INTEGRATION OF SINGLE-WALLED CARBON NANOTUBES IN POLYMERIC MATRICES THROUGH TAILORED FUNCTIONALIZATION

TESIS DOCTORAL

José Miguel González Domínguez

2011

Universidad de Zaragoza

Facultad de Ciencias

Departamento de Química Orgánica

Tesis Doctoral

Integration of Single-Walled Carbon Nanotubes in Polymeric Matrices through Tailored Functionalization

Memoria

Presentada en el Dpto. de Química Orgánica por D. José Miguel González Domínguez

para optar al Grado de Doctor en Química

José Miguel González Domínguez

Zaragoza, 2011

La **Dra. D.ª María Teresa Martínez Fernández de Landa**, Profesora de Investigación del Consejo Superior de Investigaciones Científicas (CSIC),

CERTIFICA:

Que la presente memoria titulada: "*Integration of Single-Walled Carbon Nanotubes in Polymeric Matrices through Tailored Functionalization*" presentada por el licenciado en Química **D. José Miguel González Domínguez** ha sido realizada bajo mi dirección en el Instituto de Carboquímica (ICB-CSIC) y reúne los requisitos necesarios para la obtención del Grado de Doctor, de acuerdo con la normativa vigente.

Zaragoza, 17 de octubre de 2011.

Fdo. María Teresa Martínez Fernández de Landa

EL Dr. D. JOAQUÍN BARBERÁ GRACIA, PROFESOR TITULAR Y DIRECTOR DEL DEPARTAMENTO DE QUÍMICA ORGÁNICA DE LA UNIVERSIDAD ZARAGOZA,

Como tutor de los Cursos de Doctorado del licenciado en Química D. José Miguel González Domínguez y a efectos de Profesor Ponente,

AUTORIZA:

La presentación de la memoria realizada por D. José Miguel González Domínguez, con el título *"Integration of Single-Walled Carbon Nanotubes in Polymeric Matrices through Tailored Functionalization"*, cuyo trabajo (conforme al Proyecto de Tesis aprobado por el Departamento el 21/09/2009 y ratificado por la Comisión de Doctorado el 30/09/2009) ha sido realizado en el Instituto de Carboquímica (ICB-CSIC) bajo la dirección de la Dra. D.ª María Teresa Martínez Fernández de Landa.

Y para que conste, firmo el presente informe en Zaragoza
a 17 de octubre de 2011.

"These are dark times, times without hope.
[…]What motivates a man to confront the
challenges that most of us would run from?"

Castlevania, Lords of Shadow
Konami (2011)

A todos aquellos que nunca
dudaron de que pudiera
llegar hasta aquí, y más allá.

TABLE OF CONTENTS

AGRADECIMIENTOS

Yo siempre he sido gran fan del cine. Rara vez me he perdido una gala de los Óscar, en riguroso directo, trasnochando gustosamente. Recuerdo especialmente la de 1999 cuando por primera vez yo era testigo de cómo un director de cine español era premiado, Almodóvar, por "Todo sobre mi madre", y el discurso que pronunció (¡¡de más de 1 minuto de duración!!) aún permanece en mi memoria. Aquel señor se dedicó a dar las gracias a todo ser viviente y no viviente, llegando a mencionar figuras tan atípicas en estos eventos como son la Virgen de Guadalupe o San Judas Tadeo. Yo pensaba: ¿Se puede ser más cansino? Si lo único que tenia que hacer era coger la estatuilla, decir "muchas gracias" y ya está… Pues bien, hoy por hoy y especialmente en el momento de escribir estas líneas entiendo perfectamente a aquel señor: siempre hay muchos a quienes agradecer, y mucho que agradecer. En las líneas que a continuación vienen, voy a expresar mi más profundo agradecimiento a todo aquello y todos aquellos que han hecho posible que haya llegado hasta donde ahora estoy, y lo voy a hacer a mi manera: sin convencionalismos, sin medias tintas, sin frases políticamente correctas, pero con mucha pasión y desde el corazón y la sinceridad (como todo lo que hago). Así que, estimado/a lector/a, Ud. puede pasar estas páginas si lo desea, dado que no voy a escatimar en espacio para confeccionar estos agradecimientos; pero tenga en cuenta que, a ojos de este humilde autor, esta sección es tan importante como las demás, y también que con alta probabilidad Ud. esté mencionado aquí.

No soy capaz de empezar de otro modo. Gracias a mis padres, Miguel y Eugenia, por todo. Por darme lo poco material que tenéis, que es mucho; por la paciencia, por vuestra dedicación en darnos la educación que nos ha hecho a mi hermana y a mi quienes somos. Gracias por haber estado siempre ahí, por haber confiado en nosotros, por ser nuestro pilar en los momentos bajos, y por dejar que yo haya sido vuestro pilar en vuestros malos momentos. Nunca os quepa duda de que siempre viviré con gratitud y orgullo la vida que me habéis dado, con el mismo orgullo que siempre haré que sintáis de mí, luchando a diario para llegar a ser alguien como vosotros: muy trabajadores, cumpliendo metas, con humildad y dedicación. Os quiero. Y a ti, Rocío, por ser la mejor hermana del mundo. Gracias por llevar siempre a tu hermano en un pedestal, aunque no siempre se lo merezca. Tu sensibilidad y corazón me enseña que siempre existen motivos para creer en las personas. Gracias. Y al resto de mi familia, sólo a aquellos que me han dado todo su cariño. A los que considero como mis segundos padres Manolo (Chalo) e Isabel (Tita Isa), os adoro, y a mis primas hermanas (más hermanas que primas) Mariu, Juani, Cintia, y May. El cariño y admiración que siempre me tenéis es tan grande como el que os tengo yo a vosotras. Y, ¡cómo no!, a mis sobrinos, "mis nenis", José Manuel, Adrián, Soraya y Aarón, porque sois la alegría de cada una de vuestras casas, que a su vez son también mis casas y mis alegrías. Espero que en el futuro os guste tanto la ciencia como a vuestro tito Jose. A mis primos Ricardo y David, junto con sus respectivas familias, porque ojalá la parte de familia que no he mencionado fuese como vosotros. A toda la familia que tengo en Mallorca, con los que crecí, gracias por todo lo bueno que me habéis aportado.

En el terreno profesional, y tocando muy de cerca el terreno personal, las miles de gracias que os debo a tantos que habéis trabajado conmigo, o mejor aún, a todos aquellos de los cuales he tenido el privilegio de conocer en mi periplo profesional hasta la fecha. A quien más gracias debo es a ti, Maria Teresa. Millones de gracias por haber estado ahí desde el minuto 1, por haberme brindado el honor de trabajar en tu grupo

bajo tu supervisión. Gracias por la constancia, la atención, por lo bien valorado que me he sentido, por los buenos consejos y la calidad investigadora que he podido recibir de ti. Gracias. Especial mención al afable Dr. Ánson (con "Á") por mantener siempre el equilibrio en nuestro subgrupo tras mis excesos de entusiasmo o confianza. Todo lo que me habéis enseñado, Teresa y Alejandro, es uno de los tesoros más preciados que siempre tendré en mi mochila profesional y personal, y lo guardaré junto a la profunda admiración que siempre os tendré. Y, gracias a todos aquellos compañeros que me han sufrido a lo largo de más de 4 años. A Mónica, gracias por ayudarme tanto en mis primeros pasos; a Merche, por tu bondad y profesionalidad; a Cristina, por tu calidez y valía; y unas gracias colectivas enormes a todos mis compañeros nanotuberos: a Javi, Pere, Araceli, Pablo, Manoli, Ana, Wolfgang, Edgar, Tacchini… Y, sin olvidarme de todos aquellos que han pasado por el grupo y con quien he compartido excelentes momentos: Rakel, María T., Paulina, Cristina R., Sonia M. y Armando.

Con especial cariño recordaré siempre a mis colegas y amigos con los que he tenido el honor de trabajar en este proyecto (el "composites") que tantas cosas buenas me ha dado, a todos los niveles. Un proyecto, dicho sea de paso, sin el cual hoy no estaría yo aquí finalizando este trabajo. Al grupo de Madrid, gracias a Ana y Marian, por ser tan buena gente, y por los gratos momentos que los de Zaragoza hemos compartido con vosotras. A la gente de Canadá, a mi estimadísima Yadienka (my Lady Y) millones de gracias por tu simpatía, por tu cariño y tu apoyo profesional y personal continuado, igual que a Benoit, por su amabilidad, junto con todo el grupo MNA del SIMS (Ottawa), y a Andrew y Behnam del IAR (Ottawa). Aquel septiembre de 2008 en Ottawa lo recordaré eternamente, entre otras cosas también por el cariño y amable trato que recibí de Thanh-Dung y su familia. Gracias de corazón a los que habéis sido partícipes de mis otras estancias: al Prof. Maurizio Prato y a todo su grupo en Trieste, por el excelente trato y por los buenos momentos que viví aquel diciembre de 2009; a Philippe Poulin y a todo el grupo NTG del CRPP (Bordeaux) gracias a los cuales tuve un increíble mes de julio de 2011. Al excelente servicio de análisis del ICB (con especial énfasis en Ciriaco, Elvira, Isaías e Isabel), donde la mayoría de sus integrantes han demostrado una increíble profesionalidad y sin su apoyo esta tesis habría sido casi imposible de terminar en menos de un siglo. Y, si el equipo de análisis ha sido fundamental, no lo fue menos el equipo administrativo del ICB. Gracias a Anacris (mi estimada Srta. Gracia) por su constante disposición y buen hacer, a Ana F., Don Manuel, Nacho y Maria José, porque me habéis ayudado mucho.

Gracias a los que fuisteis cómplices de mis primeros pasos en la investigación, al grupo de adsorbentes carbonosos y adsorción de la UEX, los que fuisteis mi "primera casa" y que, a pesar del paso del tiempo, nunca dejasteis de estar ahí. Gracias a Vicente, Carmen, Eduardo, Carlos y María. Y, gracias tan especiales como las anteriores, a los miembros de la UEX que siempre me han brindado su amistad y apoyo, personal y profesional en la distancia. Con mucho afecto me refiero principalmente a Mercedes T., Marina, Manuel, y Pedro C.

A mis amigos, todos aquellos que sin ser responsables de mi periplo profesional, han sido testigos directos de mis mejores momentos a lo largo de estos años. Gracias especiales mi gran amigo Sete, por ser tan buen tío, tan legal y tan buen compañero; muchas gracias por haber podido siempre contar contigo. Por extensión, muchísimas gracias a Gloria (Glow), y en general a vuestras familias en el Puerto Sagunto y Puçol donde tan bien me habéis tratado. A mis compañeros del ICB: Sabino, Iñaki A., Juan

Daniel, Marga, Isabel M., Ana C., David S., Cinthia,… no os puedo poner a todos pero en mis recuerdos sí que cabéis todos. A mi muy estimada Sra. Plou, por hacer las veces de madre estos años, por cuidarme y hacerme sentir como en mi casa desde que puse un pie en el ICB. No podía olvidarme de la Sra. del Amo y de Carmen Millán (Carmelilla) por las mismas razones. A todos aquellos que, aun estando lejos de Zaragoza, siempre me habéis ofrecido vuestra amistad, miles de gracias. A ti, Ignacio, porque (parafraseando tus propias palabras, dignas del genio que eres) encarnas los valores más sinceros de la amistad; a Olga, a quien debo siempre su cariño incondicional en la distancia; a Naomi, porque la luz de tus verdes ojos a veces se refleja en las estrellas y me llega hasta Zaragoza; a Juanjo, por ser como eres, tan buen amigo y un tío tan luchador, un ejemplo para todos. Tantas gracias debo a los que llevo mencionados como a los que a continuación citaré. Gracias a los que en estos años habéis sido mis compañeros de piso, no sólo por vivir bajo el mismo techo y compartir buenos momentos, sino también porque algunos de vosotros os habéis convertido en parte de mi familia. A mi hermano Ángel, de quien más he aprendido y del que más he aprendido a enseñar; a mis niñas polacas Joanna y Marta, por no haber dejado de estar ahí nunca; a mis amigos franceses Maelle, Juan, Clemente y Albane por tantas cosas buenas que me llevo de vosotros; y al más loco, Guerino, todo un genio y figura. ¡¡¡Gracias!!!

Si todos los buenos recuerdos, todas las vivencias, todas las cosas aprendidas, todas las veces que uno se cae, las que uno se levanta,… si todos eso cupiera en una palabra, en un símbolo, me lo tatuaría en el pecho. Mientras tanto, sólo puedo expresarlo con (muchas) palabras. No sé lo que me habrá quedado por decir, a quien me habrá quedado por mencionar, pero tened en cuenta que os debo mucho, os lo debo todo. GRACIAS a todos por haberme regalado los cuatro mejores años de mi vida. Y, si me lo permitís, quiero acabar esta sección dándole las gracias a una ciudad. Gracias Zaragoza. Gracias por ser mi casa todo este tiempo, mi refugio, mi paraíso particular. Porque viviendo en ti he tenido todo lo que más feliz me ha hecho estos cuatro años: mi trabajo (por el cual me desvivo), mis amigos, mi vida entera. Porque te adoro, a pesar del cierzo, a pesar de las ***** obras del tranvía, a pesar de las bicicletas y los autobuses,… porque lo más duro ahora será dejarte, y dejar todo lo bueno que tienes, todo lo que me has dado. Gracias, porque aunque sé que no debería, te echaré de menos, y aunque no quiera, parte de mí permanecerá aquí siempre. Pase el tiempo que pase, os lo seguiré diciendo a tod@s, GRACIAS por los cuatro mejores años de mi vida. Podrán venir tiempos igual de buenos. Nunca mejores.

"This town, is… so peaceful. The whole area used to be a sacred place. Now I can see why…"

Silent Hill 2
Konami (2001)

GLOSSARY

Acronyms for scientific and generic terms, chemicals, and experimental techniques

α: Degree of conversion (in the AIM)
AE: Activation energy
AIM: Advanced isoconversional method
BC: Block copolymer
BET: Brunnauer-Emmet-Teller method for surface area measurement
CNTs: Carbon nanotubes
CSIC: Consejo superior de investigaciones científicas (Spanish research council)
CVD: Chemical vapor deposition
DC: Direct current
DGEBA: Diglycidyl ether of bisphenol-A
ΔH: Enthalpy
DDS: 4,4'-diaminodiphenilsulfone
DLS: Dynamic light scattering
DMF: N,N'-dimethylformamide
DSC: Differential scanning calorimetry
DWCNTs: Double-walled carbon nanotubes
E': Storage modulus (DMA)
ε_b: Elongation at break (tensile tests)
EDX: Energy-dispersive X-ray spectroscopy
EO: Ethylenoxide
FA: Formic acid
FTIR: Fourier-transformed infrared spectroscopy
GF: Glass fiber
IAR: Institute for aerospace research (NRC)
ICB: Instituto de Carboquímica (CSIC), Zaragoza
ICP-OES: Induced couple plasma + optical emission spectroscopy
ICTP: Instituto de ciencia y tecnología de polímeros (CSIC), Madrid
IR: Infrared spectroscopy
LC-ESI-MS: Liquid chromatography + electrospray ionization + mass spectrometry
MS: Mass spectrometry
MWCNTs: Multi-walled carbon nanotubes
NCMs: Nanostructured carbon materials
NMP: N-methyl-2-pyrrolidone
NMR: Nuclear magnetic resonance
NRC: National research council Canada
OI: Oxygen index
PE: Polyethylene
PEEK: Poly(ether ether ketone)
PEES: Poly(1,4-phenylene ether ether sulfone)
PEI: Polyetherimide
PEO: Polyethylenoxide
PEO-*b*-PE: Diblock copolymer containing polyethylenoxide and polyethylene as adjacent blocks in each polymer chain.
PEO-*b*-PPO: Diblock copolymer containing polyethylenoxide and polypropylenoxide as adjacent blocks in each polymer chain.
PI: Purity index
PO: Propylenoxide
PPO: Polypropylenoxide
PSF: Poly(bisphenol-A ether sulfone)
PTFE: Poly(tetrafluoroethylene)
PVDF: Poly(vinylidene flouride)
SDBS: Sodium dodecylbenzenesulfonate

SEM: Scanning electron microscopy
SIMS: Steacie institute for molecular sciences (NRC), Ottawa
SWCNTs: Single-walled carbon nanotubes
σ_y: Ultimate tensile strength (tensile tests)
TEM: Transmission electron microscopy
T_{10}: Temperature of 10 wt% loss in TGA
T_g: Glass transition temperature
TGA: Thermogravimetric analysis
TGA-IR: Thermogravimetric analysis coupled to infrared spectroscopy
TGAP: Triglycidyl p-aminophenol
T_m: Maximum peak temperature in DSC
T_{max}: Temperature of maximum rate of weight loss in TGA
T_{ms}: Temperature of maximum signal in qualitative MS
THF: Tetrahydrofuran
TLC: Thin-layer chromatography
TPD-MS: Temperature-programmed desorption coupled to mass spectrometry
UNIZAR: University of Zaragoza
UV-Vis: Ultraviolet – visible range of the light spectrum
XRD: X-ray diffraction
XPS: X-Ray photoelectron spectroscopy
YM: Young's modulus (tensile tests)

Acronyms for functionalized samples and related compounds

[ox]-SWCNTs: Arc discharge SWCNTs thermally oxidized in air atmosphere (350ºC/2h)
AD: Amine-terminated derivative, isolated from reaction between TGAP and DDS
A-SWCNTs: As-grown arc discharge SWCNTs (nomenclature equivalent to SWCNT-asg)
ED: Epoxide-terminated derivative mixture, obtained from reaction between TGAP and DDS
L-SWCNTs: As-grown laser SWCNTs
NFP: N-Fmoc-6-aminohexanoyl peroxide
SW-AD: As-grown arc discharge (A-) or laser-grown (L-) SWCNTs covalently functionalized with AD *via* the *in situ* diazonium reaction
SW-DDS: As-grown arc discharge (A-) or laser-grown (L-) SWCNTs covalently functionalized with DDS *via* the *in situ* diazonium reaction
SW-DDS-ED: As-grown arc discharge (A-) or laser-grown (L-) SWCNTs covalently functionalized with DDS *via* the *in situ* diazonium reaction and then reacted with ED by nucleophilic ring opening
SWCNT-asg: As-grown arc discharge SWCNTs (nomenclature equivalent to A-SWCNTs)
SWCNT-dba: As-grown arc discharge SWCNTs functionalized with 4-aminobenzylamine *via* the *in situ* diazonium reaction
SWCNT-dca: As-grown arc discharge SWCNTs functionalized with N-Boc-ethyleneglycol-bis(2-aminoethylether)-N'-acetic acid and paraformaldehyde *via* the 1,3-dipolar cycloaddition reaction of azomethyne ylides
SWCNT-nfp: As-grown arc discharge SWCNTs functionalized with NPF *via* the alkaline reduction with Na-Naphthalene radical ion
SWCNT-oxa: As-grown arc discharge SWCNTs oxidized with nitric acid and then functionalized by amidation with N-Boc-1,6-diaminohexane
SWCNT-P2: Purified arc-discharge SWCNTs purchased from Carbon Solutions Inc.

"A famous explorer once said, that the extraordinary is in what we do, not who we are"

Tomb Raider
Square Enix (to be released in 2012)

RESUMEN

Los materiales de carbono nanoestructurados (NCMs) cero-dimensionales (fullerenos), unidimensionales (nanotubos de carbono) y bidimensionales (grafeno), son objeto de numerosos estudios en muchas disciplinas científicas debido a sus extraordinarias propiedades físicas y químicas. Una de las más importantes áreas de investigación y aplicación de los NCMs es su integración en estructuras macroscópicas tales como matrices poliméricas, donde los NCMs tienen un gran potencial para actuar como reforzante estructural, resultando en un *nanomaterial compuesto* de altas prestaciones. Sin embargo, existen importantes obstáculos (relacionados con las características superficiales y el estado físico de los NCMs) que impiden la transferencia de las excelentes propiedades de los NCMs a la matriz, siendo la química y el preprocesado de los NCMs la clave para mejorar dicha transferencia.

La presente memoria de tesis contiene los resultados de la investigación realizada en la búsqueda de diversas estrategias de modificación (covalente y no covalente) aplicadas a nanotubos de carbono de pared simple (SWCNTs), con el fin de mejorar tanto su integración en matrices poliméricas específicas como las interacciones reforzante-matriz. Se han preparado y caracterizado varias series de nanomateriales compuestos reforzados con los SWCNTs modificados, con miras al diseño racional de materiales compuestos avanzados de altas prestaciones. Se ha llevado a cabo una extensa caracterización del reforzante (antes y después de los procedimientos de modificación) y también de los nanomateriales compuestos resultantes, que ha puesto de manifiesto qué estrategia es la más apropiada para mejorar una propiedad de interés. Los resultados obtenidos permiten el uso de funcionalizaciones dirigidas buscando mejoras de propiedades específicas de los nanomateriales compuestos.

La presente tesis tiene como objetivo aportar nuevos conocimientos en el campo de los nanomateriales compuestos basados en matrices poliméricas reforzadas con SWCNTs. Para ello, se aborda el desarrollo de diversas estrategias de funcionalización que potencian la miscibilidad de los SWCNTs y su afinidad por la matriz polimérica de interés, permitiendo la integración sin uso de disolventes orgánicos. El trabajo desarrollado se enmarca en el proyecto de investigación titulado *"Multifunctional, light weight, single-walled carbon nanotube-based carbon fibre nanocomposites for*

transportation", donde han colaborado dos grupos pertenecientes al Consejo Superior de Investigaciones Científicas (CSIC) y otros dos grupos pertenecientes al Nacional Research Council (NRC) de Canadá. A lo largo de esta investigación se han buscado estrategias de funcionalización de SWCNTs en dos tipos de matrices poliméricas: una matriz termoestable de epoxi y una matriz termoplástica de poliéter éter cetona (PEEK). El trabajo realizado ha consistido en el diseño de estrategias de funcionalización de SWCNTs para su integración en ambos polímeros, y la preparación de nanomateriales compuestos con matriz epoxi. La preparación de nanomateriales compuestos de PEEK/SWCNTs, con los SWCNTs funcionalizados en el presente trabajo, se ha llevado a cabo en el Instituto de Ciencia y Tecnología de Polímeros (ICTP-CSIC), uno de los colaboradores del proyecto, y los principales resultados obtenidos se presentan en el Anexo I.

Las dos estrategias generales de funcionalización de SWCNTs investigadas con objeto de mejorar su integración en matriz epoxi se detallan a continuación:

- Funcionalización no covalente mediante dispersión de SWCNTs en varios copolímeros de bloque consistentes en distintas combinaciones de polietilen-óxido (PEO), polipropilenóxido (PPO) y polietileno (PE). El bloque de PEO actúa como un compatibilizante de epoxi, mientras que los otros bloques en los copolímeros se seleccionaron atendiendo a su mayor afinidad por los SWCNTs.
- Funcionalización covalente dirigida a la obtención de un reforzante reactivo mediante incorporación de grupos amina en la superficie de los SWCNTs, que participan en el proceso de entrecruzado de la matriz epoxi. La funcionalización con grupos amino se llevó a cabo mediante cuatro rutas químicas establecidas y también mediante una nueva propuesta consistente en la incorporación en la superficie de los SWCNTs de fragmentos derivados de la matriz epoxi (terminados en grupo amino o en oxirano) a través de la reacción de diazonio.

Las dos estrategias aplicadas a los SWCNTs para su integración en matriz de PEEK, se exponen a continuación:

- Funcionalización no covalente mediante dispersión en polímeros termoplásticos seleccionados atendiendo a su similitud estructural y compatibilidad

química con la matriz de PEEK, buscando un efecto compatibilizante entre los SWCNTs y la matriz polimérica.

- Funcionalización covalente mediante el anclaje de los SWCNTs a la matriz de PEEK, que se llevó a cabo por diferentes reacciones de esterificación entre SWCNTs carboxilados y PEEK hidroxilado.

Las estrategias de funcionalización de SWCNTs estudiadas en la presente tesis ofrecen una aportación al diseño racional de nanomateriales compuestos de altas prestaciones. Los resultados obtenidos establecen la vía para su diseño mediante estrategias de funcionalización dirigidas a la mejora de determinadas propiedades.

El contenido de la presente tesis, desglosado por capítulos, es el siguiente:

CAPÍTULO 1: Introducción general del trabajo contenido en la presente tesis.

CAPÍTULO 2: Contiene una visión general de los materiales de carbono nanoestructurados, y de los SWCNTs en particular. También se exponen las distintas rutas de funcionalización covalente empleadas en SWCNTs y su caracterización.

CAPÍTULO 3: Describe las distintas funcionalizaciones no covalentes aplicadas a los SWCNTs, mediante el recubrimiento con copolímeros de bloque basados en PEO (para su integración en epoxi) y con polímeros termoplásticos (para su integración en PEEK). Asimismo, se presenta una detallada caracterización de los SWCNTs funcionalizados no covalentemente.

CAPÍTULO 4: Se centra en el estudio del efecto de distintas funcionalizaciones de SWCNTs, covalentes y no covalentes, en el proceso de curado de la matriz epoxi, mediante calorimetría diferencial de barrido.

CAPÍTULO 5: Contiene la primera parte del trabajo relacionado con la preparación y caracterización de nanomateriales compuestos epoxi/SWCNT. En este capítulo, se estudian los materiales epoxi con SWCNTs funcionalizados covalentemente (tanto con aminas alifáticas por rutas químicas establecidas, como con fragmentos derivados de la

matriz por reacción de diazonio) en términos de morfología, propiedades mecánicas, térmicas y eléctricas.

CAPÍTULO 6: Contiene la segunda parte del trabajo relacionado con la preparación y caracterización de nanomateriales compuestos epoxi/SWCNT. En este capítulo, se estudian los materiales epoxy con SWCNTs recubiertos de copolímeros de bloque basados en PEO. Se presenta un estudio de propiedades análogo al del Capítulo 5.

CAPÍTULO 7: Presenta las conclusiones generales extraídas del presente trabajo de tesis.

ANEXO I: Reúne los principales resultados obtenidos en nanomateriales compuestos de matriz de PEEK, haciendo uso de estrategias de funcionalización covalente y no covalente descritas en los capítulos 2 y 3 respectivamente. Dichos resultados fueron obtenidos en el ICTP-CSIC, bajo la dirección de la Prof.ª M. A. Gómez-Fatou, en el marco del proyecto de investigación conjunto.

ANEXO II: Contiene una lista de contribuciones científicas generadas durante la realización de la presente tesis.

Los SWCNTs usados fueron producidos mediante el método de arco eléctrico en el Instituto de Carboquímica (ICB-CSIC). En algunos casos particulares también se utilizaron, a efectos comparativos, SWCNTs producidos por el método láser en el Steacie Institute for Molecular Sciences (SIMS-NRC).

"One who knows nothing,
can understand nothing"

Kingdom Hearts
Squaresoft (2002)

CHAPTER 1:

GENERAL INTRODUCTION AND OUTLINE

1.0. Abstract

The present thesis work deals with a series of chemical modification strategies (covalent and non-covalent) applied to single-walled carbon nanotubes (SWCNTs) in order to improve both their integration into specific polymer matrices and the filler-matrix interactions. Nanocomposite materials containing modified SWCNTs in those polymer matrices have been prepared and characterized aiming at the rational design of advanced nanocomposite materials for high-performance applications. A thorough characterization of both the filler (before and after modification) and nanocomposites properties has been conducted, emphasizing which strategy is the most suitable for enhancing a property of interest. The obtained results will allow the use of tailored functionalization strategies looking for the enhancement of specific nanocomposite features. A description of the aims and outline of the present work, as well as a brief description of the chapters' content, are provided in this first chapter.

1.1. Contextualization

Nanostructured carbon materials (NCMs), namely fullerenes (0-dimensional), carbon nanotubes (1-dimensional) and graphene (2-dimensional) are a hot topic in many scientific research areas because of their extraordinary physical and chemical properties. One of the most important areas of research and application of NCMs is their integration in macroscopic structures (such as polymer matrices) where NCMs are perfect candidates for acting as reinforcing filler, ending up in a *nanocomposite material* with improved properties. However, severe drawbacks (related to the surface characteristics of NCMs and their as-grown physical state) are hindering the full transfer of their properties, being the chemistry and pre-processing of NCMs envisioned as the key to solve these drawbacks.

1.2. Aims and purposes of the present thesis

In this context, the present thesis aims at contributing to the field of nanocomposite materials based on polymer matrices using modified SWCNTs as fillers. This thesis addresses the development of several SWCNT covalent and non-covalent functionalization strategies to enhance their miscibility and affinity for the polymer matrix,

enabling their integration without assistance of organic solvents. The work carried out lies in the framework of the project entitled *"Multifunctional, light weight, single-walled carbon nanotube-based carbon fibre nanocomposites for transportation"*, a joint research among two groups belonging to the Canadian research council (NRC) and two groups from the Spanish research council (CSIC). Two different polymer matrices are used in this project: on the one hand (and main issue of this thesis work), a thermosetting epoxy matrix based on a multifunctional precursor (TGAP) and an aromatic curing agent (DDS); on the other hand, a thermoplastic poly(ether ether) ketone (PEEK) matrix. The work carried out in this thesis consists of the design and performance of all covalent and non-covalent SWCNTs functionalization strategies to integrate the SWCNTs in both polymers and the preparation of epoxy/SWCNT nanocomposites. The preparation of PEEK/SWCNT nanocomposites has been mostly carried out at the Instituto de Ciencia y Tecnología de Polímeros (ICTP-CSIC), one of the project partners and the main results have been included as an annex.

Two general functionalization approaches, covalent and non-covalent, have been investigated for the targeted polymer matrices. For epoxy matrix, these are detailed as follows:

- The non-covalent functionalization has been carried out by dispersion and wrapping of SWCNTs in different block copolymers containing polyethylenoxide as one of the blocks. The polyethylenoxide acts as an epoxy compatibilizer, while the other blocks within copolymer chains were selected to have more affinity for SWCNTs.

- For the covalent approach, reactive fillers have been obtained by functionalizing SWCNTs with amine groups that can participate in the epoxy cross-linking process. The covalent strategy consisted of the functionalization with different terminal aliphatic amines through four well-established chemical routes, as well as a novel approach consisting of covalent attaching pre-synthesised matrix-based moieties (ending in amine or epoxide) through the *in situ* diazonium reaction.

The two general approaches (covalent and non-covalent) have also been applied to integrate SWCNTs in the PEEK matrix. The followed strategies can be summarized in:

- As non-covalent approach, the wrapping of SWCNTs with thermoplastic polymers containing aromatic residues has been undertaken. Such polymers were chosen attending to their structural similarity and chemical compatibility with the target matrix, in order to achieve a compatibilization effect in the nanocomposite.

- On the other hand, the covalent grafting of SWCNTs to a PEEK matrix was conducted by esterification reactions between carboxylated SWCNTs and hydroxilated PEEK.

The SWCNT functionalization strategies studied herein offer a systematic attempt to set the way toward the rational design of high-performance nanocomposite materials for specific properties improvement. The obtained results pave the way for tailoring and tuning of nanocomposites physical properties through SWCNT functionalization strategies.

1.3. Chapter contents

CHAPTER 2 contains an overview of NCMs, in general, and SWCNTs in particular, regarding their properties, applications and characterization. Likewise, the addressed covalent chemistry of SWCNTs and their characterization are provided.

CHAPTER 3 describes the different non-covalent modifications of SWCNTs that have been undertaken, related to the wrapping in PEO-based block copolymers (for their integration into epoxy) and thermoplastic polymers (for their integration into PEEK). A complete characterization of the wrapped fillers is presented.

CHAPTER 4 focuses on the effect of different covalent and non-covalent SWCNTs functionalization on the epoxy cross-linking reaction kinetics, as studied by differential scanning calorimetry.

CHAPTER 5 contains the first part of the work related to the manufacturing and characterization of high-performance epoxy/SWCNT nanocomposites. In this chapter, epoxy nanocomposites containing covalently functionalized SWCNTs (with both aliphatic terminal amines and matrix-based moieties) are studied and discussed, in terms of their morphology, mechanical, thermal and electrical properties.

CHAPTER 6 contains the second part of the work related to the manufacturing and characterization of high-performance epoxy/SWCNT nanocomposites. Those with block copolymer-wrapped SWCNTs used as the filler are studied in this chapter. A study of these nanocomposites analogous to the one of Chapter 5 is presented and discussed.

CHAPTER 7 presents the general conclusions drawn from the present thesis work.

ANNEX I gathers the main results attained with PEEK nanocomposites using the covalent and non-covalent strategies described in chapters 2 and 3 respectively. These results have been mostly obtained at the ICTP by the leadership of Prof. M. A. Gomez-Fatou in the framework of the aforementioned collaborative research project.

ANNEX II contains a list of the scientific contributions generated from the present thesis work.

The SWCNTs used along the present work were produced by arc-discharge at the Instituto de Carboquímica (ICB-CSIC). In some particular cases, laser SWCNTs produced at the Steacie Institute for Molecular Sciences (SIMS-NRC), one of the project partners, have also been used for comparative purposes.

"Protect your honor, and embrace your dreams. If you want to be a hero, you need to have dreams"

Final Fantasy VII Crisis Core
Square Enix (2008)

CHAPTER 2:

SINGLE-WALLED CARBON NANOTUBES. PROPERTIES, APPLICATIONS, PROCESSING AND COVALENT FUNCTIONALIZATION

2.0. Abstract

Carbon nanotubes are cutting-edge materials with exciting properties and a strong potential for applications in many fields. The single-walled type of nanotubes has been used all over the present thesis to develop high-performance nanocomposite materials. In this chapter, these nanostructured materials are presented and their general features are described. During the thesis development, the nanotubes purification, processing and characterization was undertaken and the results obtained are analyzed here. The purification *via* acid treatment was carried out mainly with nitric acid, which serves as a starting point for further functionalization approaches based on the nucleophilic attack to carboxyl groups. Many other sidewall SWCNT functionalization strategies grafting covalent moieties were also carried out, with special emphasis on obtaining primary terminal amine-functionalized nanotubes, which are of a great interest to accomplish their integration in epoxy matrix. Full experimental details, functionalization outcome and nanotubes characterization are carefully analyzed below.

2.1. Introduction

2.1.1. Carbon nanotubes. Definition, classification, features and relevance

Carbon materials have had and currently have a huge repercussion in the development of materials science and technology. Over the last two decades, new nanostructured carbon materials have emerged. These nanostructured materials have had a huge impact[1,2] and their discoverers were acknowledged by two Nobel prizes (in 1996 for the discovery of C_{60} fullerenes and in 2010 for the isolation and study of monatomic graphite layers or graphene). Since the Japanese scientist Sumio Iijima discovered Carbon Nanotubes (CNTs) in 1991,[3] and together with the raise of the new scientific discipline called Nanotechnology, there has been an enormous research effort put in this field. CNTs formally consist of a rolled-up graphene layer which could have different number of concentric tubes. The first ones in being discovered were the Multi-Walled CNTs (MWCNTs), while two years later Iijima reported the discovery of the

[1] Van Noorden, R., The trials of new carbon. *Nature* 2011, *469* (7328), 14-16.
[2] Martin, N.; Guldi, D. M.; Echegoyen, L., Carbon nanostructures-Introducing the latest web themed issue. *Chem. Commun.* 2011, *47* (2), 604-605.
[3] Iijima, S., Helical microtubules of graphitic carbon. *Nature* 1991, *354* (6348), 56-58.

Single-Walled Carbon Nanotubes (SWCNTs).[4] Despite being a totally synthetic material, it is actually considered as an additional allotropic form of carbon, such as graphite or diamond.

In a CNT two well-defined parts can be distinguished (Figure 2.1), namely *sidewall* and *endtips*, where the latter ones could be visualized as fullerene semi-spheres. Morphologically and structurally CNTs can be considered as a rolled-up graphene layer. Their physical properties, especially the electronic properties depend on the orientation of the rolled graphene layer (also referred to as *chirality* or *helicity*). Thus, three main kinds of helicities may be found leading to one of the two typical electronic behaviors (semiconducting or metallic). The so-called *chiral vector* ($\vec{C}_h$) is the magnitude which defines this physical property. The two-dimensional components (*n, m*) of this vector describe the orientation of the rolled-up graphene sheet and also account for the CNT diameter (Figure 2.1).

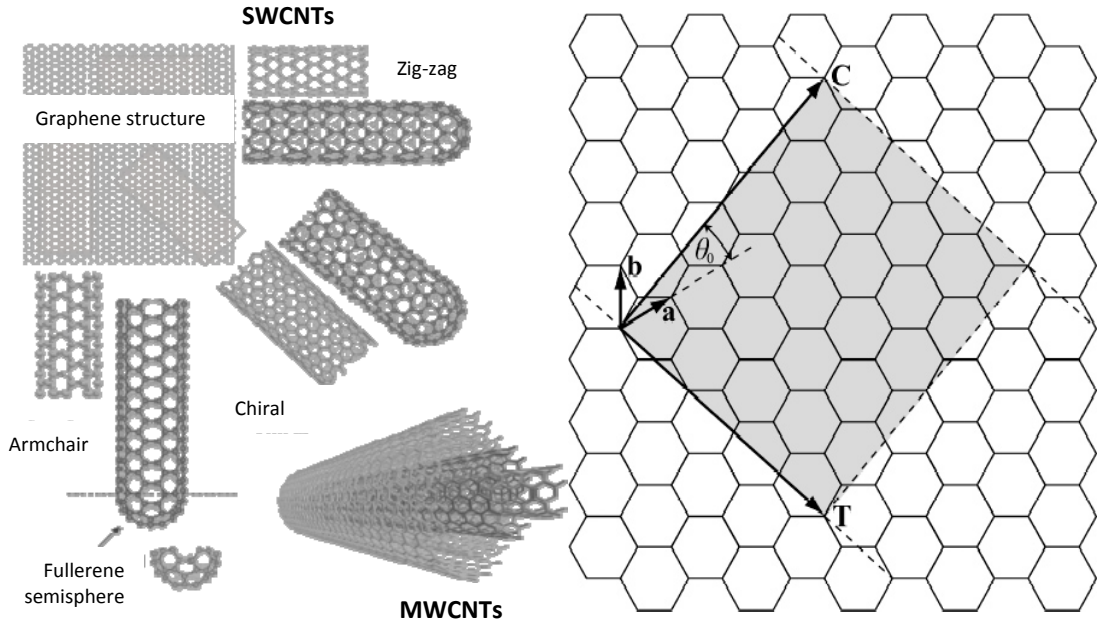

Figure 2.1. Kinds of chirality (left) and the way of obtaining the chiral vector (right) from SWCNTs.

[4] Iijima, S.; Ichihashi, T., Single-shell carbon nanotubes of 1-nm diameter. *Nature* 1993, *363* (6430), 603-605.

CNTs are being actively studied because of their fundamental interest in chemistry and physics and because of their technological applications. The extraordinary physical properties of CNTs could be summarized in the following points.

- Extraordinary electronic properties:[5] ballistic transport of electrons along the tubular axis, behavior as a quantic thread.
- Exceptional thermal properties:[6] thermal conductivity comparable to, or even higher than diamond.
- Excellent mechanical properties:[7] Young's moduli in the range of terapascals.

These facts, coupled to their extremely low density make them ideal candidates for structural reinforcement. However, these extraordinary properties as referred to isolated CNTs, and the proper transfer of these properties to the matrices (which is not straightforward) will critically depend on several factors, as will be further discussed.

The extraordinary potential of CNTs in general,[8] and SWCNTs in particular, have motivated their study in different areas, including molecular electronics,[9] advanced composite materials,[10] energy conversion and storage,[11] sensors and biosensors,[12-14] biotechnology,[15] … Furthermore, the wide range of functionalization possibilities owed by CNTs[16-20] provide even more expectations toward their applications.

[5] White, C. T.; Todorov, T. N., Carbon nanotubes as long ballistic conductors. *Nature* 1998, *393* (6682), 240-242.
[6] Berber, S.; Kwon, Y. K.; Tomanek, D., Unusually high thermal conductivity of carbon nanotubes. *Phys. Rev. Lett.* 2000, *84* (20), 4613-4616.
[7] Treacy, M. M. J.; Ebbesen, T. W.; Gibson, J. M., Exceptionally high Young's modulus observed for individual carbon nanotubes. *Nature* 1996, *381* (6584), 678-680.
[8] Dresselhaus, M. S.; Dresselhaus, G.; Avourios P.; *Carbon Nanotubes, Topics in applied physics*, 80, 1-9. Springer -Verlag Berlin Heidelberg, 2001.
[9] Avouris, P., Molecular electronics with carbon nanotubes. *Acc. Chem. Res.* 2002, *35* (12), 1026-1034.
[10] Moniruzzaman, M.; Winey, K. I., Polymer nanocomposites containing carbon nanotubes. *Macromolecules* 2006, *39* (16), 5194-5205.
[11] Arico, A. S.; Bruce, P.; Scrosati, B.; Tarascon, J. M.; Van Schalkwijk, W., Nanostructured materials for advanced energy conversion and storage devices. *Nat. Mater.* 2005, *4* (5), 366-377.
[12] Pandey, P.; Datta, M.; Malhotra, B. D., Prospects of nanomaterials in biosensors. *Anal. Lett.* 2008, *41* (2), 159-209.
[13] Martinez, M. T.; Tseng, Y. C.; Ormategui, N.; Loinaz, I.; Eritja, R.; Bokor, J., Label-Free DNA Biosensors Based on Functionalized Carbon Nanotube Field Effect Transistors. *Nano Lett.* 2009, *9* (2), 530-536.
[14] Martinez, M. T.; Tseng, Y. C.; Salvador, J. P.; Marco, M. P.; Ormategui, N.; Loinaz, I.; Bokor, J., Electronic Anabolic Steroid Recognition with Carbon Nanotube Field-Effect Transistors. *ACS Nano* 2010, *4* (3), 1473-1480.
[15] Martin, C. R.; Kohli, P., The emerging field of nanotube biotechnology. *Nat. Rev. Drug Discov.* 2003, *2* (1), 29-37.
[16] Bahr, J. L.; Tour, J. M., Covalent chemistry of single-wall carbon nanotubes. *J. Mater. Chem.* 2002, *12* (7), 1952-1958.

After two elapsed decades since the CNTs discovery, a huge amount of research has been published,[21] for both pristine and modified CNTs, and amazing progress has been developed in many areas of application, including electronic devices, membranes and catalysis. The scientific emphasis which is being put on these nanostructured materials and the exciting results that are continuously emerging suggest that further decisive progress is likely to be achieved.

In the field of materials science and technology, numerous research works have been developed with the aim of integrating SWCNTs into macroscopic structures. Different morphologies using CNTs are currently accessible, mainly as-grown CNT powder,[22] thin films or mats made of CNTs (better known as *buckypapers*[23,24]), or macroscopic fibres integrated by entangled, which can be obtained in the presence of specific polymeric materials by spinning techniques.[25-28] Fabricating CNT-based buckypapers and fibres has been to date the most efficient way to ensure a proper

[17] Dyke, C. A.; Tour, J. M., Covalent functionalization of single-walled carbon nanotubes for materials applications. *J. Phys. Chem. A* 2004, *108* (51), 11151-11159.
[18] Banerjee, S.; Hemraj-Benny, T.; Wong, S. S., Covalent surface chemistry of single-walled carbon nanotubes. *Adv. Mater.* 2005, *17* (1), 17-29.
[19] Singh, P.; Campidelli, S.; Giordani, S.; Bonifazi, D.; Bianco, A.; Prato, M., Organic functionalisation and characterisation of single-walled carbon nanotubes. *Chem. Soc. Rev.* 2009, *38* (8), 2214-2230.
[20] Peng, X. H.; Wong, S. S., Functional Covalent Chemistry of Carbon Nanotube Surfaces. *Adv. Mater.* 2009, *21* (6), 625-642.
[21] Schnorr, J. M.; Swager, T. M., Emerging applications of carbon nanotubes. *Chem. Mater.* 2011, *23*, 646-657.
[22] Journet, C.; Maser, W. K.; Bernier, P.; Loiseau, A.; delaChapelle, M. L.; Lefrant, S.; Deniard, P.; Lee, R.; Fischer, J. E., Large-scale production of single-walled carbon nanotubes by the electric-arc technique. *Nature* 1997, *388* (6644), 756-758.
[23] Rinzler, A. G.; Liu, J.; Dai, H.; Nikolaev, P.; Huffman, C. B.; Rodriguez-Macias, F. J.; Boul, P. J.; Lu, A. H.; Heymann, D.; Colbert, D. T.; Lee, R. S.; Fischer, J. E.; Rao, A. M.; Eklund, P. C.; Smalley, R. E., Large-scale purification of single-wall carbon nanotubes: process, product, and characterization. *Appl. Phys. A-Mater. Sci. Process.* 1998, 67 (1), 29-37.
[24] Anson-Casaos, A.; Gonzalez-Dominguez, J. M.; Terrado, E.; Martinez, M. T., Surfactant-free assembling of functionalized single-walled carbon nanotube buckypapers. *Carbon* 2010, *48* (5), 1480-1488.
[25] Vigolo, B.; Penicaud, A.; Coulon, C.; Sauder, C.; Pailler, R.; Journet, C.; Bernier, P.; Poulin, P., Macroscopic fibers and ribbons of oriented carbon nanotubes. *Science* 2000, *290* (5495), 1331-1334.
[26] Li, D.; Xia, Y. N., Electrospinning of nanofibers: Reinventing the wheel? *Adv. Mater.* 2004, *16* (14), 1151-1170.
[27] Dalton, A. B.; Collins, S.; Munoz, E.; Razal, J. M.; Ebron, V. H.; Ferraris, J. P.; Coleman, J. N.; Kim, B. G.; Baughman, R. H., Super-tough carbon-nanotube fibres - These extraordinary composite fibres can be woven into electronic textiles. *Nature* 2003, *423* (6941), 703-703.
[28] Dalton, A. B.; Collins, S.; Razal, J.; Munoz, E.; Ebron, V. H.; Kim, B. G.; Coleman, J. N.; Ferraris, J. P.; Baughman, R. H., Continuous carbon nanotube composite fibers: properties, potential applications, and problems. *J. Mater. Chem.* 2004, *14* (1), 1-3.

transfer of properties from the nanoscale to a bulk material.[27,29] Such properties transfer represents a critical factor for the use of a CNT-based nanocomposite material for structural, thermal or electronic applications.

2.1.2. Production and purification of SWCNTs

There are three main processes known to date to produce CNTs, which could be industrially scalable. The first used CNT synthesis technique was the electric arc discharge, a high temperature technique able to produce CNTs as discovered by Iijima and co-workers,[4] implemented by other authors.[30,22] It consists in the high-voltage discharge on a carbon-based anode which decomposes under inert atmosphere forming CNT structures deposited on the inner walls of the oven. The second technique is known as the laser ablation method, [23,31-33] In this high-temperature technique, a pulsed laser is focused on a carbon material surface provoking its vaporization in inert atmosphere and the subsequent deposition in the form of a nanostructured carbon material. Finally, the chemical vapor deposition (CVD) technique is the most employed for the CNT synthesis,[34,35] and consists of the catalytic decomposition of a carbon precursor at lower temperature than the previous methods. The CVD is a very versatile technique that allows growing on controlled positions thus obtaining CNTs with many kinds of morphological features, i.e. powder,[22] arrays or forests of aligned CNTs.[36] In the present thesis, SWCNTs mainly from the arc discharge method have been used. In some specific cases, which will be indicated, laser SWCNTs have also been employed.

---

[29] Munoz, E.; Dalton, A. B.; Collins, S.; Kozlov, M.; Razal, J.; Coleman, J. N.; Kim, B. G.; Ebron, V. H.; Selvidge, M.; Ferraris, J. P.; Baughman, R. H., Multifunctional carbon nanotube composite fibers. *Adv. Eng. Mater.* 2004, *6* (10), 801-804.

[30] Ebbesen, T. W.; Ajayan, P. M., Large-scale synthesis of carbon nanotubes. *Nature* 1992, *358* (6383), 220-222.

[31] Morales, A. M.; Lieber, C. M., A laser ablation method for the synthesis of crystalline semiconductor nanowires. *Science* 1998, *279* (5348), 208-211.

[32] Maser, W. K.; Munoz, E.; Benito, A. M.; Martinez, M. T.; de la Fuente, G. F.; Maniette, Y.; Anglaret, E.; Sauvajol, J. L., Production of high-density single-walled nanotube material by a simple laser-ablation method. *Chem. Phys. Lett.* 1998, *292* (4-6), 587-593.

[33] Kingston, C. T.; Jakubek, Z. J.; Denommee, S.; Simard, B., Efficient laser synthesis of single-walled carbon nanotubes through laser heating of the condensing vaporization plume. *Carbon* 2004, *42* (8-9), 1657-1664.

[34] Kong, J.; Cassell, A. M.; Dai, H. J., Chemical vapor deposition of methane for single-walled carbon nanotubes. *Chem. Phys. Lett.* 1998, *292* (4-6), 567-574.

[35] Cassell, A. M.; Raymakers, J. A.; Kong, J.; Dai, H. J., Large scale CVD synthesis of single-walled carbon nanotubes. *J. Phys. Chem. B* 1999, *103* (31), 6484-6492.

[36] Terrado, E.; Tacchini, I.; Benito, A. M.; Maser, W. K.; Martinez, M. T., Optimizing catalyst nanoparticle distribution to produce densely-packed carbon nanotube growth. *Carbon* 2009, *47* (8), 1989-2001.

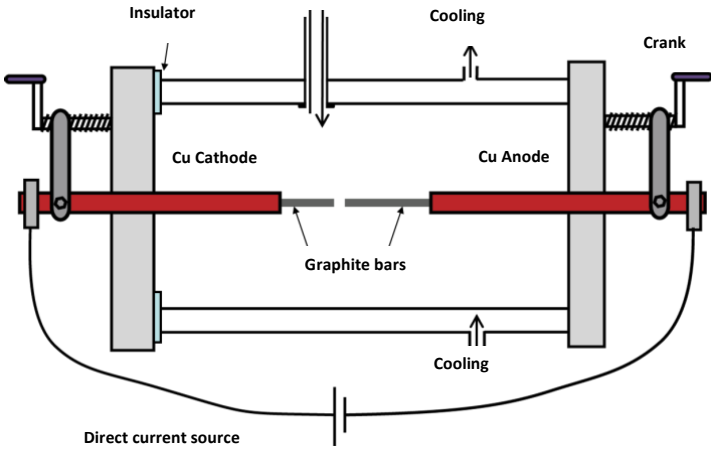

Figure 2.2. Electric arc oven scheme at the Instituto de Carboquímica (ICB-CSIC), used for the preparation of SWCNTs in the present thesis

All these methods necessarily require the use of metal catalysts when SWCNTs are produced, which cause their impurification with residual metal particles, typically Ni, Co, Fe or Y. Besides, many other carbonaceous impurities are also present in a SWCNT raw material. These are classified into amorphous carbon, and other carbon forms with different degree of graphitization (including graphitic onions and graphite particles, particularly in the high-temperature production methods). Graphite impurities consist of crystalline domains of multiple π-stacked graphene layers which can be easily identified by powder X-ray diffraction (XRD), with a sharp peak at $2\theta \sim 27^{\circ}$, as well as metallic impurities which have specific diffraction patterns depending on their crystalline lattice. Additionally, the pristine SWCNT samples appear as bundles of packed tubes in a 2D hexagonal lattice.[37] This represents another drawback in their applications, such as in nanocomposite materials, where the transfer of individual properties of SWCNTs to the matrix is hindered by the presence of bundles.

Purifying SWCNTs is a laborious task requiring one or more experimental steps prior to the SWCNT use. The interest of pure SWCNT samples regards to the experimental study of their properties and applications, and to the biological and biomedical fields. For this reason many efforts are being invested in the development of suitable purification techniques and in the experimental evaluation of the SWCNT

[37] Thess, A.; Lee, R.; Nikolaev, P.; Dai, H. J.; Petit, P.; Robert, J.; Xu, C. H.; Lee, Y. H.; Kim, S. G.; Rinzler, A. G.; Colbert, D. T.; Scuseria, G. E.; Tomanek, D.; Fischer, J. E.; Smalley, R. E., Crystalline ropes of metallic carbon nanotubes. *Science* 1996, *273* (5274), 483-487.

purity and quality. Metal particles can be greatly removed by treatment of a raw SWCNT material with refluxing inorganic acids, commonly nitric,[23,38-40] sulphuric, hydrochloric or their mixtures.[41] Other oxidizing agents in liquid phase are employed to remove metals, such as potassium permanganate,[42] or hydrogen peroxide.[43] Liquid-phase oxidative treatments of SWCNTs have proven to be even more effective if they are performed under microwave digestion conditions.[44-46] Carbonaceous impurities are sensitive to thermal treatments at a moderate temperature in air environment.[47] The current trend is to combine two or more of these methods to build a purification protocol maximizing the elimination of both metallic and carbonaceous impurities. As a common example, air oxidation followed by acid treatments is typically employed.[48-50] A softer purification route which is increasingly being used is the suspension of SWCNTs in surfactants. Through sonication of SWCNT raw material in aqueous solution of a molecular or polymeric surfactant it is possible to shape the intertube potential *via* electrostatic (in ionic surfactants) or steric/entropic (in neutral polymeric

[38] Hu, H.; Zhao, B.; Itkis, M. E.; Haddon, R. C., Nitric acid purification of single-walled carbon nanotubes. *J. Phys. Chem. B* 2003, *107* (50), 13838-13842.
[39] Martinez, M. T.; Callejas, M. A.; Benito, A. M.; Cochet, M.; Seeger, T.; Anson, A.; Schreiber, J.; Gordon, C.; Marhic, C.; Chauvet, O.; Fierro, J. L. G.; Maser, W. K., Sensitivity of single wall carbon nanotubes to oxidative processing: structural modification, intercalation and functionalisation. *Carbon* 2003, *41* (12), 2247-2256
[40] Martinez, M. T.; Callejas, M. A.; Benito, A. M.; Cochet, M.; Seeger, T.; Anson, A.; Schreiber, J.; Gordon, C.; Marhic, C.; Chauvet, O.; Maser, W. K., Modifications of single-wall carbon nanotubes upon oxidative purification treatments. *Nanotechnology* 2003, *14* (7), 691-695.
[41] Porro, S.; Musso, S.; Vinante, M.; Vanzetti, L.; Anderle, M.; Trotta, F.; Tagliaferro, A., Purification of carbon nanotubes grown by thermal CVD. *Physica E* 2007, *37* (1-2), 58-61.
[42] Hiura, H.; Ebbesen, T. W.; Tanigaki, K., Opening and purification of carbon nanotubes in high yields. *Adv. Mater.* 1995, *7* (3), 275-276.
[43] Datsyuk, V.; Kalyva, M.; Papagelis, K.; Parthenios, J.; Tasis, D.; Siokou, A.; Kallitsis, I.; Galiotis, C., Chemical oxidation of multiwalled carbon nanotubes. *Carbon* 2008, *46* (6), 833-840.
[44] Martinez, M. T.; Callejas, M. A.; Benito, A. M.; Maser, W. K.; Cochet, M.; Andres, J. M.; Schreiber, J.; Chauvet, O.; Fierro, J. L. G., Microwave single walled carbon nanotubes purification. *Chem. Commun.* 2002, (9), 1000-1001.
[45] Vazquez, E.; Georgakilas, V.; Prato, M., Microwave-assisted purification of HiPco carbon nanotubes. *Chem. Commun.* 2002, (20), 2308-2309.
[46] Schofelder, R.; Rummeli, M. H.; Gruner, W.; Loffler, M.; Acker, J.; Hoffmann, V.; Gemming, T.; Buchner, B.; Pichler, T., Purification-induced sidewall functionalization of magnetically pure single-walled carbon nanotubes. *Nanotechnology* 2007, *18* (37).
[47] Shi, Z. J.; Lian, Y. F.; Liao, F. H.; Zhou, X. H.; Gu, Z. N.; Zhang, Y. G.; Iijima, S., Purification of single-wall carbon nanotubes. *Solid State Commun.* 1999, *112* (1), 35-37.
[48] Chiang, I. W.; Brinson, B. E.; Huang, A. Y.; Willis, P. A.; Bronikowski, M. J.; Margrave, J. L.; Smalley, R. E.; Hauge, R. H., Purification and characterization of single-wall carbon nanotubes (SWCNTs) obtained from the gas-phase decomposition of CO (HiPco process). *J. Phys. Chem. B* 2001, *105* (35), 8297-8301
[49] Moon, J. M.; An, K. H.; Lee, Y. H.; Park, Y. S.; Bae, D. J.; Park, G. S., High-yield purification process of singlewalled carbon nanotubes. *J. Phys. Chem. B* 2001, *105* (24), 5677-5681
[50] Vigolo, B.; Herold, C.; Mareche, J. F.; Ghanbaja, J.; Gulas, M.; Le Normand, F.; Almairac, R.; Alvarez, L.; Bantignies, J. L., A comprehensive scenario for commonly used purification procedures of arc-discharge as-produced single-walled carbon nanotubes. *Carbon* 2010, *48* (4), 949-963.

surfactants) repulsion forces. This, particularly for polymeric surfactants, creates a free energy barrier that prevents the SWCNTs from approaching to each other, by shielding the attractive part of the intertube potential.[51] With this approach very stable-in-time suspensions of SWCNTs can be achieved. The intertube forces counteraction leads to a debundling in individual tubes in liquid media, being the effectiveness of such dispersion dependent on the surfactant nature, charge and/or molecular weight.[52] The separation of SWCNTs by surfactant action permits their isolation from colloidal mixtures,[51] hence their purification. This is an additional advantage toward many applications that require individualization as well as purification. Finally, some other less common purification techniques can be found in the literature, i.e. chromatographic separation[53] or magnetic gradient filtration.[54]

The above mentioned approaches are very often combined with centrifugation techniques. The application of the centrifugation allows the bulk purification of SWCNTs when combined with acid treatments[55,56] or surfactant purification.[56] The centrifugation of nitric acid-oxidized SWCNTs aqueous suspensions at a high speed (20000g) causes the partial sedimentation of amorphous carbon and metallic particles, leaving the purified SWCNTs in suspension, due to a different charge of these components as determined by zeta-potential measurements.[55,57,58] The steric and/or electrostatic stabilizations caused by surfactants can be combined with centrifugation

[51] Shvartzman-Cohen, R.; Nativ-Roth, E.; Baskaran, E.; Levi-Kalisman, Y.; Szleifer, I.; Yerushalmi-Rozen, R., Selective dispersion of single-walled carbon nanotubes in the presence of polymers: the role of molecular and colloidal length scales. *J. Am. Chem. Soc.* 2004, *126* (45), 14850-14857.
[52] Moore, V. C.; Strano, M. S.; Haroz, E. H.; Hauge, R. H.; Smalley, R. E.; Schmidt, J.; Talmon, Y., Individually suspended single-walled carbon nanotubes in various surfactants. *Nano Lett.* 2003, *3* (10), 1379-1382.
[53] Niyogi, S.; Hu, H.; Hamon, M. A.; Bhowmik, P.; Zhao, B.; Rozenzhak, S. M.; Chen, J.; Itkis, M. E.; Meier, M. S.; Haddon, R. C., Chromatographic purification of soluble single-walled carbon nanotubes (s-SWCNTs). *J. Am. Chem. Soc.* 2001, *123* (4), 733-734.
[54] Kim, Y. H.; Torrens, O. N.; Kikkawa, J. M.; Abou-Hamad, E.; Goze-Bac, C.; Luzzi, D. E., High-purity diamagnetic single-wall carbon nanotube buckypaper. *Chem. Mater.* 2007, *19* (12), 2982-2986.
[55] Yu, A. P.; Bekyarova, E.; Itkis, M. E.; Fakhrutdinov, D.; Webster, R.; Haddon, R. C., Application of centrifugation to the large-scale purification of electric arc-produced single-walled carbon nanotubes. *J. Am. Chem. Soc.* 2006, *128* (30), 9902-9908.
[56] Anson-Casaos, A.; Gonzalez-Dominguez, J. M.; Martinez, M. T., Separation of single-walled carbon nanotubes from graphite by centrifugation in a surfactant or in polymer solutions. *Carbon* 2010, *48* (10), 2917-2924.
[57] Hu, H.; Yu, A. P.; Kim, E.; Zhao, B.; Itkis, M. E.; Bekyarova, E.; Haddon, R. C., Influence of the zeta potential on the dispersability and purification of single-walled carbon nanotubes. *J. Phys. Chem. B* 2005, *109* (23), 11520-11524.
[58] Yu, A. P.; Su, C. C. L.; Roes, I.; Fan, B.; Haddon, R. C., Gram-Scale Preparation of Surfactant-Free, Carboxylic Acid Groups Functionalized, Individual Single-Walled Carbon Nanotubes in Aqueous Solution. *Langmuir* 2010, *26* (2), 1221-1225.

for the removal not only most of amorphous carbon and metal particles, but also of graphitic impurities.[56] Ultracentrifugation (at several hundred thousand g) in a density-gradient medium has been reported to sort SWCNTs by diameter, chirality and band gap.[59]

There is a general concern about the purity and quality of CNTs, and particularly of SWCNTs, and a proper characterization is necessary. There are several techniques to determine, either qualitatively or quantitatively, the SWCNTs purity.

- XRD is a useful technique to qualitatively assess changes in the SWCNTs states. As mentioned earlier, the different components of a SWCNT raw sample possess a particular diffraction pattern which can be identified by XRD. Graphitic impurities present a sharp peak at $2\theta = 26.5^{\circ}$, graphitic onions exhibit a knee at $2\theta = 25.8^{\circ} - 26^{\circ}$,[54] and metal particles show characteristic lattice peaks depending on the type of metal. Furthermore, the SWCNT bundles have small band signals at $2\theta \sim 10^{\circ}$, 16° and 20° corresponding to the bundles form factor.[37] The elimination of carbonaceous impurities and the SWCNT debundling can be asserted by the reduction or disappearance of their corresponding peaks. This technique is simple and non-destructive, but only provides qualitative information, being a complement for other more powerful techniques.
- Raman spectroscopy is an important technique for the characterization of graphitic and other sp^2-based materials such as SWCNTs.[60] This spectroscopy is an analytical technique that, as XRD, is applied directly to SWCNTs hence it does not require a particular sample preparation and it is non-destructive. This technique allows registering samples in any physical state, even in aqueous media. In a regular SWCNT Raman spectrum (example in Figure 2.2), three well-defined features can be distinguished:[61]
    - In the low frequency range (100-300 cm^{-1}), the radial breathing mode (RMB) bands, where the SWCNT diameter distribution (d_t) is

[59] Arnold, M. S.; Green, A. A.; Hulvat, J. F.; Stupp, S. I.; Hersam, M. C., Sorting carbon nanotubes by electronic structure using density differentiation. *Nat. Nanotechnol.* 2006, *1* (1), 60-65.
[60] Kim, U. J.; Furtado, C. A.; Liu, X. M.; Chen, G. G.; Eklund, P. C., Raman and IR spectroscopy of chemically processed single-walled carbon nanotubes. *J. Am. Chem. Soc.* 2005, *127* (44), 15437-15445.
[61] Dresselhaus, M. S.; Dresselhaus, G.; Jorio, A.; Souza, A. G.; Saito, R., Raman spectroscopy on isolated single wall carbon nanotubes. *Carbon* 2002, *40* (12), 2043-2061.

reflected, following an inverse dependence with the vibrational frequency (ν_{RBM}).[62]

$$\nu_{RBM} = \frac{A}{d_t} + B$$

- In the high frequency range (1500-2600 cm^{-1}) a characteristic resonant behavior of graphitic tangential modes, ascribed to the electronic structure of CNTs (G-band) appears. The G-band profile reveals the semiconductor or metallic character of the SWCNTs.
- In the intermediate range of frequencies (600-1100 and 2600-3000 cm^{-1}), where minor intensity bands can be detected, such as the disorder-induced (D) band, at ~1350 cm^{-1}, and its overtone (D* or G' band) at ~2700 cm^{-1}, providing information of structural defects.

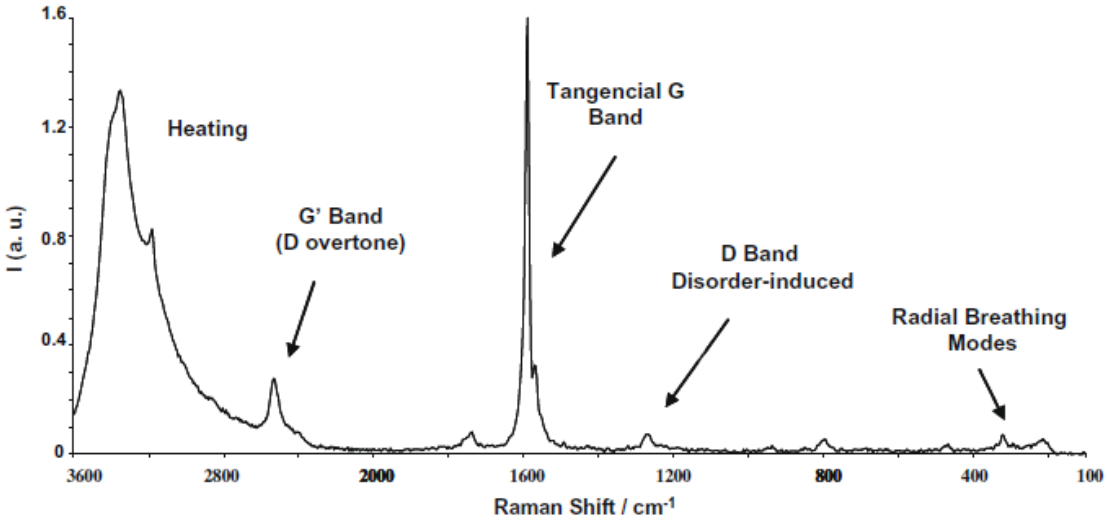

Figure 2.3. Main Raman features of a typical SWCNT sample.

These Raman features are widely used for the characterization of SWCNTs. The ratio between the D-band and the G-band is usually taken as a measure of the proportion between the graphitic and other disordered (or non-graphitized) carbon forms. As the D-band is very sensitive to the disruption of the electronic structure in the SWCNT sidewalls, a G/D ratio decrease is often assumed as an indication of covalent functionalization of SWCNTs.[63]

[62] Bachilo, S. M.; Strano, M. S.; Kittrell, C.; Hauge, R. H.; Smalley, R. E.; Weisman, R. B., Structure-assigned optical spectra of single-walled carbon nanotubes. *Science* 2002, *298* (5602), 2361-2366.
[63] Graupner, R., Raman spectroscopy of covalently functionalized single-wall carbon nanotubes. *J. Raman Spectrosc.* 2007, *38* (6), 673-683.

- Other techniques can be employed to assess the CNT purity and quality. The metal catalysts can be quantitatively determined by induced coupled plasma – optical emission spectroscopy (ICP – OES). As a representative example, after digesting the sample using an alkaline fusion with sodium peroxide and subsequent leaching to an aqueous solution, Ni and Y can be determined with ICP – OES with high accuracy.[64-66] By thermogravimetric analysis (TGA) the metal content can be estimated from the oxidized solid residue after an experiment in air atmosphere.[56] The exfoliation of SWCNT bundles can be followed by ultraviolet-visible (UV-Vis) spectroscopy.[67] Scanning (SEM) and electron (TEM) microscopies can offer images of small areas of the CNT sample, being able to show the real state of CNTs. The energy-dispersive X-ray spectroscopy (EDX) can be coupled to SEM or TEM to provide the semi-quantitative chemical composition of certain areas in a CNT sample.
- Fluorescence spectroscopy is also a useful tool to evaluate SWCNT state, because they exhibit fluorescent activity in the near infra-red (NIR) region. This feature is exclusive for individual SWCNTs, since in a bundle no emission occurs for two main reasons:[68] 1) resonant energy transference between a semiconducting SWCNT to another of lower bandgap (or to metallic ones), 2) orthogonal dispersion of rope-like distributions that induce a self-quenching of the fluorescence. For these reasons, the fluorescent emission is particularly useful for discriminating different SWCNT chiralities and conductive behaviors and to assess the individualization of SWCNTs. Chemical reactions that induce significant changes in the

[64] Montesa, I.; Munoz, E.; Benito, A. M.; Maser, W. K.; Martinez, M. T., FTIR and thermogravimetric analysis of biotin-functionalized single-walled carbon nanotubes. *J. Nanosci. Nanotechnol.* 2007, *7* (10), 3473-3476.
[65] Gonzalez, M.; Tort, N.; Benito, A. M.; Maser, W.; Marco, M. P.; Martinez, M. T., Non-Specific Adsorption of Streptavidin on Single Walled Carbon Nanotubes. *J. Nanosci. Nanotechnol.* 2009, *9* (10), 6149-6156.
[66] Gonzalez-Dominguez, J. M.; Gonzalez, M.; Anson-Casaos, A.; Diez-Pascual, A. M.; Gomez, M. A.; Martinez, M. T., Effect of Various Aminated Single-Walled Carbon Nanotubes on the Epoxy Cross-Linking Reactions. *J. Phys. Chem. C* 2011, *115* (15), 7238-7248.
[67] Grossiord, N.; Regev, O.; Loos, J.; Meuldijk, J.; Koning, C. E., Time-dependent study of the exfoliation process of carbon nanotubes in aqueous dispersions by using UV-visible spectroscopy. *Anal. Chem.* 2005, *77* (16), 5135-5139.
[68] Graff, R. A.; Swanson, J. P.; Barone, P. W.; Baik, S.; Heller, D. A.; Strano, M. S., Achieving individual-nanotube dispersion at high loading in single-walled carbon nanotube composites. *Adv. Mater.* 2005, *17* (8), 980

electronic structure of SWCNTs (such as the diazonium reaction) can be monitored by this technique.[69]

- In the evaluation of SWCNT purity, the solution-phase NIR spectroscopy stands out among all the aforementioned.[70] SWCNTs exhibit characteristic absorption bands in the NIR-Vis region which are dependent on their electronic characteristics.[71] The most intense spectral features in this region are the S_{11}, S_{22}, and M_{11} transition bands of semiconducting (S) or metallic (M) SWNCTs (in the range of ~ 300–1300 nm). This approach proposes the purity quantification through the evaluation of these bands, which belong exclusively to SWCNTs. This reliably assesses the carbonaceous purity of bulk SWCNT samples by only taking a representative portion, dispersing it in a liquid medium such as N,N'-dimethylformamide (DMF) [72,73] or aqueous solutions of common surfactants,[52,56,74] and registering the absorption spectra in the NIR region (Figure 2.3).

  The purity index (PI) can be calculated as shown in Figure 2.4, where A_t is the total area under the S_{22} band transition (typically in the range of 7750 and 11750 cm^{-1}) and A_b represents the strength of resonant transitions in a fixed diameter distribution of SWCNTs and is proportional to the semiconducting SWCNT mass. A_t is a background signal that has been attributed to near-ultraviolet resonances of carbon forms.[75] It is influenced by several factors, including absorption of carbonaceous impurities and light scattering of turbid samples. Recently, an effect of sonication, chemical functionalization

[69] Doyle, C. D.; Rocha, J. D. R.; Weisman, R. B.; Tour, J. M., Structure-dependent reactivity of semiconducting single-walled carbon nanotubes with benzenediazonium salts. *J. Am. Chem. Soc.* 2008, *130* (21), 6795-6800.
[70] Itkis, M. E.; Perea, D. E.; Jung, R.; Niyogi, S.; Haddon, R. C., Comparison of analytical techniques for purity evaluation of single-walled carbon nanotubes. *J. Am. Chem. Soc.* 2005, *127* (10), 3439-3448.
[71] Saito, R.; Dresselhaus, G.; Dresselhaus, M. S., Trigonal warping effect of carbon nanotubes. *Phys. Rev. B* 2000, *61* (4), 2981-2990.
[72] Itkis, M. E.; Perea, D. E.; Niyogi, S.; Rickard, S. M.; Hamon, M. A.; Zhao, B.; Haddon, R. C., Purity evaluation of as-prepared single-walled carbon nanotube soot by use of solution-phase near-IR spectroscopy. *Nano Lett.* 2003, *3* (3), 309-314
[73] Zhao, B.; Itkis, M. E.; Niyogi, S.; Hu, H.; Perea, D. E.; Haddon, R. C., Extinction coefficients and purity of single-walled carbon nanotubes. *J. Nanosci. Nanotechnol.* 2004, *4* (8), 995-1004.
[74] Tan, Y. Q.; Resasco, D. E., Dispersion of single-walled carbon nanotubes of narrow diameter distribution. *J. Phys. Chem. B* 2005, *109* (30), 14454-14460.
[75] Kataura, H.; Kumazawa, Y.; Maniwa, Y.; Umezu, I.; Suzuki, S.; Ohtsuka, Y.; Achiba, Y., Optical properties of single-wall carbon nanotubes. *Synt. Met.* 1999, *103* (1-3), 2555-2558.

and dispersion state of SWCNTs on the background signal has been reported.[76]

As proposed by Itkis and co-workers,[72] the PI is a measure of the carbonaceous purity in a raw SWCNT sample since it increases as the carbon impurities content decreases. If these determinations are performed at low SWCNT concentrations, light scattering contributions can be avoided.

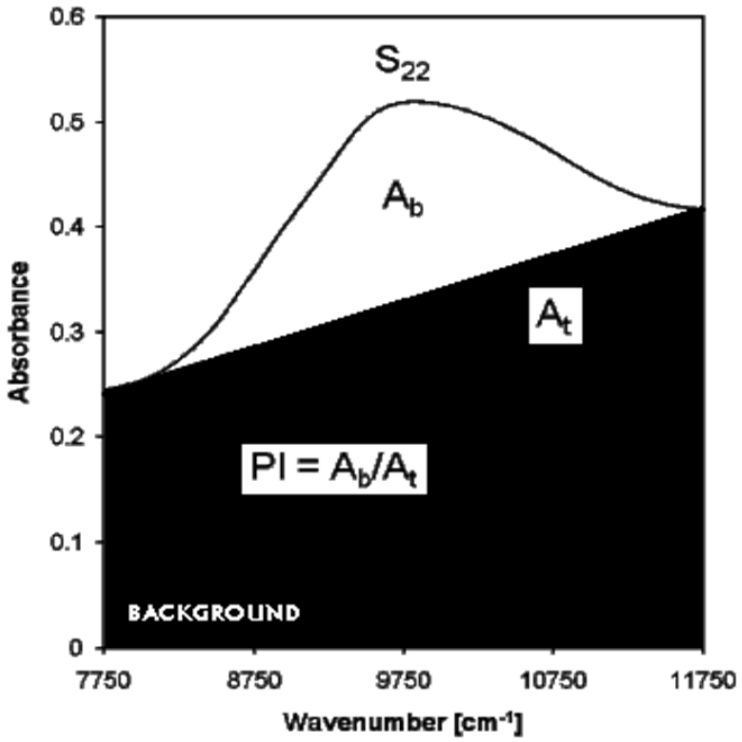

Figure 2.4. Example of a NIR absorption spectrum in an arc discharge SWCNT sample

2.1.3. Covalent functionalization of SWCNTs

One of the most interesting CNTs features is their ability to undergo a very large variety of chemical reactions which can attach almost any desirable moiety. Over the last years, CNTs have been treated as nanoscale reagents in a wide variety of different chemical processes, enabled by the particular reactivity of their sp^2-based graphene walls. CNTs chemical functionalization has been extensively analyzed in many review

[76] Naumov, A. V.; Ghosh, S.; Tsyboulski, D. A.; Bachilo, S. M.; Weisman, R. B., Analyzing absorption backgrounds in single-walled carbon nanotube spectra. *ACS Nano* 2011, *5* (3), 1639-1648.

papers,[16-20,77,78] and represents an interesting strategy toward specific applications that require chemical modifications and/or the purification of pristine tubes. Chemical covalent functionalization is believed to counteract the intertube stacking forces and to lead to debundling. This effect may be caused by the intercalation of the attached moieties.[17]

The common oxidative purification treatments represent a primary path toward covalent modification of SWCNTs. As a consequence of a liquid, gas or plasma phase oxidation, different oxygen groups are attached to the SWCNTs structure,[39,42,79,80] preferentially on (but not limited to) tips and sidewall defects. The chemical nature of the attached oxygen groups seems to depend on the kind of oxidative treatment applied to SWCNTs. Wet oxidation methods, such as those related to acid treatments differ from gas-phase methods, such as thermal treatments in air atmosphere.[81] As a matter of fact, nitric acid treatment provides a wide variety of oxygen surface groups with very different thermal stability,[82] including carboxylic, phenol and carbonyl-based moieties.[83] Besides, the nitric acid treatment induces a certain degree of structural damage to SWCNTs coupled to the oxygen functionalization and the intercalation of HNO_3 molecules within bundles.[39,40] The mixture of sulphuric and nitric acids seems to provide a more specific oxygen functionalization toward carboxylic groups,[41,84] and it

[77] Hirsch, A., Functionalization of single-walled carbon nanotubes. *Angew. Chem. Int. Ed.* 2002, *41* (11), 1853-1859.
[78] Tasis, D.; Tagmatarchis, N.; Bianco, A.; Prato, M., Chemistry of carbon nanotubes. *Chem. Rev.* 2006, *106* (3), 1105-1136.
[79] Shaffer, M. S. P.; Fan, X.; Windle, A. H., Dispersion and packing of carbon nanotubes. *Carbon* 1998, *36* (11), 1603-1612.
[80] Ago, H.; Kugler, T.; Cacialli, F.; Salaneck, W. R.; Shaffer, M. S. P.; Windle, A. H.; Friend, R. H., Work functions and surface functional groups of multiwall carbon nanotubes. *J. Phys. Chem. B* 1999, *103* (38), 8116-8121.
[81] Gonalves, A. G.; Figueiredo, J. L.; Órfão, J. J. M.; Pereira, M. F. R., Influence of the surface chemistry of multi-walled carbon nanotubes on their activity as ozonation catalysts. *Carbon* 2010, *48* (15), 4369-4381.
[82] Ansón-Casaos, A.; González, M.; González-Domínguez, J. M.; Martínez, M. T.; Influence of air oxidation in the surfactant-assisted purification of single-walled carbon nanotubes, *Langmuir* 2011, *27* (11), 7192-7198.
[83] Gorgulho, H. F.; Mesquita, J. P.; Gonçalves, F.; Pereira, M. F. R.; Figueiredo, J. L., Characterization of the surface chemistry of carbon materials by potentiometric titrations and temperature-programmed desorption. *Carbon* 2008, *46* (12), 1544-1555.
[84] Cañete-Rosales, P.; Alvarez-Lueje, A.; Bollo, S.; Gonzalez, M.; Anson-Casaos, A.; Martinez, M. T., Influence of size and oxidative treatments of multi-walled carbon nanotubes on their electrocatalytic properties, *Electrochim. Acta* 2011*(accepted)*.

can even react preferably with metallic SWCNTs of small diameter.[85] On the other hand, air oxidation induces the attachment of oxygen functionalities with a defined thermal stability, mainly lactone and anhydride groups, and minor carbonyl-based moieties, such as quinones.[82] All these oxygen functional groups enhance the SWCNT dispersibility in water, lead to stable polar suspensions of SWCNTs,[58] and can be starting points for further derivatization.

Within the vast field of CNT chemical functionalization, several routes stand out for their feasibility and versatile applications. In this thesis, specific functionalizations addressed to the integration in two different polymers have been carried out. Among them, several amination approaches have been selected and carried out in order to prepare SWCNT reactive fillers for their integration into epoxy. The most commonly employed amination route consists of the nucleophilic attack to the carboxylic groups present in CNTs after an oxidation treatment, to produce an ester or amide. This has been our first approach to obtain covalently aminated SWCNTs (SWCNT-oxa). After a proper activation of carboxylic groups and the reaction with an amine-terminated nucleophile, the amine functional group mainly sets on CNT tips, defects and on the edges of shortened open-ended CNTs.[78]

Other "less-classical" approaches take advantage of the electronic density on CNT walls to make them react *via* nucleophilic, electrophilic, cyclo-, or radical additions. A good example of radical addition is represented by the thermal decomposition of organic peroxides on SWCNTs surface.[86-88] The reductive intercalation of alkaline ions in polar aprotic solvents, which implies the negative charging of SWCNT sidewalls, has been used for further derivatizations with alkyl radicals. After the pioneer works by Billups et al.[89] and Pénicaud et al.,[90] a more recent

[85] Yang, C. M.; Park, J. S.; An, K. H.; Lim, S. C.; Seo, K.; Kim, B.; Park, K. A.; Han, S.; Park, C. Y.; Lee, Y. H., Selective removal of metallic single-walled carbon nanotubes with small diameters by using nitric and sulfuric acids. *J. Phys. Chem. B* 2005, *109* (41), 19242-19248.
[86] Peng, H.; Reverdy, P.; Khabashesku, V. N.; Margrave, J. L., Sidewall functionalization of single-walled carbon nanotubes with organic peroxides. *Chem. Commun.* 2003, *9* (3), 362-363.
[87] Peng, H.; Alemany, L. B.; Margrave, J. L.; Khabashesku, V. N., Sidewall Carboxylic Acid Functionalization of Single-Walled Carbon Nanotubes. *J. Am. Chem. Soc.* 2003, *125* (49), 15174-15182
[88] Khabashesku, V. N.; Billups, W. E.; Margrave, J. L., Fluorination of single-wall carbon nanotubes and subsequent derivatization reactions. *Acc. Chem. Res.* 2002, *35* (12), 1087-1095.
[89] Liang, F.; Sadana, A. K.; Peera, A.; Chattopadhyay, J.; Gu, Z.; Hauge, R. H.; Billups, W. E., A convenient route to functionalized carbon nanotubes. *Nano Lett.* 2004, *4* (7), 1257-1260.

article proposed the functionalization of the reduced SWCNTs with diacyl peroxides at room temperature as a simple means to derivatizate SWCNTs.[91] This approach has been carried out as the second amination route in the present thesis (SWCNT-nfp).

Prof. Maurizio Prato and his research group developed the 1,3-dipolar cycloaddition of azomethine ylides onto CNT sidewalls as a way to achieve organic functionalization and to greatly increase the CNT solubility and processability for many applications.[92] The fourth functionalization approach is an aminoacid functionalization through dipolar cycloaddition (SWCNT-dca).

In 2001, J. M. Tour and co-workers developed the derivatization of SWCNTs with *in situ* generated aryl diazonium salts,[93] a versatile and easy way to functionalize nanotubes with a large variety of chemical grafted moieties. This methodology has also been employed in the present thesis to functionalize SWCNTs with terminal primary amines from tailored matrix-based moieties (SW-DDS, SW-AD).

2.2. Experimental section

2.2.1. Materials and reagents

The SWCNTs used here were produced at the Instituto de Carboquimica (ICB-CSIC), Zaragoza, by the arc discharge method (100A, 20V), using a Ni/Y mixture as catalysts under 660 mb of helium.[22,94] For the preparation of functionalized SWCNTs with epoxy matrix-based moieties, laser-grown SWCNTs were also employed. These were prepared at the Steacie Institute for Molecular Sciences (SIMS-NRC), Canada, using an approach to the two-laser synthesis method.[33]

All other chemicals were purchased from Sigma-Aldrich and used as received without further treatment. Ultrasounds bath (45 kHz Branson 3510) and/or ultrasonic tip

[90] Pénicaud, A.; Poulin, P.; Derré, A.; Anglaret, E.; Petit, P., Spontaneous dissolution of a single-wall carbon nanotube salt. *J. Am. Chem. Soc.* 2005, *127* (1), 8-9.
[91] Martinez-Rubi, Y.; Guan, J.; Lin, S.; Scriver, C.; Sturgeon, R. E.; Simard, B., Rapid and controllable covalent functionalization of single-walled carbon nanotubes at room temperature. *Chem. Commun.* 2007, (48), 5146-5148.
[92] Tagmatarchis, N.; Prato, M., Functionalization of carbon nanotubes via the 1,3-dipolar cycloadditions. *J. Mater. Chem.* 2004, *14* (4), 437-439.
[93] Bahr, J. L.; Tour, J. M., Highly functionalized carbon nanotubes using in situ generated diazonium compounds. *Chem. Mater.* 2001, *13* (11), 3823-3824.
[94] Benito, A. M.; Maser, W. K.; Martinez, M. T., Carbon nanotubes: from production to functional composites. *Int. J. Nanotechnol.* 2005, *2* (1-2), 71-89.

(Hielscher DRH-P400S; 400W maximum power; 24 kHz maximum frequency at 60% amplitude and 50% cycle time) were employed for sonication unless otherwise stated.

2.2.2. Experimental functionalization procedures

2.2.2.1. Route 1: Functionalization *via* acid treatment + amide formation (SWCNT-oxa)

Oxidative acid treatment

Around 0.5g of as-grown SWCNTs and 150 mL of a 1.5M HNO_3 solution were placed in a round bottom flask. The system was heated up to the boiling temperature and was refluxed for 2h under constant magnetic stirring. Subsequently, the reaction medium was poured into several centrifugation vials and centrifuged at 3500 rpm for 15 min. The supernatant liquid was decanted off and the vials were refilled with aqueous HCl (pH = 1-2), bath sonicated for 30 min and centrifuged again under identical conditions. The supernatant was then decanted off and the SWCNTs were swept with deionized water, vacuum - filtered through a 1.2 μm polycarbonate membrane, and thoroughly rinsed with deionized water until the pH of the falling filtrate was neutral. As-produced oxidized SWCNTs were dried at 60ºC in a vacuum oven for 24h. These nanotubes have a high content in oxygen groups, of which carboxylic groups are desired for the following step.

Activation of carboxylated SWCNTs

200 mg of nitric acid-treated SWCNTs were bath sonicated in ~10 mL of DMF inside a round bottom flask and then 40 mL of thionyl chloride were carefully added. The flask was coupled to a reflux, and the system was kept at 120ºC for 24h under a constant magnetic stirring. Afterwards, the product was vacuum filtered through a 0.1 μm pore size polytetraflouroethylene (PTFE) membrane and washed with anhydrous tetrahydrofuran (THF). Finally it was dried under vacuum at room temperature for 2h.

Amidation of activated SWCNTs

225 mg of freshly activated SWCNTs were placed in a round bottom schlenk and bath sonicated in 100 mL of anhydrous DMF for 15 min. The suspended SWCNTs were magnetically stirred under argon atmosphere at 90ºC for about 1h. Then, ~3g of N-Boc-1,6-diaminohexane were added by injection through a septum cap using a purged syringe. The system was allowed to react under unchanged conditions for 4 days. The product was vacuum-filtrated through a 0.1 μm pore size PTFE membrane and copiously washed with methanol. Drying was carried out at 60ºC in a vacuum oven.

2.2.2.2. Deprotection of the Boc groups

Amine-SWCNTs functionalized through either the acid followed by the acyl chloride route or the 1,3-dipolar cycloaddition route were obtained as N-Boc-protected products and required the detachment of the protective group in order to render the free amine. Around 100 mg of amino-Boc SWCNTs were bath sonicated for 15 min in 25 mL of an HCl / 1,4-dioxane mixture (4% v/v HCl) and stirred at room temperature for 2h. The reaction product was vacuum filtered through a 0.1 μm pore size PTFE membrane, thoroughly washed with 1,4-dioxane and diethyl ether and vacuum dried at room temperature overnight. The deprotected SWCNTs were then sonicated for 15 min in 100mL of a diluted NaOH solution and stirred at room temperature for 24h to neutralize the ammonium salt and yield the free primary amine groups. The aqueous suspension was filtered through a 1.2 μm pore size polycarbonate membrane, rinsed with deionized water (until the falling liquid pH was neutral) and finally dried at room temperature under vacuum overnight.

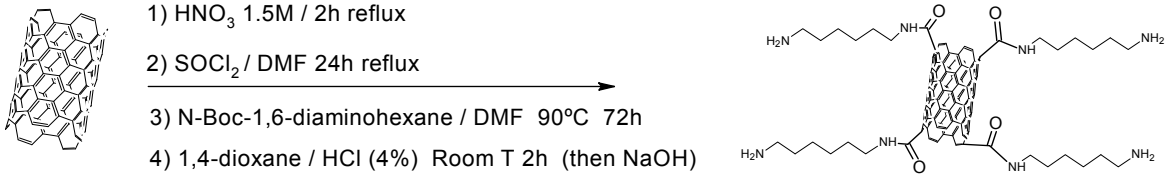

Figure 2.5. Reaction scheme for the first functionalization route

2.2.2.3. Route 2: Functionalization *via* alkaline reduction + diacyl peroxide (SWCNT-nfp)

Synthesis of the N-Fmoc-6-aminohexanoyl peroxide (NFP)

The synthesis of this organic peroxide was undertaken through reaction of hydrogen peroxide with the acyl chloride derivative of the N-Fmoc-6-aminohexanoic acid. Following the experimental protocol described by Martinez-Rubi et al.,[91] a CH_2Cl_2 solution of N-Fmoc-6-aminohexanoic acid (1.76g) was first acylated with $SOCl_2$ (3.6mL) and then precipitated in hexane. The acyl chloride (1g) was subsequently dissolved in a chloroform/diethyl ether mixture at 0ºC and a simultaneous dropwise addition of hydrogen peroxide (206 μL, 30% concentration) and pyridine (260 μL) was made. The NFP precipitate was dissolved in chloroform, purified by liquid-phase extraction with cold water, and then the pure product was precipitated from the organic phase by addition of diethyl ether. The successful synthesis of this peroxide was confirmed through ^{1}H and ^{13}C nuclear magnetic resonance (NMR) and mass spectrometry (MS), obtaining the expected signals (data not shown), which were consistent with the literature source.

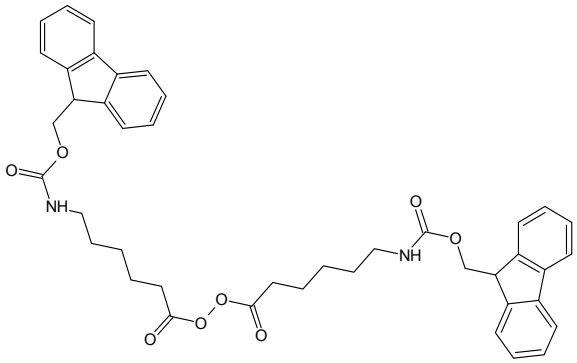

Figure 2.6. Chemical structure of the NFP organic peroxide

Reduction of SWCNTs with sodium naphthalide radical ion

400 mg of arc as-grown SWCNTs were bath-sonicated for 30 min in 30 mL of anhydrous THF inside a round-bottom schlenk flask, under an Argon (Ar) atmosphere achieved by connection to a manifold with constant gas flow. After sonication, a fine

suspension of the SWCNTs was observed, which was kept under argon at a constant magnetic stirring. In parallel, sodium naphthalide radical ion was prepared by bath-sonicating around 80 mg of small sodium pieces in a naphthalene-THF solution (7 mg/mL, anhydrous THF) for 15-20 min in Ar atmosphere. A dark green colour appeared indicating the successful radical ion synthesis (Figure 2.7). The sodium-naphthalide ion was added to the SWCNT-THF suspension with the aid of a glass syringe previously purged with Ar. Care must be taken in order to prevent the green solution contacting the outer air atmosphere; otherwise the radical ion is deactivated hence loosing its colour. About 70mL of the radical ion solution were slowly injected into the SWCNT-THF suspension, through a septum cap, until a persistent green colour was observed in the medium. The mixture was bath-sonicated for 1h and left overnight at room temperature under Ar and magnetic stirring. It was then placed in open air and poured into centrifuge vials. Centrifugation was applied at 8000 rpm for 30min, and then the supernatants were decanted and discarded. The vials were filled with wet THF, sonicated in bath for 30min and centrifuged under identical conditions. Again, supernatants were decanted and discarded. The process was subsequently repeated according to the following sequence of solvents: methanol (2 times), distilled water, HCl 5% v/v, and distilled water. SWCNTs were collected and filtered through a 0.1 μm pore size polytetraflouroethylene (PTFE) membrane, washed with isopropanol, methanol, and acetone, and finally dried under vacuum at 60ºC.

Reaction of reduced SWCNTs with NFP

150 mg of the as-processed SWCNTs were taken and subjected to an identical reduction procedure as described in the previous section, with an identical volume of the radical ion green solution. After the overnight reduction, about 1g of NFP was added to the mixture and a sudden loss of the green colour was observed. After a few hours of magnetic stirring at room temperature the reaction medium was removed from the schlenk and subjected to the same centrifugation sequence, as described above.

Deprotection of the Fmoc group

In a typical deprotection experiment, 100mg of NFP-functionalized SWCNTs were submerged in 10mL of a DMF/piperidine mixture (80:20 v/v) and bath-sonicated for a

few minutes. Then, magnetic stirring was applied for 1h at room temperature. The medium was filtered through 0.1 μm pore size PTFE membrane and washed with N,N'-dimethylformamide (DMF) until the filtrate fell colourless. Finally, it was rinsed with diethyl ether and dried under vacuum at room temperature.

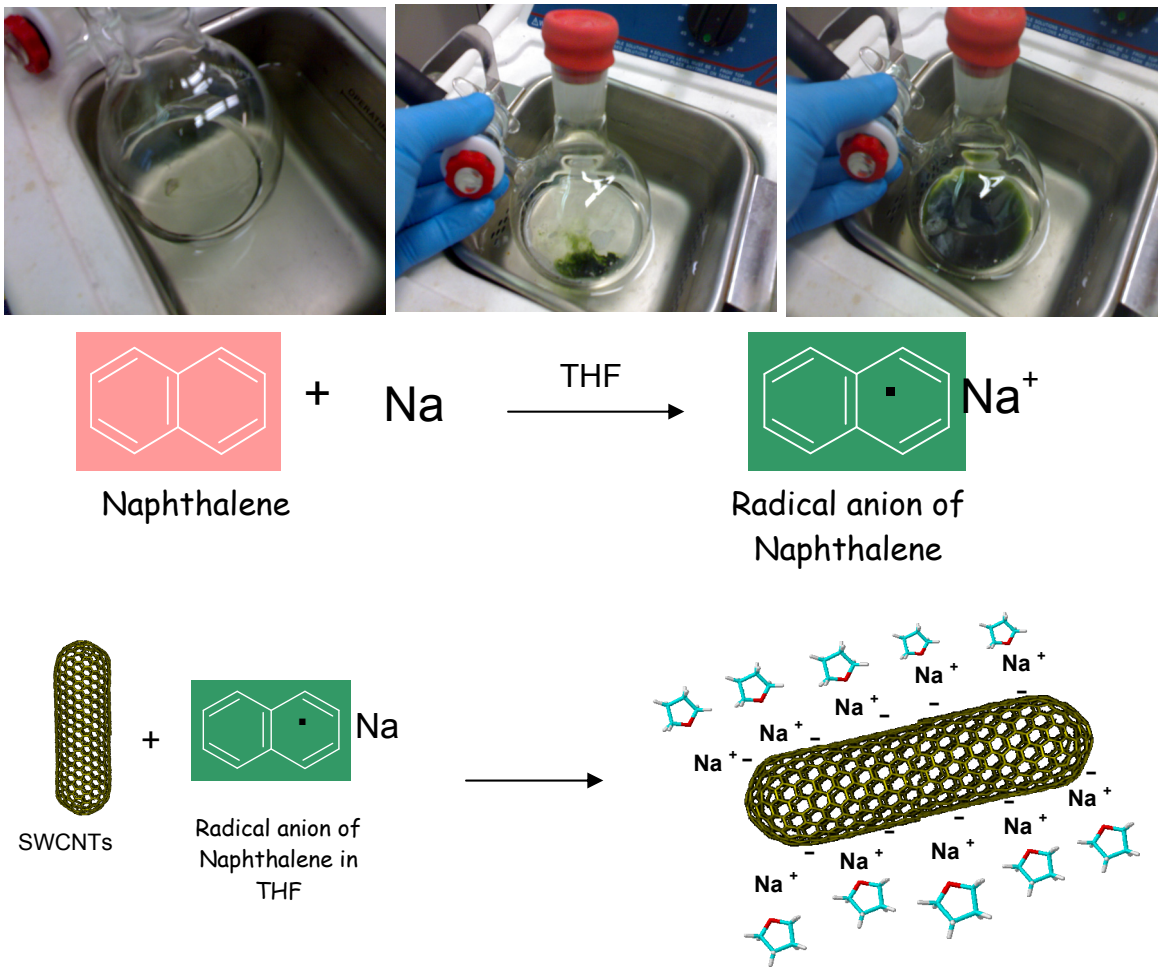

Figure 2.7. Sequential images of the preparation of the THF-radical ion in THF (above), scheme of the radical ion formation (centre), and scheme of SWCNT reduction (below).

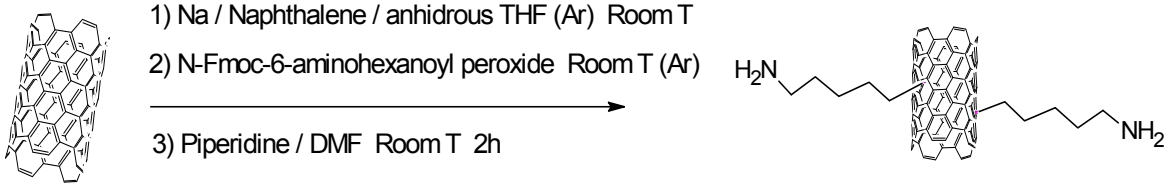

Figure 2.8. Reaction scheme for the second functionalization route

2.2.2.4. Route 3: Functionalization *via* the *1,3*- dipolar cycloaddition of azomethine ylides (SWCNT-dca)

Synthesis of the amine-terminated α-aminoacid

The synthesis of the N-Boc-protected α-aminoacid, N-Boc-ethyleneglycol-bis(2-aminoethylether)-N'-acetic acid, was carried out through the synthetic route proposed by Kordatos et al.[95] in which a commercial symmetric diamine, ethylene glycol-bis(2-aminoethylether), is monoprotected with Boc-anhydride, then alkylated with Benzyl-2-bromoacetate, and finally reduced with hydrogen.

Reaction between the α-aminoacid, an aldehyde and the SWCNTs

The 1,3-dipolar cycloaddition reaction was performed with the aforemementioned α-aminoacid and paraformaldehyde. In a typical experiment, 100mg of pristine arc SWCNTs were mixed with 100mL of DMF inside a 200 mL round-bottom flask and sonicated in an ultrasound bath (Bransonic MTH2510, 42 kHz, 130W) for about 30 min. Subsequently, 150mg of the α-aminoacid and 150mg of paraformaldehyde were added to the resuting suspensión. After two minutes of magnetic stirring at room temperature, the mixture was bath sonicated for 30 min. Then the flask was set in an oil bath at 115ºC and refluxed under a constant magnetic stirring for 4 days. During the course of the reaction, 3 more additions of the same amounts of the α-aminoacid and paraformaldehyde were made in periods of approximately 24h. These additions were carried out after cooling down to room temperature and were followed by 30 min of bath sonication. The reaction medium was vacuum-filtered (0.1 μm pore size PTFE membrane) after a period of 4 days. The solid filtrated material was washed by successive submersions in 100mL of solvents, bath sonication and filtration in the same filter type. The solvent washing sequence was: DMF (4 times) and methanol (2 times). After the last methanol filtration the sample was rinsed with diethyl ether (2 x 25mL) in the filtration equipment. The functionalized material was dried overnight under vacuum

[95] Kordatos, K.; Da Ros, T.; Bosi, S.; Vazquez, E.; Bergamin, M.; Cusan, C.; Pellarini, F.; Tomberli, V.; Baiti, B.; Pantarotto, D.; Georgakilas, V.; Spalluto, G.; Prato, M., Novel versatile fullerene synthons. *J. Org. Chem.* 2001, *66* (14), 4915-4920.

at room temperature. The N-Boc-protected derivative was subjected to the Boc group cleavage, following the experimental protocol described in section 2.2.2.2.

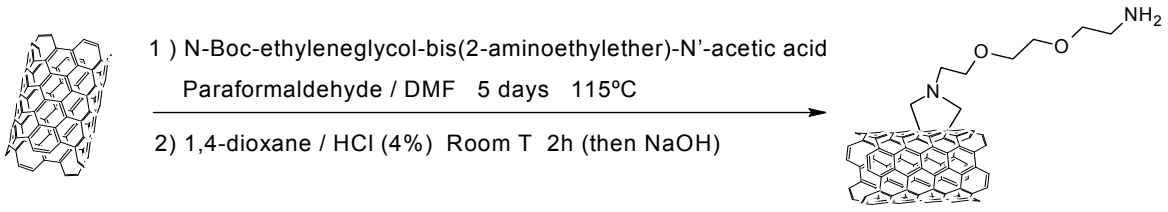

Figure 2.9. Reaction scheme for the fourth functionalization route

2.2.2.5. Route 4: Functionalization *via in situ* diazonium compounds

This specific route was carried out with different purposes. On the one hand, the functionalization of SWCNTs with terminal amines was pursued to introduce terminal amines as in previous routes. The use of this reaction was observed to be especially useful in the processing of SWCNTs to buckypapers with covalent functionalization.[24] On the other hand, the functionalization of SWCNTs with matrix-based moieties was also addressed using this functionalization strategy.

Preparation of functionalized SWCNTs with terminal amines (SWCNT-dba)

100mg of as-grown SWCNTs were bath sonicated in 25mL of DMF for 1h and then tip sonicated for 30 min (60% amplitude 0.5 cycle time). Separately, 1.3 mL of 4-amino benzylamine (10 mmol) were dissolved into 25mL of acetonitrile and bubbled with Ar for a few minutes. Both liquids were blended in a glass vial and kept at 60ºC and constant magnetic stirring. A small slit was left in the vial seal to avoid overpressure. After stabilizing the system temperature, 1mL of isoamyl nitrite was added and it was left overnight at 60ºC with constant stirring. The product was vacuum-filtered through a PTFE 0.1 μm pore size membrane and washed with DMF until the filtrate fell colourless. The functionalized SWCNTs were rinsed with diethyl ether and dried under vacuum at room temperature.

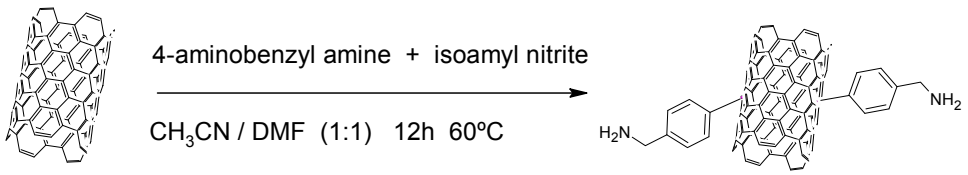

Figure 2.10. Reaction scheme for the third functionalization route applied to the functionalization of arc SWCNTs.

Functionalization of SWCNTs with matrix-based moieties via the diazonium route

The diazonium route was used to functionalize both arc and laser SWCNTs with DDS and a TGAP/DDS-derived pre-synthesised ligand.[96] In order to apply the diazonium route with matrix-based moieties a trifunctional epoxy precursor, triglycidyl p-aminophenol (TGAP), and the curing agent 4,4'-diaminodiphenylsulfone (DDS), were kindly supplied by Hunstman company and used as received for the derivatization of arc and laser SWCNTs. Their respective chemical structures are shown below.

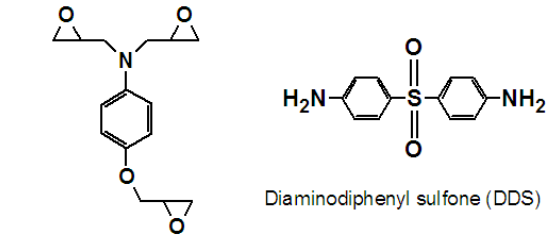

Figure 2.11. Chemical structures of TGAP and DDS molecules

SWCNT functionalization with the curing agent (SW-DDS): Looking for SWCNT functionalization with moieties having chemical affinity for TGAP/DDS systems, DDS was used as the arylamine for the *in situ* generation of the diazonium salt. In a typical experiment, 100 mg of either arc (A) or laser (L) as-grown SWCNT (8.3 mmol C) were suspended in 75 mL of DMF with the aid of a sonication bath for 1 h and an ultrasonic probe for 30min. Separately, 2.4 g of DDS (10 mmol) was slowly dissolved in 25 mL of

[96] Martinez-Rubi, Y.; González-Domínguez, J. M.; Ansón-Casaos, A.; Kingston, C.; Martínez, M. T.; Simard, B.; Tailored SWCNT functionalization optimized for compatibility with epoxy matrices, *Nanotechnology (submitted)*.

acetonitrile and degassed with argon for 5 minutes. The SWCNT suspension and the arylamine solution were mixed in a vial under constant magnetic stirring, keeping the temperature at 60 ºC. Then, 1 mL of isoamyl nitrite (7.4 mmol) was added to the mixture and the vial was sealed, leaving a small slit to prevent overpressure due to nitrogen evolution. The reaction was kept at 60 ºC overnight. The product was vacuum filtered and washed with DMF until the liquid filtrate was colorless, and rinsed with anhydrous diethyl ether to remove DMF.

SWCNT functionalization with an amine-terminated derivative via the diazonium reaction (SW-AD): An amine-terminated derivative (AD) based on the native structure of the TGAP/DDS epoxy matrix was synthesised (Figure 2.12) and used for functionalization of SWCNTs *via* the diazonium reaction. The same procedure used for the synthesis of SW-DDS samples was followed for this reaction, with either arc (A) or laser (L) as-grown SWCNTs. In this case 500 mg of the arylamine AD dissolved in 25 mL of DMF and 200 μL of isoamyl nitrite were used to functionalize 100 mg of SWCNT

Synthesis of the TGAP-DDS derivative (AD): In order to synthesize an oligomer containing free primary amine groups (AD), DDS and TGAP were mixed following a procedure similar to the curing protocol of this epoxy resin but using an excess of DDS. 1 equivalent of epoxide (TGAP) and 5 equivalents of NH_2 (DDS) were mixed at 100ºC under magnetic stirring while the temperature was increased to 150ºC at a rate of 2 ºC/min. After 40 min at 150ºC the mixture gelified and the transparent dark-yellow solid was ground in an agate mortar. Thin layer chromatography (TLC) of the solid dissolved in DMF indicated that all the TGAP had been consumed. The presence of free DDS was also detected, which was extracted with methanol through several washing cycles. The final product, AD (Figure 2.12), a pale-yellow powder, was dried overnight under vacuum at room temperature and then characterized.

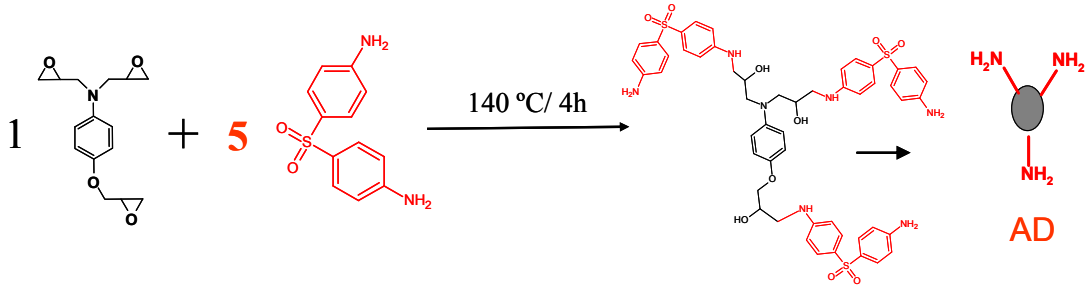

Figure 2.12. Reaction scheme for the preparation of the AD molecule

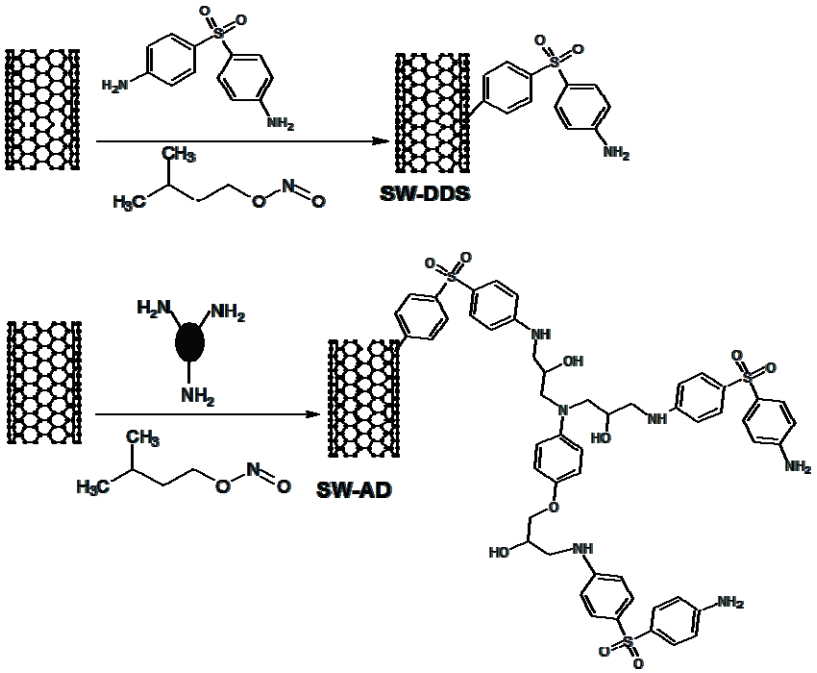

Figure 2.13. Reaction schemes for the functionalization of arc SWCNTs (A-SW) or laser SWCNTs (L-SW) with the curing agent DDS (top) and the AD derivative (bottom)

Synthesis of epoxide-functionalized SWCNTs (SW-DDS-ED): SWCNTs functionalized with DDS molecules were further employed to perform a grafting reaction with another ligand based on the TGAP/DDS native structure. In this case, the synthesised derivative possessed terminal epoxide groups, and DDS amines were used as the grafting points to the SWCNT surface. In a typical experiment, 100 mg of A-SW-DDS or L-SW-DDS (Figure 2.13) were suspended in 60 mL of DMF bath-sonicated for 30 min and tip-sonicated for 15 min. Then the previously synthesized ED derivative (Figure 2.14) dissolved in 20 mL of DMF was added and the mixture refluxed at 130 °C with magnetic stirring. After refluxing for 5 hours the product was precipitated in methanol, vacuum filtered and washed with DMF and anhydrous diethyl ether.

Synthesis of the DDS-TGAP derivative (ED): In order to synthesize an oligomer containing free epoxide groups, DDS and TGAP were mixed together in a ratio of 1:1.5 of amine to epoxide. In a typical experiment 5g of TGAP and 2g of DDS were mixed with magnetic stirring at 100ºC until DDS was completely dissolved and the mixture was kept at 140ºC for 3h. Before cooling to room temperature, 20 mL of DMF were added to the viscous mixture to dissolve the product and avoid gelification. This solution was used for characterization and SWCNT functionalization without further purification. This oligomer consists of a mixture of products with different TGAP-DDS ratios and also unreacted TGAP (as it will be shown in following sections). In Figure 2.14 the different TGAP-DDS possible functionalization products are shown, and only the grafting of the 2TGAP-1DDS molecule is depicted for simplicity.

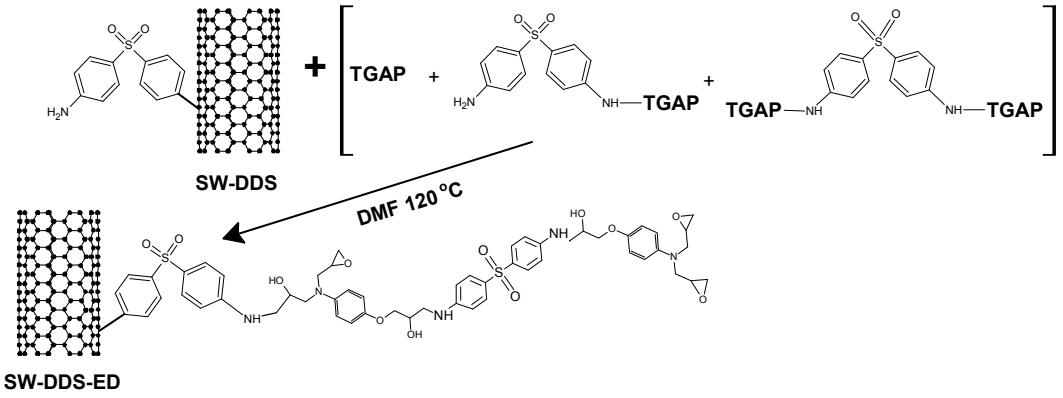

Figure 2.14. Reaction scheme of the grafting between A- or L-SW-DDS and the epoxide-terminated oligomer mixture.

2.2.3. Characterization techniques

►TGA experiments were performed on functionalized SWCNTs under nitrogen atmosphere (60 mL/min flow), and registered with a SETARAM Setsys Evolution 16/18 device at a heating rate of 10ºC/min, in the range from room temperature to 900ºC **(ICB)**.

►Thermogravimetry coupled to infrared spectroscopy (TGA–IR) analyses were performed on a Netzsch TG 209 F1 Iris® coupled to a Bruker Tensor 27 Fourier

Transform Infrared (FTIR) spectrometer via a TGA A588 TGA-IR module. The system was run with BOC HP argon (grade 5.3) gas and residual oxygen was trapped with a Supelco Big- Supelpure Oxygen/water trap. Transfer lines between the TG instrument, mass spectrometer and FTIR spectrometer were heated to a temperature of 200 °C. The detailed experimental conditions of the measurement have been previously reported by the NRC partners.[97] **(SIMS)**

►The amount of free primary amine groups was quantified using the Kaiser test, which was designed to monitor solid-state protein coupling.[98] Later on, it has successfully been applied to characterize amino-functionalized CNTs.[99] The intramolecular redox reaction undergone by the ninhydrin molecules in the presence of primary amines (Kaiser reaction) was carried out using the standard procedure on ~2mg of amino-functionalized SWCNTs. The reaction extent was measured by UV-Visible spectroscopy (Shimadzu UV-2401 PC Spectrophotometer) on the supernatant in the range of 450-650 nm, and the absorbance at the maximum was used to determine the number of free amines in functionalized SWCNTs. The procedure was applied at least twice to ensure repeatability, and the reported are average values. **(ICB)**

►Raman spectra were recorded on different equipments. For SWCNTs functionalized with matrix-based moieties, a Renishaw inVia micro-Raman spectrometer was used. Samples were measured in a dry powder format using a 514 nm laser focused to approximately 1 μm through a 50x objective. Laser power density at the sample was maintained below 3 kW/cm^2 to avoid laser heating effects. **(SIMS)** For the rest of SWCNT samples, Raman spectroscopy was performed using a HORIBA Jobin Yvon Raman spectrometer model HR 800 UV, working with a 532 nm laser. The spectra were analysed, base-line corrected and normalized with the NGS LabSpec software. **(ICB)**

►Elemental analysis were performed using a Thermo Flash 1112 analyzer. For a typical C, H, and N determination, samples are burnt in pure oxygen at 950°C in the

[97] Kingston, C. T.; Martinez-Rubi, Y.; Guan, J. W.; Barnes, M.; Scriver, C.; Sturgeon, R. E.; Simard, B., Coupled thermogravimetry, mass spectrometry, and infrared spectroscopy for quantification of surface functionality on single-walled carbon nanotubes. *Anal. Bioanal. Chem.* 2010, *396* (3), 1037-1044.
[98] Kaiser, E.; Colescot, R. L.; Bossinger, C. D.; Cook, P. I., Color test for detection of free terminal amino groups in solid-phase synthesis of peptides. *Anal. Biochem.* 1970, *34* (2), 595.
[99] Quintana, M.; Prato, M., Supramolecular aggregation of functionalized carbon nanotubes. *Chem. Commun.* 2009, (40), 6005-6007.

presence of V_2O_5. Combustion products pass through an oxidant bed of CuO at 950°C to be converted into NO_x, CO_2, and H_2O. Then, a bed of Cu metal at 500°C transforms NO_x into N_2. The gases are separated in a polar chromatographic column, and quantified by thermal conductivity. For oxygen content analysis, samples are heated to 1080°C, and the pyrolisis products are reduced to CO in a carbon black bed. Due to the experimental setup, data are provided without interference of moisture. Elemental composition is expressed as a weight percent. **(ICB)**

►Nickel and Yttrium were quantitatively determined by the ICP-OES method. Samples were first digested by alkaline fusion with sodium peroxide, and then leached to an aqueous solution which was analyzed in a Jobin-Ybon 2000 ICP instrument. **(ICB)**

►Liquid chromatography electrospray ionization mass spectrometry (LC-ESI-MS) analysis were performed on an Alliance 2795-996PDA-ZQ 2000 (Waters-Micromass) liquid chromatograph-mass spectrometer. The liquid chromatograph was equipped with Sunfire C18, 2.1x100mm, 3.5 μm column. Mobile phase solvents were acetonitrile with 0.1% formic acid (FA) and water with 0.1% FA. Gradient elution was as follows: for AD 30% acetonitrile/water/FA for 5 min then gradient to 50% in 20 min and for ED a gradient from 10% to 60% acetonitrile/water/FA in 30 min, followed by 5 min. 95% acetonitrile/water/01.% FA at flow rate 0.2 ml/min. The mass spectrometer was equipped with pneumatically-assisted electrospray ionisation source, operating in positive mode. The source temperature was set at 80 °C, an electrospray capillary was set at 3.5 kV with a cone voltage set at 20V. Data were collected in centroid mode between 200-1800 m/z with sweep time 0.5 second. **(SIMS)**

►Solid-state absorption spectroscopy in the mid infrared region (FTIR) was performed using a Bruker VERTEX 70 spectrometer. Functionalized SWCNTs were pelletized in spectroscopic grade KBr prior to their analysis. **(ICB)**

►Absorption spectroscopy in the NIR region was performed using a Bruker VERTEX 70 spectrometer. An aqueous suspension of each SWCNT sample (0.1 g/L) in sodium dodecyl benzene sulfonate (SDBS) surfactant (1 wt%) was made with the aid of an ultrasound bath. The suspended SWCNTs were measured inside 2mL quartz cells. The sample absorbance was adjusted within the range of 0.4 – 0.5, by dilution with the 1

wt% SDBS solution. Background correction was effected with the same surfactant solution. **(ICB)**

►The electrical conductivity of several SWCNT samples was measured using a Keithley 4200-SCS equipment working in a two-point probe configuration at 20V. SWCNT samples (~100mg) were previously pelletized in polyvinylidene difluoride (PVDF) and measured with each probe placed in different faces of the pellet. **(ICB)**

► TEM micrographies were taken with a JEOL-2000 FXII electron microscope, working at 200kV and with 0.28nm point-to-point resolution. **(UNIZAR)**

2.3.Results and discussion

2.3.1. Brief analysis of the SWCNT pristine materials

Both of the SWCNTs used in the present chapter, arc- and laser-grown respectively, have particular characteristics of their respective preparation procedures. Table 2.1 summarizes the most relevant differences between both kinds of SWCNTs. Despite laser SWCNTs present lower metal content, higher purity and a narrower diameter distribution, their dispesibility is worse than arc SWCNTs. This is an important issue in the nanocomposites field which will be extensively discussed in following sections.

Table 2.1. As-grown arc (A) and laser (L) SWCNT characterization data

Sample	Metal residue (%) (TGA) *	T_{max} (°C) (TGA) *	PI (NIR)	RBM (cm^{-1}) (Raman)	D (nm)* (Raman)
Arc SWCNTs	13-20	441.1	0.037-0045	145-205	1.69-1.16
Laser SWCNTs	4-11	459.2	0.075-0.087	159-204	1.52-1.17

* In air, from room temperature to 900 ºC at a heating rate of 5 ºC/min. T_{max} corresponds to the temperature of maximum rate of weight loss. D is the diameter distribution.

2.3.2. Characterization of SWCNTs functionalized with aliphatic primary amines

The covalent functionalization of arc discharge SWCNTs with terminal amines have been performed with four different approaches which have ended up in attachment of apliphatic primary amines on the SWCNTs surface. A general scheme of these sepcific functionalizations (described in the expermiental section) is shown in Figure 2.15.

The degree of functionalization was determined from TGA experiments under inert atmosphere (Figure 2.16). Weight losses observed upon non-isothermal heating reveal the presence of covalently attached functional groups. The weight loss up to 100ºC corresponds to residual moisture within SWCNT samples. This moisture content is especially visible in SWCNT-oxa and SWCNT-dca samples, consistent with their higher hydrophilicity as they bear large amounts of surface oxygen groups. The progressive desorption of the chemical groups starts at 100 ºC. Weight losses between 100-700ºC for the functionalized SWCNTs are listed in Table 2.2. As-grown SWCNTs experience a small weight loss (4.3%) which comes from certain native surface groups.[39] The rest of SWCNT samples experience higher weight loss values, which follow the order: SWCNT-oxa > SWCNT-nfp > SWCNT-dca > SWCNT-dba. To calculate the extent of functionalization, weight loss values together with the molecular weight of the different moieties were employed, and the following equation was applied:

$$X = \frac{R(\%) \cdot Mw(g/mol)}{L(\%) \cdot 12 g/mol} \qquad [1]$$

Where X stands for the number of carbon atoms in the SWCNT sample per each covalent functional group, *R(%)* is the residual mass at 700ºC in the TGA plot, *L(%)* is the weight loss in the range of 100-700ºC, and *Mw* is the molecular weight of the desorbed moieties. This calculation considers SWCNT samples to be entirely constituted by carbon, which is indeed an approximation. Functional groups desorbed in the SWCNT-asg sample were discounted in the calculations since they are not a direct consequence of the functionalization. In Table 2.2, X values for the functionalized sam-

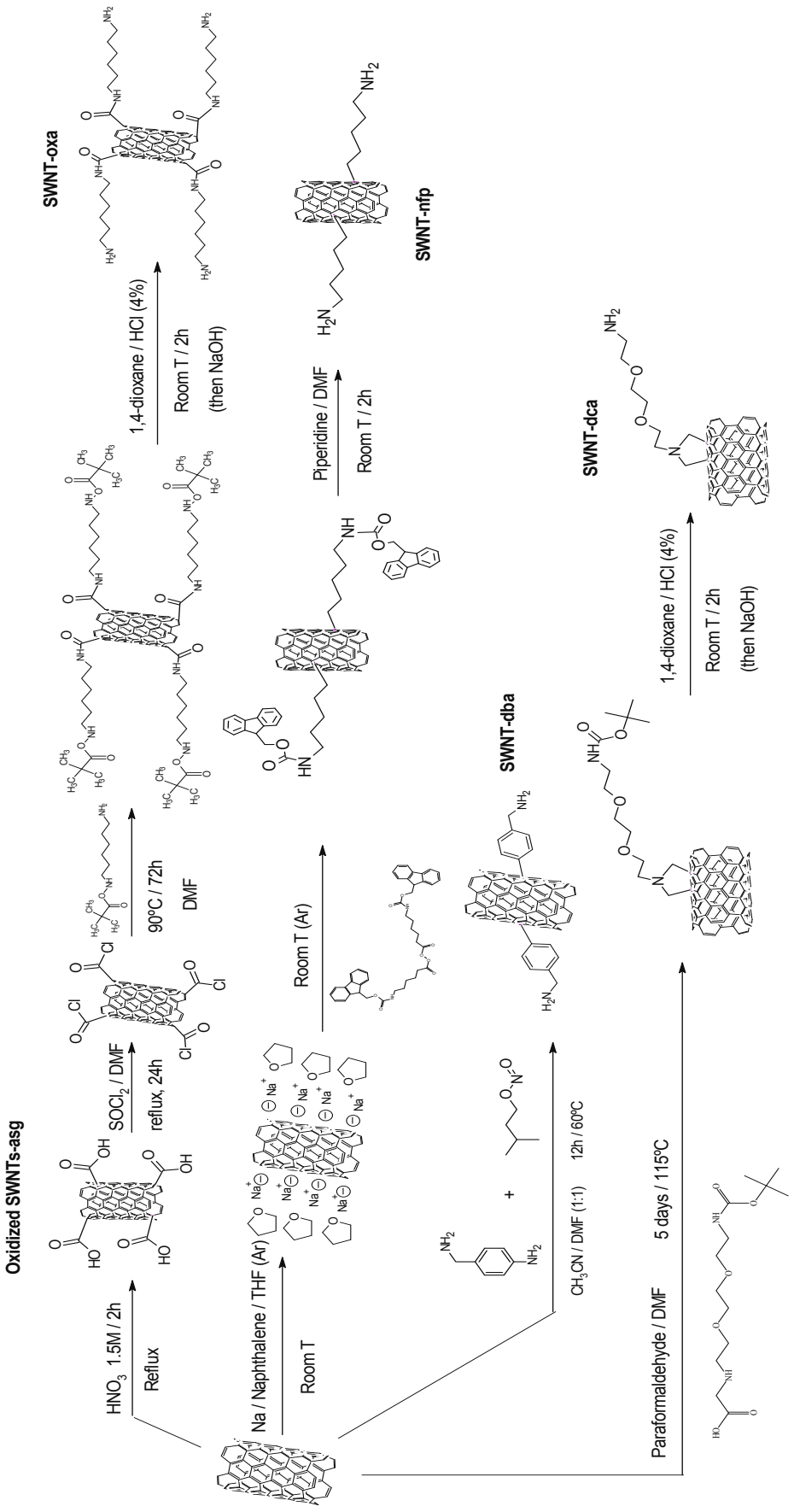

Figure 2.15. Overview scheme for the arc SWCNT covalent functionalization with terminal aliphatic amines

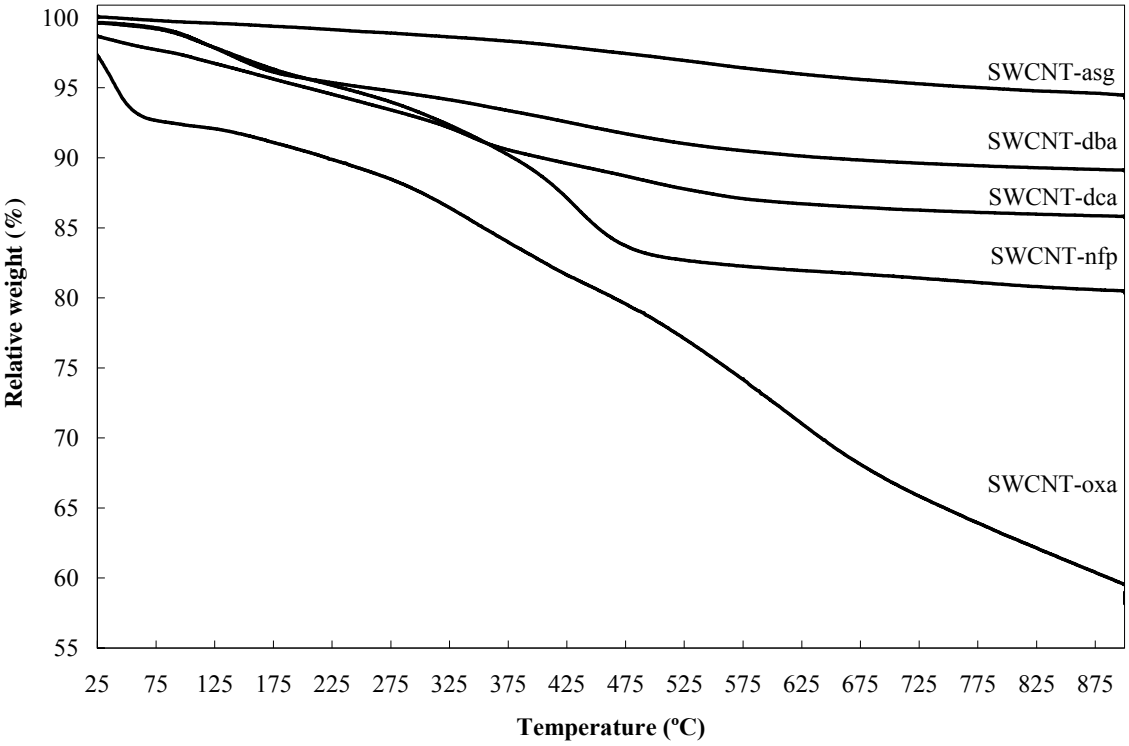

Figure 2.16. TGA plots for as-grown (SWCNT-asg) and covalently functionalized arc SWCNT samples

ples are displayed, and the functionalization degree follows the order: SWCNT-oxa > SWCNT-nfp > SWCNT-dba > SWCNT-dca. It is worth mentioning that the TGA-derived degree of functionalization in SWCNT-oxa includes the desorption of other oxygen groups which are not involved in the functionalization process. However, this does not change the fact that SWCNT-oxa present the highest degree of functionalization, as will be shown below.

The amount of free amines was determined by the Kaiser test, whose results can be found in Table 2.2. The functionalization extent determined by the Kaiser test follows a trend identical to TGA data with the exception of SWCNT-nfp which appears to have less amine groups than expected. The classical oxidation-amidation approach generates the highest number of amines, while the 1,3-dipolar cycloaddition gives the lowest functionalization degree.

Table 2.2. Thermogravimetric data and Kaiser test results

	TGA weight loss in % (from 100 to 700ºC, inert atmosphere)	**Extent of functionalization**	
		X values (1 functional group per X carbon atoms)*	Amine content (μmol/gCNT)**
SWCNT-asg	4.3	---	---
SWCNT-oxa	25.4	31	340
SWCNT-nfp	17.1	34	64
SWCNT-dba	9.0	88	198
SWCNT-dca	11.0	115	20

* Calculated from TGA data using Equation 1

** Calculated from Kaiser test data as the difference between unfunctionalized (SWCNT-asg) and functionalized samples.

The identification of the grafted functionalities was conducted through FTIR spectroscopy. Figure 2.17 shows solid-state FTIR spectra of all the SWCNT samples. The as-grown SWCNT sample (SWCNT-asg) shows no relevant IR features except the band at 1559 cm^{-1} which corresponds to the C=C phonon modes.[100] A wide band at around 1190 cm^{-1} (C-O stretching vibration) is also visible, ascribed to the aforementioned native surface groups, and consistent with the weight loss observed in TGA (Table 2.2). Oxidized SWCNTs present a band at 1722 cm^{-1} that can be attributed to the C=O stretching vibration of carboxylic groups. The presence of carboxylic groups can also be confirmed by the band at 1584 cm^{-1}, typical of the carboxylate anion.[101,102] At 1217 cm^{-1}, the C-O stretching vibrations of esters[101] and phenolic groups can be observed.[101,102] CNTs treated with nitric acid is a complex heterogeneous material with a wide variety of oxygen groups.[83] All the aminated SWCNTs have a common band in the range of 1630-1640 cm^{-1} which can be assigned to the N-H deformation vibration of primary amine groups, and a double band at 2915 / 2848 cm^{-1} (Csp^3 – H vibrations). This doublet presents the lowest intensity in the SWCNT-dca sample, which has the lowest functionalization degree. In the SWCNT-oxa sample, the C=O stretching band downshifts to 1700 cm^{-1}, due to the formation of amide bonds, and the presence of unreacted groups is detected through the carboxylate band (1585 cm^{-1}) as well as the band at 1216 cm^{-1}. In SWCNT-dca sample, a band at 1147 cm^{-1} indicates the presence

[100] Kuhlmann, U.; Jantoljak, H.; Pfander, N.; Bernier, P.; Journet, C.; Thomsen, C., Infrared active phonons in single-walled carbon nanotubes. *Chem. Phys. Lett.* 1998, *294* (1-3), 237-240.

[101] Cross, A. D.; Jones, R. A.; *An Introduction to Practical Infrared Spectroscopy*, Ed. Butterworths, London 1969.

[102] Coates, J.; *Interpretation of Infrared Spectra, a practical approach*, in: *Encyclopedia of Analytical Chemistry*, Ed. R. A. Meyers, John Wiley & sons Ltd., Chichester, 2000, pp10815-10837.

of aliphatic ether groups, and the band at 1206 cm^{-1} corresponds to the C-N stretching vibration in tertiary amines, both contained in the attached moiety (see Figure 2.16). The SWCNT-nfp sample has a band at 1447 cm^{-1} consistent with the C-H bending in methylene groups, and another at 748 cm^{-1} that could be ascribed to the rocking vibrations of successive $(CH_2)_n$ ($n \geq 3$).[102] In SWCNT-dba sample, different bands corresponding to the benzene ring of the attached moiety are observed: two located at 1515 cm^{-1} and 1615 cm^{-1} (C=C stretching) and another one at 814 cm^{-1} (C-H in-plane vibration of a 1:4 disubstituted benzene).

As a consequence of covalent functionalization, SWCNT Raman features are altered, particularly the D-band (1300-1400 cm^{-1}). This band is usually taken as an indication of covalent functionalization,[63] when comparing its relative intensity to the G-band (1500-1700 cm^{-1}). Usually, an increase in the D-band intensity is observed after a covalent attachment onto SWCNT surface. As can be observed in Figure 2.18, the G/D ratios of functionalized SWCNTs are significantly lower than that of the SWCNT-asg sample.

NIR purity data and the ICP metal content of the different SWCNT samples are displayed in Table 2.3. The NIR purity ratio is a quantitative measurement of the purity of SWCNT samples,[72] relative to the whole carbon content. The PI is calculated as the ratio of the baseline subtracted peak area and the total peak area for the SWCNT S_{22} transition between 7750 and 11750 cm^{-1} (see Figure 2.4). In our functionalized SWCNTs, NIR purity ratios are visibly affected by the functionalization route. The nitric acid treatment causes a nearly two-fold increase in the SWCNT-asg purity, while the amidation step lowers this ratio to approximately the initial value. Sidewall addition reactions yield higher PIs, particularly the alkaline reduction, which causes a ~50% increase in the PI of SWCNT-asg. The bundles exfoliation induced by negatively charging the SWCNTs, combined with the centrifugation could have caused the removal of carbonaceous impurities hence increasing the NIR ratio. TEM images of a reduced SWCNT-asg sample (deposited on a copper grid and subsequently deactivated in open air) are shown in Figure 2.19. Note that the bundles thickness (typically of ~20 tubes) is much lower and the intertube distance is slightly increased, which seems to indicate some degree of bundles exfoliation.

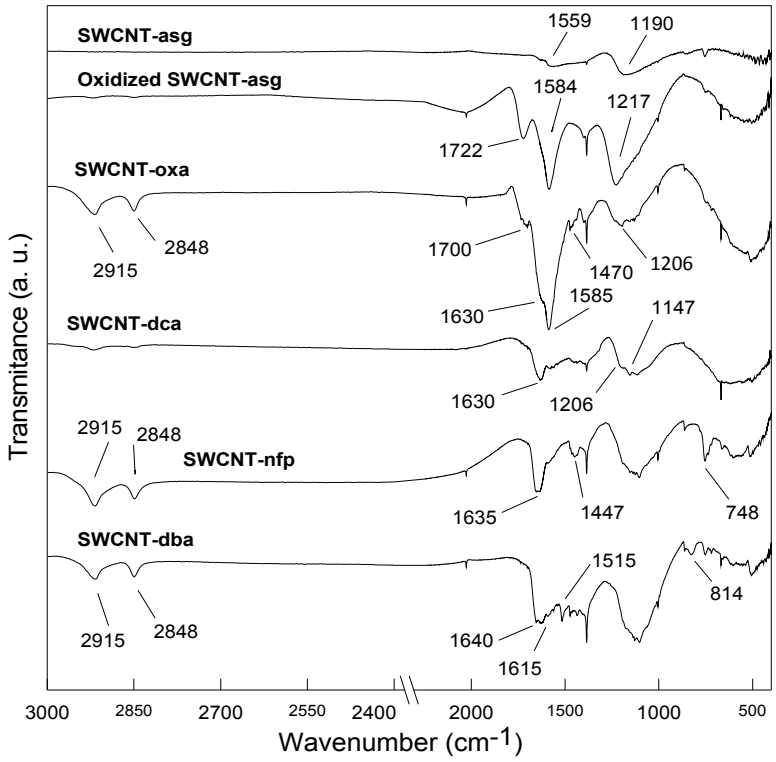

Figure 2.17. FTIR spectra for SWCNT-asg and the functionalized SWCNT samples

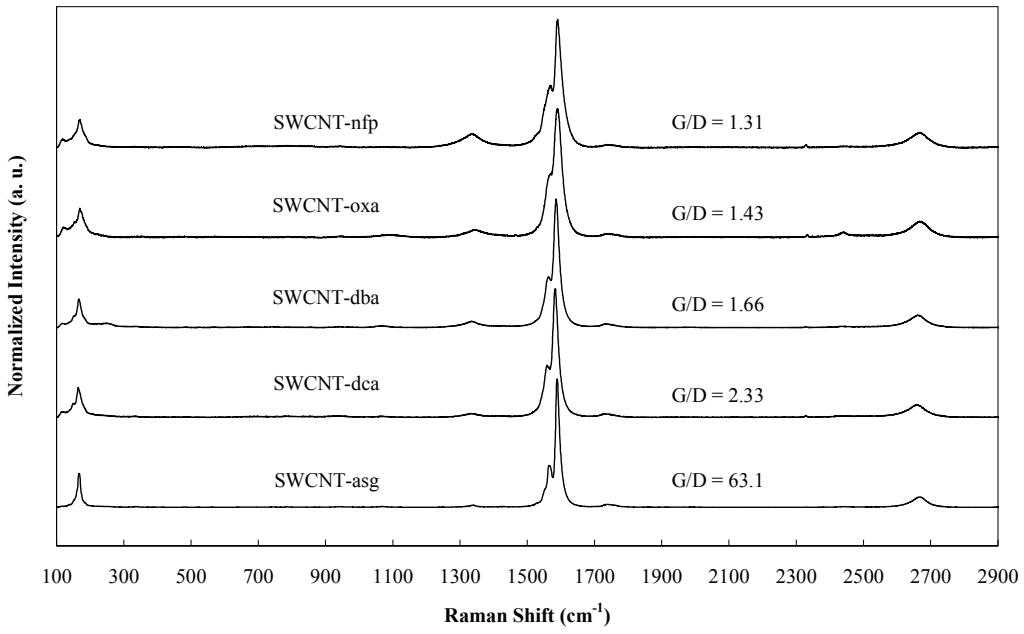

Figure 2.18. Raman spectra for the set of SWCNT samples

Table 2.3. NIR purity index and metal content for the different SWCNT samples

	PI	Metal Content (ICP-OES)	
		Ni (%)	Y (%)
SWCNT-asg	0.027* / 0.045**	13.13	6.64
Oxidized SWCNTs***	0.047	3.94	0.65
SWCNT-oxa	0.031	3.27	0.42
Reduced SWCNT****	0.063		
SWCNT-nfp	0.055	10.3	1.73
SWCNT-dba	0.052	6.14	14.5
SWCNT-dca	0.053	12.1	2.03

* NIR purity index of SWCNT-asg employed for the nitric acid treatment and the subsequent amidation reaction
** NIR purity index of SWCNT-asg employed for the rest of functionalization procedures and for composite blends
*** SWCNT-asg oxidized with nitric acid (see experimental section)
**** Arc SWCNTs after the first alkaline reduction cycle (see experimental section)

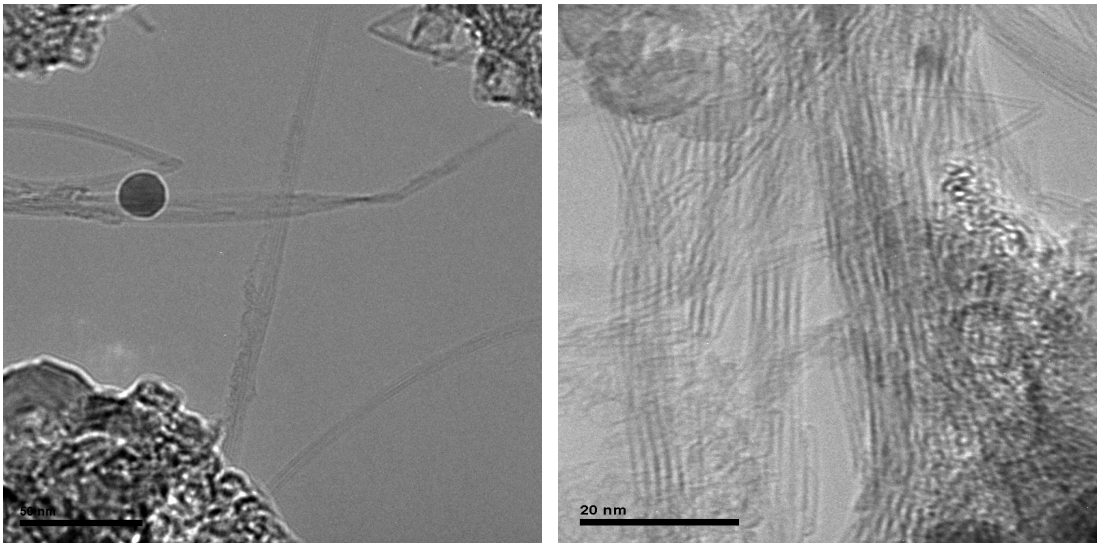

Figure 2.19. TEM images of reduced arc SWCNTs after deactivation of the negative charging by exposure to open air.

As-grown SWCNTs possess a total metallic content of around 20 wt%, which corresponds to the catalysts remaining from the SWCNT synthesis. As expected, the nitric acid treatment yields SWCNTs with a noticeably reduced amount of metals (~77% reduction). SWCNTs aminated through carboxylic activation (SWCNT-oxa) present similar metal content to nitric acid-treated SWCNTs. The lower amount of metals present in the SWCNT-oxa sample compared to the rest of functionalized

SWCNTs is due to the nitric acid treatment that precedes the amination step. SWCNTs functionalized through alkaline reduction (SWCNT-nfp) and 1,3-dipolar cycloaddition (SWCNT-dca) present a ~30-40% reduction in the metal content. While in SWCNT-nfp, the removal of metals could arise from the negative charging and exfoliation of SWCNTs (which may detach the impurities), in the SWCNT-dca it has been reported as an effect of the organic functionalization.[103]

2.3.3. Characterization of SWCNTs functionalized with matrix-based moieties

For the obtention of amine-terminated SWCNTs were functionalized with the curing agent DDS and the TGAP-DDS derivative (AD), a higher molecular weight oligomer containing terminal amino groups with a chemical structure analogous to the cured epoxy resin network of interest. The composition of the AD derivative was analyzed by LC-ESI-MS and the results are shown in Figure 2.20. As can be observed, the main product in the AD derivative is the 1TGAP-3DDS adduct, obtained as a mixture of regioisomers (α or β-amino alcohol) from the nucleophilic ring opening of the epoxide by amine groups.

The curing agent DDS and the AD derivative were covalently attached to the SWCNT sidewalls through diazotization reaction, as represented in Figure 2.13. Due to their structural similarity with the matrix, the covalent functionalization of the nanotubes with the AD derivative should improve the affinity of the nanotubes for the epoxy polymer matrix and help maintaining the stability of the dispersion during the cross-linking process. In addition, this higher molecular weight functionality could show improved affinity in comparison to the smaller DDS fragments. Figure 2.21 shows the Raman spectra of pristine L-SWCNT and A-SW-DDS / L-SW-DDS samples obtained using a 514 nm excitation laser. The most characteristic features of the Raman spectrum of SWCNT (Figure 2.3) are visible here.

[103] Georgakilas, V.; Voulgaris, D.; Vazquez, E.; Prato, M.; Guldi, D. M.; Kukovecz, A.; Kuzmany, H., Purification of HiPCO carbon nanotubes via organic functionalization. *J. Am. Chem. Soc.* 2002, *124* (48), 14318-14319.

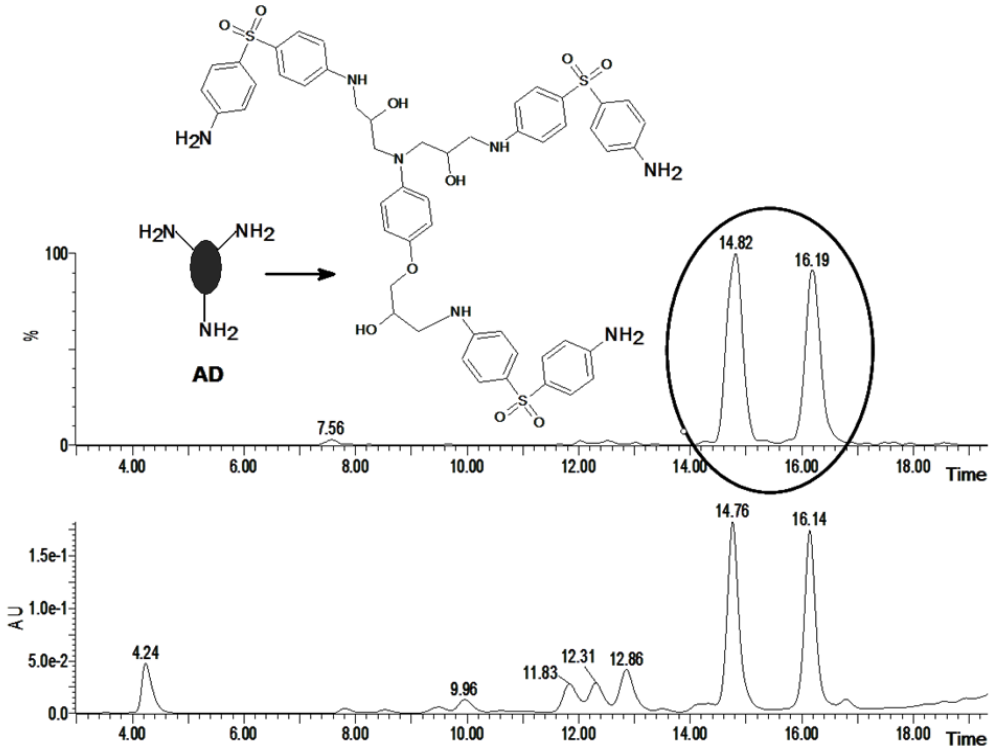

Figure 2.20. LC-ESI-MS analysis of the TGAP-DDS derivative (AD) retention times of 14.82 and 16.19 min correspond to a peak mass of $[M+H]^+$ = 1022.4 (1TGAP-3DDS).

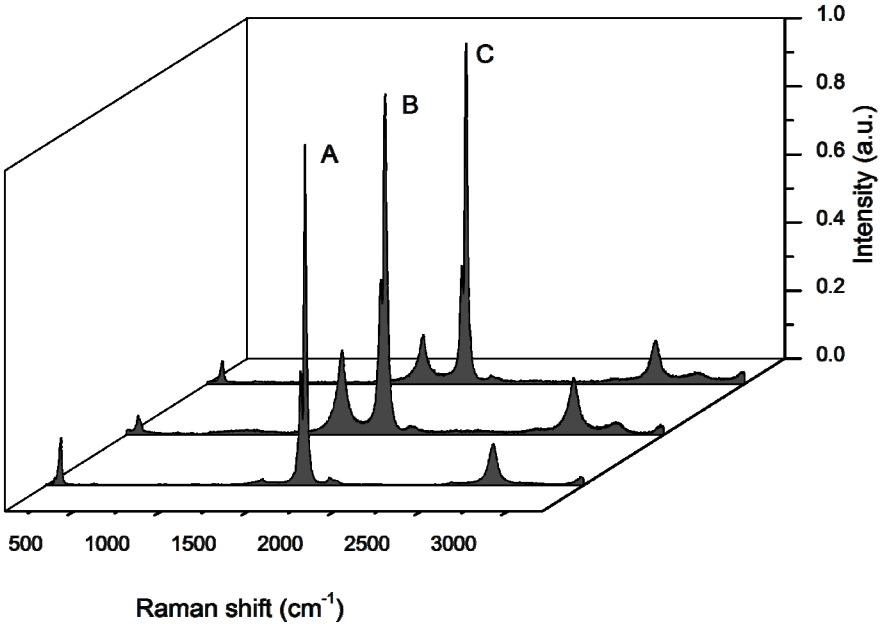

Figure 2.21. Raman spectra of a) pristine L-SWCNT, b) A-SW-DDS and c) L-SW-DDS after base line correction and normalized to the intensity of the D-band. Excitation laser 514 nm.

The G to D band intensity ratio (G/D) of A-SWCNT and L-SWCNT changes from 33.3 to 3.85 and from 50 to 7.14 respectively after the diazonium reaction with DDS. A blank reaction was carried out in identical conditions but in absence of isoamyl nitrite. The Raman spectrum of this sample (Blank A-SW-DDS) showed a smaller change of G/D than the functionalized samples. These results are summarized in Table 2.4.

Figure 2.22 shows the Raman spectra obtained for pristine A-SWCNT and SW-AD samples. After the diazonium reaction of arc and laser-SWCNT with the synthesized ligand AD, the Raman spectra of functionalized samples show a smaller decrease on the G/D value compared to SW-DDS samples (Table 2.4). These results are indicative of a lower addition density of the AD derivative to the nanotubes sidewall, probably due to a lower reactivity of the AD derivative compared to DDS. A higher molecular weight amine is known to generate lower functionalization degree, usually ascribed to steric hindrance.[104] A similar observation has been reported when using the "grafting to" approach to functionalize nanotubes with polymer chains.[105]

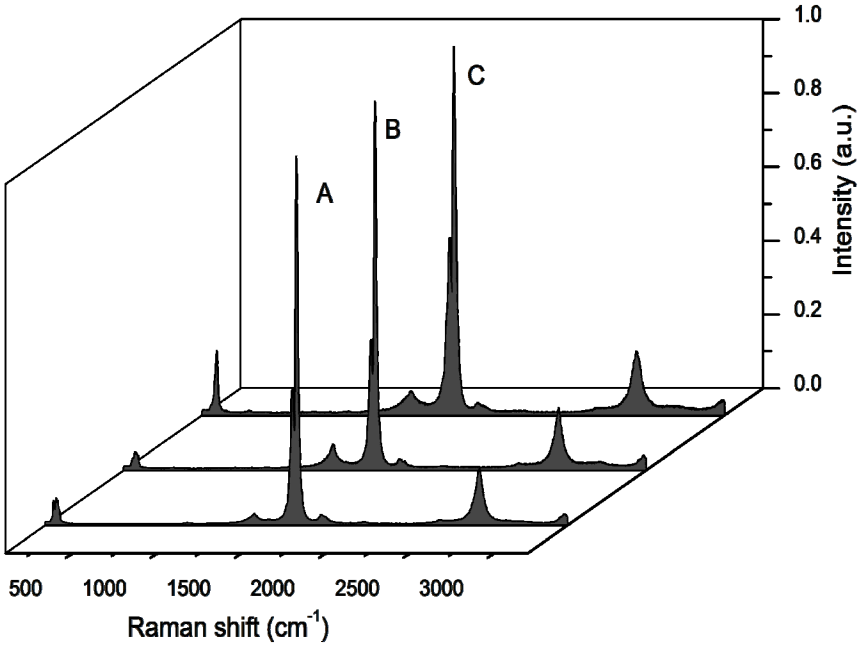

Figure 2.22. Raman spectra of a) pristine A-SWCNT, b) A-SW-AD and c) L-SW-AD after base line correction and normalized to the intensity of the G-band. Excitation laser: 514 nm.

[104] Jimeno, A.; Goyanes, S.; Eceiza, A.; Kortaberria, G.; Mondragon, I.; Corcuera, M. A., Effects of Amine Molecular Structure on Carbon Nanotubes Functionalization. *J. Nanosci. Nanotechnol.* 2009, *9* (10), 6222-6227.

[105] Li, J.; He, W. D.; Yang, L. P.; Sun, X. L.; Hua, Q., Preparation of multi-walled carbon nanotubes grafted with synthetic poly(L-lysine) through surface-initiated ring-opening polymerization. *Polymer* 2007, *48* (15), 4352-4360.

Table 2.4. Raman and TGA data obtained for SWCNT samples functionalized with matrix-based moieties.

Samples	G/D* λ_{exc} = 514 nm	TGA wt loss (%) until 700 ºC**	X values (1 functional group per X carbon atoms)***
A-SWCNT	33.3	3	-
A-SW-DDS	3.85	11	164
A- SW-AD	14.3	12	597
A- SW-DDS-ED	4.05	20	
L-SWCNT	50	2	-
L- SW-DDS	7.14	12	164
L- SW-AD	20	11	758
L- SW-DDS-ED	6.25	23	
Blank A-SW-DDS	22.2	6	-

* From Raman spectra, after base line correction and normalized to the G-band intensity.
** Including ~ 2 wt% loss due to DMF solvent in amine functionalized samples
*** Using Equation (1). The metal content (20 % and 11 % for A-SWCNT and L-SWCNT respectively) was taken into account in this case.

The covalent functionalization is also supported by electrical conductivity measurements. About 100 mg of either pristine A-SWCNT or A-SW-DDS were mixed with ~5 wt% PVDF and pressed at 3 tons in a 13 mm diameter cylindrical mould. DC pellet conductivities were measured at room temperature in a two-probe configuration (see experimetal section). The obtained conductivity values were 10.8 and $4.5 \cdot 10^{-2}$ S/cm for A-SWCNT and A-SW-DDS respectively. The reduction (which is about three orders of magnitude) is in agreement with the literature. According to some theoretical studies, covalent sidewall functionalization of metallic or semiconducting SWCNTs originates a localized electronic state near the nanotube Fermi level.[106,107] This impurity state produces a drastic drop in the electrical conductivity of metallic SWCNTs.[107] Since sidewall functionalization through the diazonium salts route is selective towards metallic SWCNTs[108,109], the conductivity decrease measured for A-SW-DDS could be interpreted as a chemical inhibition of the metallic SWCNTs contribution.

TG data and IR of the thermally desorbed gases from the functionalized L-SW-

[106] Zhao, J. J.; Park, H. K.; Han, J.; Lu, J. P., Electronic properties of carbon nanotubes with covalent sidewall functionalization. *J. Phys. Chem. B* 2004, *108* (14), 4227-4230.
[107] Park, H.; Zhao, J. J.; Lu, J. P., Effects of sidewall functionalization on conducting properties of single wall carbon nanotubes. *Nano Lett.* 2006, *6* (5), 916-919.
[108] Strano, M. S.; Dyke, C. A.; Usrey, M. L.; Barone, P. W.; Allen, M. J.; Shan, H. W.; Kittrell, C.; Hauge, R. H.; Tour, J. M.; Smalley, R. E., Electronic structure control of single-walled carbon nanotube functionalization. *Science* 2003, *301* (5639), 1519-1522.
[109] Ghosh, S.; Rao, C. N. R., Separation of Metallic and Semiconducting Single-Walled Carbon Nanotubes Through Fluorous Chemistry. *Nano Res.* 2009, *2* (3), 183-191.

DDS sample is given in Figure 2.23. Thermal desorption data show a total mass loss of 12 % upon heating to 700°C, markedly higher than that obtained for unfunctionalized nanotubes or the diazonium blank reaction (see Table 2.4). The dTG data show two discrete mass-loss events centered at ~225°C, ~425°C and accounting for ~2 wt% and ~10 wt% respectively. Similar results were obtained for A-SW-DDS samples (Table 2.4). The IR spectrum associated to the event at low temperature (data not shown) can be unambiguously assigned to residual DMF present even after previous drying of the samples. On the other hand, the IR absorption spectrum associated with the higher temperature desorption event shows bands that are indicative of the covalent attachment of DDS to the nanotubes and the presence of free amine groups. The shoulder at 3400 cm^{-1} (-NH stretching vibration) and the bands at 1620 cm^{-1} (N-H deformation of primary amine), 1501, 1270 and 747 cm^{-1} (mono-substituted benzene ring) coincide with the gas phase spectrum of aniline, while the bands at 1375-1340 cm^{-1} correspond to sulfur dioxide. Both species simultaneously desorbed during the decomposition of the covalently attached moiety on SW-DDS samples. It is worth mentioning that the band at 1620cm^{-1} was not identified on the IR spectrum of Blank A-SW-DDS samples (data not shown).

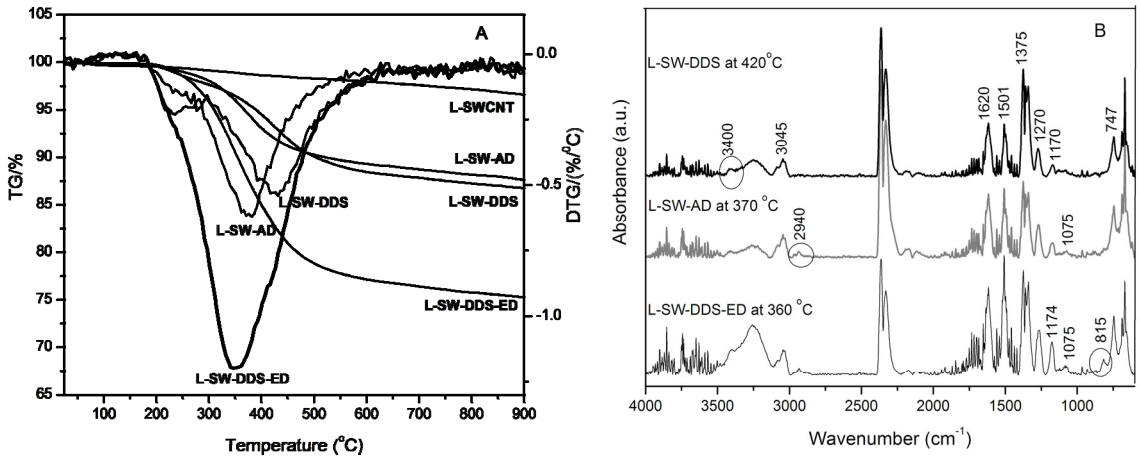

Figure 2.23. A) TGA of as-grown L-SWCNT and functionalized L-SW-DDS, L-SW-AD and L-SW-DDS-ED sample under desorption conditions; B) gas-phase IR spectra of the species desorbed from functionalized SWCNT samples at the T_{max}.

On the other hand, as observed in Figure 2.23a and table 2.4, the L-SW-AD sample shows a total mass loss of 11 % upon heating to 700°C, very similar to the value

of L-SW-DDS. However, as was observed by Raman spectroscopy their G/D ratios are significantly different. This result is compatible with the higher molecular weight of the fragment attached to the nanotubes sidewalls in L-SW-AD samples. The IR spectrum associated to the L-SW-AD mass loss event is very similar to the one observed for L-SW-DDS samples except for some changes in the relative intensity of the signals. Specifically, the intensity of the bands associated to SO_2 (1375-1340 cm^{-1}) is very similar to the intensity of NH deformation band (1620 cm^{-1}) indicating a lower SO_2/NH ratio of the desorbed moiety than L-SW-DDS, in agreement with the structure of the AD derivative (Figure 2.13). Additionally, new bands can be observed at ~2940 cm^{-1} which corresponds to the stretching vibration of C_{sp3} - H containing fragments, and a small broad band at 1075 cm^{-1} assigned to C-O stretching vibrations, further indication of the successful attachment of the AD derivative to the nanotube sidewalls.[96]

With respect to the second matrix-based derivative (ED), as can be determined by LC-ESI-MS analysis, Figure 2.24, the conditions employed for the synthesis of the ED derivative produced a complex mixture of different adducts from the ring opening of the epoxide by amine groups. The major components of this mixture are unreacted TGAP, and different isomers of adducts 1DDS-1TGAP and 1DDS-2TGAP. A solution of this mixture and SW-DDS samples was refluxed in DMF at 120ºC (see experimental section) in order to create a covalent connection between DDS-functionalized SWCNT and the epoxide-containing molecules in the ED derivative. This functionalization was shown in Figure 2.14.

Figure 2.23b includes TGA-IR results obtained for L-SW-DDS-ED samples. The thermal desorption data show a total mass loss of 23 % upon heating to 700°C, 11% higher than the value obtained for SW-DDS samples indicating the successful attachment of species present in the ED derivative mixture. The IR spectrum of the fragments desorbed at the temperature of maximum decomposition rate (360 °C) is also included in Figure 2.23b. The IR spectra of L-SW-AD and L-SW-DDS-ED are very similar; however, a clear difference is the higher intensity of the band at 1501 and 1075 cm^{-1} and a new band at 815 cm^{-1} that can be assigned to 1-4 disubstituted benzene rings in L-SW-DDS-ED. These features indicate a different decomposition pathway for this latter sample.

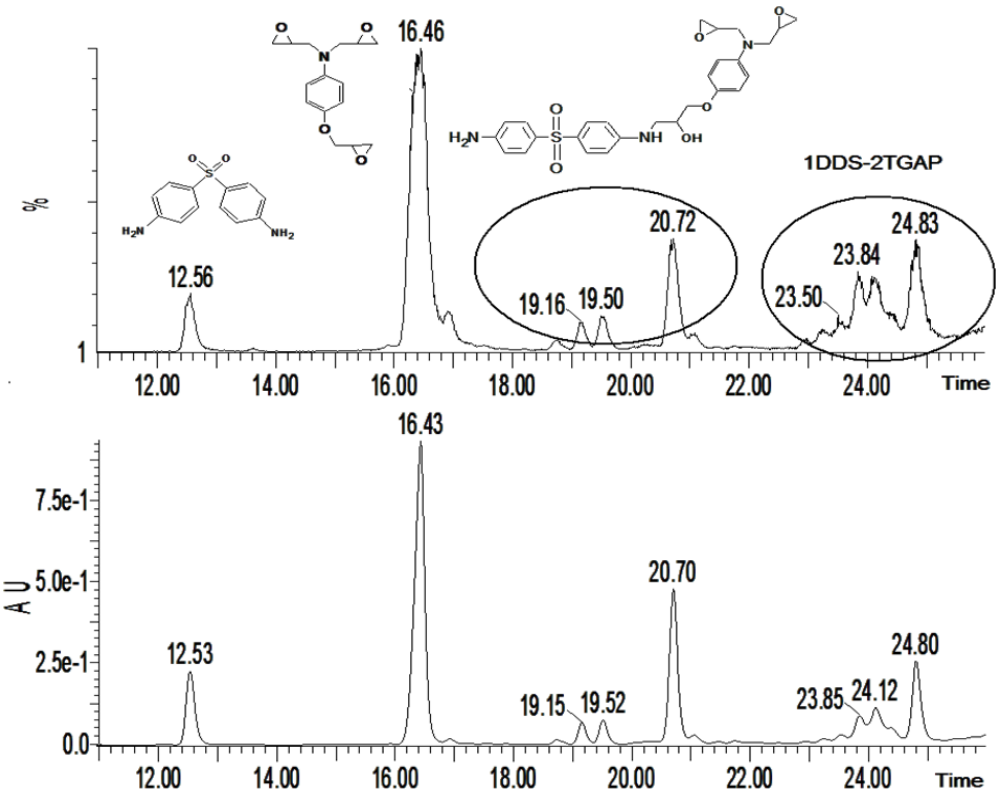

Figure 2.24. LC-ESI-MS analysis of the DDS-TGAP derivative (ED). t = 12.56 min $[M+H]^+$ 297.3(DDS); t = 16.46 min $[M+H]^+$ 278.3 (TGAP); t = 19.16, 19.50 and 20.72 min $[M+H]^+$ 526 (1DDS-1TGAP); t = 23.50, 23.84 and 24.83 min $[M+H]^+$ 803.6 (1DDS-2TGAP).

The extent of functionalization was supported with elemental analysis. In Table 2.5 elemental compositions of the different samples are displayed, being the oxygen content determined in separate experiments. The metal amount has not been examined, so the total percentage does not add up to 100%. However, some useful information can be drawn from elemental characterization. Both laser- and arc-grown SWCNTs contain a small amount of oxygen, in the range of 2-3%, indicative of the existence of oxygen functional groups in the pristine samples. The diazonium reaction with DDS in both kinds of SWCNT induces an increase in the sulphur content, reaching ~2%. In parallel, there is an increase in the nitrogen content also in the range of 2-3%. The diazonium blank reaction exhibits a minor amount of nitrogen (probably due to remaining DMF traces) and almost no presence of sulphur, which corroborates the successful grafting in SW-DDS samples. Furthermore, the nitrogen content only increased slightly after coupling SW-DDS with the ED derivative while the sulphur content slightly decreased, which would be in agreement with the introduction of grafted molecules present in the ED mixture. However, such a small increase in the nitrogen content could be indicating

that mainly the TGAP monomer has been grafted to the SW-DDS samples rather than higher molecular weight oligomers. The diazonium grafting of the AD ligand gives a slightly lower nitrogen content than the SW-DDS samples while the nitrogen/sulfur ratio is higher than that of SW-DDS samples which is in agreement with the lower degree of functionalization of the AD derivative (compared to DDS), as stated by X values in TGA data (table 2.4).

Table 2.5. Elemental analysis for different SWCNT samples functionalized with matrix-based moieties.

Samples	%O	%C	%H	%N	%S
A-SWCNTs	1.92	72.8	0.3	0.1	0.0
A-SW-DDS		68.3	1.2	2.5	2.1
A- SW-AD		69.8	1.3	2.3	1.1
A- SW-DDS-ED		69.0	1.9	2.8	1.8
L-SWCNT	2.98	83.5	0.3	0.2	0.0
L- SW-DDS		79.6	1.5	3.2	2.4
L- SW-AD		84.0	1.2	1.9	1.0
L- SW-DDS-ED		76.7	2.4	3.6	2.2
Blank A-SW-DDS*		72.8	1.1	0.9	0.1

* Blank diazonium reaction with arc SWCNTs without adding isoamyl nitrite

Solid-state FTIR spectra (Figure 2.25) gave knowledge about the different covalently attached moieties. While only a set of functionalized A-SWCNTs are represented, equivalent results were obtained for the analogous laser SWCNT (data not shown). As-produced A-SWCNTs do not show any significant feature, except for a band located at 1559 cm^{-1} due to the CNT C=C phonon modes.[100,110] The wide band at about 1150 cm^{-1} corresponds to the C-O stretching modes due to native oxygen functional groups,[39] which is consistent with TGA data. The other visible bands in A-SWCNTs (centered at 750 and 1610 cm^{-1}) could be attributed to moisture contained in the SWCNT sample. When A-SWCNTs are functionalized different features arise and can be assigned to the attached functional groups. After the functionalization process *via* the diazonium reaction with DDS the most significant feature of A-SW-DDS samples is the band at 1650 cm^{-1} which stands for the N-H deformation in primary amines.[101] In addition, different bands corresponding to aromatic rings are also present. The band at 1590 cm^{-1} can be assigned to the C=C in-plane deformation of the DDS

[110] Kim, U. J.; Liu, X. M.; Furtado, C. A.; Chen, G.; Saito, R.; Jiang, J.; Dresselhaus, M. S.; Eklund, P. C., Infrared-active vibrational modes of single-walled carbon nanotubes. *Phys. Rev. Lett.* 2005, *95* (15).

benzene rings, and the intense 1:4 ring substitution vibration modes are visible at 1098 (in-plane) and 828 (out-of-plane) cm^{-1}.[101] The sulfone bands can be identified at 1136 (symmetric SO_2 stretching) and 1286 (asymmetric SO_2 stretching) cm^{-1} together with a visible knee at 1165 cm^{-1}, a typical feature in diphenyl sulfones.[111] In the case of the diazonium functionalization with the AD oligomer (A-SW-AD), the IR spectrum is very similar to that of the A-SW-DDS, except for the band at 1500 cm^{-1} which can be assigned to the N-H deformation in secondary amines,[101] contained within the AD molecular structure. The joint presence of the 1650 and 1500 cm^{-1} bands support the attachment of the AD ligand with free NH_2 groups. For the A-SW-DDS-ED sample, the same profile as the A-SW-DDS sample is present, with the following differences: the primary amine band at 1650 cm^{-1} is noticeably less intense relative to the 1590 cm^{-1} C=C in-plane deformation of the DDS benzene rings, which evidences the consumption of primary amines trough the coupling reaction. The remaining signal is probably coming from unreacted SW-DDS and/or coupling of the 1DDS-1TGAP adduct which contains free amine groups. The appearance of a band at 1276 cm^{-1} together with an association of several weak bands at about 900 cm^{-1} indicates the presence of epoxide rings.[112]

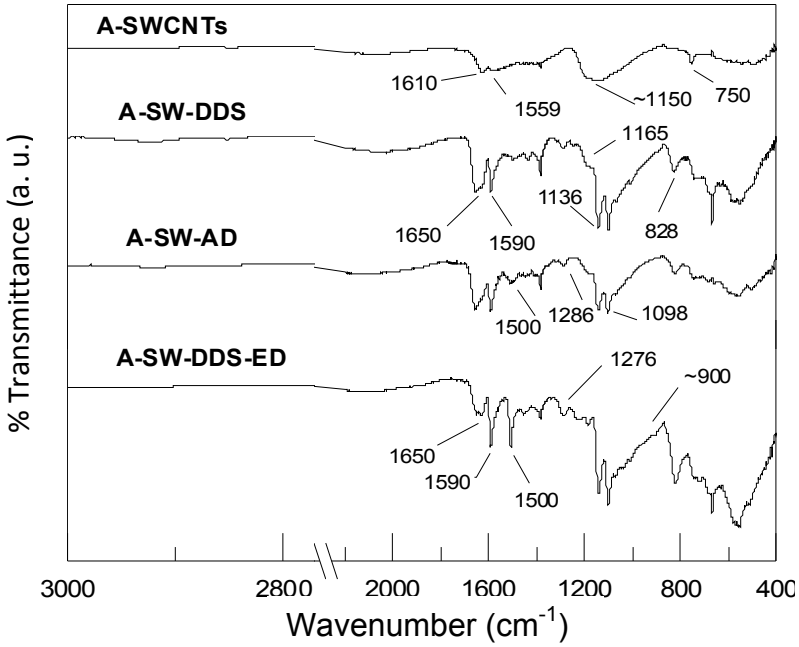

Figure 2.25. Solid-state FTIR spectra for a set of functionalized A-SWCNT

[111] Schreiber, K. C., Infrared Spectra of Sulfones And Related Compounds. *Anal. Chem.* 1949, *21* (10), 1168-1172.
[112] Patterson, W. A., Infrared Absorption Bands Characteristic of the Oxirane Ring. *Anal. Chem.* 1954, *26* (5), 823-835.

2.4. Conclusion

In the present chapter different approaches to covalent functionalization SWCNTs are reported. The functionalization pathways aim at providing covalently-modified SWCNTs with terminal primary amines (or oxirane rings), which are of special interest for further developing composite materials based on epoxy matrix. Each approach has its own features and functionalization degree, that have been carefully analyzed through multiple techniques.

- The classical carboxylation + amidation reaction has been undertaken using a nitric acid treatmen which serve as both purification means and a source of carboxylic groups, which were amidated with a diamine. Functionalization is assumed to set mainly in tips and sidewall defects.
- The alkaline reduction with sodium naphthalide provides highly exfoliated and reactive SWCNTs. The reaction of reduced SWCNTs with a diacyl peroxide using an established protocol[91] provides a sidewall-functionalized material with aliphatic terminal amines.
- The *in situ* generation and reaction of aryl diazonium salts with SWCNTs[93] provided sidewall-functionalized with a wide variety of covalent moieties. This approach was first used to obtain covalently aminated SWCNTs using 4-aminobenzylamine as the arylamine. The diazonium route also allowed to covalently functionalize SWCNTs with tailored molecules derived from the chemical structure of the targeted epoxy matrix. As a matter of fact, SWCNTs were functionalized *via* the diazonium route with the curing agent DDS and two pre-synthesised derivatives made with the epoxy precursor (TGAP) and the curing agent, which provided terminal aromatic amines or epoxide rings with a definite molecular architecture.
- The 1,3-dipolar cycloaddition of azomethine ylides on SWCNTs surface was used to functionalize SWCNTs with a specific α-aminoacid providing an amine-terminated material with higher purity than the pristine sample. This was accomplished using the experimental protocol designed by the Prato group.[113]

[113] Georgakilas, V.; Tagmatarchis, N.; Pantarotto, D.; Bianco, A.; Briand, J. P.; Prato, M., Amino acid functionalisation of water soluble carbon nanotubes. *Chem. Commun.* 2002, (24), 3050-3051.

The purity of samples was thoroughly assessed using diverse analytical techniques. NIR optical absorption revealed that the PI increased and the metal content (quantified with ICP-OES) was reduced after most of the functionalization protocols, being more drastically removed in the functionalization route preceded by nitric acid treatment.

The functionalization degree could be estimated by TGA and the aliphatic amine content was measured with the Kaiser test. In general, the functionalization of SWCNTs with terminal aliphatic amines exhibited higher functionalization degrees than SWCNTs functionalized with matrix-based moieties, which is in consonance with the higher molecular weight of the attached moiety in the latter case. The functionalziation degree was also characterized by other techniques such as elemental analysis or Raman spectroscopy.

In summary, many functionalized SWCNT samples were performed and analized. These materials were employed for integration into epoxy matrix toward the development of high-performance epoxy nanocomposite materials, which will be described in following chapters.

"The closer you get to the light,
the greater your shadow becomes"

Kingdom Hearts
Squaresoft (2002)

CHAPTER 3:

NON-COVALENT MODIFICATIONS OF SINGLE-WALLED CARBON NANOTUBES

3.0. Abstract

In order to develop efficiently reinforced nanocomposite materials with SWCNTs, an approach based on non-covalent interactions of SWCNTs with specific macromolecules has been undertaken. The wrapping of SWCNTs with amphiphilic block copolymers (BCs), based on polyethylenoxide (PEO) was used, since the SWCNTs dispersion in this type of BC aqueous solutions causes their purification and debundling, being the resulting filler specially attractive to reinforce epoxy matrices. Similar works were conducted through the wrapping of SWCNTs with thermoplastic polymers in other liquid media, with the aim of improving the compatibility of the filler in a PEEK matrix. The effect of wrapping in the morphology and purity of SWCNTs as well as the rational choice of the wrapping polymers are explained.

3.1. Introduction

3.1.1. General context

CNTs exhibit exceptional nanoscale properties, such as high aspect ratio, low density, outstanding electrical properties, high strength and high stiffness. SWCNTs, in particular, have been at the forefront of novel nanoscale investigations due to their unique structure-dependent electronic and mechanical properties.[1] SWCNTs have a high potential to improve the mechanical, physical and electrical properties of polymers.[2] Polymer/CNT composites are expected to preserve the good processability of the matrix and also the excellent functional properties of CNTs. SWCNTs are mostly synthesised as bundles of aligned tubes, packed in a triangular 2D compact lattice due to van der Waals interactions.[3] Their applications and excellent performance are referred to individual tubes and the SWCNTs self-assembling in bundles hinders their dispersibility in both aqueous and organic media, making as-grown SWCNTs difficult to process. Bundling and low adhesion to matrices represent the main obstacle in developing

[1] Baughman, R. H.; Zakhidov, A. A.; de Heer, W. A., Carbon nanotubes - the route toward applications. *Science* 2002, *297* (5582), 787-792.
[2] Thostenson, E. T.; Ren, Z. F.; Chou, T. W., Advances in the science and technology of carbon nanotubes and their composites: a review. *Compos. Sci. Technol.* 2001, *61* (13), 1899-1912.
[3] Thess, A.; Lee, R.; Nikolaev, P.; Dai, H. J.; Petit, P.; Robert, J.; Xu, C. H.; Lee, Y. H.; Kim, S. G.; Rinzler, A. G.; Colbert, D. T.; Scuseria, G. E.; Tomanek, D.; Fischer, J. E.; Smalley, R. E., Crystalline ropes of metallic carbon nanotubes. *Science* 1996, *273* (5274), 483-487.

SWCNTs technological potential.[4-6] Poorly dispersed CNT–polymer composites have reduced effects in transferring the CNTs properties, leading to low tensile strength or low thermal conductivity. The effective utilization of CNTs in composite applications strongly depends on the ability to homogeneously disperse them throughout the matrix.[4] Good interfacial bonding is also required to achieve load transfer from the CNTs to the matrix, resulting in an optimum transfer of nanoscale properties to the macroscale.[5] Load transfer can be achieved by several mechanisms which include chemical bonding and/or weak van der Waals interactions between the tubes and the matrix. Several techniques have been utilized to enhance dispersion and adhesion of CNTs to polymeric matrices, such as physical blending,[7] addition of compatibilizers,[8] *in situ* polymerization,[9,10] or chemical functionalization.[11] Among them, some kind of physical blending or non covalent functionalization is preferred in cases where preserving the physical state and electronic structure of CNTs is desired.

Steric repulsion among polymer-decorated tubes can be employed for the stabilization of CNTs dispersions (Figure 3.1). Polymers are efficient steric stabilizers, and among them, BCs stand out. They interact with CNTs *via* weak van der Waals - type bonding, resulting in polymer wrapped, adsorbed or extreme–connected nanotubes.[12] This causes steric repulsions between polymer layers which, because of the entropy alteration, lead to a separation of the tubes. Besides, polymer chains remain

[4] Thostenson, E. T.; Li, C. Y.; Chou, T. W., Nanocomposites in context. *Compos. Sci. Technol.* 2005, *65*, 491-516.
[5] Andrews, R.; Weisenberger, M. C., Carbon nanotube polymer composites. *Curr. Opin. Solid State Mater. Sci.* 2004, *8* (1), 31-37.
[6] Bal, S.; Samal, S. S., Carbon nanotube reinforced polymer composites - A state of the art. *Bull. Mater. Sci.* 2007, *30* (4), 379-386.
[7] Qian, D.; Dickey, E. C.; Andrews, R.; Rantell, T., Load transfer and deformation mechanisms in carbon nanotube-polystyrene composites. *Appl. Phys. Lett.* 2000, *76* (20), 2868-2870.
[8] Diez-Pascual, A. M.; Naffakh, M.; Gomez, M. A.; Marco, C.; Ellis, G.; Gonzalez-Dominguez, J. M.; Anson, A.; Martinez, M. T.; Martinez-Rubi, Y.; Simard, B.; Ashrafi, B., The influence of a compatibilizer on the thermal and dynamic mechanical properties of PEEK/carbon nanotube composites. *Nanotechnology* 2009, *20* (31), 5707-5720.
[9] Cochet, M.; Maser, W. K.; Benito, A. M.; Callejas, M. A.; Martinez, M. T.; Benoit, J. M.; Schreiber, J.; Chauvet, O., Synthesis of a new polyaniline/nanotube composite: "in-situ" polymerisation and charge transfer through site-selective interaction. *Chem. Commun.* 2001, (16), 1450-1451.
[10] Viswanathan, G.; Chakrapani, N.; Yang, H. C.; Wei, B. Q.; Chung, H. S.; Cho, K. W.; Ryu, C. Y.; Ajayan, P. M., Single-step in situ synthesis of polymer-grafted single-wall nanotube composites. *J. Am. Chem. Soc.* 2003, *125* (31), 9258-9259.
[11] Cao, L.; Chen, H. Z.; Wang, M.; Sun, J. Z.; Zhang, X. B.; Kong, F. Z., Photoconductivity study of modified carbon nanotube/oxotitanium phthalocyanine composites. *J. Phys. Chem. B* 2002, *106* (35), 8971-8975.
[12] Shvartzman-Cohen, R.; Levi-Kalisman, Y.; Nativ-Roth, E.; Yerushalmi-Rozen, R., Generic approach for dispersing single-walled carbon nanotubes: The strength of a weak interaction. *Langmuir* 2004, *20* (15), 6085-6088.

adsorbed on the SWCNT surface after the dispersion process,[13] which may become useful if the dispersant provides additional advantages for the SWCNT further applications.

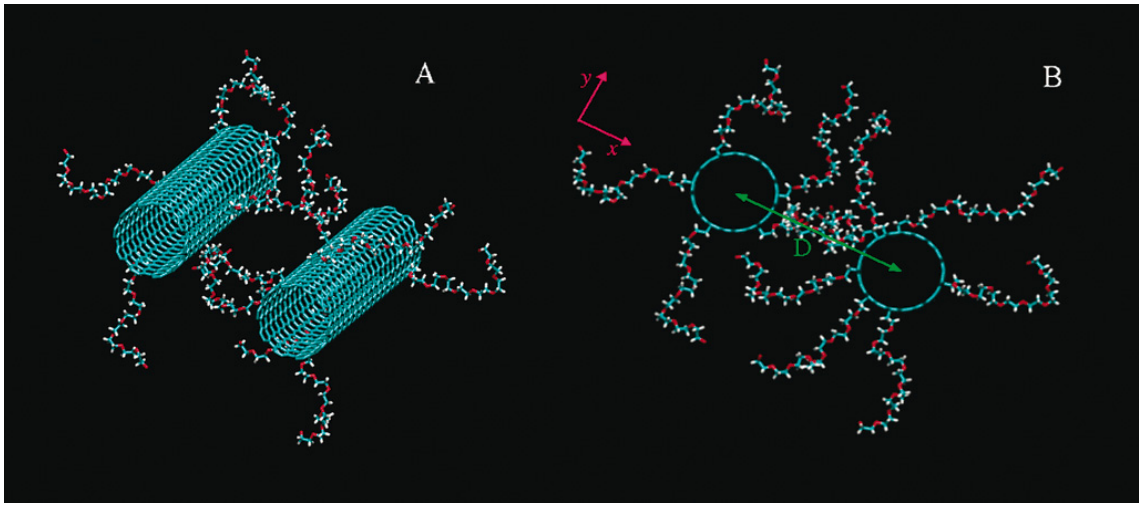

Figure 3.1. Schematic illustration of PEO-decorated SWCNTs, showing the repulsive interaction spawned by the dispersing polymer in (A) perspective view, and (B) projection in the perpendicular plane of A. Image taken from Ref. 16

There are two main groups of polymers used to disperse and non-covalently modify CNTs:[14] those whose interactions with CNTs alter their electronic structure, and those which mainly modify the intertube interactions (from strongly attractive to repulsive) by physical and entropic actuation. Regarding the latter ones, pure homopolymeric chains could disperse and sterically interact with SWCNTs for their further use as fillers in polymer matrices, being the compatibilization effect dependent on the choice of the dispersing agent. On the other hand, BCs have been proven to be excellent promoters of wetting and adhesion. Choosing a BC with one of the blocks chemically compatible with the target matrix, the other block more compatible with SWCNTs, and co-dispersing them, provides a way to prepare SWCNT – Polymer nanocomposites with a good dispersion state.[15] It is remarkable the role of the BC

[13] Bandyopadhyaya, R.; Nativ-Roth, E.; Regev, O.; Yerushalmi-Rozen, R., Stabilization of individual carbon nanotubes in aqueous solutions. *Nano Lett.* 2002, *2* (1), 25-28.
[14] Szleifer, I.; Yerushalmi-Rozen, R., Polymers and carbon nanotubes - dimensionality, interactions and nanotechnology. *Polymer* 2005, *46* (19), 7803-7818.
[15] Yerushalmi-Rozen, R.; Szleifer, I., Utilizing polymers for shaping the interfacial behavior of carbon nanotubes. *Soft Matter* 2006, *2* (1), 24-28.

solvent in the previous dispersion stage which, if chosen properly, could selectively dissolve the blocks, affecting to surface interactions in a very specific way.

In addition to the steric stabilization and debundling, the non-covalent interaction of SWCNTs with such dispersing agents leads to a certain degree of purification, based on the fact that the surfactant action allows the selective isolation of SWCNTs from their colloidal mixtures,[16] mainly composed of amorphous and graphitic carbon particles and remaining metal catalysts. This effect can be maximized when combining the dispersion with centrifugation cycles.[17] Thus, a multipurpose approach can be conceived dealing with non-covalent interactions between SWCNTs and targeted polymers which would enable a SWCNT compatibilization effect in specific polymer matrices, coupled to the SWCNT debundling and removal of undesired impurities.

In the present chapter, the selective dispersion of SWCNTs based on non-covalent interactions is addressed by using thermoplastics and BCs especially chosen for further SWCNT integration into specific polymers. The development of high-performance polymer/SWCNT composite materials is envisioned.

3.1.2. Non-covalent interactions of SWCNTs toward PEEK matrix

Thermoplastic polymers can be used as dispersants and wrapping agents to obtain a specific filler for further development of nanocomposite materials with another thermoplastic matrix. The wrapping thermoplastics must be chosen attending to their compatibilization effect toward thermoplastic matrices of interest, which is determined by the chemical nature of the monomeric unity. The wrapping of SWCNTs in thermoplastic polymers is used for the preparation of high-performance poly(ether ether ketone) (PEEK) – based nanocomposite materials. Thermoplastic wrapping polymers with aromatic residues and oxygen groups have been selected due to their structural similarity and chemical affinity to the target matrix (Figure 3.2).

[16] Shvartzman-Cohen, R.; Nativ-Roth, E.; Baskaran, E.; Levi-Kalisman, Y.; Szleifer, I.; Yerushalmi-Rozen, R., Selective dispersion of single-walled carbon nanotubes in the presence of polymers: the role of molecular and colloidal length scales. *J. Am. Chem. Soc.* 2004, *126* (45), 14850-14857.
[17] Anson-Casaos, A.; Gonzalez-Dominguez, J. M.; Martinez, M. T., Separation of single-walled carbon nanotubes from graphite by centrifugation in a surfactant or in polymer solutions. *Carbon* 2010, *48* (10), 2917-2924.

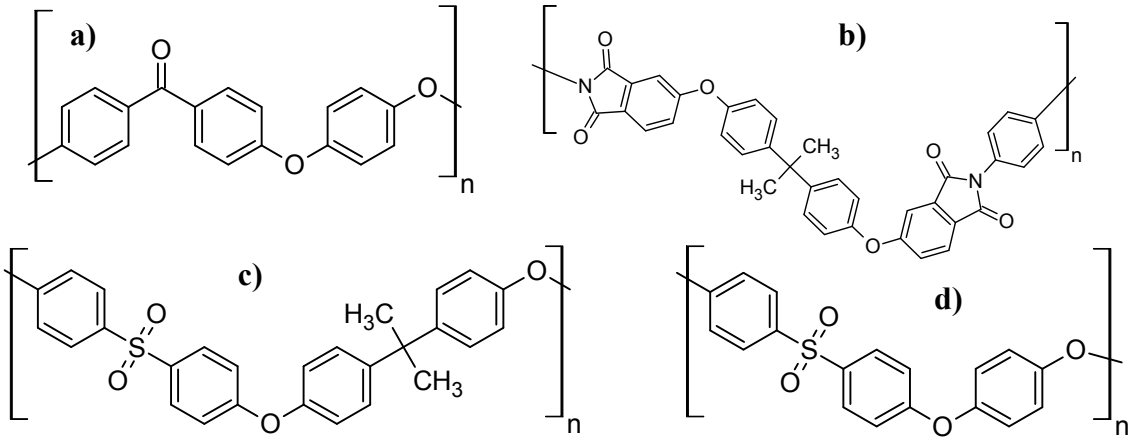

Figure 3.2. Chemical structures of thermoplastic polymers a) Poly(ether ether ketone), PEEK; b) Polyetherimide, PEI; c) Poly(bisphenol-A ether sulfone), PSF; and d) Poly(1,4-phenylene ether ether sulfone), PEES.

Polyetherimide (PEI, Figure 3.2b) is an amorphous amber-coloured polymer that is miscible with[18-20] and structurally similar to PEEK (Figure 3.2a). It has been selected as a compatibilizer due to its high hydrophobic character, commercial availability and chemical compatibility with both components of the composite. In addition, it presents excellent mechanical properties, even at elevated temperature, and exceptional thermo-oxidative stability,[21] which causes the enhancement of the PEEK matrix thermal features.[20] Over the last decades, several papers related to the morphological[19,22] and thermal[18,20,23,24] characterization of PEEK/PEI mixtures have been published. Furthermore, some studies dealing with PEI-based composites have been recently reported, the most relevant being those published by Rath et al,[25,26] where the compatibilizing effect of a third component on liquid crystal polymer/PEI blends has

[18] Crevecoeur, G.; Groeninckx, G., Binary blends of poly(ether ether ketone) and poly(ether imide) - miscibility, crystallization behavior, and semicrystalline morphology. *Macromolecules* 1991, *24* (5), 1190-1195.
[19] Hudson, S. D.; Davis, D. D.; Lovinger, A. J., Semicrystalline morphology of poly(aryl ether ether ketone) poly(ether imide) blends. *Macromolecules* 1992, *25* (6), 1759-1765.
[20] Ramani, R.; Alam, S., Composition optimization of PEEK/PEI blend using model-free kinetics analysis. *Thermochim. Acta* 2010, *511* (1-2), 179-188.
[21] Yano, K.; Usuki, A.; Okada, A.; Kurauchi, T.; Kamigaito, O., synthesis and properties of polyimide clay hybrid. *J. Polym. Sci. A-Polym. Chem.* 1993, *31* (10), 2493-2498.
[22] Bicakci, S.; Cakmak, M., Development of structural hierarchy during uniaxial drawing of PEEK/PEI blends from amorphous precursors. *Polymer* 2002, *43* (1), 149-157.
[23] Jenkins, M. J., Crystallisation in miscible blends of PEEK and PEI. *Polymer* 2001, *42* (5), 1981-1986.
[24] Bicakci, S.; Cakmak, M., Kinetics of rapid structural changes during heat setting of preoriented PEEK/PEI blend films as followed by spectral birefringence technique. *Polymer* 2002, *43* (9), 2737-2746.
[25] Rath, T.; Kumar, S.; Mahaling, R. N.; Mukherjee, M.; Das, C. K.; Pandey, K. N.; Saxena, A. K., The flexible PEI composites. *Polym. Compos.* 2006, *27* (5), 533-538.
[26] Rath, T.; Kumar, S.; Mahaling, R. N.; Khatua, B. B.; Das, C. K.; Yadaw, S. B., Mechanical, morphological and thermal properties of in situ ternary composites based on poly(ether imide), silicone rubber and liquid crystalline polymer. *Mater. Sci. Eng. A* 2008, *490* (1-2), 198-207.

been investigated. Nevertheless, PEI had never been used as a compatibilizer for polymer/SWCNT composites. The bisphenol-A and phenyl moieties of PEI would strongly interact with the matrix chains due to their chemical similarity, as well as with SWCNTs due to π-π interactions of its aromatic rings with the sp^2-bonded carbon hexagonal networks. Moreover, the PEI imide rings have high polarity and are able to undergo polar interactions (e.g. dipole-dipole interactions or hydrogen bonds) with the oxygen groups of SWCNTs, either native or induced by chemical treatments. The aforementioned selective affinities enhance the interfacial adhesion between the SWCNTs and the matrix, hence the resulting properties of the nanocomposites.

Polysulfones are high performance amorphous thermoplastics well known for their toughness and stability at high temperatures.[27] Transparent, rigid and high-strength polymers, they exhibit excellent impact resistance over a wide temperature range and are highly resistant to water, steam, acids and oxidizing agents.[28] Their structure is formed by a monomeric unit which contains phenyl, ether and sulfone moieties. The phenyl rings give thermal stability to the polymer, enhanced by the high degree of resonant stabilization. Sulfone groups are electron-withdrawers, and their proximity to benzene rings provides high thermal and oxidative resistances.[29] The ether groups confer some flexibility, which leads to an inherent toughness.[29] These thermoplastics, widely used for medical and household applications, are also employed in the electronics and automotive industries. In this thesis, they were chosen as compatibilizers due to their similar structure to the PEEK matrix, miscibility with it at a very low polysulfone content,[30] chemical compatibility with both components of the composite and solubility in common organic solvents. The sp^2 hexagonal networks of the SWCNTs are expected to undergo π interactions with the aromatic moieties of the polysulfones. Furthermore, the oxygen groups (mainly carboxylic, but also others as phenol or aldehyde) generated onto the surface and tips of acid-treated SWCNTs are capable of forming strong hydrogen bonds with the highly polar segments of the

[27] Nandan, B.; Kandpal, L. D.; Mathur, G. N., Poly(ether ether ketone)/poly(aryl ether sulphone) blends: thermal degradation behavior. *Eur. Polym. J.* 2003, *39* (1), 193-198.
[28] Summers, G. J.; Ndawuni, M. P.; Summers, C. A., Chemical modification of polysulfone: anionic synthesis of dipyridyl functionalized polysulfone. *Polymer* 2001, *42* (2), 397-402.
[29] Balashova, I. M.; Danner, R. P.; Puri, P. S.; Duda, J. L., Solubility and diffusivity of solvents and nonsolvents in polysulfone and polyetherimide. *Ind. Eng. Chem. Res.* 2001, *40* (14), 3058-3064.
[30] Ni, Z., The preparation, compatibility and structure of PEEK–PES blends. *Polym. Adv. Technol.* 1994, *5* (9), 612-614.

polysulfone chains. Likewise, the phenyl and bisphenol-A moieties of the compatibilizers would interact with the polymer matrix through π-π stacking. Therefore, the dual affinity of the polysulfones with the filler and matrix is expected to rule the wrapping process and the compatibilization effect. In the literature, several papers have been focused on the morphological,[30] thermal[27] and mechanical characterization[31] of PEEK/Polysulfones mixtures. However, there is no previous attempt to employ this family of thermoplastics as compatibilizers for polymer/CNT composites.

3.1.3. Non-covalent interactions of SWCNTs toward epoxy nanocomposites

PEO-based BCs have been selected for their compatibility with epoxy matrices in the present thesis. BCs have attracted special attention in toughening epoxy resins, since when blended with epoxy systems they generate self-assembled nanostructures that mitigate brittleness of the cured resin.[32,33] The self-assembly process is possible due to the coexistence of a resin-miscible "epoxyphilic" block with a less miscible "epoxyphobic" block. The epoxyphilic block is typically PEO which is fully miscible with epoxy monomers. Polypropylenoxide (PPO),[34] poly(ethylene-*alt*-propylene)[35] or even fluorinated blocks[36] are typically used as the epoxyphobic block. High epoxyphilic block volume fractions lead to the formation of vesicular morphologies in epoxies, even at very low BC loadings.[37] These micelles and vesicles lead to mechanical improvements (higher fracture resistance)[38] and changes in the glass transition

[31] Shibata, M.; Fang, Z. J.; Yosomiya, R., A study of blends of poly(ether ether ketone ketone) and poly(ether sulphone): Effect of the addition of poly(ether ether ketone) oligomer. *Polym. Polym. Compos.* 1996, *4* (7), 483-488.
[32] Ruzette, A. V.; Leibler, L., Block copolymers in tomorrow's plastics. *Nat. Mater.* 2005, *4* (1), 19-31.
[33] Ruiz-Perez, L.; Royston, G. J.; Fairclough, J. P. A.; Ryan, A. J., Toughening by nanostructure. *Polymer* 2008, *49* (21), 4475-4488.
[34] Mijovic, J.; Shen, M. Z.; Sy, J. W.; Mondragon, I., Dynamics and morphology in nanostructured thermoset network/block copolymer blends during network formation. *Macromolecules* 2000, *33* (14), 5235-5244.
[35] Dean, J. M.; Verghese, N. E.; Pham, H. Q.; Bates, F. S., Nanostructure toughened epoxy resins. *Macromolecules* 2003, *36* (25), 9267-9270.
[36] Ocando, C.; Serrano, E.; Tercjak, A.; Peña, C.; Kortaberria, G.; Calberg, C.; Grignard, B.; Jerome, R.; Carrasco, P. M.; Mecerreyes, D.; Mondragon, I., Structure and properties of a semifluorinated diblock copolymer modified epoxy blend. *Macromolecules* 2007, *40* (11), 4068-4074.
[37] Dean, J. M.; Lipic, P. M.; Grubbs, R. B.; Cook, R. F.; Bates, F. S., Micellar structure and mechanical properties of block copolymer-modified epoxies. *J. Polym. Sci. B-Polym. Phys.* 2001, *39* (23), 2996-3010.
[38] Dean, J. M.; Grubbs, R. B.; Saad, W.; Cook, R. F.; Bates, F. S., Mechanical properties of block copolymer vesicle and micelle modified epoxies. *J. Polym. Sci. B-Polym. Phys.* 2003, *41* (20), 2444-2456.

temperature.[39] Some studies have revealed a thermo-reversible response of BC/epoxy systems.[40]

In SWCNT-based nanocomposite materials there is special concern about improving dispersion and interfacial adhesion between the nanotubes and the polymer matrix. BCs have been shown to be excellent dispersing agents for SWCNTs.[14] The difference in lyophilicity between blocks provides a suitable means for SWCNT integration into epoxy resins by exploiting the selective interactions of lyophobic blocks with SWCNTs and the lyophilic interaction of the resin with PEO blocks. There have been very few attempts in incorporating BC-dispersed CNTs into epoxy resins; Disperbyk-2150 has been used as the BC for multi-walled carbon nanotubes dispersion.[41-43] The chemical composition of the different blocks in this BC is unknown, and as a consequence, their affinities for epoxy or nanotubes, respectively remain also unexplained. A recent work reports the use of CNTs grafted with a synthetic acrylic-based diblock copolymer to enhance their dispersion into an epoxy matrix.[44]

For the preparation of nanocomposite materials based on an epoxy system, specific BCs have been selected with one of its blocks being PEO and with a particular lyophilicity difference between blocks within the BC chains (Figure 3.3). BCs based on PEO and PPO have been employed (Figure 3.3a and b), with two different block compositions. On the one hand, the diblock copolymer (referred to as PEO-*b*-PPO) and, on the other hand, the triblock PEO-*b*-PPO-*b*-PEO copolymer (referred to as its commercial name, Pluronic). The third BC used in this thesis was selected with a more hydrophobic block to produce a higher lyophilicity difference with PEO. This has been accomplished by using polyethylene (PE) as de adjacent block in the BC (Figure 3.3c).

[39] Thio, Y. S.; Wu, J. X.; Bates, F. S., Epoxy toughening using low molecular weight poly(hexylene oxide)-poly(ethylene oxide) diblock copolymers. *Macromolecules* 2006, *39* (21), 7187-7189.
[40] Tercjak, A.; Larrañaga, M.; Martin, M. D.; Mondragon, I., Thermally reversible nanostructured thermosetting blends modified with poly(ethylene-b-ethylene oxide) diblock copolymer. *J. Therm. Anal. Calorim.* 2006, *86* (3), 663-667.
[41] Li, Q. Q.; Zaiser, M.; Koutsos, V., Carbon nanotube/epoxy resin composites using a block copolymer as a dispersing agent. *Phys. Stat. Sol. A* 2004, *201* (13), R89-R91.
[42] Cho, J.; Daniel, I. M., Reinforcement of carbon/epoxy composites with multi-wall carbon nanotubes and dispersion enhancing block copolymers. *Scripta Mater.* 2008, *58* (7), 533-536.
[43] Cho, J.; Daniel, I. M.; Dikin, D. A., Effects of block copolymer dispersant and nanotube length on reinforcement of carbon/epoxy composites. *Compos. Part A* 2008, *39* (12), 1844-1850.
[44] Gilbert, A. C. C.; El Bounia, N. E.; Pere, E.; Billon, L.; Derail, C., Dispersion improvement of carbon nanotubes in epoxy resin using amphiphilic block copolymers, *Advances in Structural Analysis of Advanced Materials*, Karama, M.,Ed. Trans Tech Publications Ltd: Stafa-Zurich, 2010;Vol.112,pp 29-36.

This BC will be referred to as PEO-*b*-PE. All these BCs are commercially available and water-soluble, which provides additional advantages for their further use.

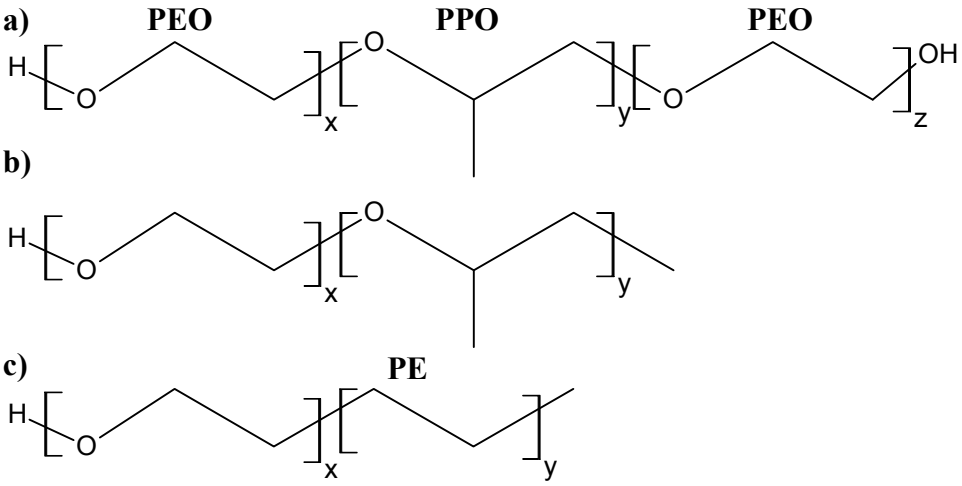

Figure 3.3. Chemical structures of the different BCs employed in this thesis, based on PEO. a) Pluronic, b) PEO-*b*-PPO, c) PEO-*b*-PE.

3.1.4. SWCNT dispersion and wrapping

The evaluation of the SWCNTs outcome (in terms of their physical state, purity, etc.) after inducing non-covalent interactions with the selected wrapping agents is described in this chapter. Unfortunately, there is a lack of standards and uniform characterization methods to unambiguously determine a successful CNT dispersion.[45] This is a general concern that can be overcome by the convolution of many analytical techniques that individually provide particular insights into the dispersion state. Each technique has its own limitations, but combining different techniques, the SWCNT dispersion and wrapping can be reasonably assessed. Besides, extensive theoretical and semi-empiric parameters could be calculated in order to quantify or predict the state of dispersion of CNTs (as the Flory-Huggins or DLVO theories).[45,46] Among the numerous available techniques capable of evaluating dispersion and wrapping of CNTs, this thesis will focus on the following:

[45] Green, M. J., Analysis and measurement of carbon nanotube dispersions: nanodispersion versus macrodispersion. *Polym. Int.* 2010, *59* (10), 1319-1322.
[46] Coleman, J. N., Liquid-Phase Exfoliation of Nanotubes and Graphene. *Adv. Funct. Mater.* 2009, *19* (23), 3680-3695.

- X-Ray diffraction (XRD): As commented in the former chapter, powder XRD is a useful bulk technique to qualitatively observe not only the presence of carbonaceous and metallic impurities, but also the bundling of individual SWCNTs. The hexagonal crystal lattice typical of SWCNT bundles appear at low diffraction angles (typically at 2θ ~ 10º, 16º and 20º).[3,12] The disappearance of these peaks can be attributed to the debundling of SWCNTs, likely by the steric stabilization of individual tubes in a successful dispersion.
- Transmission electron microscopy (TEM): As a microscopic technique, it only allows observing small regions of the filler but it reveals the true state of the sample. The wrapping of SWCNTs by the dispersing polymer can directly be seen. With observations in many zones, and with the complement of other techniques, TEM provides very useful insights but with time-consuming and often expensive means. Important caution must be taken in the sample preparation to avoid re-aggregation of the sample;[45] diluted suspensions are desirable to minimize this effect.
- Raman spectroscopy: The radial breathing mode (RBM) bands of SWCNTs are very sensitive to the environment of individual tubes; in fact, RBM bands are very likely to be much influenced by the nanotubes packing, doping and wrapping.[47,48] An upshift in the RBM peaks has been stated as an effect of polymer intercalation between individual SWCNTs within a bundle.[49]
- NIR spectroscopy: The purity index (PI) can be obtained from this technique, as stated by Itkis and co-workers[50] (see section 2.1.2).
- Zeta potential: The repulsive forces between individual SWCNTs during a liquid-phase dispersion can be also due (apart from steric considerations) to electrostatic repulsions caused by the polar segments or ionizable groups contained in the dispersant. This repulsion is also effective in preventing re-

[47] Rols, S.; Righi, A.; Alvarez, L.; Anglaret, E.; Almairac, R.; Journet, C.; Bernier, P.; Sauvajol, J. L.; Benito, A. M.; Maser, W. K.; Munoz, E.; Martinez, M. T.; de la Fuente, G. F.; Girard, A.; Ameline, J. C., Diameter distribution of single wall carbon nanotubes in nanobundles. *Eur. Phys. J. B* 2000, *18* (2), 201-205.
[48] Britz, D. A.; Khlobystov, A. N., Noncovalent interactions of molecules with single walled carbon nanotubes. *Chem. Soc. Rev.* 2006, *35* (7), 637-659.
[49] Valentini, L.; Biagiotti, J.; Kenny, J. M.; Santucci, S., Morphological characterization of single-walled carbon nanotubes-PP composites. *Compos. Sci. Technol.* 2003, *63* (8), 1149-1153.
[50] Itkis, M. E.; Perea, D. E.; Niyogi, S.; Rickard, S. M.; Hamon, M. A.; Zhao, B.; Haddon, R. C., Purity evaluation of as-prepared single-walled carbon nanotube soot by use of solution-phase near-IR spectroscopy. *Nano Lett.* 2003, *3* (3), 309-314.

aggregation of SWCNTs even at short distances, hence leading to a high-quality dispersion. The zeta potential allows quantifying this electrostatic repulsion since it correlates with the dispersion quality in cases where this repulsion is important.[46] The nature of the zeta potential arises from the double electrical layer formed during the electrostatic or polar stabilization of SWCNTs, and, it can be indirectly measured by dynamic light scattering (DLS) on diluted suspensions. A successful and stable-in-time suspension of SWCNTs is typically achieved for zeta values of around 20 mV or higher (in absolute value), in cases where the system has major electrostatic contributions. With only polar interactions the zeta value can be lower, but other contributions different from electrostatic stabilizations (i.e. steric effects) could contribute to the stability and they are not quantified by this parameter. With this experimental technique particle size distribution is intrinsically obtained, which provides additional information in the quality and state of SWCNT dispersion. This technique is known for being rapid and effective.[45]

- Thermogravimetric analysis (TGA): The amount of wrapping polymers adsorbed on the SWCNTs surface can be quantified by TGA. The selective pyrolisis of the polymer in inert atmosphere at moderate temperatures (typically above 300ºC) can be used to estimate the weight loss associated with the remaining dispersant. For polymers with a high content on aromatic moieties, this technique is somewhat more difficult to apply since they tend to leave a noticeable amount of solid residue, which must be taken into account in the estimation.

3.2. Experimental section

3.2.1. Materials and reagents

For the preparation of BC-wrapped SWCNTs, nanotubes were produced at the Instituto de Carboquimica (ICB-CSIC), Zaragoza, by the arc discharge method (100A,

20V), using a Ni/Y mixture as catalysts under 660mb of helium.[51,52] For the preparation of SWCNTs wrapped by thermoplastic polymers, laser-grown SWCNTs were also employed. These were prepared at the Steacie Institute for Molecular Sciences (SIMS-NRC), Canada, using an approach to the two-laser synthesis method.[53]

The thermoplastic wrapping polymers and BCs were all purchased from different commercial sources. **PEI**, was provided by Sigma-Aldrich in pellet form (M_w ~ 30,000 g·mol^{-1}, T_g = 217 ºC, $d_{25ºC}$ = 1.27 g·cm^{-3}, batch #17030PD). **PSF** (M_n ~ 22,000 g·mol^{-1}, T_g = 190ºC, $d_{25ºC}$ = 1.24 g·cm^{-3}, batch #06222AR), and **PEES** (M_w ~ 38,000 g·mol^{-1}, T_g = 192ºC, $d_{25ºC}$ = 1.37 g·cm^{-3}, batch #14814JN), were also provided by Sigma–Aldrich in pellet form. **Pluronic F-68** (EO_{76}-PO_{29}-EO_{76}, M_w ~ 8,400 g·mol^{-1}, batch #027K0027, waxy powder) and **PEO-*b*-PE** (M_n ~ 2,250 g·mol^{-1}, $d_{25ºC}$ = 1.05 g·cm^{-3}, batch #04015HD, lentil form), were purchased from Sigma-Aldrich, while **PEO-*b*-PPO** (M_w ~ 8,750 g·mol^{-1}, batch #402512, waxy powder) was acquired from PolySicences Inc.

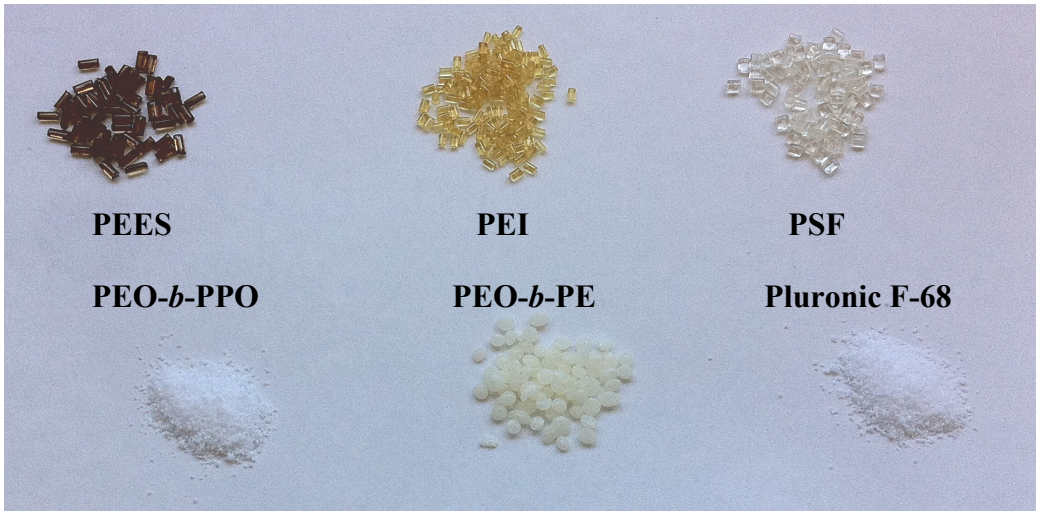

Figure 3.4. Real images of the wrapping agents employed in the present thesis.

[51] Journet, C.; Maser, W. K.; Bernier, P.; Loiseau, A.; delaChapelle, M. L.; Lefrant, S.; Deniard, P.; Lee, R.; Fischer, J. E., Large-scale production of single-walled carbon nanotubes by the electric-arc technique. *Nature* 1997, *388* (6644), 756-758.
[52] Benito, A. M.; Maser, W. K.; Martinez, M. T., Carbon nanotubes: from production to functional composites. *Int. J. Nanotechnol.* 2005, *2* (1-2), 71-89.
[53] Kingston, C. T.; Jakubek, Z. J.; Denommee, S.; Simard, B., Efficient laser synthesis of single-walled carbon nanotubes through laser heating of the condensing vaporization plume. *Carbon* 2004, *42* (8-9), 1657-1664.

Ultrasounds bath (45 kHz Branson 3510) and/or ultrasonic tip (Hielscher DRH-P400S; 400W maximum power; 24 kHz maximum frequency at 60% amplitude and 50% cycle time) were employed for sonication unless otherwise stated.

3.2.2. Experimental procedures

3.2.2.1. Wrapping of SWCNTs in thermoplastic polymers

This wrapping was conducted in liquid media using organic solvents. For the preparation of PEI-wrapped SWCNTs, arc-grown SWCNTs (PI = 0.037) were treated in a reflux of HNO_3 1.5 M, at 150 ºC for 2h, and then centrifuged. This process reduced their metal content by approximately 75%, and caused nearly two-fold increase in PI, which demonstrates the effectiveness of the purification step. During the treatment, oxygenated groups are formed which increase the polar character of the CNTs and therefore improve the anchoring of compatibilizers and their adhesion to the polymer matrix. More details on the experimental procedure of acid treatment and the characterization of oxidized SWCNTs are given in sections 2.2.2.1 and 2.3.2 respectively. Laser-grown SWCNTs were used without further purification. Then, 25 mL of a PEI chloroform solution (1.5% w/w) was mixed with ~370 mg of SWCNTs (either laser as grown or acid treated arc discharge) with bath sonication for 5 min. Each mixture was treated with ultrasonic tip for 60 min. The resulting dispersion was observed to be highly stable. Subsequently, it was filtered using a 0.2 μm pore size PTFE membrane and dried under vacuum at 60ºC for 2h to assure total evaporation of the solvent. In order to homogenize the particle size, the resulting solid was milled in an agate mortar.

For the wrapping of SWCNTs with PEES and PSF, the arc-grown material was subjected to a more aggressive oxidation treatment. These SWCNTs were purified following an experimental procedure inspired in the method developed by Yu et al.[54] Arc SWCNTs were refluxed in HNO_3 7M at 150ºC for 4h.* The resulting mixture was bath sonicated for 30min, and centrifuged at 3,500 rpm for 15min. The supernatant was decanted off, and the sediments were re-dispersed in H_2O/HCl at pH ~ 2. Centrifugation

[54] Yu, A. P.; Bekyarova, E.; Itkis, M. E.; Fakhrutdinov, D.; Webster, R.; Haddon, R. C., Application of centrifugation to the large-scale purification of electric arc-produced single-walled carbon nanotubes. *J. Am. Chem. Soc.* 2006, *128* (30), 9902-9908.

was repeated twice to maximize the removal of amorphous carbon impurities.[55] The final sediment was redispersed in deionized water, sonicated for 3h, and centrifuged at 13,000 rpm several times. The resulting SWCNT dispersions were observed to be stable for several weeks;[56] they were filtered through 1.2μm pore size polycarbonate membranes, dried in an oven at 80–100ºC, and milled in an agate mortar. As stated before, the carboxylic groups counteract the van der Waals attractive forces between CNTs and increase their polar character, which enhances the anchoring of compatibilizers and their integration into the polymer matrix. Laser-grown SWCNTs were again used without further purification.

The wrapping was performed in organic media: 25 mL of a PSF 1,4-dioxane or PEES 1-methyl-2-pyrrolidone (NMP) solution (both at 1.5% w/w) were mixed with ~260 mg of SWCNTs (either laser as-grown or acid treated arc-discharge) with bath sonication for 5min. Each mixture was treated with ultrasonic tip for 60 min. The resulting dispersion was observed to be highly stable. Then it was filtered using a 0.1 μm pore size PTFE membrane and finally dried under vacuum at 60ºC during 2 or 24h (for 1,4-dioxane or NMP, respectively) to assure evaporation of the solvent. In order to homogenize the particle size, the resulting solid was milled in an agate mortar.

It is worth noting that SWCNTs can be dispersed[57] and even exfoliated by sonication and dilution in NMP.[46,58] Nevertheless, the role of the NMP in this work is to allow the wrapping of the SWCNTs by the polysulfones in liquid medium. The sonication process in NMP (or 1,4-dioxane) weakens the intertube interactions, thus facilitating the intercalation of the polymer among the CNT bundles. After the drying

[55] Hu, H.; Yu, A. P.; Kim, E.; Zhao, B.; Itkis, M. E.; Bekyarova, E.; Haddon, R. C., Influence of the zeta potential on the dispersability and purification of single-walled carbon nanotubes. *J. Phys. Chem. B* 2005, *109* (23), 11520-11524.

[56] Anson-Casaos, A.; Gonzalez-Dominguez, J. M.; Terrado, E.; Martinez, M. T., Surfactant-free assembling of functionalized single-walled carbon nanotube buckypapers. *Carbon* 2010,*48*(5),1480-1488.

*** Note:** During the course of the research project in whose framework this thesis work has been developed, the purification method consisting of nitric acid treatment + centrifugation cycles (inspired in reference 54) was tuned up. The work dealing with the SWCNT wrapping in polysulfones was conducted with this kind of purified nanotubes (instead of those formerly used for the wrapping in PEI) since they exhibited higher PIs (PI = 0.075).

[57] Furtado, C. A.; Kim, U. J.; Gutierrez, H. R.; Pan, L.; Dickey, E. C.; Eklund, P. C., Debundling and dissolution of single-walled carbon nanotubes in amide solvents. *J. Am. Chem. Soc.* 2004, *126* (19), 6095-6105.

[58] Giordani, S.; Bergin, S. D.; Nicolosi, V.; Lebedkin, S.; Kappes, M. M.; Blau, W. J.; Coleman, J. N., Debundling of single-walled nanotubes by dilution: Observation of large populations of individual nanotubes in amide solvent dispersions. *J. Phys. Chem. B* 2006, *110* (32), 15708-15718.

step, the solvent is removed, leading to a solid SWCNT dispersion. To assure that the effective debundling attained in the dispersions is promoted by the wrapping in the polysulfones, a control sample was prepared by sonicating under identical conditions a similar amount of acid-treated SWCNTs in this solvent. Upon evaporation of the NMP, the SWCNTs present approximately the same bundle diameter than before the sonication step, which suggests that the debundling is induced by the insertion of the polysulfones among the bundles.

3.2.2.2. Wrapping of SWCNTs in amphiphilic PEO-based BCs

For the wrapping by Pluronic F-68, arc SWCNTs (PI = 0.037) were refluxed in 1.5M HNO_3 as described above for the PEI-wrapped SWCNTs. After that, 25 mL of a Pluronic F68 aqueous solution (20 g/L) to 100 mg of acid treated SWCNTs (PI = 0.050). Tip sonication was applied for 60 min at 50% oscillation amplitude and 50% cycle time. The resulting dispersion was centrifuged at 6,000 rpm during 35min and the supernatant solution was decanted from the sediment. The supernatant was sonicated again for 4h under identical tip conditions. The homogeneity of the dispersion was controlled with optical microscopy (Zeiss AX10 optical microscope) and light scattering (using a Beckman Coulter LS 13 320 equipment, capable of measuring particle sizes from 0.04 to 2000 microns). Light scattering measurements were performed after each hour of tip sonication until a steady average particle size (calculated by modelling the suspended particles as spheres) of 40nm is reached, which is the lower detection limit of the equipment. It was finally filtered at room temperature under vacuum, using 3µm pore size polycarbonate filters. An illustrative scheme for this preparation is shown in Figure 3.5.

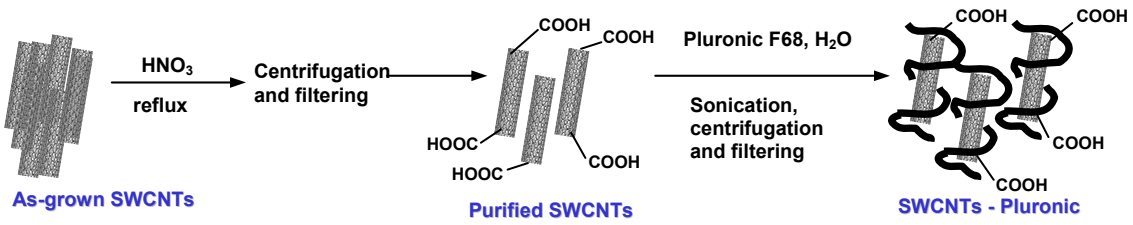

Figure 3.5. Illustrative scheme for the wrapping of SWCNTs in Pluronic F-68

For the preparation of SWCNTs wrapped in PEO-*b*-PPO or PEO-*b*-PE, arc-grown SWCNTs were employed without further treatment. Besides, oxidized SWCNTs were also employed. Oxidized SWCNTs ([ox]-SWCNTs, hereafter) were obtained by thermal treatment of as-grown SWCNTs in air atmosphere at 350ºC for 2h.[59] In a typical experiment, 25mL of 1 wt% aqueous solution of the BC were blended with 100mg of either SWCNTs or [ox]-SWCNTs. The mixture was bath sonicated for 10min and then tip sonicated for 1h. The resulting suspension was centrifuged for 1h at 13,000rpm. The supernatant was decanted off and used for further characterization. Wrapped SWCNTs were obtained after dilution of the supernatant in a 15-fold excess of acetone (wrapped as-grown SWCNTs) or methanol (wrapped [ox]-SWCNTs) and overnight settlement. The observed precipitate was recovered by filtration in a 10μm pore size PTFE membrane, and drying in a vacuum oven at room temperature.

3.2.3. Characterization techniques

►TGA experiments were performed on BC-wrapped SWCNTs under CO_2 atmosphere (60mL/min flow), and heating rate of 5ºC/min by using the same equipment described in section 2.2.3 **(ICB)**. For thermoplastic-wrapped SWCNTs, TGA experiments were carried out using a TA-Q500 thermobalance, at a heating rate of 10ºC/min, under both inert (nitrogen) and oxidizing (dry air) atmospheres under dynamic conditions, from room temperature to 900ºC, with a gas purge rate of 150 mL/min. All the analyses were performed on samples with an average mass of 10mg. **(ICTP)**

► Raman spectroscopy was performed as stated in section 2.2.3. **(ICB)**

►Absorption spectroscopy in the NIR region was measured on the supernatants obtained from the wrapping process in the same equipment described in section 2.2.3. **(ICB)** The sample absorbance was adjusted within the range of 0.4 – 0.5, by dilution with the original 1 wt% BC solution. Background correction was effected with the same solution.

[59] Anson-Casaos, A.; Gonzalez, M.; Gonzalez-Dominguez, J. M.; Martinez, M. T., Influence of Air Oxidation on the Surfactant-Assisted Purification of Single-Walled Carbon Nanotubes. *Langmuir* 2011, *27* (11), 7192-7198.

►TEM micrographies were taken with the equipment described in section 2.2.3. **(UNIZAR)** Samples were prepared by drop casting several diluted supernatant drops on a carbon-coated copper grid.

►XRD was used to characterize crystalline phases. Patterns were collected using a Bruker D8 Advance diffractometer using a Cu tube as X-ray source (λ CuK_α = 1.54 Å) a tube voltage of 40 kV and a current of 40 mA. The results were analyzed with the fitting software Topas 2.1 in Bragg-Brentano geometry in the range 2θ = [3º–60º], with steps of 0.05º and 3 s accumulation time. **(ICB)**

►Zeta potential was measured using a Zetasizer Nano ZS device from Malvern company. The device measures the particle size distribution through the DLS approach by irradiating with a He-Ne laser at 633nm. The Zeta value is internally calculated from the electrophoretical mobility using Henry's equation. Supernatants were measured before filtration by diluting them in deionized water at 1/6 ratio. Measurements were carried out in disposable polystyrene dip cells (code DTS1061). **(ICB)**

►Laser diffraction measurements, in order to elucidate the average particle size were performed by using a Beckman Coulter LS 13 320 equipment, capable of measuring particle sizes from 0.04 to 2000 microns. A ~50mL aliquot of the liquid supernatant after centrifugation was systematically diluted with deionised water until achieving sufficient optical transparency; then, measurements are taken at regular time intervals enough number of times to assure data repeatability. **(ICB)**

3.3. Results and discussion

3.3.1. Characterization of thermoplastic-wrapped SWCNTs

TGA under air atmosphere was carried out to obtain information about the thermo-oxidative stability of the SWCNT samples, determine the amount of polymer wrapping in SWCNTs, and determine their metallic residue. The temperatures of maximum rate of weight loss (T_{max}) for the wrapped SWCNTs are collected in Table 3.1. The polymer weight wrapping the SWCNTs in all cases ranges from ~7 – 11 wt%,

being slightly higher for arc SWCNTs, probably due to the acid treatment, which enhances the polar character at the SWCNTs surface.

Table 3.1. TGA characterization parameters for thermoplastic-wrapped SWCNTs

SWCNT Sample	Polymer content (wt%)	Metal residue (wt%)	T_{max} (ºC)*
Laser (as-grown)	-	4-11	493
Arc (as-grown)	-	13-20	459
Arc (purified, PI = 0.050)**	-	3.2	541
Arc (purified, PI = 0.075)***	-	1.8	698
Laser (PEI-wrapped)	6.9	4.1	488
Laser (PEES-wrapped)	8.5	4.1	493
Laser (PSF-wrapped)	7.1	4.3	490
Arc (PEI-wrapped)	8.3	3.3	532
Arc (PEES-wrapped)	11.2	1.7	560
Arc (PSF-wrapped)	9.6	1.8	556

* In air, from room temperature to 900 ºC at a heating rate of 5 ºC/min. T_{max} corresponds to the temperature of maximum rate of weight loss.
** SWCNTs used for wrapping in PEI or Pluronic
*** SWCNTs used for wrapping in PSF or PEES

The T_{max} values in air atmosphere do not significantly change for laser SWCNTs while they visibly decrease in arc SWCNTs upon wrapping in thermoplastics. This could be explained by the previous oxidation of arc SWCNTs. Higher thermo-oxidative stability is associated with purer and less defective materials.[60,61] Moreover, the position of T_{max} peak is also strongly affected by the amount and nature of the metal impurities. The residual mass corresponds to the oxidized catalyst particles, and provides an indication of the abundance of metal in the samples. As expected, purified arc-grown SWCNTs, with lower content of metal impurities, present improved thermo-oxidative stability compared to as-grown laser-SWCNTs.

Figure 3.6 shows TEM images of acid treated arc SWCNTs wrapped in PEI. Small nanotube bundles shrouded in PEI can be visualized in the micrographs.[62] The

[60] Arepalli, S.; Nikolaev, P.; Gorelik, O.; Hadjiev, V. G.; Bradlev, H. A.; Holmes, W.; Files, B.; Yowell, L., Protocol for the characterization of single-wall carbon nanotube material quality. *Carbon* 2004, *42* (8-9), 1783-1791.
[61] Smith, M. R.; Hedges, S. W.; LaCount, R.; Kern, D.; Shah, N.; Huffman, G. P.; Bockrath, B., Selective oxidation of single-walled carbon nanotubes using carbon dioxide. *Carbon* 2003, *41* (6), 1221-1230.
[62] Diez-Pascual, A. M.; Gonzalez-Dominguez, J. M.; Martinez-Rubi, Y.; Naffakh, M.; Anson, A.; Martinez, M. T.; Simard, B.; Gomez, M. A., Synthesis and properties of PEEK/Carbon nanotube

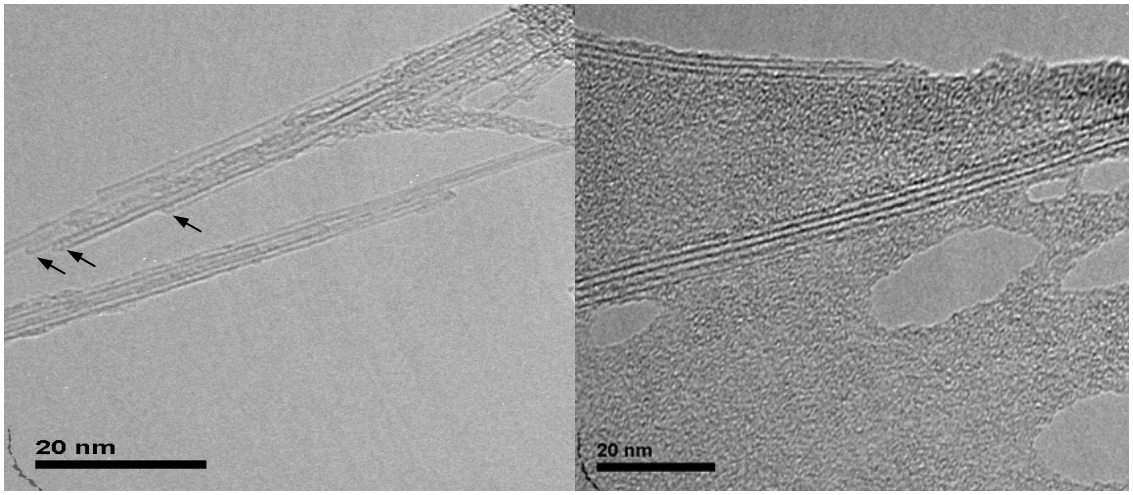

Figure 3.6. TEM images of PEI-wrapped arc SWCNTs.

open ends in the SWCNTs structure (pointed with arrows in Figure 3.6) are a direct consequence of the nitric acid treatment. Typical TEM micrographs of arc-purified and laser-grown SWCNTs wrapped in PEES are displayed in Figure 3.7. Good homogeneity in the dispersions, without agglomerates, was observed from the images; this confirms the efficiency of the wrapping process in liquid media. It is important to notice that the effective debundling attained in the wrapped SWCNTs is caused by the presence of the polysulfone, which impedes the re-aggregation of the nanotubes after the evaporation of the solvent. Small CNT bundles (2–4 individual tubes), which appear as fine stripes, are clearly shrouded in the amorphous polymer. No voids or discontinuities are found between the nanotube and polymer phases; the polysulfone wraps around the bundles forming a tight interfacial layer. In general, wrapped laser-grown SWCNTs present thicker bundles than arc-purified CNTs.

XRD diffractograms for PEI-wrapped and as-grown arc SWCNTs are presented in Figure 3.8. The peaks corresponding to SWCNT bundles (appearing at low diffraction angles[3]), such as that observed at $2\theta = 6^{\circ}$, decreases after the purification and wrapping processes. X-ray diffraction patterns of the different SWCNTs wrapped in polysulfones are shown in Figure 3.9. Intense bundle lattice peaks, appearing at low diffraction angles (see the arrows marked on the plot), can be seen in the diffractogram of pristine laser-grown SWCNTs (Figure 3.9a). The synthesis procedure of these nanotubes provi-

Nanocomposites. In *Polymer Nanotube Nanocomposites*, Wiley, Ed. Scrivener Publishing: Salem, 2010; pp 281-313.

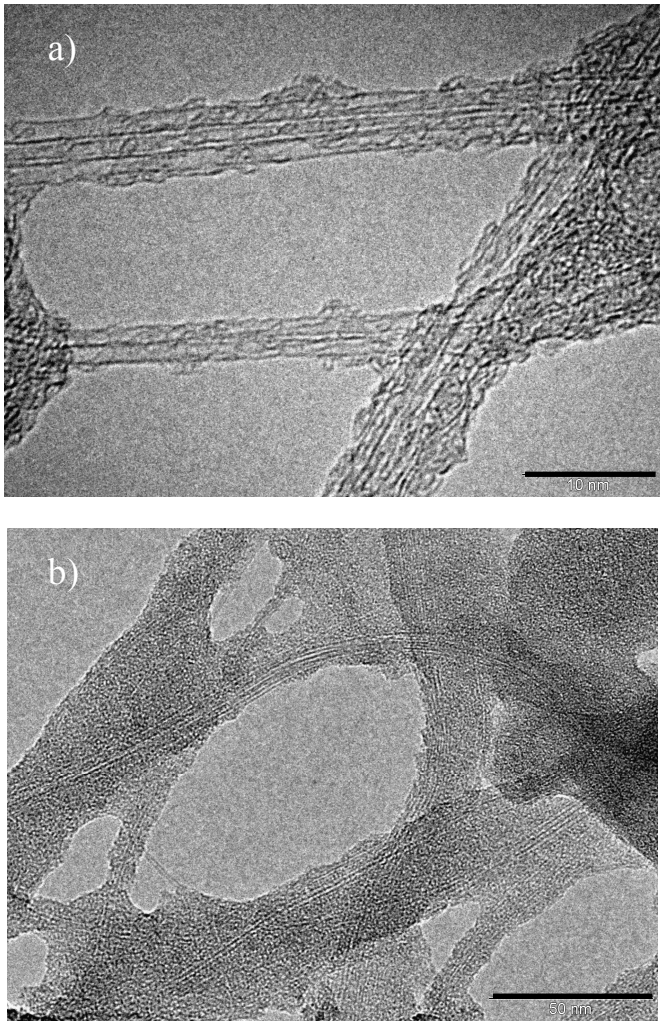

Figure 3.7. TEM images of (a) purified SWCNTs for PEES wrapping, scale bar = 10nm; (b) PEES-wrapped laser SWCNTs, scale bar = 50nm.

des a material with thick rope-like bundles of CNTs which are present since they were used without further purification. The wrapping process in the polysulfones induced nanotube disaggregation, as revealed by the noticeable diminution or disappearance of the bundle peaks. These peak reduction is more pronounced in PEES-wrapped SWCTs. Notice that the main feature bands of the pure polysulfones are low intense and appear in the angular range $2\theta = 17–25^{\circ}$; therefore, they practically do not interfere with the bundle lattice peaks, as seen in Figure 3.9b. In the arc-purified SWCNTs (Figure 3.9b), the absence of metal catalysts diffractions (Ni peaks at $2\theta = 44.4^{\circ}$ and 51.9°) evidences the successful removal of metallic impurities during the purification treatment. Moreover, most of the bundle peaks in the non-wrapped arc-purified SWCNTs could hardly be detected (only a slightly visible maximum at $2\theta = 6^{\circ}$), which might point to a

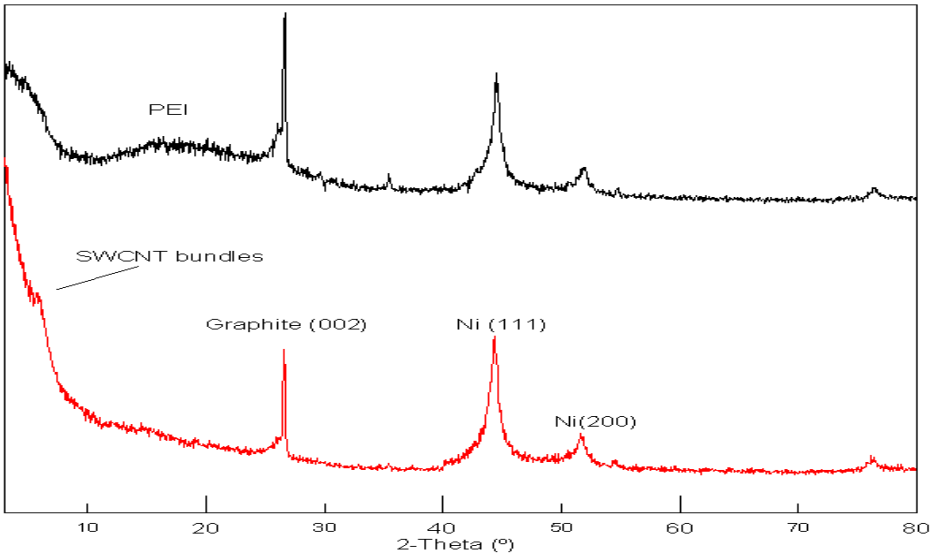

Figure 3.8. XRD plots for as-grown (red) and acid-treated + PEI-wrapped (black) arc SWCNTs

pre-debundling induced by the purification process. The indicated lattice peak practically disappears when the nanotubes are dispersed in PEES. The polysulfone bands seem to contribute slightly to the diffraction pattern of the arc-purified wrapped SWCNTs (Fig. 3.9b), being this influence stronger for those shrouded in PEES, as revealed by the higher intensity ratio of its bands in comparison with the graphite peak ($2\theta = 26.6º$). This is perfectly consistent with the polysulfone content measured by TGA (see Table 3.1). On the whole, the comparison of the different diffractograms indicates that the acid-treated SWCNTs wrapped in the polysulfones and PEI can be considered as efficiently debundled.

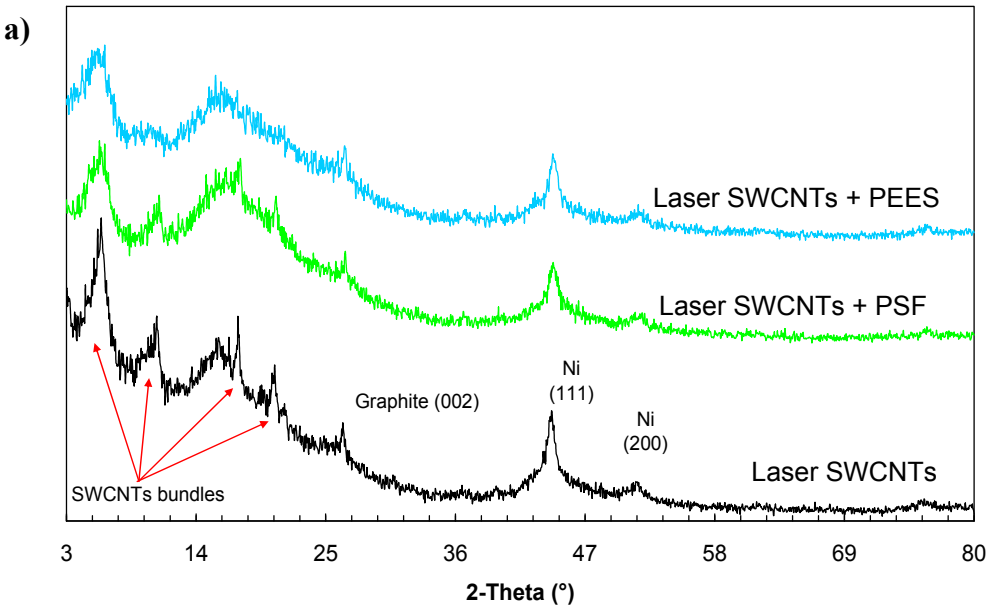

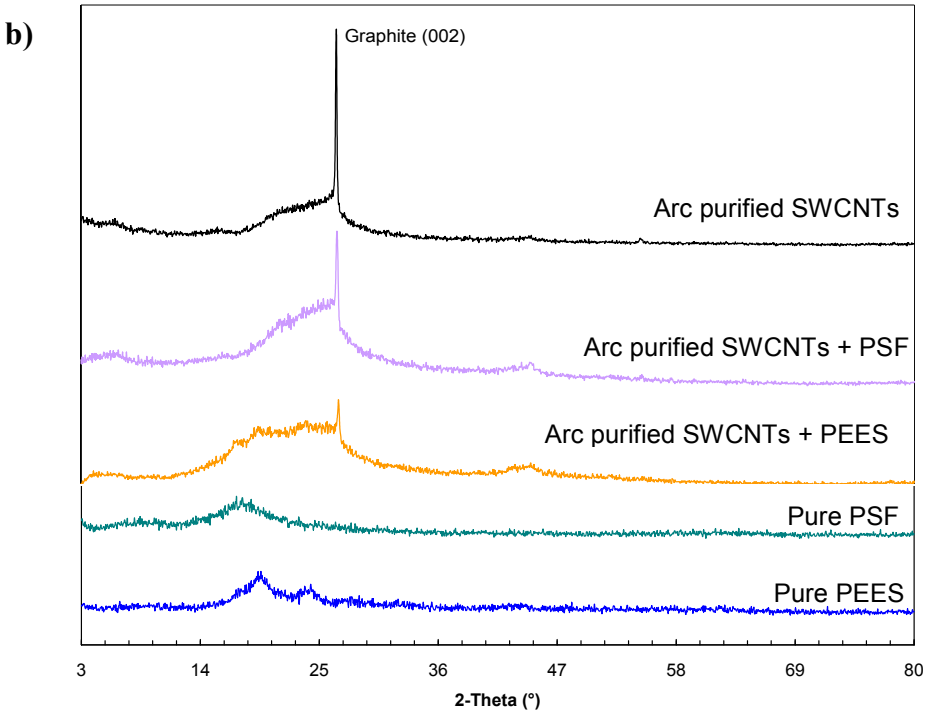

Figure 3.9. X-Ray diffractograms of different arc and laser SWCNT samples wrapped in PEES and PSF.

Raman spectroscopy was also applied to characterize these dispersions. The Raman spectra of the SWCNTs and their dispersions in both polysulfones (Figure 3.10) were recorded to analyze possible changes in the bands due to the CNT disaggregation. All the samples display almost identical spectra, with four main features,[63] as described in section 2.1.2. The Raman spectra of arc-purified (Figure 3.10a) and laser-grown (Figure 3.10b) SWCNTs showed that the dispersion of SWCNTs in both polysulfones produced modifications in the G/D intensity ratios, indicating changes in their vibrational modes. The Raman shift of the RBM is inversely proportional to the SWCNT diameter, and reflects the tube diameter distribution in the SWCNTs excited with this particular wavelength. The position of the RBM, as stated before, has been reported to be strongly influenced by the nanotube packing, doping and wrapping.[47,48] In the case of arc-purified SWCNTs, no appreciable change is found in the RBM after the dispersion process in the thermoplastic polymers, which could be a consequence of the previous shift due to the purification treatment. In contrast, for laser-grown SWCNTs (Figure 3.10c), a pronounced upshift of ~12 cm^{-1} is observed in the maximum RBM pe-

[63] Dresselhaus, M. S.; Dresselhaus, G.; Jorio, A.; Souza, A. G.; Saito, R., Raman spectroscopy on isolated single wall carbon nanotubes. *Carbon* 2002, *40* (12), 2043-2061.

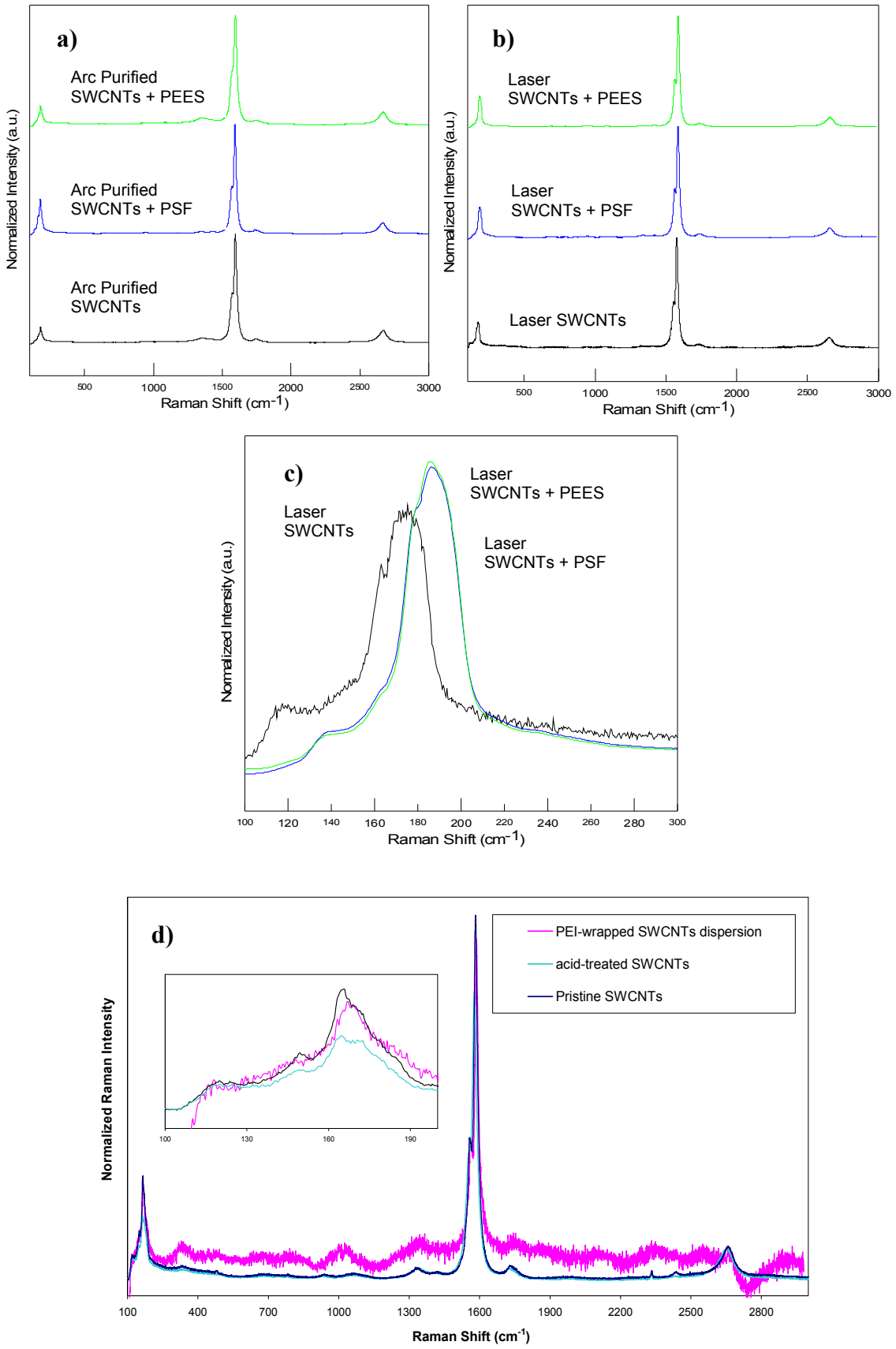

Figure 3.10. Raman spectra of a) arc purified, and b) laser-grown SWCNTs wrapped in PEES and PSF; c) inset containing RBM of Fig. 3.10b; d) Raman spectra of pristine, nitric acid-treated and PEI-wrapped arc SWCNTs, with inset of the RBM bands.

ak from the pristine nanotubes to the polysulfone-wrapped materials. This is a clear indication of the debundling caused by the polysulfones, as this RBM displacement has been previously attributed to a polymer intercalation among individual SWCNTs in a bundle.[49] These observations are in good agreement with those derived from the X-ray diffractograms. A similar discussion (as the aforementioned for the wrapping in polysulfones) can be made in the case of PEI-wrapped SWCNTs (Figure 3.10d).

3.3.2. Characterization of amphiphilic BC-wrapped SWCNTs

3.3.2.1. Dispersions of arc SWCNTs in Pluronic F-68

Good homogeneity in the SWCNTs–Pluronic supernatants was observed by optical microscopy (images not shown), with no appearance of macroscopic agglomerates. Laser diffraction experiments indicated that all particle sizes in the aqueous medium after the whole process were below 40 nm, which was the lower detection limit of the device (see experimental section). However, the particle size measured by DLS exhibited a different result. In DLS measurements, the liquid supernatant exhibited a narrow monomodal particle size distribution centered at 148nm. This supernatant liquid contained a very stable SWCNT suspension as inferred from the zeta values. The average zeta potential was -28.6 mV (being the sample conductivity 0.0527 mS/cm), which evidences a strong polar character of the SWCNT suspension. The SWCNTs surface oxygen groups (produced by nitric acid treatment) and the dipole moments of Pluronic chains suggest the participation of noticeable electrostatic stabilization. These suspensions were observed periodically during at least two years after their preparation and no visible aggregates or deposits were detected. Besides, NIR purity index of the final supernatant was 0.060 (almost double of the starting material).

X-Ray diffractograms of the Pluronic-wrapped SWCNTs after filtration (Figure 3.11) showed bundles lattice peak ($2\theta = 6^{o}$) disappearance,[12,64] indicating bundle disaggregation. Diffractograms showed that the dispersion-centrifugation process

[64] Gonzalez-Dominguez, J. M.; Castell, P.; Anson, A.; Maser, W. K.; Benito, A. M.; Martinez, M. T., Block Copolymer Assisted Dispersion of Single Walled Carbon Nanotubes and Integration into a Trifunctional Epoxy. *J. Nanosci. Nanotechnol.* 2009, *9* (10), 6104-6112.

removed most of graphitic impurities (main peak at 2θ = 26.6º) from the pristine SWCNTs.[17,64] Other features are the decrease of metallic content (Ni peaks at 2θ = 44.4º and 51.9º) and the presence of a broad band (in the 2θ range from 14º to 30º) due to Pluronic. Raman spectroscopy, Figure 3.12a, indicated that the dispersion of SWCNTs in Pluronic produced a G/D band intensity ratio alteration. G/D ratio decreased from an average of 20 (in pristine SWCNTs) to an average of 10 (Pluronic-wrapped SWCNTs), as averaged from more than twenty different spectra of each sample. This was a consequence of changes in vibrational modes due to SWCNTs wrapping by the BC.

Raman spectroscopy supported the debundling of SWCNTs due to the RBM displacement (Figure 3.12b). The SWCNT packing, doping and wrapping have influence on the radial character of RBM band, which involves the tube diameter distribution.[47,48] In Figure 3.12b, an upshift of 2.5 cm^{-1} is observed in the maximum RBM peak from the pristine SWCNTs to the SWCNTs–Pluronic material. As mentioned before, this fact is attributed to the effect of polymer intercalation between SWCNTs.[49]

TEM micrographies (Figure 3.13) showed individual polymer-wrapped nanotubes and small bundles (3–4 tubes) also wrapped by the BC. TGA analysis in a

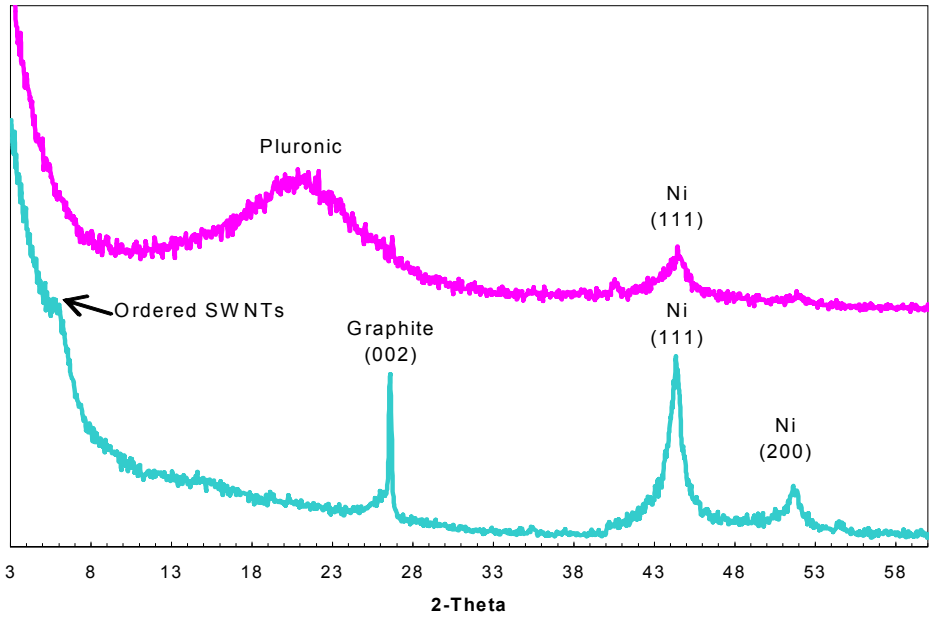

Figure 3.11. X-ray diffractograms of pristine SWCNTs (below) and Pluronic-wrapped SWCNTs (above).

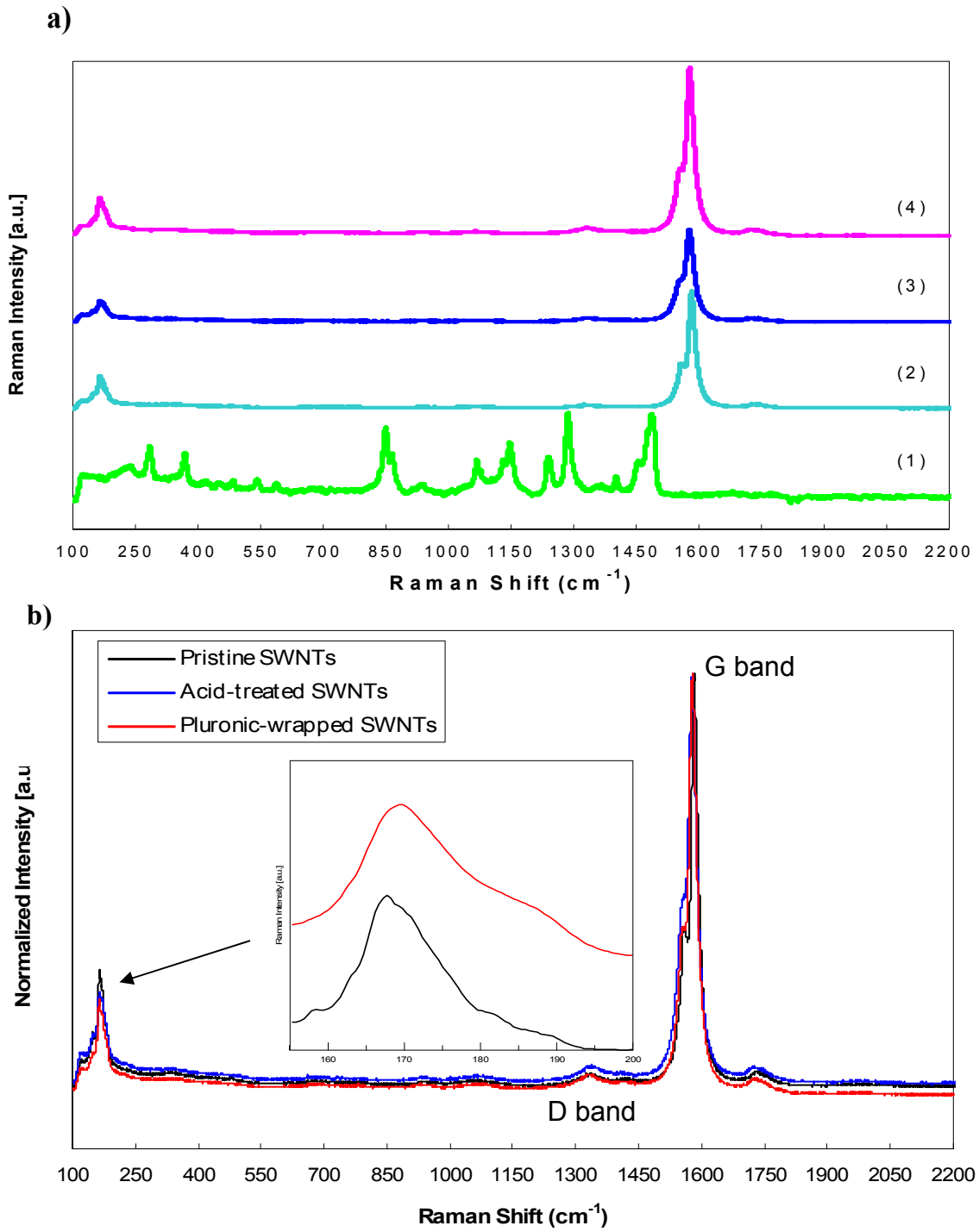

Figure 3.12. a) Raman spectra of different materials based on SWCNTs and Pluronic: (1) Pluronic F68, (2) Pristine SWCNTs, (3) acid treated SWCNTs, (4) Pluronic-wrapped SWCNTs solid material and b) inset of the RBM part of the Raman spectra in Figure 2a, where maximum peaks displacement can be seen.

CO_2 atmosphere (Figure 3.14) showed that in the final solid material, composed by Pluronic-wrapped SWCNTs, about 30 wt% of the total mass corresponds to Pluronic, which showed a maximum degradation peak at 320ºC.

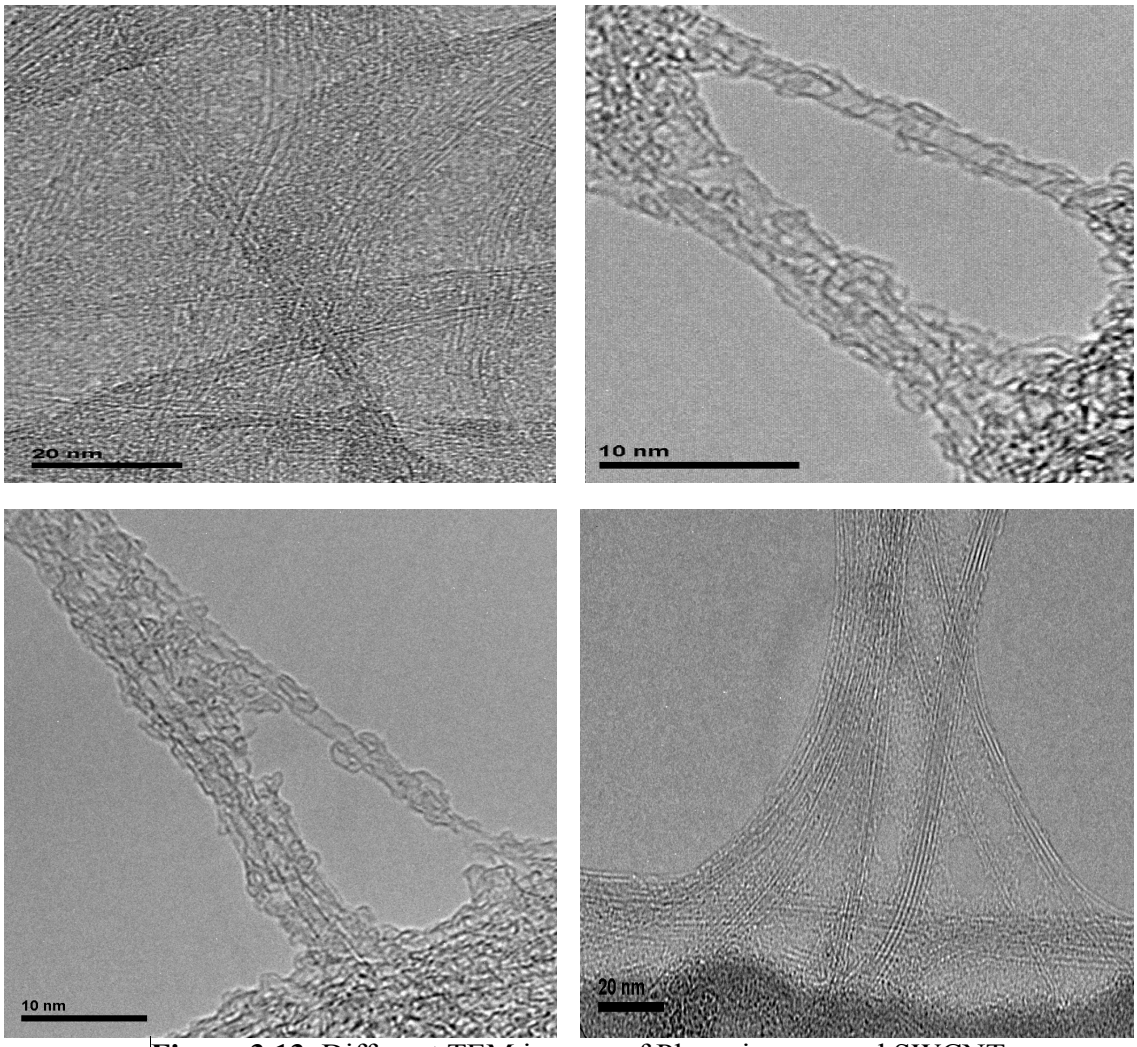

Figure 3.13. Different TEM images of Pluronic-wrapped SWCNTs

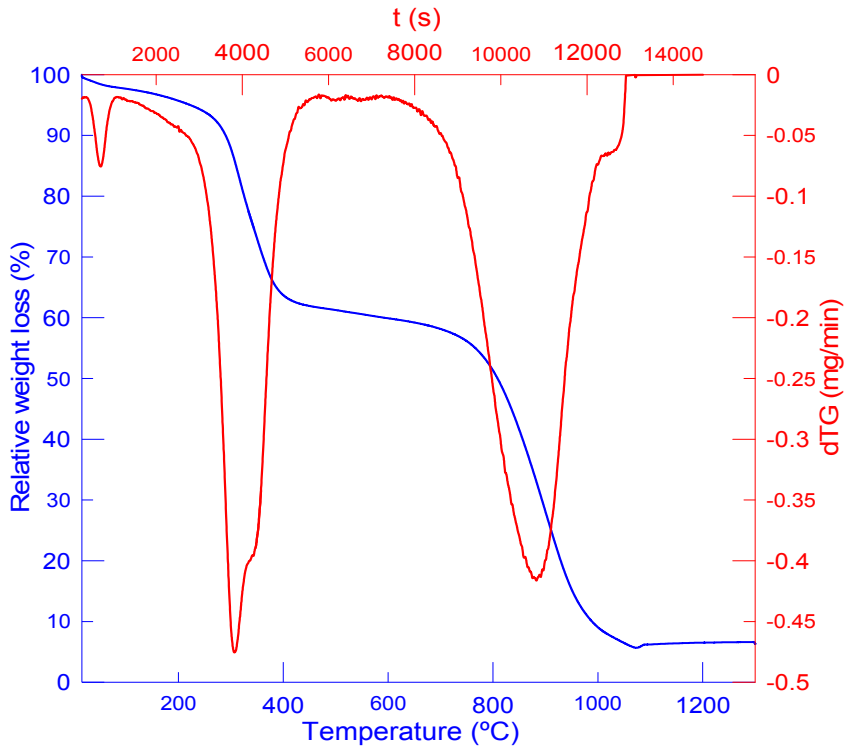

Figure 3.14. TG and dTG plots for the solid Pluronic-wrapped SWCNTs

3.3.2.2. Dispersions of arc SWCNTs in PEO-based diblock copolymers

The characterization of the obtained supernatants after centrifugation was conducted through the DLS technique and NIR spectroscopy. The results obtained for both BCs (Table 3.2) are very similar when using as-grown SWCNTs. A noticeable PI improvement is achieved, as compared to the pristine SWCNT material, almost threefold increase. The centrifugation of arc SWCNTs after suspension in the BC solution is capable of removing carbonaceous and metallic impurities. Particle sizes are lower than those achieved for Pluronic-wrapped acid-treated SWCNTs, and the zeta potential values are visibly lower. The difference in zeta values between PEO-*b*-PPO and PEO-*b*-PE could be due to the fact that the latter one presents lower polarity owing to the PE segment. PEO-*b*-PE wrapping of [ox]-SWCNTs, provides a filler with significant differences as compared to its as-grown counterpart (table 3.2). A five-fold increase in PI of [ox]-SWCNTs is revealed upon wrapping process. The PI achieved for wrapped [ox]-SWCNTs as compared to as-grown wrapped SWCNTs is almost double. This is due to the effect of surface oxidation of the pristine material.[59] Regarding particle size and zeta potential, these are also different when [ox]-SWCNTs are employed in the wrapping process. The particle size increases, and the zeta potential decreases in wrapped [ox]-SWCNTs as compared to their as-grown counterpart.

Table 3.2. PI and DLS parameters for pristine samples and supernatants containing PEO-based BC-wrapped SWCNTs. BC initial concentration = 1 wt%; SWCNT initial concentration = 0.4 wt%; centrifugation speed = 13000rpm

BC	Type of SWCNTs	Average particle size (nm)	Zeta potential (mV)	PI*
	As-grown			0.045
	[ox]			0.046
PEO-*b*-PPO	As-grown	138.7	-9.05	0.148
PEO-*b*-PE	As-grown	113.0	-6.38	0.147
	[ox]	150.8	-2.08	0.249

***Note:** During the course of the project, the starting quality of the as-grown arc SWCNTs was noticeably improved. For this reason, the work package dealing with PEO-based diblock copolymers was carried out with better as-grown SWCNT material, without acid treatment, as their starting purity (PI = 0.045) matched that of the acid-treated SWCNTs previously used in the Pluronic wrapping (PI = 0.050), but avoiding the disadvantages of the SWCNT nitric treatment (see Chapter 6).

Strong polar interactions between surface oxygen groups and BC dipoles occur, which strongly bounds the BC on SWCNTs surface. These oxygen groups introduced by air oxidation are mainly quinones and anhydrides,[59] which are non-ionizable. This would agree with the decrease in zeta potential, since ionizable oxygen groups (such as carboxylic group) would contribute to the electrical double layer in aqueous solution, favouring the electrostatic stabilization mechanism. In air-oxidized SWCNTs, surface oxygen groups boost the steric stabilization (instead of the electrostatic one) due to favourable polar interactions between SWCNTs surfaces and BC.

TGA plots obtained for the filtrated wrapped SWCNTs are displayed in Figure 3.15. The weight loss from room temperature to ~150ºC can be ascribed to the moisture present in the sample. The weight loss experienced by the sample from 100ºC to 600ºC in CO_2 atmosphere is used to elucidate the content on BC.[64] In Figure 3.15a, the solid material containing as-grown SWCNTs wrapped by PEO-*b*-PE presents a sharp single weight loss centred at ~400ºC upon pyrolisis in CO_2 atmosphere (ascribed to the own BC, as shown in Figure 3.15b), while as-grown SWCNTs wrapped in PEO-*b*-PPO show a lower weight loss, whose maximum is centred at ~350ºC. The BC content for both wrapped SWCNTs is 26 wt% and 65 wt% for PEO-*b*-PPO and PEO-*b*-PE respectively. The subsequent weight loss from 600ºC on, corresponds to the degradation of SWCNTs, since gasification of carbon materials through thermo-oxidative reaction with CO_2 occurs in this range of temperature, being all the previous weight losses attributed to the thermal desorption of attached species on SWCNT surface.[17]

[ox]-SWCNTs present a well defined thermal stability, with a steep loss around 600ºC caused by the desorption of surface oxygen groups.[59] [ox]-SWCNTs wrapped in PEO-*b*-PE show a noticeably higher amount of BC (90 wt%), indicating the higher capacity of these SWCNTs to retain BCs during the dispersion process (due to strong polar interactions between oxygen surface groups and BC). This fact suggests that the entropic (steric) contribution acquires greater signifi-cance when wrapping [ox]-SWCNTs rather than as-grown ones.

The purification and physical state of SWCNTs after wrapping was further characterized by XRD. X-Ray diffractograms of these samples are depicted in Figure 3.16. The remaining BC amount is observed in the range of 2θ ~ 20º-25º, due to the se-

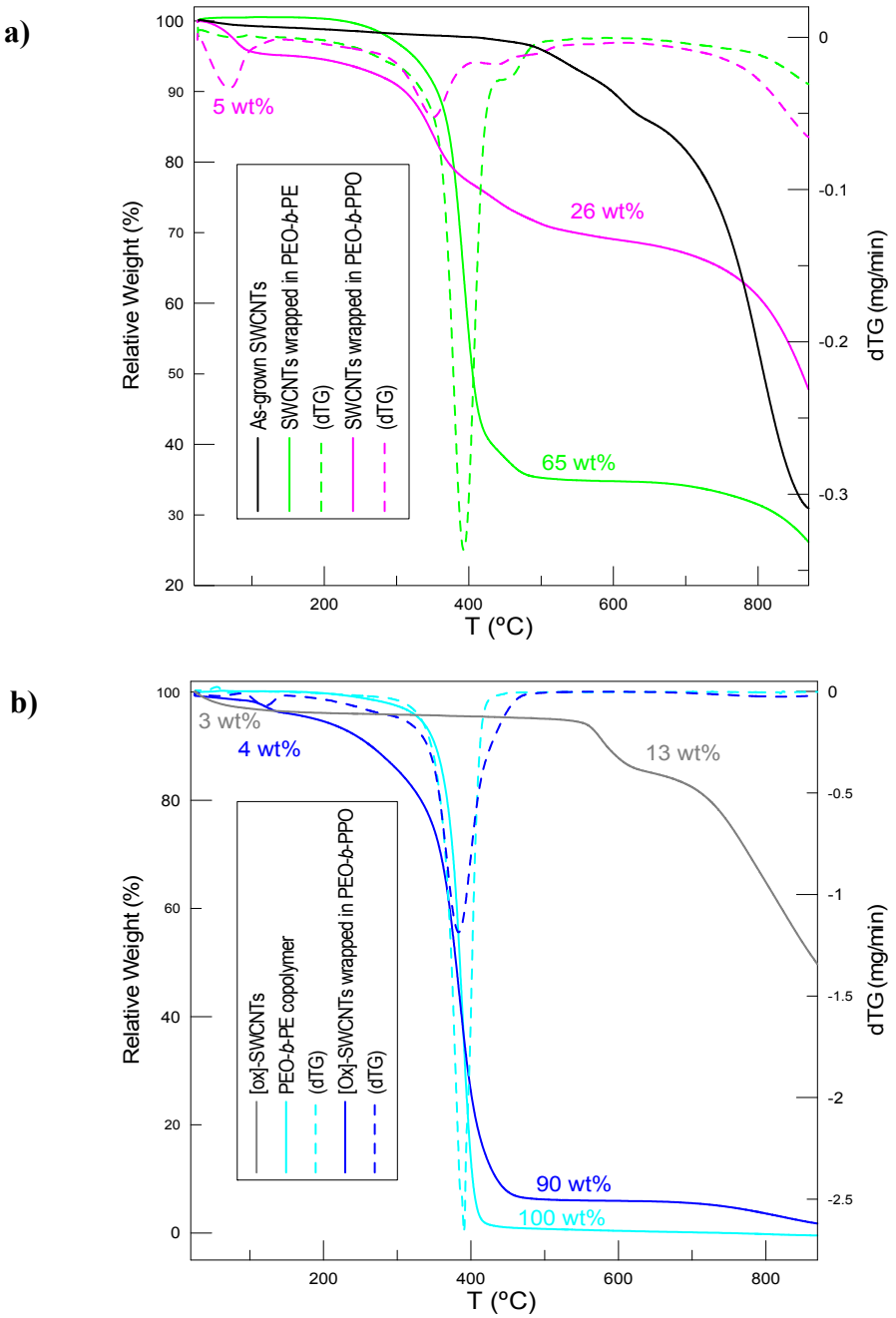

Figure 3.15. TGA plots for a) arc SWCNTs and b) [ox]-SWCNTs wrapped in the indicated PEO-based diblock copolymers after filtration, jointly with their respective pristine samples.

micrystalline nature of these polymers. The BC TGA peaks are especially visible in the PEO-*b*-PE cases, owing to the larger amount adsorbed on SWCNTs and [ox]-SWCNTs (see Figure 3.15) as compared to SWCNTs wrapped by PEO-*b*-PPO. Moreover, the visible peak contribution of the SWCNTs bundles form factor ($2\theta = 6^{\circ}$) totally disappears when PEO-*b*-PE is used, while it is still visible when wrapping SWCNTs with PEO-*b*-PPO. This would indicate that the former BC is more efficient in debundl-

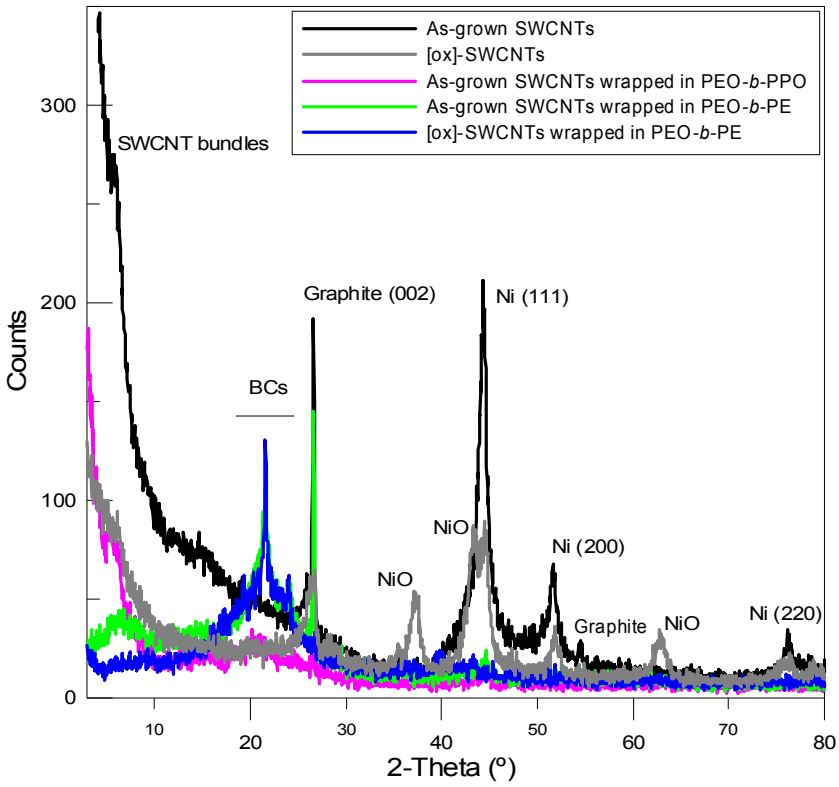

Figure 3.16. XRD plots for arc as-grown, [ox]-SWCNTs and different BC-wrapped materials.

ing SWCNTs than the latter one. The steric (entropic) interactions between the BC and SWCNTs seem to be stronger in PEO-*b*-PE, having a more pronounced liophilicity difference between blocks within BC chains. This would result in a more efficient debundling effect for PEO-*b*-PE than for PEO-*b*-PPO. In both cases, the steric effect of a BC has been observed to cause greater debundling than purely electrostatic stabilization mechanisms, such as that induced by ionic surfactants (i.e. SDBS).[17] It is worth noting that the oxidation of SWCNTs also promotes their debundling, as observed by the decrease in the $2\theta = 6^{\circ}$ peak intensity, possibly due to the insertion of oxygen functional groups on SWCNTs surface.

The peaks corresponding to crystalline domains of graphite (mainly that at $2\theta = 26.6^{\circ}$) and Ni diffraction peaks are visible in the as-grown SWCNTs sample. After wrapping in PEO-based diblock copolymers, all these impurity peaks disappear in a higher or lower degree, reasserting a significant improvement in the SWCNTs purity. Metallic particles are practically eliminated in as-grown SWCNTs after the wrapping process in both BCs. However, graphitic impurities are more efficiently removed using

PEO-*b*-PPO rather than PEO-*b*-PE. This fact could be explained in terms of different self-assembling potential of both BCs. The solvent in which the wrapping process took place was water that perfectly dissolves PEO, PPO is only partly water-soluble, while PE is completely insoluble in water. As a consequence, PEO-*b*-PE has a higher potential to form stable micelles in solution,[65] particularly in our study, where we are clearly above the critical micelle concentration. This would explain the higher potential of PEO-*b*-PE to debundle SWCNTs, since amphiphilic BC micelles can encapsulate individual SWCNTs.[66] On the other hand, PEO-*b*-PPO would be mainly dissolved and co-dispersed with as-grown SWCNTs in aqueous solution, providing also entropic interactions which would allow stabilizing SWCNTs and separate them from graphitic particles which are more efficiently removed after centrifugation in PEO-*b*-PPO than in PEO-*b*-PE.

Considering [ox]-SWCNT diffractograms, new peaks coming from the oxidation of Ni catalysts appear, together with those mentioned earlier, and a reduction of the graphite peak intensity at 26.6º is observed (~70 counts in [ox]-SWCNTs). The wrapping of [ox]-SWCNTs in PEO-*b*-PE provides again a material with no observable Ni (or NiO) diffraction peaks, and graphite peaks. In this case, the previous oxidation of SWCNTs allows the PEO-*b*-PE copolymer to remove the remaining graphite impurities along with the rest of metallic impurities, since the oxidation process leads to the partial debundling of SWCNTs. Besides, [ox]-SWCNTs wrapped in PEO-*b*-PE presents the highest degree of debundling among all the studied samples.

Raman spectroscopy provided additional insights into the debundling of SWCNTs by the BCs. The general Raman profile of these samples (Figure 3.17a) shows the typical features of SWCNTs.[63] In Figure 3.17b an inset of the RBM part of the spectra is shown. The effect of polymer intercalation between individual SWCNTs within a bundle is observed, as an upshift of the RBM maximum peak position.[49] The PEO-*b*-PPO causes an upshift of 3 cm^{-1}, similar to that achieved for Pluronic wrapping on acid-treated SWCNTs,[64] and PEO-*b*-PE induces an even larger upshift (8cm^{-1}), conf-

[65] Li, B.; Li, L. Y.; Wang, B. B.; Li, C. Y., Alternating patterns on single-walled carbon nanotubes. *Nat. Nanotechnol.* 2009, *4* (6), 358-362.
[66] Kang, Y. J.; Taton, T. A., Micelle-encapsulated carbon nanotubes: A route to nanotube composites. *J. Am. Chem. Soc.* 2003, *125* (19), 5650-5651.

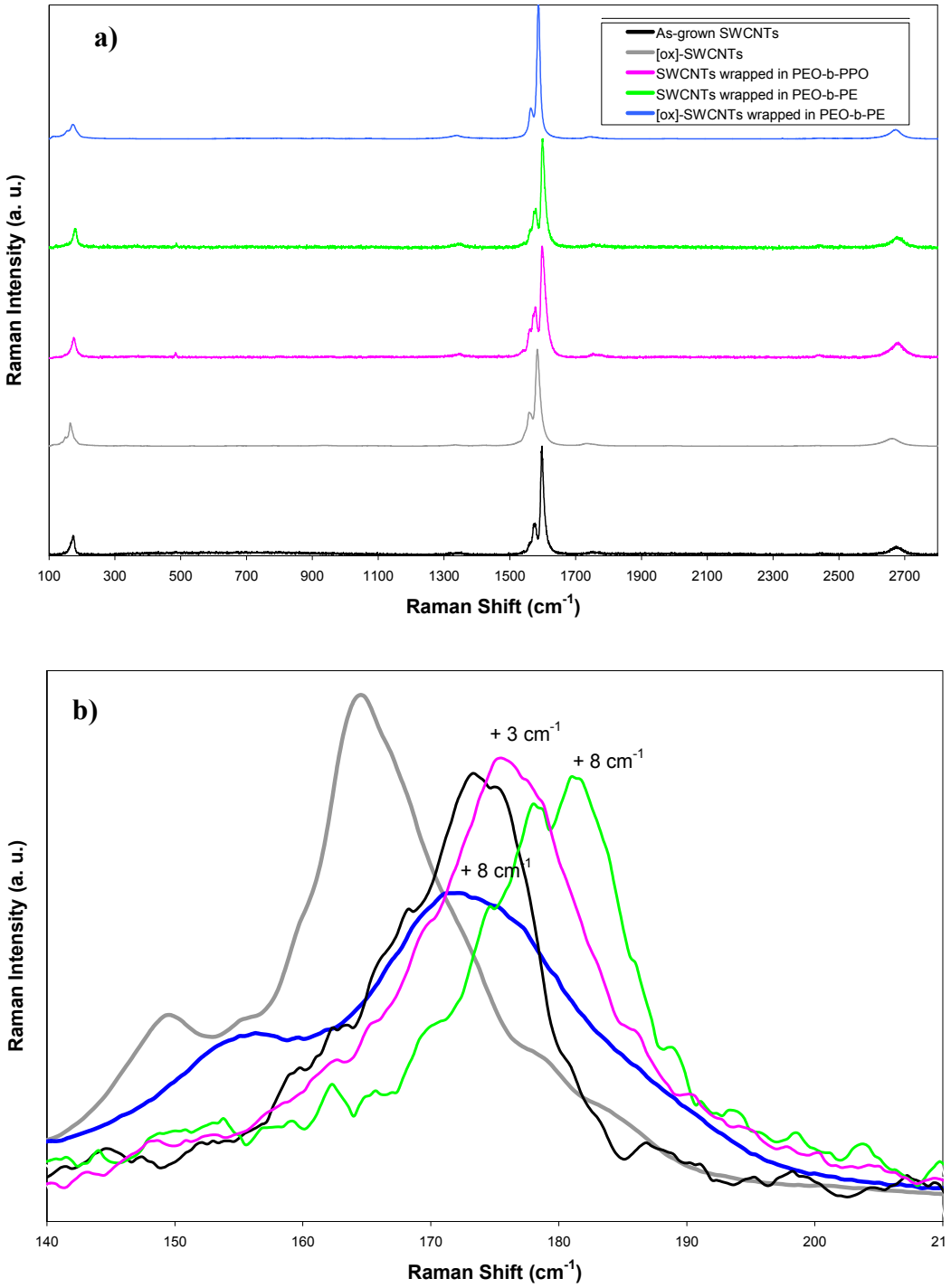

Figure 3.17. a) Raman spectra of pristine and diblock copolymer-wrapped SWCNTs; b) inset of the RBM part of spectra in Figure 3.17a.

irming its higher potential to unbundle SWCNTs (either as-grown or oxidized), which is in agreement with XRD results.

In Figure 3.18, TEM images of both kinds of SWCNTs wrapped in the PEO-based diblock copolymers are shown. There are no relevant differences between

samples containing as-grown SWCNTs. In general, as-grown SWCNTs wrapped in PEO-*b*-PE (Figure 3.18a) seem to present thinner bundles and slightly higher number of individual SWCNTs, while those wrapped in PEO-*b*-PPO present slightly thicker bundles and a higher degree of entanglement (Figure 3.18b). In comparison to the pristine ones, these wrapped SWCNTs have a more disentangled and unbundled view, with almost no presence of metal particles and carbon impurities. The BCs are clearly visible surrounding the tubes. When [ox]-SWCNTs are wrapped in PEO-*b*-PE (Figure 3.18c and d, the sample appears totally unbundled. As can be seen in Figure 3.18d, a thick layer of BC is surrounding individual SWCNTs.

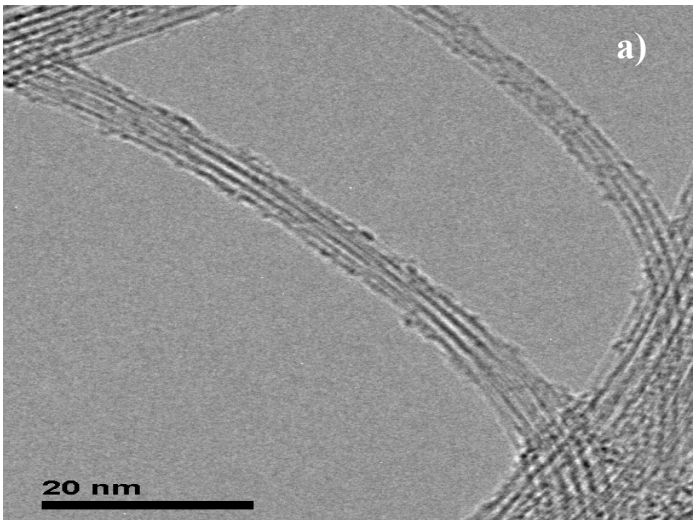

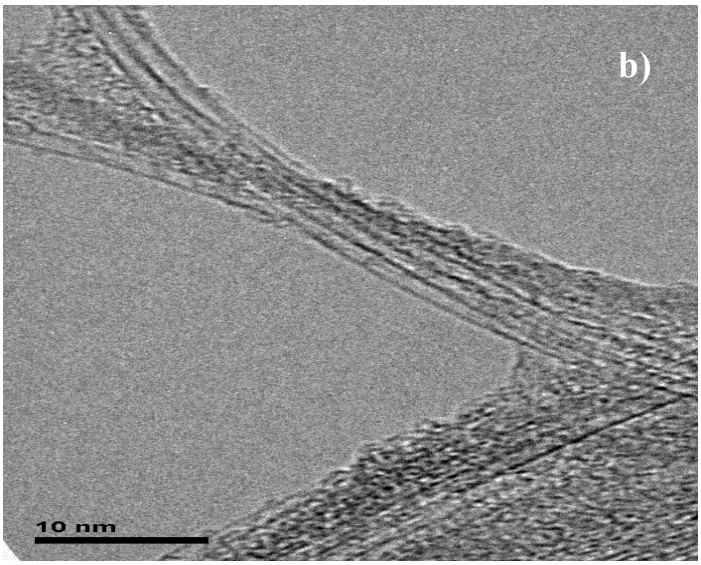

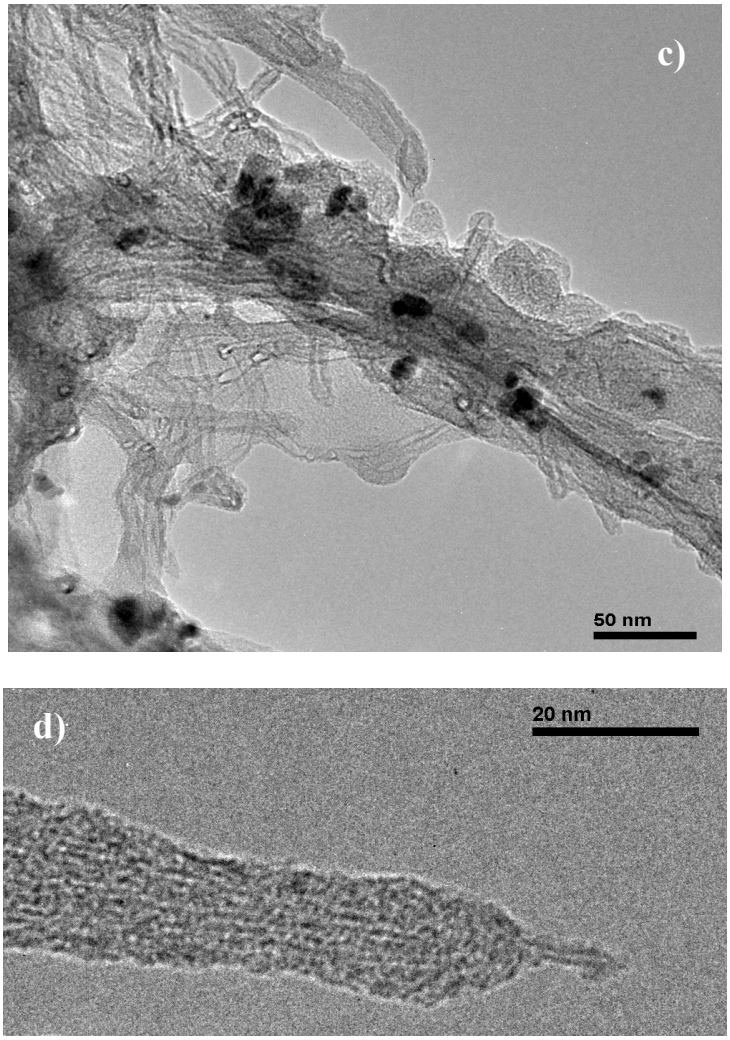

Figure 3.18. TEM images of as-grown SWCNTs wrapped in a) PEO-*b*-PE, and in b) PEO-*b*-PPO; c) and d) are different images of [ox]-SWCNTs wrapped in PEO-*b*-PE.

3.4. Conclusion

In the present chapter, different non-covalent modifications of SWCNTs have been carried out and the resulting materials have been extensively characterized. The remaining dispersant adsorbed on SWCNTs has been quantified by TGA, while the dispersion process and the resulting wrapped SWCNTs have been characterized through several techniques, including XRD, Raman spectroscopy and TEM.

The wrapping of arc and laser SWCNTs with the chosen thermoplastic polymers has been proposed as a way to improve the SWCNT integration into target high-

performance thermoplastic matrices, such as PEEK. The wrapping thermoplastics were rationally chosen in terms of chemical affinity and structural similarity with the target matrix. The sonication of as-grown laser or nitric acid-treated arc SWCNTs in organic solvent solution of PEI, PSF or PEES provided unbundled SWCNTs with reduced metallic content and potential to be used as fillers for PEEK matrices. On the other hand, wrapping of arc SWCNTs with PEO-based amphiphilic BCs has been proposed as a way to improve their integration into high-performance epoxy matrices. The choice of the BCs was made attending to the relative affinities of the different blocks in the epoxy and SWCNTs respectively. PEO was selected as the polymer block with more affinity to epoxy, while PPO or PE were selected for their better affinity with SWCNTs. The wrapping process has been conducted in water, a selective solvent for PEO.

The dispersion of nitric acid-treated SWCNTs in Pluronic F68 aqueous solution resulted in a highly purified and highly debundled SWCNT material, suitable for its integration into epoxy matrices. Additionally, the wrapping of as-grown arc SWCNTs in PEO-based diblock copolymers provided similar results. The obtained PIs were as high as 0.148 and an extraordinary reduction in the metal content have been achieved. However, there was a difference in the ability to remove graphitic impurities between both diblock copolymers. While SWCNTs wrapped in PEO-*b*-PPO exhibited almost no trace of graphite, those wrapped in PEO-*b*-PE still contained a certain amount of graphite, as seen by XRD. This would be due to the liophilicity differences between blocks within each BC. PEO-*b*-PE exhibits higher liophilicity difference, which would boost its micelle formation in aqueous solution, and that seems to favour the debundling of SWCNTs. In contrast, PEO-*b*-PPO presents a lower liophilicity difference between blocks, which would mainly cause the co-dispersion of SWCNTs and enhancement of graphite removal during centrifugation. This would also explain the higher potential of PEO-*b*-PE to debundle SWCNTs than PEO-*b*-PPO. If air-oxidized SWCNTs are employed for the wrapping in PEO-*b*-PE, a totally debundled filler and a high degree of purification (PI = 0.249) are achieved. The previous oxidation of the sample in air allows achieving a higher degree of purification (including the removal of graphite and metals) and even higher degree of debundling as compared to as-grown SWCNTs. This could be attributed to the fact that air-oxidized SWCNTs are partly purified and debundled.

The as-prepared wrapped SWCNT fillers have been incorporated into the aforementioned target polymer matrices. The experimental details and characterization of the resulting nanocomposites will be described in following chapters.

"The world is born… from zero.
The moment zero becomes one is
the moment the world springs to life"

Metal Gear Solid 4: Guns of the Patriots
Konami (2008)

CHAPTER 4:

INTEGRATION OF FUNCTIONALIZED SWCNTs INTO AN EPOXY MATRIX. INFLUENCE ON THE CROSS-LINKING SYSTEM KINETICS

4.0. Abstract

Arc-discharge SWCNTs modified by non-covalent interactions with Pluronic F68 BC or by covalently attaching different alyphatic primary amine moieties were integrated into a high performance epoxy system without using solvents. The aim of the present chapter is to study the influence of these SWCNT fillers on the matrix cross-linking reactions. The study was conducted through differential scanning calorimetry (DSC) and by using the so-called "advanced isoconversional kinetic method". The integration of Pluronic-wrapped SWCNTs caused a decrease in the matrix activation energy during the early stages of the curing process, suggesting that Pluronic induced an improvement in the mobility of reactants. On the other hand, SWCNTs aminated through sidewall addition reactions participate in cross-linking processes. It has been determined that the type and chemical nature of the amine moieties play an important role in the dispersibility and reactivity of SWCNTs in the epoxy, but the functionalization degree and metal content do not seem to affect the epoxy curing process. Unfunctionalized SWCNTs or those aminated on tips and edges do not show any evidence of a covalent anchoring to the matrix (suggested by an increase in the curing enthalpy and minor changes in the glass transition temperature).

4.1. Introduction

Due to their superior physical properties, CNTs offer unique possibilities for a wide variety of applications, including molecular electronics, biotechnology, sensors, and particularly as polymer matrix filler for high-performance composites. Considering their high mechanical strength and aspect ratio, CNTs are actively being used as nanoscale reinforcers to enhance the performance of polymer composite materials.[1-3]

[1] Spitalsky, Z.; Tasis, D.; Papagelis, K.; Galiotis, C., Carbon nanotube-polymer composites: Chemistry, processing, mechanical and electrical properties. *Prog. Polym. Sci.* 2010, *35* (3), 357-401.
[2] Tasis, D.; Tagmatarchis, N.; Bianco, A.; Prato, M., Chemistry of carbon nanotubes. *Chem. Rev.* 2006, *106* (3), 1105-1136.
[3] Bose, S.; Khare, R. A.; Moldenaers, P., Assessing the strengths and weaknesses of various types of pre-treatments of carbon nanotubes on the properties of polymer/carbon nanotubes composites: A critical review. *Polymer* 2010, *51* (5), 975-993.

Epoxy resins are considered as one of the most important thermosetting materials, and are widely used as matrices for advanced composites.[4-6] These materials are being used in a wide number of industrial applications due to their high durability, high strength, light weight, process flexibility, etc.

The epoxy cross-linking is a very complex process that arises from the thermally-activated reaction of the multiple amine groups of a "hardener" (or curing agent) with the monomer's multiple oxirane rings by means of nucleophilic ring opening, and it is composed of several stages (including primary amine addition, secondary amine addition and etherification) which are often overlapped.[7] The epoxide-to-amine ratio and the temperature heating program are essential parameters in a curing process, and they influence the matrix toughness and stiffness. These parameters will be fixed in the present thesis for an equal series of samples, but could slightly vary from one series to another.

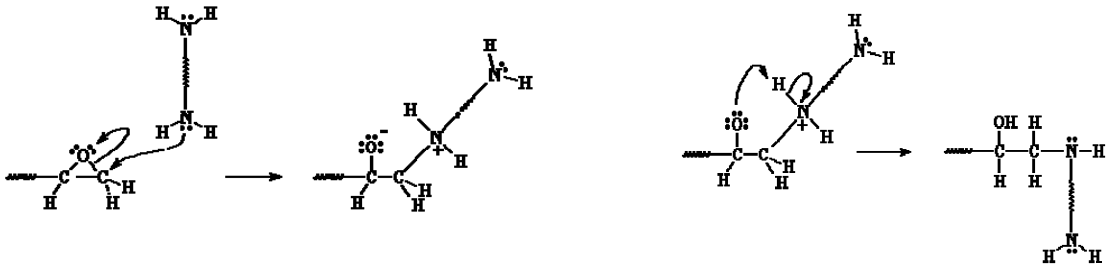

Figure 4.1. Schematic mechanism for the primary amine addition to an oxirane ring, the first step within the epoxy cross-linking process.

The chemical reactions involved lead to a heavily cross-linked structure, which could be understood as a "big single-molecule" polymer, (Fig. 4.2.) with specific features dependent on the type and degree of cross-linking. This structure leads to a stiff, insoluble, electrical insulating material but with an inherent brittleness.

[4] May, C., *Epoxy resins. Chemistry and technology*. Marcel Dekker: New York, 1988.
[5] Prime, R.; Turi, E., *Thermal characterization of polymeric materials*. Academic Press: New York, 1997
[6] Guo, P.; Chen, X. H.; Gao, X. C.; Song, H. H.; Shen, H. Y., Fabrication and mechanical properties of well-dispersed multiwalled carbon nanotubes/epoxy composites. *Compos. Sci. Technol.* 2007, *67* (15-16), 3331-3337.
[7] George, G. A.; Cash, G. A.; Rintoul, L., Cure monitoring of aerospace epoxy resins and prepregs by Fourier transform infrared emission spectroscopy. *Polym. Int.* 1996, *41* (2), 169-182.

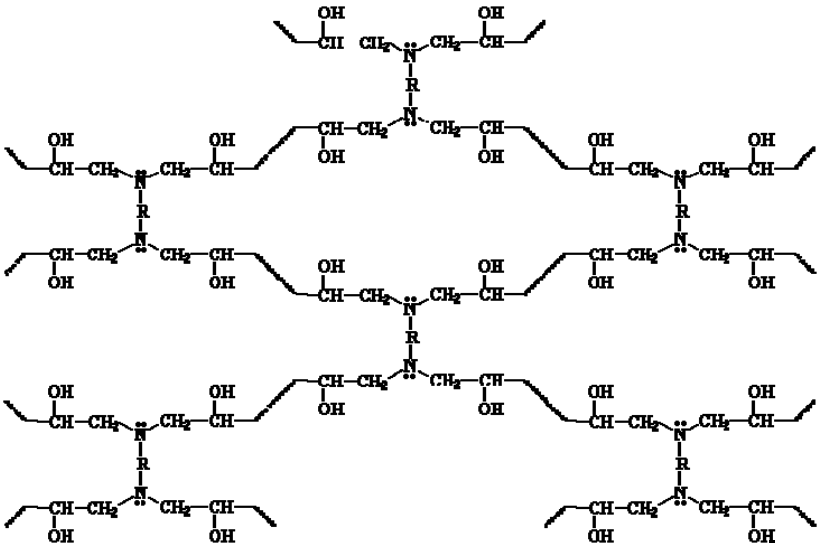

Figure 4.2. Chemical cross-linked structure of a model epoxy network.

For many decades, the use of epoxy resins in the composites field has almost exclusively been limited to bifunctional epoxy precursors (i.e. two oxiane rings per monomer molecule), derived from diglycidyl ether of Bisphenol A (DGEBA).[4-6,8] Recently, an increasing interest has arised in multifunctional epoxy precursors specially in tri[9] and tetrafunctional[10] epoxies. The interest, particularly in aromatic glycidylic and aromatic aminoglycidylic multifunctional epoxies, lies in the fact that they are very appreciated as high performance materials in coatings and aircraft skin manufacturing due some outstanding physical properties, such as their higher temperature resistance and lower shrinkage upon curing. This could be related to the morphology of cross-linking, because in epoxies having more than two reactive groups the density of cross-linking is higher, leading to better features as higher glass transition temperatures, higher impact resistance, higher modulus, and, generally better thermomechanical properties. Besides, there barely have been attempts to study these systems with the addition of CNTs.

[8] Loos, M. R.; Pezzin, S. H.; Amico, S. C.; Bergmann, C. P.; Coelho, L. A. F., The matrix stiffness role on tensile and thermal properties of carbon nanotubes/epoxy composites. *J. Mater. Sci.* 2008, *43* (18), 6064-6069.

[9] Carrasco, F.; Pages, P.; Lacorte, T.; Briceno, K., Fourier transform IR and differential scanning calorimetry study of curing of trifunctional amino-epoxy resin. *J. Appl. Polym. Sci.* 2005, *98* (4), 1524-1535.

[10] Xie, H. F.; Liu, B. H.; Yuan, Z. R.; Shen, J. Y.; Cheng, R. S., Cure kinetics of carbon nanotube/ tetrafunctional epoxy nanocomposites by isothermal differential scanning calorimetry. *J. Polym. Sci.B-Polym. Phys.* 2004, *42* (20), 3701-3712.

In the field of nanocomposite materials based on thermosetting epoxy matrices, the use of CNTs as fillers is of a critical interest in lightweight aerospace and automotive applications; hence a huge research effort has been undertaken in this field.[1-3,11] The incorporation of CNTs into an epoxy system is carried out before the curing reaction and their presence affects the cross-linking reactions during the curing stage of manufacturing. The in-depth study of these effects is highly necessary[12,13] to identify the filler impact during the formation of the thermosetting architecture, whose glass transition temperature (T_g) may be altered. The thermomechanical stability and overall performance in the working conditions can be influenced or even tailored through the filler choice.

Several studies have been performed with this aim. By using isothermal or nonisothermal differential scanning calorimetry (DSC) measurements, an accelerating effect of CNTs at the early stages of the curing process has been determined[10,14-17] in different epoxy systems. The most accepted explanation for this fact seems to be the high thermal conductivity of the filler[14] and/or the presence of surface oxygen groups,[10,15,16] which may act as catalysts for epoxide rings opening. The incorporation of CNTs into epoxy matrices also seems to lower the overall cross-linking degree of the thermosetting network[15,17] as inferred from curing enthalpies and T_g values. However, full understanding of this issue is still lacking,[12] especially regarding T_g changes, due to the disparity of some results and the wide variety of materials and experimental procedures employed.

[11] Sahoo, N. G.; Rana, S.; Cho, J. W.; Li, L.; Chan, S. H., Polymer nanocomposites based on functionalized carbon nanotubes. *Prog. Polym. Sci.* 2010, *35* (7), 837-867.
[12] Allaoui, A.; El Bounia, N., How carbon nanotubes affect the cure kinetics and glass transition temperature of their epoxy composites? - A review. *Express Polym. Lett.* 2009, *3* (9), 588-594.
[13] Gerson, A. L.; Bruck, H. A.; Hopkins, A. R.; Segal, K. N., Curing effects of single-wall carbon nanotube reinforcement on mechanical properties of filled epoxy adhesives. *Composites: Part A* 2010, *41* (6), 729-736.
[14] Puglia, D.; Valentini, L.; Armentano, I.; Kenny, J. M., Effects of single-walled carbon nanotube incorporation on the cure reaction of epoxy resin and its detection by Raman spectroscopy. *Diam. Relat. Mater.* 2003, *12* (3-7), 827-832.
[15] Tao, K.; Yang, S. Y.; Grunlan, J. C.; Kim, Y. S.; Dang, B. L.; Deng, Y. J.; Thomas, R. L.; Wilson, B. L.; Wei, X., Effects of carbon nanotube fillers on the curing processes of epoxy resin-based composites. *J. Appl. Polym. Sci.* 2006, *102* (6), 5248-5254
[16] Zhou, T. L.; Wang, X.; Liu, X. H.; Xiong, D. S., Influence of multi-walled carbon nanotubes on the cure behavior of epoxy-imidazole system. *Carbon* 2009, *47* (4), 1112-1118
[17] Qiu, J. J.; Wang, S. R., Reaction kinetics of functionalized carbon nanotubes reinforced polymer composites. *Mater. Chem. Phys.* 2010, *121* (1-2), 295-301.

In the field of CNT composites, there is a great interest in the incorporation of covalently functionalized fillers.[3,11] The aim of CNT covalent modification is to enhance solubility of CNTs in organic solvents, whose ultimate goal is to achieve homogeneous dispersion in the polymer matrix. According to the literature, the use of solvents can lead to a decrease of T_g values, even after careful evaporation.[12,18,19] In epoxy composites the primary amine functional group is of special interest due to its high nucleophilicity and similar reactivity to those of the curing agent. Amine-functionalized CNTs have been integrated into an epoxy matrix using a solvent-assisted integration method and their effect on the curing process was evaluated by DSC.[17,20] In these works it was reported that the effect of aminated CNTs was a reduction in the curing enthalpy and an increase in the activation energy. However, an in-depth evaluation of the effect of covalent functionalities on the dispersion behavior of CNTs into epoxy matrices in the absence of solvents is still lacking. This evaluation would be of particular interest for the evaluation of the chemical affinity between the functionalized fillers and the host matrix. There is also a lack of systematic studies with different functionalization routes and different amine moieties, coupled to a full characterization of the functionalized filler.

In the present chapter, SWCNTs have been integrated into a trifunctional epoxy system. The filler consisted of SWCNTs wrapped by Pluronic F68 BC or SWCNTs covalently functionalized with different moieties ending in a primary amine, following diverse chemical routes. The moieties have different chemical nature and inevitably lead to different functionalization degrees. Aminated and Pluronic-wrapped SWCNTs have been respectively integrated without using solvents into a trifunctional epoxy system. The effect of the different SWCNTs on the curing reaction of the epoxy matrix and the T_g values of the as-prepared nanocomposites has been studied using nonisothermal DSC scans and Isoconversional kinetic calculations. The previous characterization of the filler has been taken into account in order to correlate the SWCNTs effect with the observed phenomena.

[18] Grady, B. P., Recent Developments Concerning the Dispersion of Carbon Nanotubes in Polymers. *Macromol. Rapid Commun.* 2010**,** *31* (3), 247-257.
[19] Moniruzzaman, M.; Winey, K. I., Polymer nanocomposites containing carbon nanotubes. *Macromolecules* 2006**,** *39* (16), 5194-5205.
[20] Valentini, L.; Armentano, I.; Puglia, D.; Kenny, J. M., Dynamics of amine functionalized nanotubes/epoxy composites by dielectric relaxation spectroscopy. *Carbon* 2004, *42* (2), 323-329.

4.2. Experimental section

4.2.1. Materials and reagents

SWCNTs used in this chapter were the same as described in section 2.2.1.

A trifunctional epoxy precursor, triglycidyl p-aminophenol (TGAP), whose trade name is Araldite MY 0510, was used as the polymeric matrix precursor. It is a yellowish liquid with low viscosity at room temperature and a molecular weight of 300 g/mol. Aradur HT 976, (4,4'-diaminodiphenylsulfone) in the following, DDS, was chosen as the curing agent. Given the higher reactivity of the primary *vs.* the secondary amine, DDS presents a negative substitutional effect with TGAP precursor,[21] and may lead to good features in the network's morphology.

The chemical structures of both the precursor and the curing agent are shown in Figure 4.3. For all the samples processed in the present chapter, TGAP and DDS were mixed at stoichiometric ratio, assuming functionality for TGAP and DDS 3 (three oxirane rings per molecule) and 4 (two amine groups per molecule with two valences each) respectively.

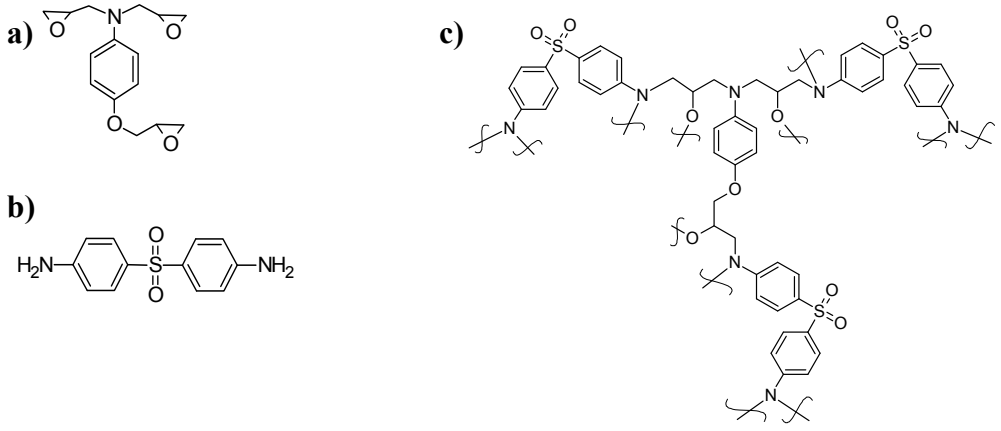

Figure 4.3. Chemical structures of a) the epoxy precursor, b) the hardener, and c) the TGAP+DDS cross-linked structure.

[21] Liu, H. P.; Uhlherr, A.; Varley, R.; Bannister, M. K., Influence of substituents on the kinetics of epoxy/aromatic diamine resin systems. *J. Polym. Sci. A-Polym. Chem.* 2004, *42* (13), 3143-3156.

4.2.2. Epoxy nanocomposite blends preparation

The mixtures were prepared using an electrical heater with magnetic stirring (300 rpm). In a typical blending, 1g of TGAP was mixed with 0.67g of DDS for the neat matrix preparation. The optimum mixing time and temperature were set as 60ºC / 15-30 min, these details will be discussed in a following section. Nanocomposite blends were prepared by premixing TGAP with the corresponding amount of SWCNTs (at 60ºC, 45 min) followed by tip sonication (Hielscher DRH-UP400S, 50% amplitude, continuous cycle application, 15min). Then, DDS is stepwise added at 60ºC in a time period no longer than 30 min.

For the non-covalently modified SWCNTs samples, several amounts of Pluronic-wrapped SWCNTs were added in the following percentages: 0.1, 0.25, 0.50, 1.0, 2.0 wt% (all of them in wt% of wrapped SWCNTs) and 2.0 wt% of nitric acid treated SWCNTs. Amino-functionalized and as-grown SWCNTs were integrated using the same protocol, at a loading of 0.5 wt % (8.35 mg of SWCNTs into 1.67 g of TGAP+DDS). These samples were also registered in the absence of DDS; the same amount of SWCNTs was maintained, and the SWCNT loading was recalculated.

Two representative blanks were also prepared; one of them was made by applying the premixing protocol to bare TGAP (followed by incorporation of DDS in stoichiometric ratio) and the other blank was performed adding to the TGAP the same amount of Pluronic contained in the sample with 2 wt% Pluronic-wrapped SWCNTs (10.0 mg of Pluronic per TGAP gram).

4.2.3. Characterization techniques

► DSC measurements were made in a Mettler DSC-823e equipment, calibrated using an indium standard (heat flow calibration) and an indium-lead-zinc standard (temperature calibration). Nonisothermal experiments were performed from room temperature to 320 ºC (samples with curing agent) or 400 ºC (samples without curing agent) at different heating rates (2, 5, 10, and 20 ºC/min) on ~10 mg (with curing agent) or ~3 mg (without curing agent) of sample, exactly weighed, placed into standard 40 μL aluminium crucibles, under a 100 mL/min flow of N_2. T_g values were taken as the

inflection point of the heating DSC curves after nonisothermal curing inside the equipment, in the subsequent cooling cycle (at 20 ºC/min). Enthalpy values (ΔH) were calculated from the area under the exothermic curing peak. The onset (starting temperature of a thermal process), and maximum peak temperatures (T_m) were taken from numerical evaluation of the obtained curves. The DSC data obtained at different heating rates (2, 5, 10 and 20 ºC/min) were subjected to the model-free calculations of the so-called "advanced isoconversional method" developed by Vyazovkin,[22-24] which allows obtaining activation energy (AE) plots versus the degree of conversion (α) and has extensively been applied to many epoxy systems and also to CNT-epoxy composites.[25-27]

In the dynamic curing process the degree of conversion (α) was calculated as follows:

$$\alpha = H_T / H_{dyn} \quad [1]$$

where H_T is the heat released up to a temperature T obtained by integration of the calorimetric signal up to this temperature, and H_{dyn} is the total reaction heat associated with the complete conversion of all reactive groups. The conditions of mixing were optimized for the TGAP+DDS system, which will be further discussed.

4.2.4. Kinetic study

In highly cross-linked systems such as an epoxy thermoset, the curing or cleavage reaction undergoes a complex mechanism with several, often overlapping, stages. Isoconversional kinetic methods assume that the reaction rate at a constant α

[22] Vyazovkin, S., Advanced isoconversional method. *J. Therm. Anal.* 1997, *49* (3), 1493-1499.
[23] Vyazovkin, S., Evaluation of activation energy of thermally stimulated solid-state reactions under arbitrary variation of temperature. *J. Comput. Chem.* 1997, *18* (3), 393-402.
[24] Vyazovkin, S., Modification of the integral isoconversional method to account for variation in the activation energy. *J. Comput. Chem.* 2001, *22* (2), 178-183.
[25] Vyazovkin, S., Thermal Analysis. *Anal. Chem.* 2010, *82* (12), 4936-4949.
[26] Gonzalez-Dominguez, J. M.; Castell, P.; Anson, A.; Maser, W. K.; Benito, A. M.; Martinez, M. T., Block Copolymer Assisted Dispersion of Single Walled Carbon Nanotubes and Integration into a Trifunctional Epoxy. *J. Nanosci. Nanotechnol.* 2009, *9* (10), 6104-6112.
[27] Gonzalez-Dominguez, J. M.; Anson-Casaos, A.; Castell, P.; Diez-Pascual, A. M.; Naffakh, M.; Ellis, G.; Gomez, M. A.; Martinez, M. T., Integration of block copolymer-wrapped single-wall carbon nanotubes into a trifunctional epoxy resin. Influence on thermal performance. *Polym. Degrad. Stab.* 2010, *95* (10), 2065-2075.

value is only a function of the temperature (equation [2]). Therefore, the assumption of a specific reaction order is not necessary.

$$\left(\frac{d\ln(d\alpha/dt)}{dT^{-1}}\right)_{\alpha} = -\frac{(AE)_{\alpha}}{R} \qquad [2]$$

This model-free approach allows individual activation energy (AE) values to be obtained for a particular α, $(AE)_\alpha$, considering single-step contributions to the overall reaction. These variations provide representative mechanistic information.[28] Several integral methods of the isoconversional approach have been proposed over the past years. In this study we have used the integral "advanced isoconversional method" (AIM), developed by S. Vyazovkin.[22-24] It considers a continuous variation of the AE throughout a thermally activated process, which is a more realistic approach than considering AE to be constant.[29] With a set of $n \geq 3$ experiments at different heating rates (β), equation [3] can be applied, thus obtaining each $(AE)_\alpha$ value:

$$\beta \cdot g(\alpha) = k_0 \cdot \frac{RT^2}{(AE)_{\alpha}} \cdot e^{\frac{-(AE)_{\alpha}}{RT}} \qquad [3]$$

where k_0 is the rate constant at infinite temperature, and g(α) is a function representing a model of the reaction mechanism. The AE appears as a constant value throughout the reaction in single step processes, while in multi-step reactions AE has a variable value. This methodology does not require knowledge of g(α), since all the information is implicitly included in the measurements. As there are no formal solutions, calculations must be solved numerically. This prevents having to select a g(α) function, with its associated errors, thus leading to more accurate results.

The standard procedure followed in all samples was a dynamic scan from 25 to 320 ºC at the different mentioned scan rates, a second dynamic scan from 25 to 320 ºC at 20 ºC/min showed the glass transition and no residual enthalpy. The activation energy can be determined at any particular value of α and evaluated numerically by a set of

[28] Vyazovkin, S.; Sbirrazzuoli, N., Mechanism and kinetics of epoxy-amine cure studied by differential scanning calorimetry. *Macromolecules* 1996, *29* (6), 1867-1873.
[29] Vyazovkin, S.; Wight, C. A., Kinetics in solids. *Annu. Rev. Phys. Chem.* 1997, *48*, 125-149.

experimental heating programs. Using this activation energy dependency and with the DSC software (STARe Mettler Toledo) simulations of isothermal curing at any temperature of interest can be made. Thus, we were able to predict the time necessary to reach a certain α at the different selected temperatures.

4.4. Results and discussion

4.4.1. Dispersion of SWCNTs in epoxy

TGAP/SWCNT mixtures coming from the premixing stage (described in the experimental section) were drop-casted in a glass slide and capped with a thin (0.5 mm thick) glass cover. These samples were observed in an optical microscope (Zeiss AXIO, coupled to a Cannon digital camera, 50X magnification, pictures shown in Figure 4.4).

The epoxy blend containing SWCNT-asg exhibited a bad dispersibility, with frequent lumps within a smooth background (Figure 4.4a). In a similar way, acid-treated SWCNTs present a very irregular and aggregated aspect (Figure 4.4b). The worst dispersibility was observed for the SWCNT-oxa sample (Figure 4.4c), which showed a highly agglomerated aspect, already visible to the naked eye. In contrast, the solvent-free mixing protocol provides a highly homogeneous epoxy blend with no visible agglomerates in the case of Pluronic-wrapped SWCNTs (Figure 4.4d), which is visibly different from that of the aforementioned. For TGAP mixtures containing SWCNT-nfp, SWCNT-dca, and SWCNT-dba the aspect was very smooth and homogeneous, without visible aggregates (images not shown), and similar to that observed for Pluronic-wrapped SWCNTs in Figure 4.4d.

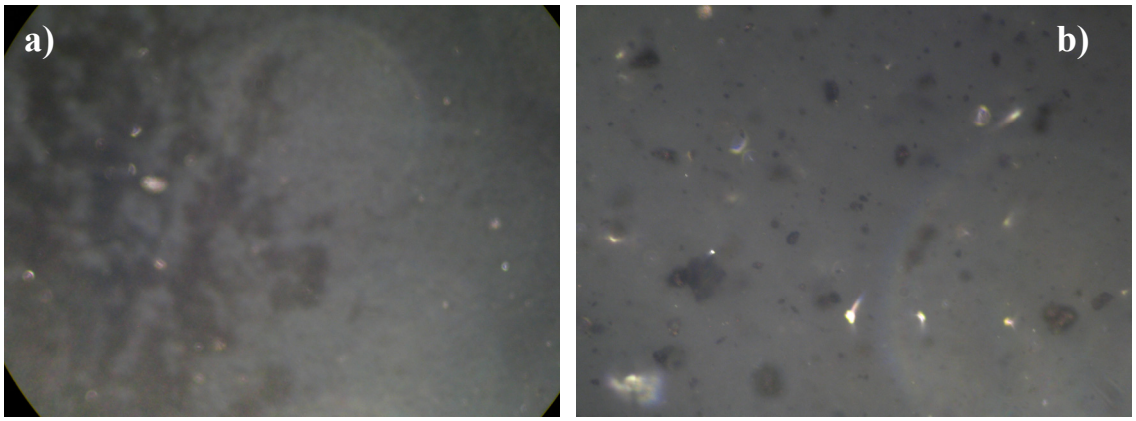

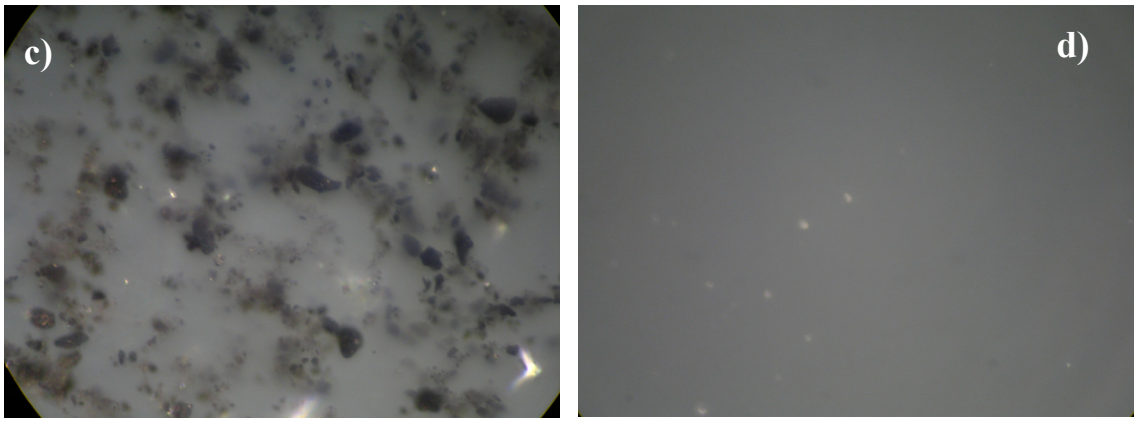

Figure 4.4. Optical images of TGAP/SWCNT mixtures before adding the curing agent. Approximate filler ratio = 0.84 wt%; a) SWCNT-asg b) nitric acid-treated SWCNTs c) SWCNT-oxa d) Pluronic-wrapped SWCNTs. NOTE: Dark spots are SWCNT aggregates, while bright spots are small entrapped bubbles or voids.

These observations are a relevant proof of the importance of a SWCNT modification route toward the dispersibility and integration into an epoxy matrix. The solvent-free integration protocol allows assessing the chemical affinity and dispersibility of a given type of SWCNT in the epoxy system, and as a primary conclusion, nitric acid treatments provide the worst behavior, even worse than bare as-grown SWCNTs. This could be ascribed to the compaction of the sample and has important consequences that will be further discussed. On the whole, it is clear how SWCNT dispersibility can be modified from different approaches. In particular, grafting amino groups on SWCNTs surface in most of the cases (except for SWCNT-oxa) has evidenced a drastically lower degree of agglomeration, accounting for an enhanced chemical affinity between the polymer matrix and the filler. According to literature results,[30] this fact should mostly prevent CNTs re-agglomeration during the curing reaction which will be critical for the further development of such composite materials. Besides, Pluronic-wrapped SWCNTs exhibit a greatly improved state of dispersion as well, spawned by the enhanced miscibility of the wrapped filler in comparison to the bare acid treated or pristine SWCNTs. The presence of the BC will also have important implications that will be analyzed.

[30] Ma, P. C.; Mo, S. Y.; Tang, B. Z.; Kim, J. K., Dispersion, interfacial interaction and re-agglomeration of functionalized carbon nanotubes in epoxy composites. *Carbon* 2010, *48* (6), 1824-1834.

4.4.2. General considerations about TGAP/DDS system curing and optimization of mixing conditions

As stated earlier, the epoxy cross-linking is due to the nucleophilic ring opening of the precursor's oxirane rings by the hardener's amine groups, gathering three main (overlapped) processes i.e. primary amine addition, secondary amine addition and etherification. In the absence of the curing agent, nonisothermal heating causes the autocuring of the TGAP monomer, through the spontaneous formation of hydroxyl groups from oxirane rings and subsequent etherification with other oxirane rings. This latter mechanism is known to happen at higher temperatures than those involving the amines of the curing agent.[31] The observed DSC features are significantly different in each case, and a representative example is depicted in Figure 4.5. Unlike TGAP/DDS samples, the TGAP autocuring overlaps with its degradation at the exothermic peak temperatures, becoming a pulverulent black solid and thus no T_g could be measured in the absence of DDS.

The conditions of TGAP and DDS mixing were optimized by performing nonisothermal heating scans at 20 ºC/min in the DSC device to stoichiometric mixtures of TGAP and DDS. Samples were registered right after mixing, in order to prevent further reaction between both reagents. Optimum mixing time and temperature were determined comparing reaction enthalpies and checking homogeneity of samples. In Table 4.1 some different tested conditions are shown. At 60ºC, results indicate that the enthalpy values are constant up to 30 min of mixing. Then, at 60 min ΔH decreases aro-

Table 4.1. Nonisothermal curing results of different TGAP/DDS mixing conditions from scans at 20ºC/min

Mixing Conditions				
Mixing T (ºC)	**Time (min)**	**T_m (ºC)**	**Onset (ºC)**	**ΔH (J/g)**
60	5	238.37	197.21	694.40
60	15	237.11	195.67	694.61
60	30	238.11	193.31	694.03
60	60	238.21	185.23	591.90
120	5	236.27	188.54	629.59

[31] Choi, W. S.; Shanmugharaj, A. M.; Ryu, S. H., Study on the effect of phenol anchored multiwall carbon nanotube on the curing kinetics of epoxy/Novolac resins. *Thermochim. Acta* 2010, *506* (1-2), 77-81.

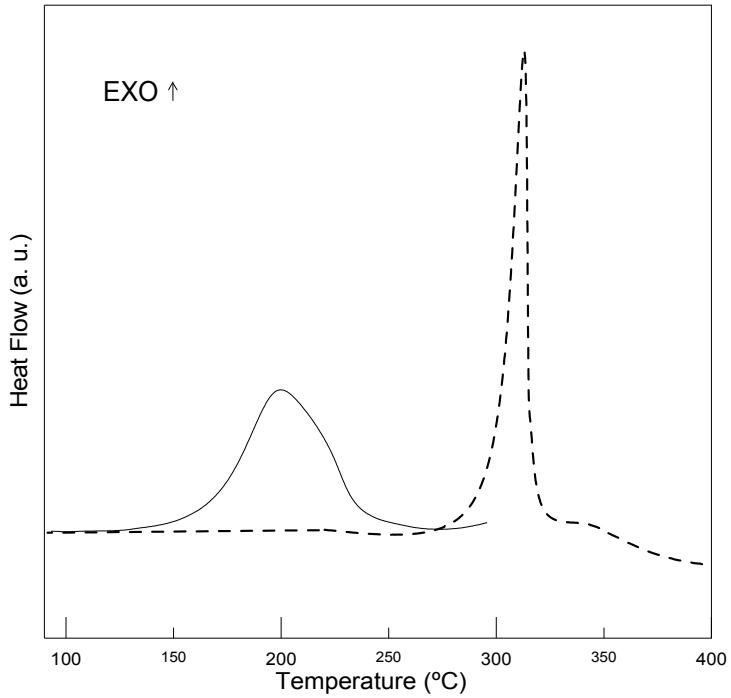

Figure 4.5. Example of DSC nonisothermal heatings for epoxy or epoxy/SWCNT blends in the presence (-) or absence (---) of the curing agent, at equal heating rate.

und 100 J/g which evidences that the cross-linking has already taken place during the mixing step.

In contrast, at 120ºC only 5 min of mixing are necessary to observe an enthalpy loss. From these data, it was established that the optimum conditions would be those capable of providing an homogeneous blend but without losing enthalpy, i.e. avoiding the curing in the mixing process. The most suitable temperature for this was 60 ºC, and the lowest time suitable to observe homogeneous mixture was 15 min. Therefore, all the epoxy blends were prepared at 60 ºC in a time period between 15 and 30 min, until reaching a homogeneous blend. The addition of Pluronic did not alter the mixing conditions, as it exhibited total miscibility with the epoxy.

4.4.3. Curing kinetics in Pluronic-wrapped SWCNT / epoxy blends

Kinetics of epoxy-based systems has been studied and reported from several classic Arrhenius-based approaches[32-34] over decades. In particular, the TGPA + DDS

[32] Kissinger, H. E., Reaction kinetics in differential thermal analysis. *Anal. Chem.* 1957, *29* (11), 1702-1706.

system kinetics was first studied by R. D. Patel et al.[35] They found out first-order kinetics up to 80% of curing completion at least, and reported kinetic data calculated from classical Arrhenius-based equations.

In order to apply the AIM, four nonisothermal scans at different heating rates were collected.[26] As an example, the different nonisothermal scans of the TGAP/DDS + 0.25% SWCNTs – Pluronic sample can be seen in Figure 4.6a. It is worth noting that the maximum peak temperature varies with the heating rate. From these thermograms, conversion curves can be obtained (Figure 4.6b) and activation energy (AE) *vs.* α plots can be determined (Figure 4.6c). It has to be mentioned that close to the end of the curing process, the activation energy increases due to a diffusion hindering effect. Using the activation curves, isothermal conversion plots at different temperatures can be estimated (Figure 4.6.d).

Figure 4.7 shows AE *vs.* α plots for all samples studied. The shape of the curves shows no significant AE variation in the central range of conversions, an acceleration effect (i.e. sharp drop in the AE curve) in the early stages and a hindering effect in the latter stages. On the average, activation energy, in the constant AE-behaving part of the curing process is between 65 and 70 kJ/mol, which is in agreement with bibliographical data for the TGAP/DDS epoxy system.[9,35] It also indicates that SWCNTs had no direct effect on the mechanism during the cross-linking reactions because of the similarity of AEs at intermediate values of α. This is consistent with the fact that the overall reaction is ruled by diffusional processes, despite carboxylic groups which are present in SWCNTs ends and sidewall defects could react in the system.[36]

From isoconversional plots and tables, different times to reach certain α for each temperature and sample can be obtained. This allows inferring reaction rates in the different stages of reaction for each sample. The observations of activation energies and

[33] Ozawa, T., Critical investigation of methods for kinetic-analysis of thermoanalytical data. *J. Therm. Anal.* 1975, *7* (3), 601-617.
[34] Ozawa, T., Modified method for kinetic-analysis of thermoanalytical data. *J. Therm. Anal.* 1976, *9* (3), 369-373.
[35] Patel, R. D.; Patel, R. G.; Patel, V. S., Investigation of kinetics of curing of triglycidyl-p-aminophenol with aromatic diamines by differential scanning calorimetry. *J. Therm. Anal.* 1988, *34* (5-6), 1283-1293.
[36] Bekyarova, E.; Thostenson, E. T.; Yu, A.; Itkis, M. E.; Fakhrutdinov, D.; Chou, T. W.; Haddon, R. C., Functionalized single-walled carbon nanotubes for carbon fiber-epoxy composites. *J. Phys. Chem. C* 2007, *111* (48), 17865-17871.

isothermal curves (Figure 4.7) indicated that at low temperatures and α values, Pluronic effect was to lower activation energy at the earliest stages of reaction. It implies that equal α values are reached at lower times, suggesting an improvement in mobility of reactants. This effect disappeared at higher temperatures and α values because the intrinsic high reactivity of the system.

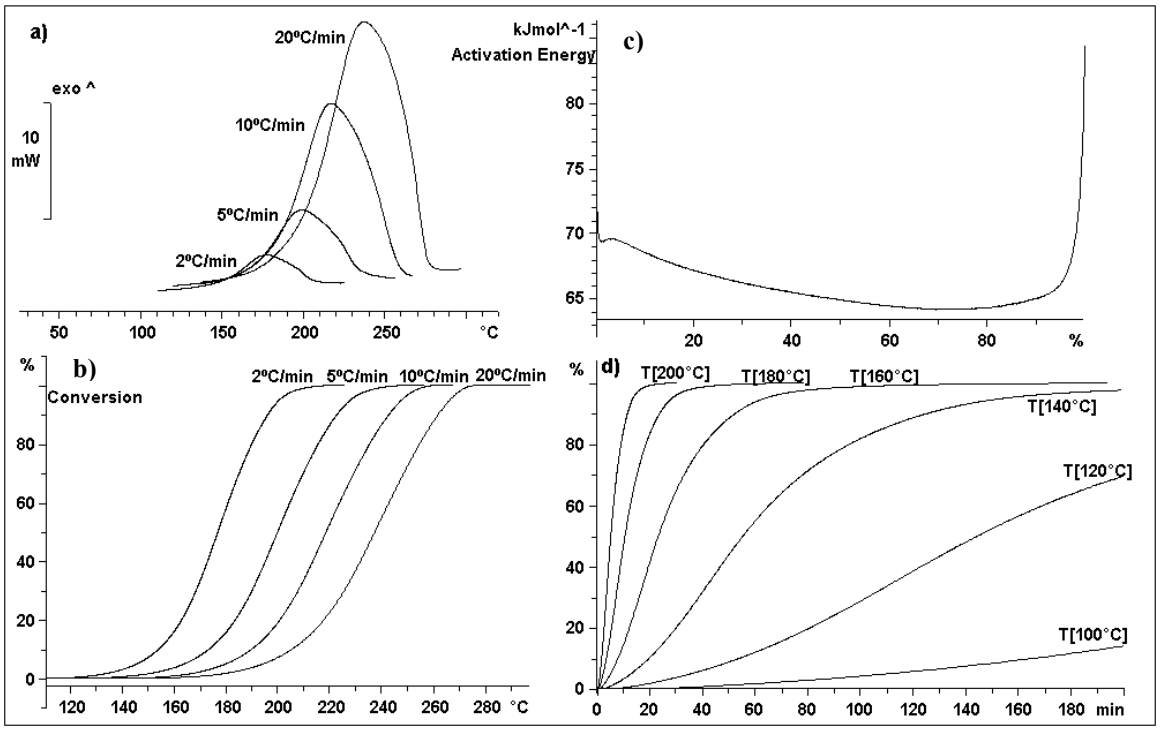

Figure 4.6. Representative schematic steps of cross-linking studies of TGAP/DDS + 0.25 % SWCNTs-Pluronic in AIM application: a) Nonisothermal curing curves at four different heating rates, b) AIM equations to obtain AE *vs.* α, c) Representation of conversion curves for each heating rate, d) Application of AIM equations to simulate isothermal curing conditions.

The presence of SWCNTs, as said before, did not seem to affect the system α and kinetics in the range of constant AE values (~ 20% < α < 80%). The AE exhibits little variation, but in the early stages it is clearly evidenced how the two samples which did not contain Pluronic (TGAP/DDS and TGAP/DDS + 2% acid treated SWCNTs) had the highest activation energies at the beginning, which indicates lower intrinsic reactivity in absence of Pluronic. For TGAP/DDS + 2% acid treated SWCNTs, the highest hindering effect at the end of the curing process is observed. That is consistent with the fact that cross-linking mechanisms undergo by diffusional effect,[4,5] and it is

very likely that Pluronic (in the low amounts that it is incorporated here) is facilitating the mobility of species during the reaction resulting in lower initial activation energies.

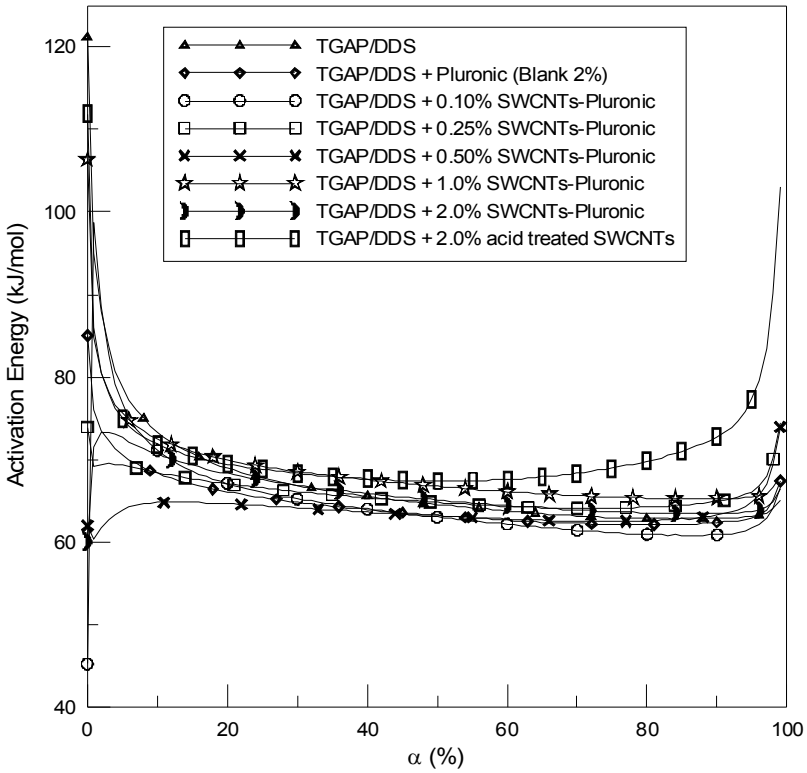

Figure 4.7. Activation energy *vs.* degree of conversion plots for samples in this section.

4.4.4. Curing kinetics in aminated SWCNT/epoxy blends

Nonisothermal DSC scans of the epoxy + amino-SWCNTs were registered in presence and absence of the curing agent DDS.[37] The presence of primary amine groups on the SWCNTs surface provides a reactive filler toward the TGAP oxirane rings, hence a possible covalent anchoring to the epoxy matrix. The covalent anchoring is expected to enhance the filler-matrix adhesion, improving the mechanical properties. For this reason, the DSC study of TGAP/SWCNT blends was particularly useful in this case. The aminated SWCNTs used in this study were those functionalized *via* carboxylic activation (SWCNT-oxa), alkaline reduction + diacyl peroxide (SWCNT-nfp), 1,3-dipolar cycloaddition of azomethyne ylides (SWCNT-dca) and diazonium compounds

[37] Gonzalez-Dominguez, J. M.; Gonzalez, M.; Anson-Casaos, A.; Diez-Pascual, A. M.; Gomez, M. A.; Martinez, M. T., Effect of Various Aminated Single-Walled Carbon Nanotubes on the Epoxy Cross-Linking Reactions. *J. Phys. Chem. C* 2011, *115* (15), 7238-7248.

with 4-aminobenzyl amine (SWCNT-dba). Experimental details of their synthesis and characterization are given in Chapter 2.

Thermodynamic parameters extracted from nonisothermal DSC scans at 5ºC/min are listed in Table 4.2. The incorporation of non-functionalized SWCNTs (SWCNT-asg) into the TGAP/DDS epoxy, increases ΔH (by 16.7 J/g) and increases slightly the T_g (by 1.6 ºC). The latter is consistent with an increase in the rigidity of the system, and also with the fact that the nanofiller presence does not hinder the cross-linking process, unlike other authors' findings in epoxy/SWCNT composites with bifunctional epoxy monomers.[15,17] The absence of organic solvents during our experimental procedure of preparation could contribute to these different findings. The solvent-free integration of SWCNT-asg results in apparently homogeneous mixtures with the epoxy probably due to favourable physical interactions (i.e. π-π stacking of aromatic species, polar interactions with SWCNT native surface groups …) which would enhance the intimate contact between matrix and filler. The opposite behavior was observed for the nitric acid-treated SWCNTs in the previous section, where the presence of aggregates was dominant.

The increase in enthalpy could be due to the native surface groups present on SWCNT-asg, which undergo chemical changes during the curing process and thereby increase its reaction heat. Given that there is no significant change in the curing onset or maximum peak temperature (T_m), we assume that as-grown SWCNTs do not produce any catalytic effect. Thus, the effects of functionalized SWCNTs can be entirely ascribed to the functional groups and not to metals, as it has been previously suggested.[12]

Functionalized SWCNT samples (SWCNT-dba, SWCNT-dca and SWCNT-nfp) exhibit a clear decrease of the curing enthalpy (of 18.8, 7.9 and 17.3 J/g, respectively), compatible with a decrease in the extent of curing conversion as the epoxide/amine ratio is modified, as observed by other authors.[17,20] Additionally, the involvement of SWCNT attached amines in the enthalpy changes can be confirmed by observing the SWCNT-dca sample which showed the lowest extent of functionalization (see Chapter 2), since it exhibits considerably lower ΔH decrease. T_g values experience a noticeable increase in comparison with the neat matrix (of 7.3, 8.7 and 7.8 ºC for composites containing

SWCNT-dba, SWCNT-dca and SWCNT-nfp respectively), indicating the successful cross-linking between the filler and the matrix hence an efficient covalent anchoring. Both onset and T_m values decrease, pointing to a catalytic effect of the amine groups in the epoxy medium.

Contrary to the behavior shown by sidewall functionalized samples, the SWCNT-oxa sample does not show catalytic behavior or decrease in enthalpy. Its DSC parameters are nearly those of SWCNT-asg but with a higher ΔH. Since SWCNT-oxa has the highest functionalization degree, this striking fact can only be explained by the extremely bad dispersibility of nitric acid-treated SWCNTs into epoxy throughout solvent-free techniques. The SWCNT-oxa amino groups are unable to develop their catalytic effect since they do not reach proper contact with the parent matrix, albeit the high ΔH suggests that oxygen groups (highly abundant in SWCNT-oxa) experience thermal modifications during the curing process, raising the reaction heat.

Table 4.2. DSC parameters obtained for different TGAP/DDS/SWCNT and TGAP/SWCNT mixtures heated at a rate of 5ºC/min.

Filler*	With DDS				Without DDS		
	Onset (ºC)	T_m (ºC)	ΔH (J/g)	T_g (ºC)**	Onset (ºC)	T_m (ºC)	ΔH (J/g)
Neat Epoxy	167.5	199.7	203.9	209.9	301.3	312.9	497.7
SWCNT-asg	167.5	199.0	220.6	211.5	298.0	309.2	439.5
SWCNT-oxa	168.5	200.7	256.9	211.0	311.2	323.6	509.2
SWCNT-nfp	162.3	197.6	186.6	217.7	298.7	309.7	364.0
SWCNT-dba	166.3	198.1	185.1	217.2	297.7	309.0	440.0
SWCNT-dca	164.6	196.4	196.0	218.6	295.8	306.6	351.8

* SWCNT content is 0.5 wt% (in the presence of DDS) or 0.835 wt% (in absences of DDS).
** T_g values are obtained during the cooling stage (-20 ºC/min) after non-isothermal curing

In the absence of the curing agent (Table 4.2), onset and T_m changes are small except for the TGAP/SWCNT-oxa mixture, in which both parameters increase by about 10ºC. The rest of the samples show catalytic effects that can only be explained by the amino groups actuation since no DDS is present. For all the TGAP mixtures with sidewall-functionalized SWCNTs, a large decrease in the ΔH (up to 145.9 J/g, for SWCNT-dca sample) is observed. This is perfectly consistent with an enhanced dispersion of functionalized SWCNTs in the TGAP monomer by the solvent-free technique. Well-dispersed SWCNTs can act as a physical hindrance to the monomer

mobility and thus lower the reaction heat.[15] This premise has been used by other authors for the DSC evaluation of the SWCNT dispersion in epoxy matrices,[38] considering the total heat of reaction being influenced mainly by those SWCNTs that are optimally dispersed. In this sense, the incorporation of sidewall-functionalized SWCNTs into the epoxy matrix leads to an improved degree of dispersion as compared to SWCNT-asg or SWCNT-oxa, which is reflected in the DSC parameters. The enhanced dispersion would be directly caused by the attached moieties.

AE *vs.* α plots for TGAP/DDS + amino-SWCNT samples at a 0.5 wt% loading are depicted in Figure 4.8. Isoconversional plots show a fairly linear section which takes most of the curing process (α ~ 10-90%). This section, which would stand for the propagation of the amine-oxirane ring openings,[7] has an average AE value of 65-70 kJ/mol, consistent with literature data for TGAP/DDS curing studies using classical Arrhenius-based equations.[35] In the extreme stages of the curing process there is a significant dependence of AE with α. Regarding the initial steps of curing (up to α ~ 10%), which can be considered mostly conducted by the primary amine reaction with oxirane rings, the neat TGAP/DDS sample shows no practical AE dependence on the conversion. However, the incorporation of SWCNTs leads to different behaviors depending on the functionalization route. The presence of SWCNT-asg and SWCNT-oxa in the TGAP/DDS system causes a sudden increase of AE at the beginning of the curing process, reaching the constant value at α ~10%. This could be considered as a decelerating effect. This effect would arise upon viscosity increase during the initiation of curing, as it undergoes mainly by diffusional control.

The lower initial values of AE, corresponding to SWCNT-asg and SWCNT-oxa blends, could be attributed to an enhanced thermal diffusivity which would promote the initiation of the curing reaction. Furthermore, the oxygen groups on SWCNT-asg and SWCNT-oxa surfaces could also create hydrogen-bridge bonds with TGAP upon oxirane opening, and this fact is well known to affect the reaction course and the eventual cross-linking density.[39] For the composite blend containing SWCNT-oxa, the filler's larger amount of surface oxygen groups would cause a more sharpened AE

[38] Kim, S. H.; Lee, W. I.; Park, J. M., Assessment of dispersion in carbon nanotube reinforced composites using differential scanning calorimetry. *Carbon* 2009, *47* (11), 2699-2703.
[39] Bellenger, V.; Verdu, J.; Francillette, J.; Hoarau, P.; Morel, E., Infrared study of hydrogen-bonding in amine-cross-linked epoxies. *Polymer* 1987, *28* (7), 1079-1086.

increase. In the SWCNT-oxa blend, no influence of the amine groups is observed, as it shows a similar behavior to that containing SWCNT-asg.

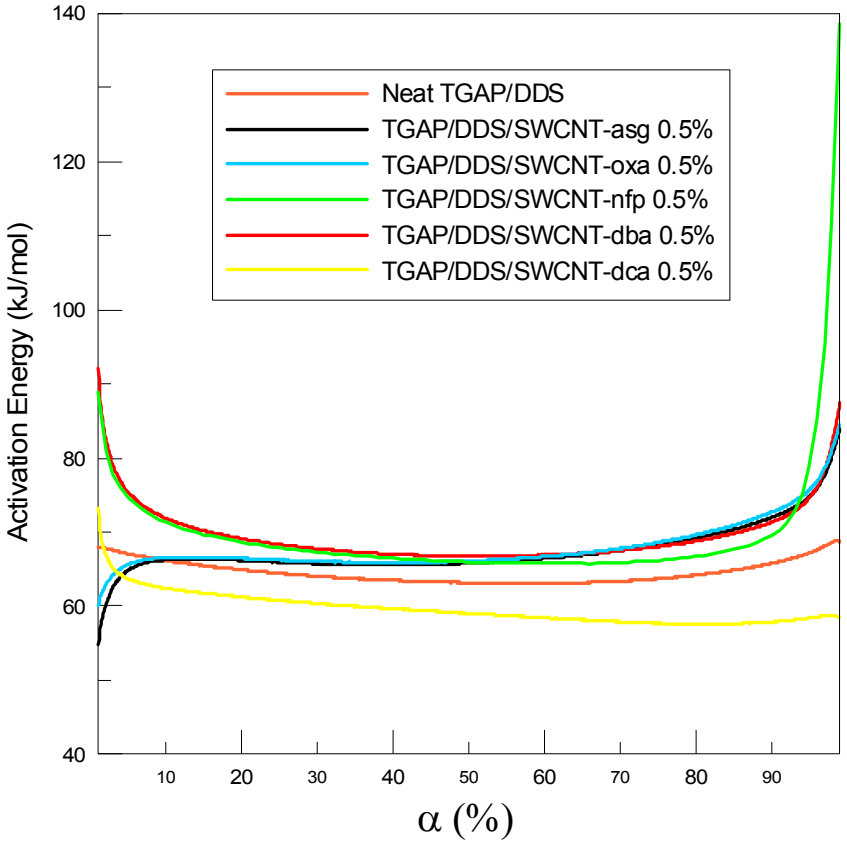

Figure 4.8. AE plots for the neat epoxy resin and TGAP/DDS/SWCNT samples at a 0.5 wt% ratio

For the rest of functionalized samples, the opposite effect appears in the initial curing stages. The higher AE initial values for these samples could be explained as an effect of oxirane rings pre-opening by the surface amino groups present in these SWCNTs. During the blend manufacturing, terminal amines could have partly reacted with oxirane rings, raising the viscosity of the system, as was experimentally observed. Since any of the amine moieties on SWCNTs are more reactive than amines coming from DDS,* the successful covalent interaction between TGAP and functionalized SWCNTs is suggested, and this effect would exceed that of an enhanced thermal

* Nucleophilicity and basicity of an aromatic amine such as DDS is lower as compared to an aliphatic one because the direct linking to a benzene ring partly delocalizes the electron pair on the nitrogen atom. All the functional groups from SWCNTs studied in this chapter contain aliphatic or benzylic amines so their basicity and nucleophilicity are expected to be higher than DDS amines and thus their reactivity toward oxirane rings.

diffusivity, as stated for SWCNT-asg epoxy blends. Besides, a sharp drop of AE occurs, which can be perfectly compatible with an accelerating effect spawned by the surface amino groups on SWCNTs.

The strongest acceleration is caused by the SWCNT-dca, that reach an average AE value ~5 KJ/mol lower than that of the neat matrix. According to the chemical nature of the covalent moieties, the one attached to SWCNT-dca is structurally the most similar to the epoxy cross-linked network, due to the ethylenoxide (EO) groups. This could generate an additional affinity based on non-covalent interactions that would decrease the viscosity and promote the curing reaction by counteracting the diffusional hindrance. In the previous section it has been shown how small amounts of EO accelerate initial stages of TGAP/DDS curing upon integration of Pluronic-wrapped SWCNTs, due to an increase in the mobility of chemical species.

With respect to the latter stages of curing, the neat matrix and SWCNT-dca composite do not show a significant dependence of AE with α, but the rest of composites exhibit a sharp increase of AE. Taking into account that the etherification reactions would predominate in the latter stages, this increase in AE could be ascribed to a hindrance of these reactions by surface groups in SWCNTs (namely –OH or amine). Indeed, other authors have reported a delay on epoxy etherification reactions with OH-containing SWCNTs, which raise the curing temperature at this stage.[31] More interestingly, these effects do not depend on the functionalization degree, although seem to be strongly dependent on the dispersibility of the filler, which is influenced by the chemical nature of the attached moiety and consequently by the functionalization route.

Figure 4.9 shows the isoconversional plots for TGAP/SWCNT mixtures, where 0.835 wt% corresponds to the final recalculated SWCNT ratio in the absence of DDS. AE plots in these blends show the course of the self-curing and degradation of the TGAP monomer, which presents a variable dependence of AE with α. In the initial stages of conversion (up to α ~ 25%), the effect of all SWCNT samples on the TGAP self-curing is to hinder its initiation. The reaction between surface (either amine or oxygen) groups would compete with the oxirane self-opening. During the next stage of conversion, a linear section with AE~100 kJ/mol is observed, with no influence of SWCNTs. The most noticeable AE dependences (in the form of a peak) arise from α ~

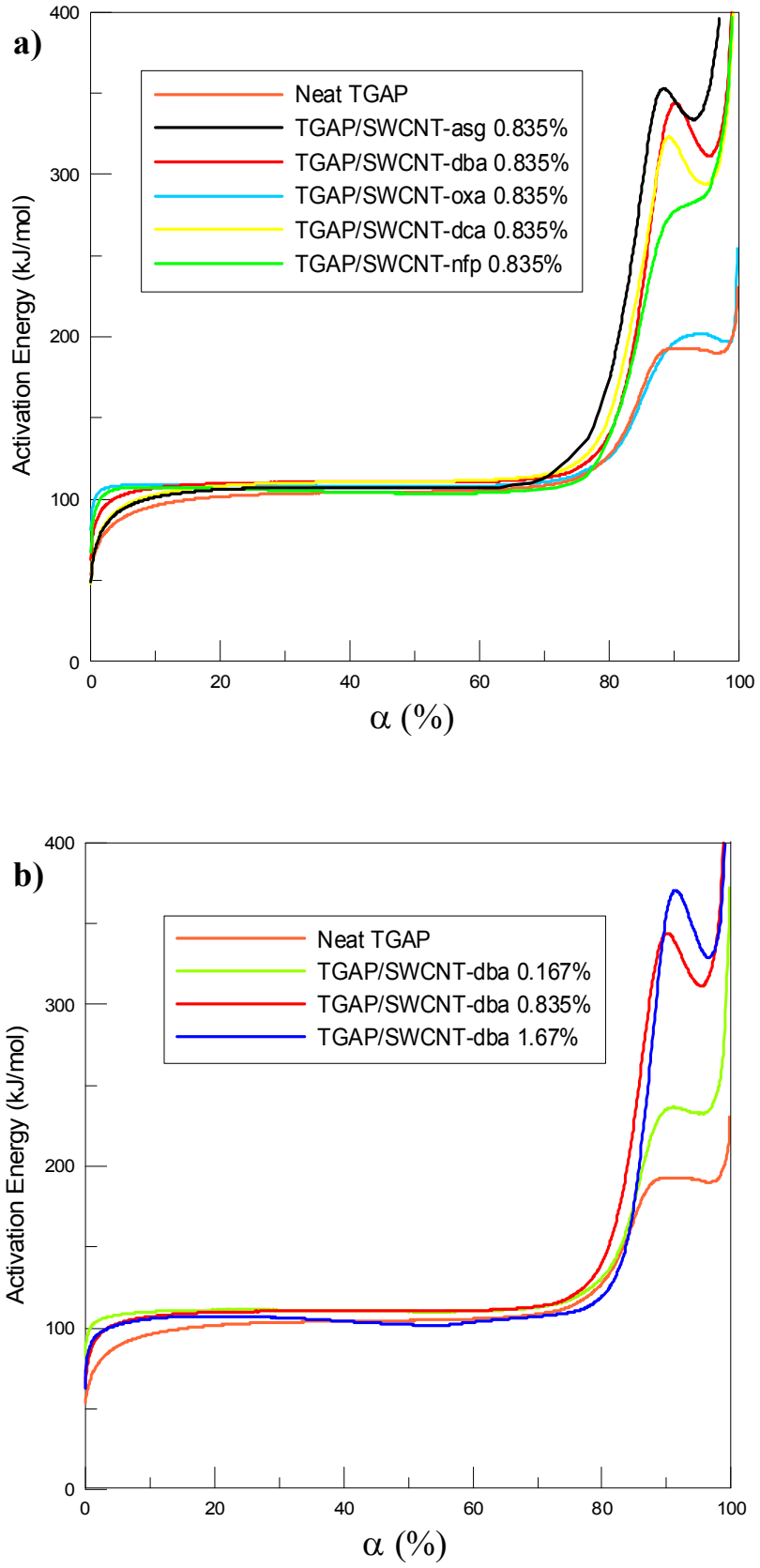

Figure 4.9. AE plots for the epoxy monomer and different TGAP/SWCNT mixtures: a) effect of different functional groups at a fixed loading, and b) effect of loading for SWCNT-dba sample.

75% on, moment in which the autocuring is much likely overlapping with degradation. In this stage the presence of SWCNTs greatly raises the AE (as determined from the SWCNT-asg sample). The rest of functionalized SWCNTs exhibit an upshift of the peak and lower AE values. This behavior correlates with the thermal stability observed for these SWCNTs in TGA (see section 2.3.2), suggesting that the degradation of the TGAP monomer is intimately related to the stability of the filler functional groups.

To study the effect of the amount of functionalized SWCNTs in the nonisothermal TGAP heating, a series of composite samples were recorded using SWCNT-dba at different loadings (Figure 4.9b). The nanotube content plays an important role in this matter since the AE peak at the highest conversions progressively rises in intensity and shifts toward higher α values (i.e. temperatures). The successful integration by solvent-free method of SWCNTs not only catalyzes the TGAP/DDS curing but also prevents the monomer degradation.

4.4.4.1. Effect of the SWCNT purity on curing kinetics

In order to distinguish effects which may come from the impurities generated during the functionalization procedures, the DSC study was fully repeated using the high purity SWCNT material (SWCNT-P2 hereafter), purchased from Carbon Solutions Inc. These SWCNTs (referred to as P2, batch # 02-369) were produced by the arc discharge technique similar to our SWCNT-asg. Then, according to the manufacturer's specifications, they were purified through air oxidation followed by an unspecified treatment to remove the residual catalyst. SWCNTs purity is >90% and metal content is 4-7 wt%, as determined by TGA in air. Our NIR measure-ments on this sample in 1 wt% SDBS gave a purity index of 0.157.

The observed values do not differ much from those obtained for SWCNT-asg in the same conditions. The nearly unchanged onset, T_g and T_m point to the same behavior as the SWCNT-asg sample. The curing enthalpy in the presence of DDS is higher for SWCNT-P2 than for SWCNT-asg, which could be ascribed to its higher purity.

Table 4.3. DSC parameters obtained for different TGAP/DDS/SWCNT and TGAP/SWCNT mixtures heated at a rate of 5ºC/min.

Filler*	With DDS				Without DDS		
	Onset (ºC)	T_m (ºC)	ΔH (J/g)	T_g (ºC)**	Onset (ºC)	T_m (ºC)	ΔH (J/g)
Neat Epoxy	167.5	199.7	203.9	209.9	301.3	312.9	497.7
SWCNT-asg	167.5	199.0	220.6	211.5	298.0	309.2	439.5
SWCNT-P2	167.5	199.2	242.9	212.0	300.2	310.7	423.8

* SWCNT content is 0.5 wt% (in the presence of DDS) or 0.835 wt% (in absences of DDS).
** T_g values are obtained during the cooling stage (-20 ºC/min) after non-isothermal curing.

Isoconversional kinetic curves of these samples are shown in Figure 4.10. The SWCNT-P2 sample presents an activation energy profile very similar to that of the SWCNT-asg in both cases, with and without DDS. Slight differences can be observed between both unfunctionalized fillers that come from their different purity and surface oxygen content. Therefore, the initial purity of the filler, is not a major influence in the curing process, being the dispersibility and grafted amines the most relevant factors involved. Chemical purification treatments do not cause visible effect as long as they do not drastically affect the filler's dispersibility (as nitric acid treatment does).

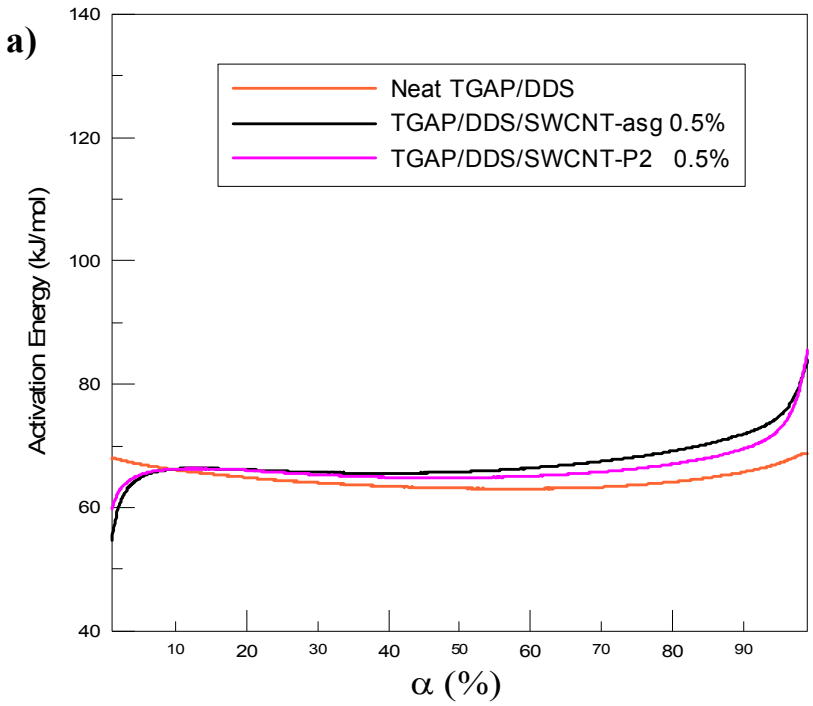

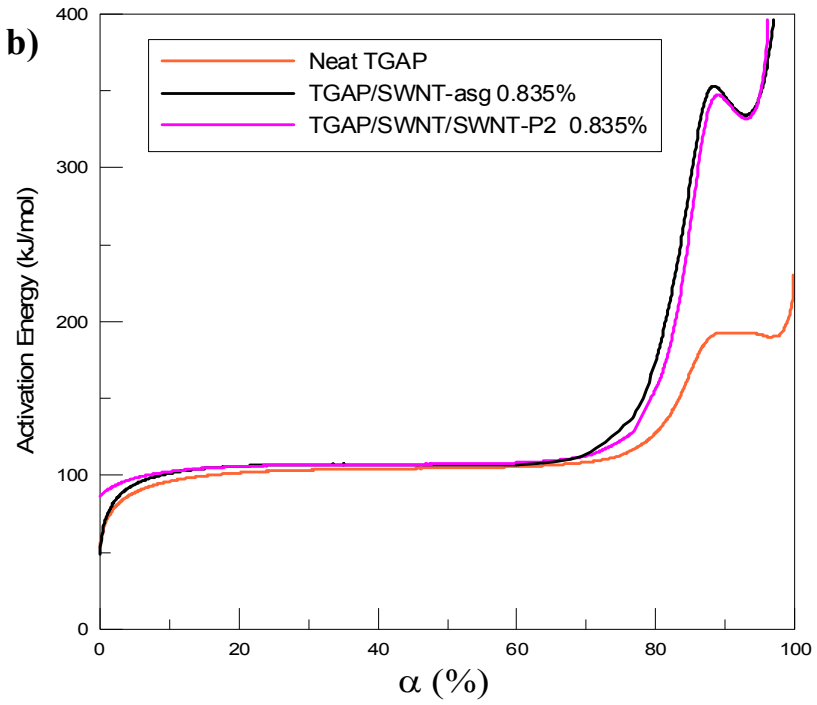

Figure 4.10. Activation energy plots for different unfunctionalized SWCNTs in epoxy, a) in the presence, or b) absence of the curing agent DDS.

4.5. Conclusion

The integration of Pluronic-wrapped and different amino-functionalized SWCNTs into a high performance trifunctional epoxy resin (TGAP/DDS) has been successfully carried out by means of solvent-free dispersion. The dispersibility of these SWCNTs was checked using optical microscopy in some TGAP/SWCNT mixtures before adding the hardener. Microscopic observation revealed a very smooth and fine morphology for Pluronic-wrapped and sidewall-functionalized SWCNTs, while as-grown SWCNTs or those undergoing nitric acid oxidation exhibited bad dispersibility and a high level of aggregation. TGAP/SWCNT and TGAP/DDS/SWCNT blends were subjected to DSC nonisothermal scans and a kinetic study of the filler effect on the curing kinetics was conducted using the Vyazovkin's AIM. AE *vs.* α plots, show a constant value (65-70 kJ/mol) for the intermediate stage of conversion (α ~ 25-70%) in all cases. In the extreme stages, there is a noticeable dependence of AE with α, which differs from a type of filler to another. As regards to blends containing Pluronic-wrapped SWCNTs, AE vs α plots show that Pluronic BC provides initial and final AE

values lower than the nitric acid-treated SWCNTs (2 wt%) sample. This fact points to a positive effect of this BC on the epoxy curing kinetics (at the low loadings incorporated), possibly by promoting the species mobility as the cross-linking reactions mainly undergo by diffusional control.

In epoxy/amino-SWCNT blends, the incorporation of non-functionalized SWCNTs, or those which undergo nitric acid oxidation prior to amination, raises the curing enthalpy with slight increase of T_g in the TGAP/DDS epoxy matrix and causes a sudden increase in the AE of the initial curing stages. Aminated SWCNTs through different sidewall addition reactions exhibit a decrease in enthalpy and a big increase in T_g coupled to a sharp decrease in AE during the initial curing stages of TGAP/DDS, consistent with an effective covalent anchoring of SWCNT amino groups to the target matrix. Further studies in the absence of the curing agent reveal the hindrance of autocuring and degradation of the TGAP monomer by the SWCNTs, regardless of the functionalization degree albeit dependent on the SWCNT loading. The remaining metal catalysts do not seem to be the cause of all these facts; nevertheless, the dispersibility of SWCNTs (influenced by the attached moiety and the functionalization procedure) plays a crucial role in the solvent-free integration. The type and chemical nature of the attached covalent moieties are directly responsible of these effects, but not the functionalization degree. The initial purity of the SWCNT sample did not show to cause a determinant influence on the curing process, as studied in a high purity commercial arc-discharge sample.

The results herein offer useful insights into the design of an epoxy-SWCNT composite material, without negatively affecting the cross-linking reactions while promoting (in the case of aminated SWCNTs) the covalent anchoring, and enhancing the filler-matrix adhesion. Manufacturing and full characterization of these composite materials will be reported in the following chapter.

"If you don't try to save one life,
you'll never save any".

Resident Evil Degeneration
Capcom (2008)

CHAPTER 5:

HIGH-PERFORMANCE EPOXY/SWCNT NANOCOMPOSITES, PART I: MATRIX REINFORCEMENT WITH COVALENTLY-FUNCTIONALIZED SWCNTs.

5.0. Abstract

Functionalization of SWCNTs with covalently grafted amine moieties provides reactive fillers with potential for covalent anchoring to an epoxy matrix. Manufacturing and characterization of a high performance epoxy system reinforced with as-grown and aminated SWCNTs throughout different approaches are presented. This chapter includes the preparation of epoxy nanocomposites containing SWCNTs aminated with aliphatic terminal amines and those epoxy nanocomposites reinforced with SWCNTs functionalized with matrix-based moieties. The proper choice of grafted moiety and integration protocol makes feasible to tune the physical properties of the nanocomposites. The functionalization with terminal aliphatic amines leads to nanocomposite materials with specific improvements in some of the epoxy physical properties, which enables the tailored design of the composites properties through functionalization. As it will be shown, the amination *via* the diazonium reaction with 4-aminobenzyl amine is especially effective in enhancing the tensile and impact properties of the epoxy composites and leads to one of the highest increases in elastic modulus ever reported for the integration of aminated CNTs into epoxy resin. Nanocomposites incorporating aminated SWCNTs throughout the 1,3-dipolar cycloaddition reaction stand out for their thermo-oxidative stability and thermo-mechanical properties. In the case of SWCNTs functionalized with matrix-based moieties, the improvements in thermal and mechanical properties are even higher, lying among the best ever reported for epoxy/CNT nanocomposites. This study suggests that a highly enhanced interfacial bonding between matrix and filler is achieved, coupled to an improved dispersion. The electrical conductivity measurements suggest the possibility to tune the nanocomposites insulating or conductive behavior. Finally, the incorporation of as-produced SWCNTs into the TGAP/DDS epoxy matrix leads to composite materials with the highest electrical conductivity among all the studied samples.

5.1. Introduction

Epoxy resins are a classic example of thermosetting polymers for light-weight applications in aerospace and automotive industries. Epoxy monomers with high number of oxirane rings per molecule (multifunctional monomers) are currently being utilized in this field of applications. Their use includes structural applications, coatings,

adhesives, insulation, *etc.* However, fundamental flaws in epoxy performance (such as high brittleness, moduli and stiffness below the required level, high electrical resistance, among others) often restrict their range of use. The addition of a filler to enhance physical properties has been carried out extensively in recent decades. Within this context, SWCNTs are ideal candidates because of their extraordinary properties,[1,2] and their potential reinforcing role if a suitable transfer of properties is achieved from the nano to the macroscale. This is indeed a major challenge when dealing with polymer/SWCNT nanocomposites, where the bundling tendency, insolubility in most of liquid media and lack of adhesion to the matrix reported for SWCNTs represent the main obstacles for the full exploitation of these materials. Thus, the reported results are inferior to those predicted from theoretical studies.[3]

Numerous pre-processing procedures have been applied in order to address this problem, among which, SWCNT covalent modifications are increasingly being employed.[4] The covalent grafting of amine groups on SWCNT surfaces has a special advantage since these functional groups are able to actively participate in the curing process, reacting with the oxirane rings and becoming an integrated element in the matrix owing to covalent bonds between the filler and the cross-linked epoxy structure. The functionalization of CNTs, mainly MWCNTs, with amines has been observed to lower the degree of agglomeration and to enhance the filler-matrix adhesion,[5] leading to remarkable improvements in the mechanical properties of epoxy matrices at low loadings.[6]

[1] Treacy, M. M. J.; Ebbesen, T. W.; Gibson, J. M., Exceptionally high Young's modulus observed for individual carbon nanotubes. *Nature* 1996, *381* (6584), 678-680.
[2] Tans, S. J.; Devoret, M. H.; Dai, H. J.; Thess, A.; Smalley, R. E.; Geerligs, L. J.; Dekker, C., Individual single-wall carbon nanotubes as quantum wires. *Nature* 1997, *386* (6624), 474-477.
[3] Salvetat, J. P.; Bonard, J. M.; Thomson, N. H.; Kulik, A. J.; Forro, L.; Benoit, W.; Zuppiroli, L., Mechanical properties of carbon nanotubes. *Appl. Phys. A-Mater. Sci. Process.* 1999, *69* (3), 255-260.
[4] Bose, S.; Khare, R. A.; Moldenaers, P., Assessing the strengths and weaknesses of various types of pre-treatments of carbon nanotubes on the properties of polymer/carbon nanotubes composites: A critical review. *Polymer* 2010, *51* (5), 975-993.
[5] Gojny, F. H.; Nastalczyk, J.; Roslaniec, Z.; Schulte, K., Surface modified multi-walled carbon nanotubes in CNT/epoxy-composites. *Chem. Phys. Lett.* 2003, *370* (5-6), 820-824.
[6] Zhu, J.; Peng, H. Q.; Rodriguez-Macias, F.; Margrave, J. L.; Khabashesku, V. N.; Imam, A. M.; Lozano, K.; Barrera, E. V., Reinforcing epoxy polymer composites through covalent integration of functionalized nanotubes. *Adv. Funct. Mater.* 2004, *14* (7), 643-648.

Other studies also state significant improvements of epoxy/amine-CNT as compared to the parent matrix,[7] i.e. ~25-70% improvement in storage modulus and ~10-45% improvement in tensile strength. However, to date, only very few studies have been reported on the integration of covalently aminated SWCNTs into epoxy matrices.[6,8]

The general aim of covalently grafting amine groups onto CNTs is to seek an enhancement of SWCNT miscibility and dispersibility in organic media, together with providing a matrix-reactive filler. This feature is exploited towards the integration of functionalized SWCNTs in the epoxy, usually by the use of solvents. However, the presence of organic solvents in the epoxy matrix usually presents some disadvantages (inhomogeneous filler distribution upon evaporating[9] or decreases in parameters such as Vickers hardness,[10] flexural modulus[10] and glass transition temperature T_g[11]); for this reason, the resulting performance of the composite may be aggravated as compared to what is expected. In this chapter a comprehensive characterization of a series of amine-SWCNT/epoxy composites with SWCNT covalent anchoring to the matrix is provided.

The integration of SWCNTs functionalized with aliphatic terminal amines was carried out without organic solvents in order to ascertain the chemical compatibility with the matrix and the properties improvement as a direct consequence of the SWCNT functionalization. Discussion is given in relation to the filler-matrix dispersion behavior and chemical affinity, which is a direct consequence of the functionalization route, as previously shown by DSC[12] (see section 4.4.3). The integration of SWCNTs functionalized with matrix-based moieties was carried out not only solvent-free, but also through solvent-processing in order to show the different behavior of the grafted

[7] Spitalsky, Z.; Tasis, D.; Papagelis, K.; Galiotis, C., Carbon nanotube-polymer composites: Chemistry, processing, mechanical and electrical properties. *Prog. Polym. Sci.* 2010, *35* (3), 357-401.
[8] Wang, S. R.; Liang, Z. Y.; Liu, T.; Wang, B.; Zhang, C., Effective amino-functionalization of carbon nanotubes for reinforcing epoxy polymer composites. *Nanotechnology* 2006, *17* (6), 1551-1557.
[9] Grady, B. P., Recent developments concerning the dispersion of carbon nanotubes in polymers. *Macromol. Rapid Commun.* 2010, *31* (3), 247-257.
[10] Lau, K. T.; Lu, M.; Lam, C. K.; Cheung, H. Y.; Sheng, F. L.; Li, H. L., Thermal and mechanical properties of single-walled carbon nanotube bundle-reinforced epoxy nanocomposites: the role of solvent for nanotube dispersion. *Compos. Sci. Technol.* 2005, *65* (5), 719-725.
[11] Allaoui, A.; El Bounia, N., How carbon nanotubes affect the cure kinetics and glass transition temperature of their epoxy composites? - A review. *Express Polym. Lett.* 2009, *3* (9), 588-594.
[12] Gonzalez-Dominguez, J. M.; Gonzalez, M.; Anson-Casaos, A.; Diez-Pascual, A. M.; Gomez, M. A.; Martinez, M. T., Effect of various aminated single-walled carbon nanotubes on the epoxy cross-linking reactions. *J. Phys. Chem. C* 2011, *115* (15), 7238-7248.

functional groups in the nanocomposite properties. The curing and manufacturing of such epoxies are expected to provide nanocomposite materials with enhanced physical properties while conserving the original cross-linked architecture at the interface. On the whole, it was evidenced that both functionalization approach and the integration protocol are important in tuning the nanocomposites physical properties in a simple and reproducible way.

5.2. Experimental section

Functionalization of as-grown arc-discharge SWCNTs (SWCNT-asg) with aliphatic terminal amines was conducted through several procedures, covalently grafting primary amine-ended moieties:

- Nitric acid oxidation, carboxylic activation with $SOCl_2$ and amide formation using N-boc-1,6-diaminohexane (SWCNT-oxa).
- Alkaline reduction with sodium-naphthalide ions and sidewall radical addition of aminohexanoic acid-derived acyl peroxide (SWCNT-nfp).
- Sidewall addition of benzylamine through in situ generated diazonium salt of 4-aminobenzylamine (SWCNT-dba).
- 1,3-dipolar cycloaddition of azomethyne ylides with an amine-terminated α-aminoacid (SWCNT-dca).

A detailed description of the functionalization procedures and SWCNT characterization can be found in section 2.2.2 (summary shown in Figure 2.15).

For the functionalization of SWCNTs with matrix-based moieties, the experimental procedure followed was based on the *in situ* formation of an aryl diazonium and reaction with arc-discharge or laser SWCNT sidewalls, as described by Bahr et al.[13] Detailed experimental procedures can also be found in section 2.2.2 (a summary scheme of these functionalizations is depicted in Figure 5.1. By this means, the DDS molecule was used as the arylamine to perform the diazonium route. Besides, two derivatives were synthesized using TGAP and DDS. The first derivative, AD,

[13] Bahr, J. L.; Tour, J. M., Highly functionalized carbon nanotubes using in situ generated diazonium compounds. *Chem. Mater.* 2001, *13* (11), 3823-3824.

contained terminal amine groups and the second one, ED, contained terminal epoxide rings.

5.2.1. Preparation of epoxy/SWCNT nanocomposites

Nanocomposites containing SWCNTs functionalized with aliphatic terminal amines were prepared by mixing TGAP and DDS in stoichiometric ratio (100/67),[14] while for nanocomposites based on SWCNTs functionalized with matrix-based moieties the epoxy reagents were mixed in a slightly off-stoichiometric ratio (100/60).[15] Neat baseline epoxy (TGAP/DDS) was prepared by directly blending TGAP and DDS at 60ºC for 15min. Different nanocomposites containing 0.1, 0.5 and 1 wt % of as-grown or functionalized SWCNTs were prepared by a solvent-free protocol including hot stirring and sonication.[16] In a typical experiment, 1g of TGAP was mixed with the required filler amount and magnetically stirred at 60ºC for 45min. Then, the mixture was subjected to tip sonication for 15min, having external refrigeration with a water bath at room temperature. After 2min of stirring at 60ºC, the DDS was slowly incorporated stepwise, within a time period between 15-30 min (as indicated in section 4.4.2.).

To study the influence of a solvent in the integration, in a parallel preparation protocol, the integration was carried out by pre-dispersion of SWCNTs in organic solvent (DMF) at a fixed loading of 0.5 wt% SWCNTs. The suspension of SWCNT in DMF was added to the epoxy monomer and mixed by mechanical stirring and bath sonication for 30 min. The DMF was removed at 70 ºC under vacuum and mechanical stirring for 2h, and finally dried for 3h at 120 ºC under the same conditions. The epoxy blank samples were prepared using both procedures respectively but without adding SWCNTs, in order to verify the effect of the preparation protocol on the properties of

[14] Gonzalez-Dominguez, J. M.; Diez-Pascual, A. M.; Anson-Casaos, A.; Gomez-Fatou, M. A.; Martinez, M. T., Epoxy composites with covalently anchored amino-functionalized SWNTs: towards the tailoring of physical properties through targeted functionalization. *J. Mater. Chem.* 2011, *21* (20), 14948-14958.
[15] González-Domínguez, J. M.; Martínez-Rubí, Y.; Díez-Pascual, A. M.; Ansón-Casaos, A.; Gómez-Fatou, M. A.; Simard, B.; Martínez, M. T., Reactive fillers based on SWCNTs functionalized with matrix-based moieties for the preparation of epoxy composites with superior and tuneable properties, *Nanotechnology (submitted).*
[16] Gonzalez-Dominguez, J. M.; Castell, P.; Anson, A.; Maser, W. K.; Benito, A. M.; Martinez, M. T., Block Copolymer Assisted Dispersion of Single Walled Carbon Nanotubes and Integration into a Trifunctional Epoxy. *J. Nanosci. Nanotechnol.* 2009, *9* (10), 6104-6112.

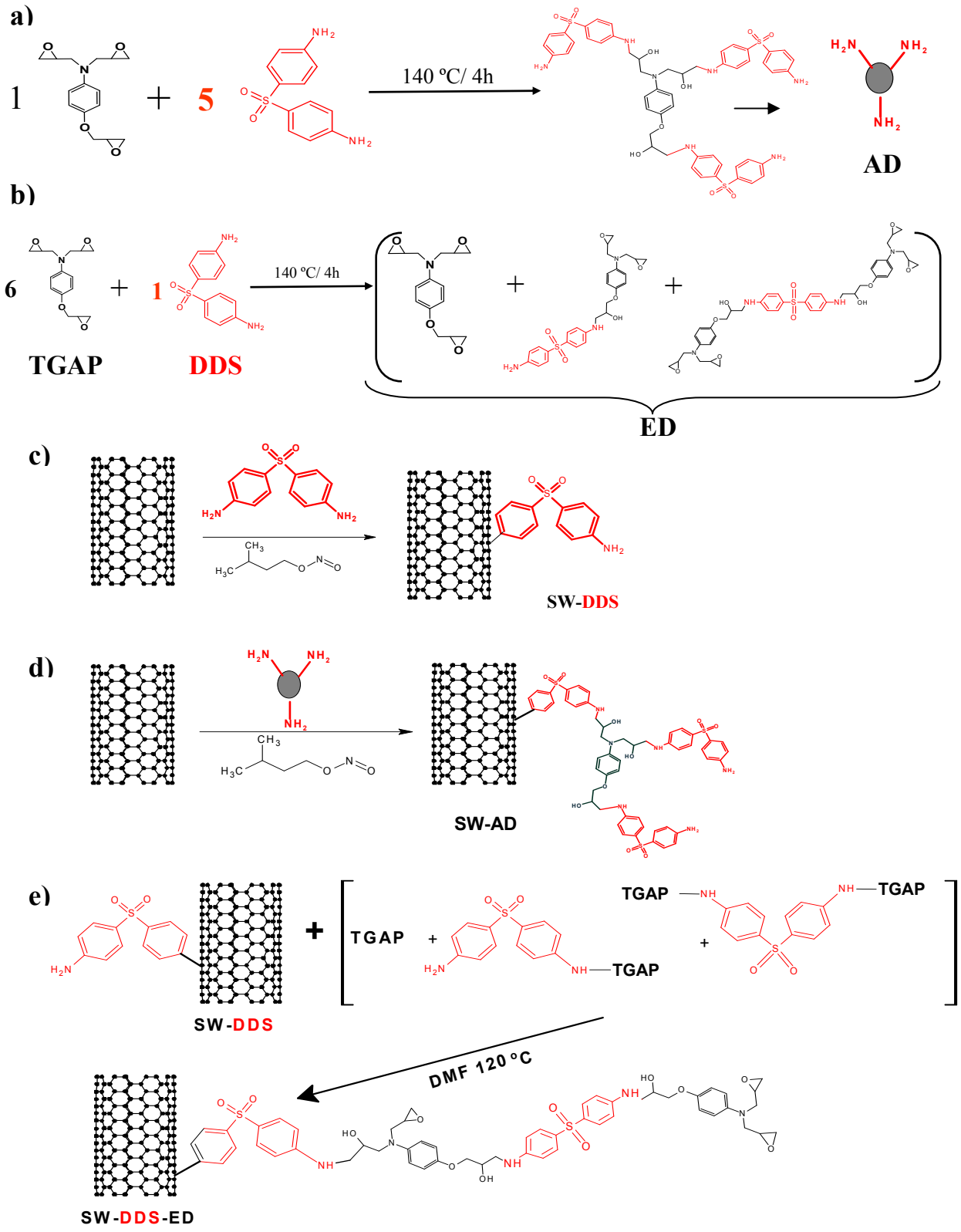

Figure 5.1. a) preparation of the AD derivative, b) preparation of the ED derivative mixture, c) functionalization of SWCNTs with DDS *via* the diazonium reaction, d) functionalization of SWCNTs with AD *via* the diazonium reaction, e) functionalization of SWCNTs with the ED derivative mixture by nucleophilic ring opening. For the sake of clarity, TGAP moieties are displayed in black while DDS moieties appear in red.

the matrix. The curing was performed by casting the epoxy or composite blends into a steel dish mould (2mm thick) sealed by 3mm thick teflon plates, followed by heating at 160ºC for 45 minutes and 200ºC for 30min in a Perkin Elmer hydraulic press coupled to a Greaseby Specac controlled heater, under 3 tonnes of pressure. The samples were removed from the mould, transferred to a Carbolite LHT4/30 oven and postcured at 200ºC for 4 hours.

5.2.2. Characterization techniques

► SEM experiments were made in a scanning electron microscope (Hitachi S3400N), working in the secondary electrons mode at a high voltage 15 kV and a distance of 5 mm. Cured samples were fractured and the edge was sputtered with a 10nm gold layer prior to their observation. **(ICB)**

► The nanocomposites thermal and thermo-oxidative stability was analyzed by TGA in both nitrogen and air atmospheres (at 50 mL/min flow rate). Epoxy nanocomposites based on SWCNTs functionalized with aliphatic terminal amines were analyzed in the same conditions specified in section 2.2.3. **(ICB)** Epoxy nanocomposites containing SWCNTs functionalized with matrix-based moieties were registered in a Mettler TA-4000/TG-50 thermobalance, at a heating rate of 10ºC/min. The temperature was scanned from room temperature to 800ºC under dry air or nitrogen atmosphere. All experiments were carried out on samples with an average mass of 150 mg. **(ICTP)**

► The dynamic mechanical performance of the samples was analysed using a Mettler DMA 861 dynamo-mechanical analyser. Experiments were performed in the tensile mode at a frequency of 1 Hz. A dynamic force of 6 N oscillating at fixed frequency and amplitude of 30 μm was used. The relaxation spectra were recorded in the temperature range between -100ºC and 325ºC, at a heating rate of 2ºC/min. The specimen dimensions were ~19.5 × 5 × 2 mm^3. **(ICTP)**

► Tensile mechanical properties of the composites were measured with an INSTRON 4204 tester at room temperature (23 ± 2ºC), using a crosshead speed of 1 mm/min and a load cell of 1 kN. Dogbone specimens (Type 1BB) were employed, as specified in the UNE-EN ISO 527-2 standard. Both sample surfaces were surface-polished prior to the

measurements. At least five specimens for each type of composite were tested to ensure repeatability. **(ICTP)**

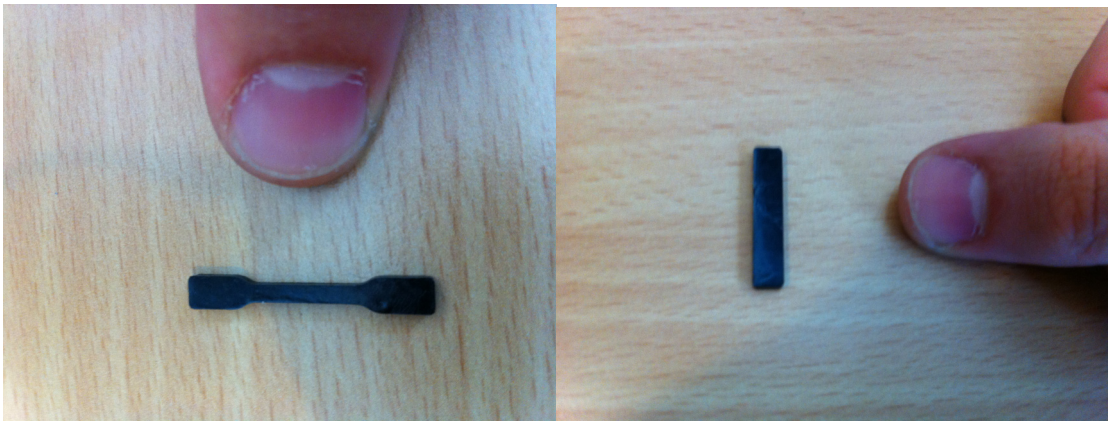

Figure 5.2. Typical dog-bone tensile (left side) and DMA (right side) test samples.

► Charpy impact strength measurements were carried out using a CEAST Fractovis dart impact tester. A hammer mass of 1.096 kg impacted at a constant velocity of 3.60 ms^{-1} (giving a total kinetic energy at impact of 7.10 J) on notched specimen bars with dimensions 33 × 10 × 3 mm^3, as described in the UNE-EN ISO 179 standard. Measurements were performed at 23 ± 2ºC and 50 ± 5% relative humidity. The presented data correspond to the average value of at least 5 specimens. **(ICTP)**

► Raman spectra were recorded on the same equipment stated in section 2.2.3. **(SIMS)** For Raman mapping the top surface of 2 mm thick Epoxy/SWCNT composites were successively polished using 600, 800 and 1200 grit grinding paper. Mapping of the SWCNT concentration distribution was done using a spectral imaging mode. Raman images were acquired for 80 μm x 120 μm regions at 1 μm intervals in X and Y using a 50x objective and an excitation wavelength of 785 nm.

► Electrical conductivity was measured in nanocomposite samples under the same conditions described in section 2.2.3. The specimen measurements were ~19.5 × 5 × 2 mm^3. Test samples were placed in a sandwich-like arrangement using two copper sheets (0.2mm thick). Measurements were carried out in a two-probe configuration, with the two probes placed on each of the ~19.5 × 5 mm^2 rectangular surfaces of the test sample. **(ICB)**

► AFM measurements were performed with a Multimode SPM from Veeco Instruments (Santa Barbara, US), equipped with Nanoscope V controller and JV-scanner (10μm scan size in XY, and 2.5μm Z-range), The system included the HarmoniX option which allows force-distance curves to be acquired in real time during tapping mode operation and map mechanical properties to be extracted as additional data channels.[17] Soft silicon tapping mode cantilevers with off-axis tip design and reflective backside Al-coating (tip radius 10nm, spring constant 4 N/m, fundamental vertical resonance 70kHz, torsional resonance 1200 kHz) were used, optimized for large bandwidth acquisition of the force distance data (type HMX, Veeco Probes, Camarillo, US). Probes were mounted in a cantilever holder with large dither piezo (model MFMA, Veeco Instruments, Santa Barbara, US). Electrical mapping was carried out using tips Using cantilever SCM-PIC made of Sb-doped W with 0.01-0.025 Ω•cm resistivity coated with 20nm of Pt/Ir and 3nm Cr. Cured composites were cut with an ultramicrotome, thoroughly polished and attached to a steel sample holder with silver painting prior to the AFM measurements. Calibration of the modulus was performed by comparing the HarmoniX-data with a polymer sample of known modulus in the expected range. **(ICB)**

5.3. Results and discussion

5.3.1. Epoxy nanocomposites containing SWCNTs with aliphatic terminal amines

SEM observation

SEM images were taken of fractured edge surfaces of the composites and representative examples are shown in Figure 5.3. The epoxy nanocomposite containing SWCNT-asg (Fig. 1a) exhibits a very irregular distribution of the filler, with frequent entanglements (highlighted with circles in Fig. 5.3a). The filler consists of long SWCNT bundles that appear to have been pulled out from the bulk matrix during the fracture. The incorporation of SWCNT-oxa gives a similar fracture edge overview (not shown), much like that of solvent-free integrated nitric acid-treated SWCNTs in the

[17] Sahin, O.; Erina, N., High-resolution and large dynamic range nanomechanical mapping in tapping-mode atomic force microscopy. *Nanotechnology* 2008, *19* (44).

same epoxy resin, as it will be shown in the following chapter.[18] Epoxy composites with the other functionalized SWCNTs exhibit substantially different features. The fracture edge contains randomly dispersed SWCNTs without visible agglomerates. The length of bundles is noticeably shorter, which could be indicative of breakage, instead of a pulling-out. Thus, the epoxy composites containing sidewall-functionalized SWCNTs seem to present better filler-matrix adhesion and enhanced dispersion within the matrix, as a direct consequence of functionalization.

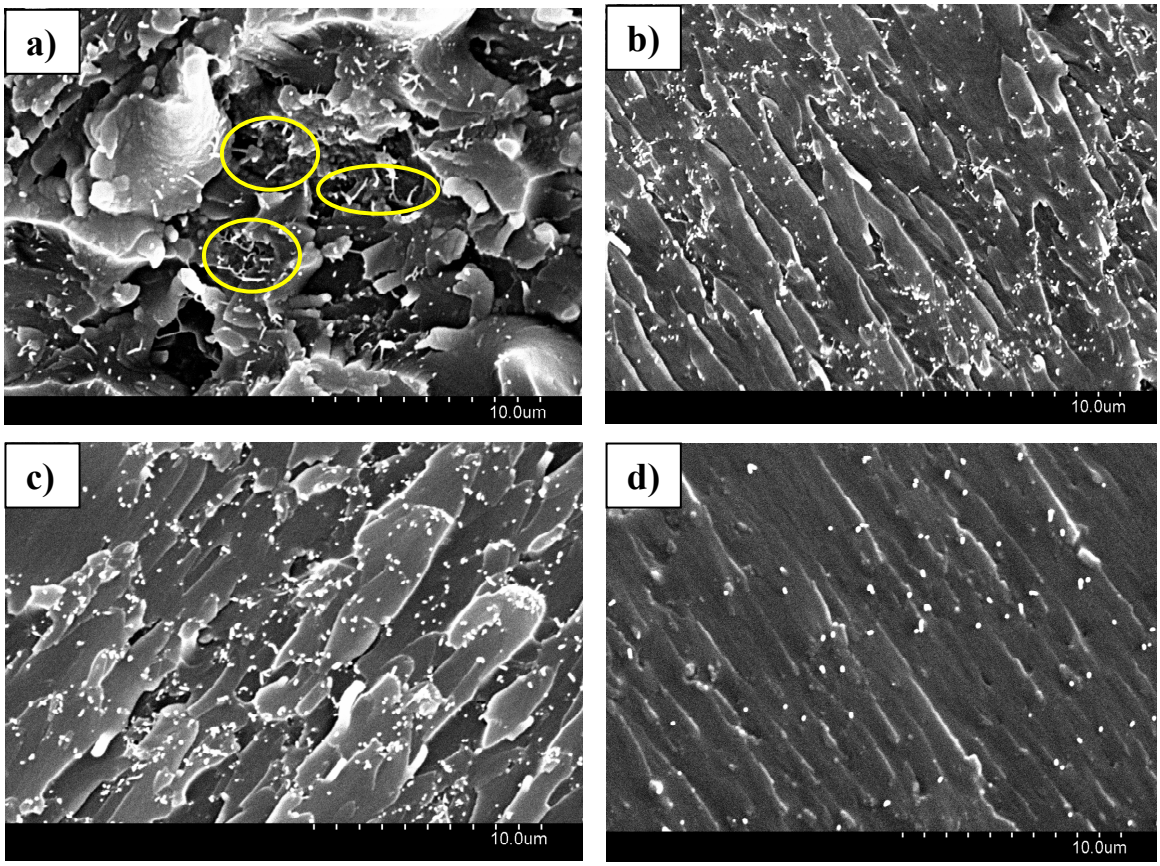

Figure 5.3. Fracture surface SEM images of epoxy nanocomposites containing (a) 1 wt % SWCNT-asg; (b) 0.5 wt % SWCNT-dca; (c) 1 wt % SWCNT-nfp; (d) 0.5 wt % SWCNT-dba.

It is worthy of note that the SWCNT-dba composite (Figure 5.3d) shows a larger dispersion enhancement. Furthermore, the protruded bundles across the fracture edge

[18] Gonzalez-Dominguez, J. M.; Anson-Casaos, A.; Diez-Pascual, A. M.; Ashrafi, B.; Naffakh, M.; Backman, D.; Stadler, H.; Johnston, A.; Gomez, M.; Martinez, M. T., Solvent-Free Preparation of High-Toughness Epoxy-SWCNT Composite Materials. *ACS Appl. Mater. Interfaces* 2011, *3* (5), 1441-1450.

appear extremely short (mostly as dots), indicative of a higher breakage of the SWCNTs spawned by a more efficient covalent anchoring.

Thermal and thermo-oxidative stability

Information about thermal and thermo-oxidative features can be inferred from TGA in nitrogen and air atmospheres. Thermograms obtained in inert environment exhibit a single weight loss centred at about 390ºC, while those registered in oxidative atmosphere show two consecutive weight losses, centred around 370ºC and 440ºC respectively.[19] Table 5.1 indicates the different parameters obtained from the TGA plots, including the temperatures of maximum rate of weight loss (T_{max}) and the temperatures corresponding to 10% weight loss (T_{10}), for composites with 0.5 wt % SWCNTs.

Table 5.1 Data extracted from TGA plots in air and N_2 atmosphere of the neat matrix and composites with 0.5 wt % SWCNTs. T_{10} = temperature corresponding to 10% weight loss; T_{max} = temperature of maximum rate of weight loss; the subscripts 1 and 2 refer to the first and second degradation stages, respectively. ΔT is the difference between $T_{max}1$ and $T_{max}2$. R_{700} = residue at 700ºC. Numbers in parenthesis indicate the standard deviation

	Air atmosphere					**N_2 atmosphere**			
	T_{10}/ºC (±2)	**$T_{max}1$/ºC (±2)**	**$T_{max}2$/ºC (±4)**	**ΔT (ºC)**	**R_{700}/wt% (±0.06)**	**T_{10}/ºC (±2)**	**T_{max}/ºC (±2)**	**R_{700}/wt% (±0.1)**	**OI (%)**
Neat TGAP/DDS	347.9	363.9	533.9	170.0	0.10	349.9	386.3	23.7	26.7
TGAP/DDS/SWCNT-asg	353.1	374.6	544.4	169.8	0.92	351.5	391.9	27.5	28.5
TGAP/DDS/SWCNT-oxa	352.1	363.6	540.7	177.1	0.65	353.4	393.7	25.8	27.8
TGAP/DDS/SWCNT-dca	351.3	386.4	544.5	158.1	0.73	354.8	395.3	26.5	28.1
TGAP/DDS/SWCNT-dba	351.5	371.2	547.3	176.1	0.85	352.5	394.4	27.2	28.4
TGAP/DDS/SWCNT-nfp	351.2	380.5	536.9	156.4	1.28	351.2	392.6	26.4	28.1

The solvent-free incorporation of SWCNT-asg leads to an enhancement in thermal and thermo-oxidative stability since T_{max} increases ~6ºC and $T_{max}1$ and $T_{max}2$

[19] Gonzalez-Dominguez, J. M.; Anson-Casaos, A.; Castell, P.; Diez-Pascual, A. M.; Naffakh, M.; Ellis, G.; Gomez, M. A.; Martinez, M. T., Integration of block copolymer-wrapped single-wall carbon nanotubes into a trifunctional epoxy resin. Influence on thermal performance. *Polym. Degrad. Stab.* 2010, *95* (10), 2065-2075.

rise ~10ºC each. The incorporation of functionalized SWCNTs leads to higher degradation temperatures in most cases as compared to the neat epoxy matrix or the epoxy composites containing SWCNT-asg. The most remarkable features are those coming from SWCNT-dca composites in nitrogen atmosphere, where T_{10} increases by about 5ºC and T_{max} rises by 9ºC as compared to the TGAP/DDS sample. This is approximately 3ºC higher than the SWCNT-asg composite in both parameters at 0.5 wt% loading. The rest of nanocomposites containing functionalized SWCNTs do not exhibit significant improvements in comparison to the TGAP/DDS/SWCNT-asg sample, but all of them possess higher thermal stability than the parent matrix. In air environment, the SWCNT-dca composite shows the highest $T_{max}1$ value, which is 22ºC higher than the neat matrix and 12ºC higher than the composite with the same amount of unfunctionalized SWCNTs. This indicates that the SWCNT-dca composites are more suitable for high-temperature applications in oxidative environments than pristine epoxy.

The flame retardant ability of a material can be estimated through the oxygen index (OI) from the char residue wt% at 700ºC in inert atmosphere. This parameter can be easily calculated through the Van Krevelen empirical equation [1], where CR is defined as the final char residue found under N_2 atmosphere.[20] The limiting OI (in %), at which a material can be considered flammable, is ≤26%. The TGAP/DDS sample exhibits an OI value close to the flammable behavior, and all the composite samples show visible non-flammable behavior. This enhancement has no dependence on the functionalization route except for the SWCNT-oxa composite, which exhibits lower enhancement.

$$OI(\%) = 17.5 + 0.4 \cdot (CR) \qquad [1]$$

Further discussion on the thermal and thermo-oxidative stability of these samples is given in reference 14.

Dynamic mechanical characterization

[20] van Krevelen, D. W., Some basic aspects of flame resistance of polymeric materials. *Polymer* 1975, *16* (8), 615-620.

The dynamic mechanical properties of the different epoxy/SWCNT composites were studied in order to ascertain changes in their stiffness as a function of temperature. DMA tests over a wide temperature range are sensitive to the transitions and relaxation processes of the resin in the composite, and provide information about the CNT-matrix interfacial bonding. The summary of the room temperature storage moduli (E′) and glass transition temperatures (T_g) of the different composites is shown in Figure 5.4. E′ of the neat epoxy matrix (Fig. 5.4a) is 3.42 GPa, and it decreases by ~18% upon subjecting the matrix to the same preparation procedure as the composite samples. This indicates that the hot stirring and sonication steps cause some damage to the parent matrix with the used curing cycle. This damage could arise from the polymer chains scission upon heating and/or sonicating, which would lower the cross-linking degree at a given TGAP/DDS ratio, hence diminishing the matrix stiffness.

The nanocomposites incorporating 0.1 wt% SWCNT loading clearly shows that all functionalized SWCNTs are able to compensate the effect of the preparation protocol, and to raise E′ close to the value of the neat matrix, with the exception of SWCNT-oxa, whose composite shows similar E′ to that of the blank sample. At higher loadings, the differences between the various samples are more pronounced. At 0.5 wt% loading, the SWCNT-oxa composite still remains below the neat matrix, despite having storage modulus above the blank sample. All the other composite samples exhibit similar E′ values, which are on average 58% higher than that of the blank sample. With respect to the 1 wt% loading, the largest E′ enhancement is found for the SWCNT-dca composite (77% improvement in comparison to the blank sample and almost 45% in comparison to the neat epoxy). The SWCNT-oxa composite slightly surpasses the neat matrix modulus, while the other composites exhibit a very high E′, with those of samples containing functionalized SWCNTs clearly above those of the composites with non-functionalized SWCNTs.

This significant increase in the storage modulus, hence in the composite stiffness, results from improved interfacial bonding CNT-epoxy, since the amino groups grafted on the CNT surface reacted with the epoxide rings during the curing processes. It is worthy of note that E′ improvements achieved in some of our composites with functionalized SWCNTs are among the highest reported for analogous epoxy composi-

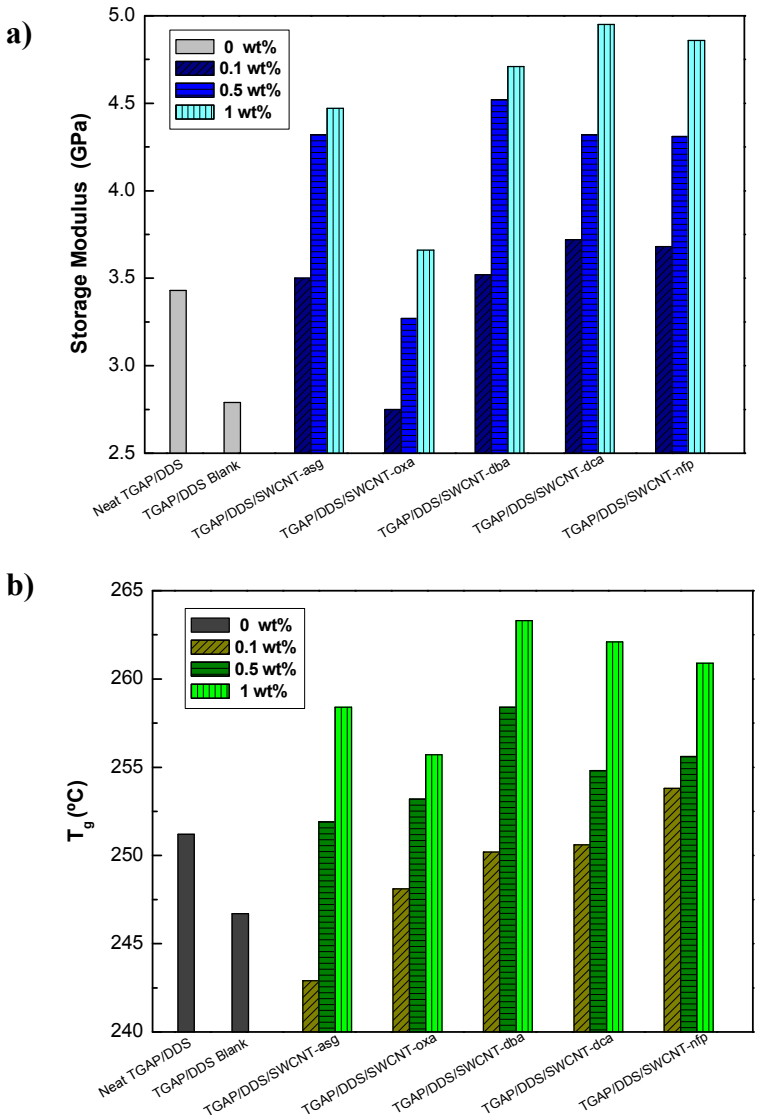

Figure 5.4. Data extracted from the DMA tests: (a) Storage moduli E´; and (b) Glass transition temperatures, T_g

tes containing other amino-functionalized CNTs (either SWCNTs or MWCNTs) with similar loading.[6,8,21,22] For nanocomposites with 0.5 wt% of aminated SWCNTs loading, the highest E´ increment is achieved for the SWCNT-dba nanocomposites, exhibiting higher E´ improvement than that obtained by Wang et al.[8] with aminated SWCNTs at the same loading. For composites with a 1 wt % CNT loading, the SWCNT-dca nanoco-

[21] Spitalsky, Z.; Matejka, L.; Slouf, M.; Konyushenko, E. N.; Kovarova, J.; Zemek, J.; Kotek, J., Modification of carbon nanotubes and its effect on properties of carbon nanotube/epoxy nanocomposites. *Polym. Compos.* 2009, *30* (10), 1378-1387

[22] Liu, L.; Etika, K. C.; Liao, K. S.; Hess, L. A.; Bergbreiter, D. E.; Grunlan, J. C., Comparison of Covalently and Noncovalently Functionalized Carbon Nanotubes in Epoxy. *Macromol. Rapid Commun.* 2009, *30* (8), 627-632.

Table 5.2. Comparative chart between mechanical and thermomechanical properties from literature data and nanocomposites samples in the present section.

Ref.	Type of CNTs	Amine moiety	CNT loading (wt%)	E' (25ºC) improvement*	Present Results**	T_g change*	Present Results**	YM improvement*	Present Results**	σ_y improvement*	Present Results**
8	SWCNTs	Aryl-NH_2	0.5	24.6%	32.1% (SWCNT-dba, 0.5 wt%)	-11.3ºC	+7.3ºC (SWCNT-dba, 0.5 wt%)				
6	SWCNTs	CO-NH-R-NH_2	1 and 4	~31.5% @ 1 wt%	44.3% (SWCNT-dca, 1 wt%)			30.5% @ 1 wt%	54.8% (SWCNT-dba 1wt%)	25% @ 1 wt%	43% (SWCNT-dba, 1 wt%)
21	MWNTs	CO-NH-R-NH_2	0.5 and 1	~25% @ 1wt%						~38.5% @ 0.5wt%	30% (SWCNT-dba, 0.5 wt%)
		Aryl-CO-NH-R-NH_2		~44% @ 1wt%						~30.8% @ 0.5wt%	
22[a]	MWNTs	NH-$(CH_2$-CH_2-$NH)_n$-CH_2-CH_3	1	~16.7%		~(-6ºC)	+12.2ºC (SWCNT-dba, 1 wt%)				
25	MWNTs	CO-NH-R-NH_2	1			+8ºC					
26	SWCNTs	CO-NH-R-NH_2	0.3			+2ºC	+3ºC (SWCNT-nfp 0.1 wt%)				
27	MWNTs	CH(COOH)-CH_2-CO-NH-R-NH_2	0.1 – 1			+11ºC @ 1 wt%	+12.2ºC (SWCNT-dba, 1 wt%)			~45% @ 1wt%	43% (SWCNT-dba, 1 wt%)
30	DWNTs[b]	NH_2	0.1 – 0.5					14.9% @ 0.5 wt%	38.7% (SWCNT-dba, 0.5 wt%)	8.35% @ 0.5 wt%	30% (SWCNT-dba, 0.5 wt%)
	MWNTs							8.5% @ 0.5 wt%		0.27% @ 0.5 wt%	
31	DWNTs	NH_2	0.1 – 1					~6.4% @ 1wt%	54.8% (SWCNT-dba 1wt%)	~1.7% @ 1 wt%	43% (SWCNT-dba, 1 wt%)
32	SWCNTs	CO-NH-R-NH_2	≤ 0.1							1.9% @ 0.1 wt%	5.2% (SWCNT-dba, 0.1 wt%)
33	MWNTs	CO-NH-R-NH_2	0.25 - 0.75					~37.5% @ 0.5 wt%	38.7% (SWCNT-dba, 0.5 wt%)	~30% @ 0.5 wt%	30% (SWCNT-dba, 0.5 wt%)
34	SWCNTs	NH-R-NH_2	0.5			+10ºC	+7.3ºC (SWCNT-dba, 0.5 wt%)	31.6%	38.7% (SWCNT-dba, 0.5 wt%)	24.7%	30% (SWCNT-dba, 0.5 wt%)
35	MWNTs	R-CO-NH-R-NH_2	0.1 – 2							~31.5% @ 1 wt%	43% (SWCNT-dba, 1 wt%)

* Referred to their respective baseline epoxy matrices

** Compared to the best results obtained for the epoxy composites in the present study, with respect to the TGAP/DDS neat matrix. In parenthesis, the compared filler type and loading are specified.

a Data on the baseline epoxy matrix was extracted from: Etika, K. C.; Liu, L.; Hess, L. A.; Grunlan, J. C., The influence of synergistic stabilization of carbon black and clay on the electrical and mechanical properties of epoxy composites. *Carbon* 2009, 47 (13), 3128-3136.

b Double-walled carbon nanotubes

mposite showed higher enhancement than those composites reported by Zhu et al,[6] Liu et al.[22] and Spitalsky et al.[21] Working with aminated MWCNTs, Spitalsky et al[21] reported much higher improvement using functionalization with aryl diazonium than with carboxylation + amidation, which is in agreement with our results. A brief comparison of mechanical and thermomechanical results between our samples and relevant literature data is provided in Table 5.2.

Figure 5.4b compares the T_g values for the different samples prepared, extracted from the tan δ curves in DMA experiments. The T_g is a reversible transition in non-crystalline materials from a glassy to a rubbery-like state. An upshift in T_g can be interpreted as an increase of the system rigidity (stiffness) while a downshift is typically a consequence of a plasticizing effect. The evolution of the damping factor (tan δ, ratio of loss to storage modulus) as a function of temperature (Fig. 5.5) displays three relaxations peaks. The transition at the lowest temperatures (β relaxation) is related to the crankshaft rotation of the hydroxyl ether segments of the crosslinked network in the glassy state.[23] The relaxation that appears at the highest temperatures (α_1 relaxation) corresponds to the glass transition, while the other relaxation is the α_2 transition of the cured network.[24] The addition of SWCNTs leads to an increase in both β and α_1 transition temperatures of the neat epoxy (initially at about -50ºC and 251ºC, respectively), whilst the α_2 transition temperature remains generally almost unchanged.

It can be observed that the blank sample shows a T_g that is about 4ºC lower than the neat epoxy, owing to the processing steps. T_g data for the composites with the lowest loadings (0.1 wt %) are at least in the range between the values of the neat epoxy and the blank sample, except for the composite with non-functionalized SWCNTs, which exhibits a noticeable decrease. At higher loadings, nanocomposite materials exhibit significant increases in the T_g as compared to the reference samples, with the increments being more pronounced for samples with 1 wt % loading. The functionalized SWCNTs are incorporated into the matrix through the formation of strong covalent bonds, becoming part of the cross-linked network hence leading to an increase in the T_g.

[23] Yi, F. P.; Zheng, S. X.; Liu, T. X., Nanostructures and surface hydrophobicity of self-assembled thermosets involving epoxy resin and Poly(2,2,2-trifluoroethyl acrylate)-block-Poly(ethylene oxide) amphiphilic diblock copolymer. *J. Phys. Chem. B* 2009, *113* (7), 1857-1868.
[24] Varley, R. J.; Hodgkin, J. H.; Simon, G. P., Toughening of a trifunctional epoxy system - Part VI. Structure property relationships of the thermoplastic toughened system. *Polymer* 2001, *42* (8), 3847-3858.

The largest increment is obtained for the composite incorporating 1 wt% of SWCNT-dba (about 16.5ºC higher than the blank sample), with the other samples with functionalized SWCNTs possessing similar T_g values, which are higher than the T_g value of the composite with non-functionalized SWCNTs.

The increments observed in the T_g are higher than those reported for analogous epoxy/amino-functionalized CNT composites[8,25-27] (see Table 5.2), which showed lower increases and, in some cases, a reduction in T_g values.[8,22] Data from Table 5.2 evidences that amine functionalization by the 1,3-dipolar cycloaddition reaction of an azomethine ylide has shown to be the best route for improving T_g, not only among the routes reported in this paper, but also using others reported in the literature involving plasma processing[27] or carboxylation-amidation with several aliphatic and aromatic diamines.[25,26] This reasserts the reinforcing potential of our fillers, which behave as powerful enhancers of crosslinking and adhesion to the matrix.

A comparison of tan δ curve for neat epoxy and the two composite systems that possess the highest and lowest T_g is shown in Figure 5.5. The height of the α_1 peak decreases with the addition of the SWCNTs, owing to an increase in the rigidity of the systems. In the case of SWCNT-oxa reinforced composites, the height of this peak remains almost unaffected by increasing SWCNT content, whereas there is a noticeable decrease in height for those incorporating SWCNT-dba as the concentration rises. This reflects the more effective chain restriction ability caused by SWCNT-dba functionalization, ascribed to the CNT-epoxy interfacial covalent bonding that strongly hinders molecular movements. Moreover, this fact is consistent with the higher T_g values of composites with SWCNT-dba in comparison to those including SWCNT-oxa. On the other hand, the broadening of the α_1 peak with the addition of CNTs is also related to restrained chain mobility that occurs in the composites, hence covering a wider temperature range.[28] The SWCNTs disturb the relaxation of adjacent polymer

[25] Shen, J. F.; Huang, W. S.; Wu, L. P.; Hu, Y. Z.; Ye, M. X., The reinforcement role of different amino-functionalized multi-walled carbon nanotubes in epoxy nanocomposites. *Compos. Sci. Technol.* 2007, *67*, 3041-3050.
[26] Petrea, C. M.; Andronescu, C.; Pandele, A. M.; Garea, S. A.; Iovu, H., Epoxy-based nanocomposites with amine modified single walled carbon nanotubes. *E-Polymers* 2010, art. #020.
[27] Tseng, C. H.; Wang, C. C.; Chen, C. Y., Functionalizing carbon nanotubes by plasma modification for the preparation of covalent-integrated epoxy composites. *Chem. Mater.* 2007, *19* (2), 308-315.
[28] Lin, M. S.; Lee, S. T., Mechanical behaviors of fully and semi-interpenetrating polymer networks based on epoxy and acrylics. *Polymer* 1997, *38* (1), 53-58.

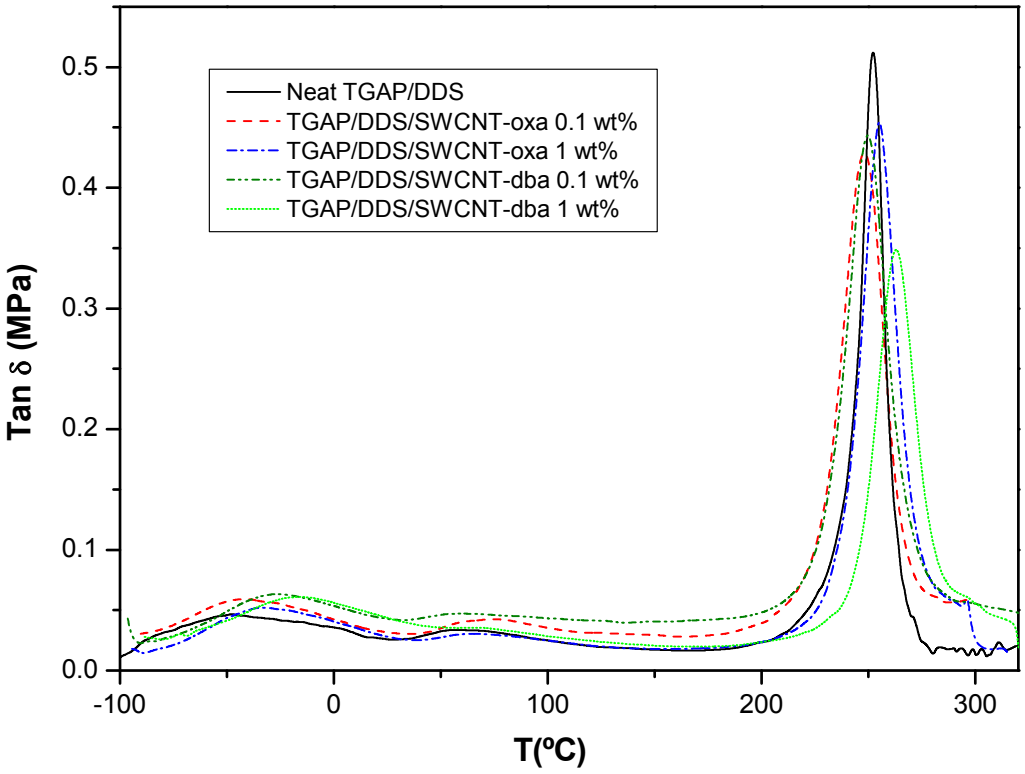

Figure 5.5. Damping factor (tan δ) curves vs temperature for the neat epoxy matrix and some composite samples containing SWCNT-oxa and SWCNT-dba

chains, which would behave differently from those farther away from the nanofiller, leading to a broadening in the relaxation peaks. Similar phenomena have been reported for other composites incorporating covalently grafted SWCNTs to the polymer matrix.[29]

Static mechanical properties

The static mechanical properties of the composites were also studied; representative stress-strain curves of samples incorporating 0.5 wt % loading are given in Figure 5.6. The Young's modulus (YM), elongation at break (ε_b) and strain to failure (σ_y) obtained from all performed tensile tests are listed in Table 5.3. YM of the neat epoxy matrix is about 3.1 GPa, decreasing by ~14% with the sonication and stirring processes. The incorporation of 0.5 wt % unfunctionalized SWCNTs causes a ~30% in-

[29] Diez-Pascual, A. M.; Martinez, G.; Gonzalez-Dominguez, J. M.; Anson, A.; Martinez, M. T.; Gomez, M. A., Grafting of a hydroxylated poly(ether ether ketone) to the surface of single-walled carbon nanotubes. *J. Mater. Chem.* 2010, *20* (38), 8285-8296.

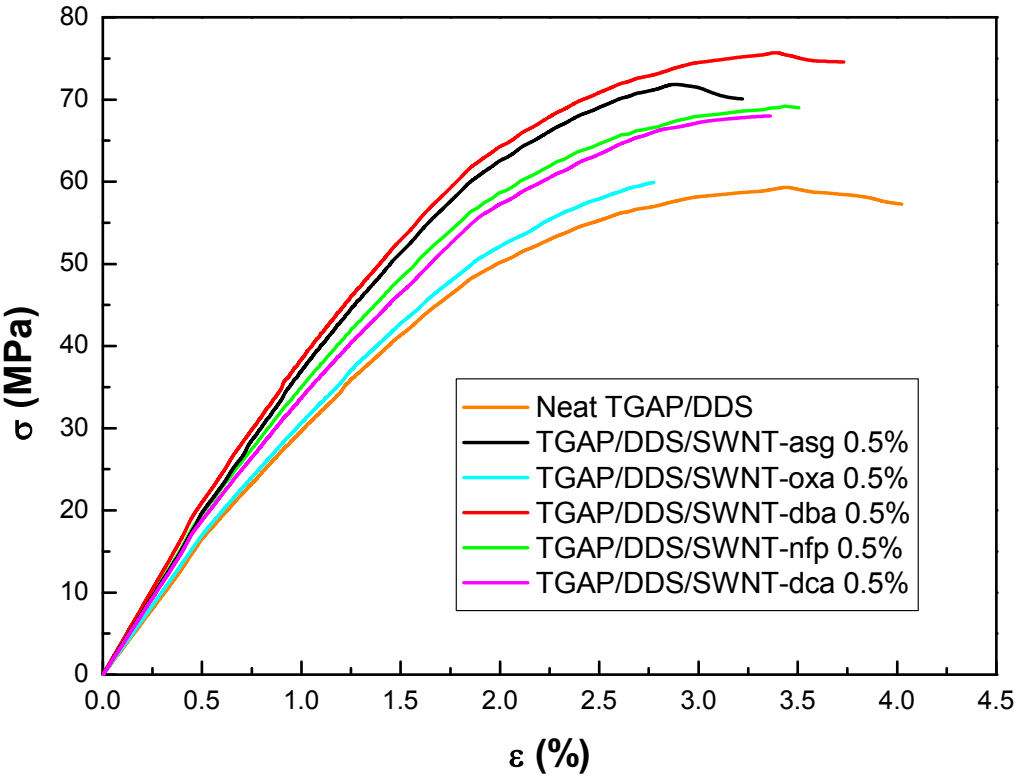

Figure 5.6. Damping factor (tan δ) curves *vs.* temperature for the neat epoxy matrix and some composite samples containing SWCNT-oxa and SWCNT-dba

crease in YM, as compared to the neat matrix (48% in comparison to the blank sample). This improvement is comparable to those attained by the addition of the same amount of SWCNT-nfp or SWCNT-dca. However, the incorporation of SWCNT-oxa leads to a marginal YM enhancement (barely a 4% increase) probably owing to inhomogeneous dispersion of the filler and undeveloped SWCNT-matrix interfacial bonding, hence poor load transfer ability. The largest increase in YM for a 0.5 wt % loading is found for the SWCNT-dba composite, which exhibits nearly 38% improvement as compared to the neat TGAP/DDS sample (about 60% improvement in comparison to the blank). This is an increase of 8% compared to the composite containing unfunctionalized SWCNTs, suggesting that the diazonium route is the functionalization that leads to the highest degree of anchoring (at 0.5 wt% loading). Similar behavior was found for the other concentrations tested. At 1 wt% loading, the SWCNT-dba composite exhibits about 75% higher modulus than the blank sample, while the increment for the SWCNT-asg composite is around 64%. The exceptional modulus enhancements attained in these composites indicate the existence of strong epoxy-CNT interfacial bonding, capable of transferring the stress load and preventing the sliding of nanotube bundles during

tension. With regard to the tensile strength, the trends observed are similar to those described for the modulus. The σ_y value of the blank sample is slightly lower than that of neat TGAP/DDS, and it experiences an increase of around 35% upon addition of 0.5 wt% SWCNT-asg (21% increase in comparison to the TGAP/DDS neat matrix). Comparable results in σ_y are found again for composites with the same amount of SWCNT-nfp and SWCNT-dca, while the largest increase is observed for the SWCNT-dba composite (29% and 9% improvement as compared to the neat matrix and the SWCNT-asg composite, respectively, and 44% enhancement with regard to the blank sample). At 1 wt % loading, this type of composite shows 43% strength enhancement in comparison with the neat epoxy (10% higher modulus than the composite incorporating unfunctionalized SWCNTs and almost 60% higher than the blank sample). The aforementioned improvements for YM values are among the highest reported in the literature for other amino-functionalized CNTs/epoxy composites[6,30-35] at the same filler loading (see Table 5.2).

The data regarding σ_y improvement in epoxy are generally higher than those found in the literature using other aminated CNTs, except for the results presented by Spitalsky et al.[21] where MWCNTs have been aminated by both carboxylation + amidation and diazonium route + amidation, and Tseng et al.[27] aminated by plasma + diamine treatment (see Table 5.2). This suggests that most of the functionalization routes employed in this work are highly effective in improving the SWCNT dispersibility and the SWCNT-epoxy interfacial adhesion, resulting in large improve-ment of the tensile strength. The SWCNT-dba composite is capable of absorbing larger amounts of energy before breaking, beyond the effect of unfunctionalized SWCNTs, which is also reflected

[30] Gojny, F. H.; Wichmann, M. H. G.; Fiedler, B.; Schulte, K., Influence of different carbon nanotubes on the mechanical properties of epoxy matrix composites - A comparative study. *Compos. Sci. Technol.* 2005, *65* (15-16), 2300-2313.
[31] Gojny, F. H.; Wichmann, M. H. G.; Kopke, U.; Fiedler, B.; Schulte, K., Carbon nanotube-reinforced epoxy-compo sites: enhanced stiffness and fracture toughness at low nanotube content. *Compos. Sci. Technol.* 2004, *64* (15), 2363-2371.
[32] Zhao, Y.; Mannhalter, B.; Hong, H. P.; Welsh, J. S., Mechanical Properties of Epoxy nanocomposites reinforced with very low content of amino-functionalized single-walled carbon nanotubes. *J. Nanosci. Nanotechnol.* 2010, *10* (9), 5776-5782.
[33] Li, S. Q.; Wang, F.; Wang, Y.; Wang, J. W.; Ma, J.; Xiao, J., Effect of acid and TETA modification on mechanical properties of MWCNTs/epoxy composites. *J. Mater. Sci.* 2008, *43* (8), 2653-2658.
[34] Zhao, Y.; Barrera, E. V., Asymmmetric diamino functionalization of nanotubes assisted by BOC protection and their epoxy nanocomposites. *Adv. Funct. Mater.* 2010, *20* (18), 3039-3044.
[35] Chen, X. H.; Wang, J. F.; Lin, M.; Zhong, W. B.; Feng, T.; Chen, J. H.; Xue, F., Mechanical and thermal properties of epoxy nanocomposites reinforced with amino-functionalized multi-walled carbon nanotubes. *Mater. Sci. Eng. A* 2008, *492* (1-2), 236-242.

Table 5.3. Tensile parameters for the neat epoxy matrix and nanocomposite samples at different SWCNT loadings.

	Filler loading (wt%)	YM (GPa)	σ_y (MPa)	ε_b (%)
Neat TGAP/DDS	0	3.1 ± 0.1	58 ± 1	4.0 ± 0.2
Blank	0	2.7 ± 0.3	52 ± 4	3.6 ± 0.4
TGAP/DDS/SWCNT-asg	0.1	3.2 ± 0.2	60 ± 3	4.5 ± 0.2
	0.5	4.1 ± 0.4	70 ± 5	3.1 ± 0.4
	1	4.5 ± 0.2	76 ± 3	2.5 ± 0.5
TGAP/DDS/SWCNT-oxa	0.5	3.3 ± 0.3	62 ± 4	2.8 ± 0.2
TGAP/DDS/SWCNT-nfp	0.5	4.0 ± 0.2	69 ± 3	3.6 ± 0.3
TGAP/DDS/SWCNT-dba	0.1	3.4 ± 0.1	61 ± 5	4.9 ± 0.4
	0.5	4.3 ± 0.1	75 ± 2	3.7 ± 0.2
	1	4.8 ± 0.3	83 ± 4	3.1 ± 0.3
TGAP/DDS/SWCNT-dca	0.5	4.0 ± 0.3	66 ± 3	3.4 ± 0.4

in the ε_b values. This latter parameter is about 4% and3.6% for the neat matrix and the blank sample, respectively. For composites with 0.5 wt% loading, the use of SWCNT-dba as the filler provides the closest value to the neat matrix (only ~8% decrease in ε_b), whereas the unfunctionalized nanotubes lead to a 22% decrease; this means that the former filler induces the most ductile fracture among all the studied samples. This is a very significant result as the general trend in epoxy/SWCNT composites is the drastic reduction of ε_b upon filler incorporation,[6,36] providing a more fragile fracture behavior and being detrimental to materials toughness in most cases. Similar trends were found for the other concentrations tested.

What is particularly significant is that, at 0.1 wt% loading, the SWCNT-dba composite shows an increase in elongation at break up to ~5%, which is a 22% increment as compared to the relatively brittle neat epoxy matrix. This fact would point to an effective breakage of SWCNTs during the material failure, instead of a simple pull-out (in consonance with microscopic observations), which again shows the strong reinforcement effect by these amino-functionalized SWCNTs and the potential of these TGAP/DDS composites in high-stress structural applications at room temperature. From the area under the stress-strain curve, first evidence is given for improved toughness of the SWCNT-dba composites in comparison to the neat matrix. With strong covalent bonding, the functionalized nanotubes can maintain or even increase the strain to

[36] Rafiee, M. A.; Lu, W.; Thomas, A. V.; Zandiatashbar, A.; Rafiee, J.; Tour, J. M.; Koratkar, N. A., Graphene Nanoribbon Composites. *ACS Nano* 2010, *4* (12), 7415-7420.

failure, thus leading to an increase in impact resistance. A detailed discussion is given in the following, by impact strength characterization.

DMA and tensile measurements demonstrated that the solvent-free dispersion of as-grown arc-discharge SWCNTs leads to visible enhancements in the mechanical and thermo-mechanical properties of the TGAP/DDS matrix. Covalent amination of SWCNTs can improve these parameters beyond the effect of unfunctionalized SWCNTs. However, SWCNTs aminated on tips and defect sites show poor improvement in mechanical performance, ascribed to poor dispersibility. These results are consistent with the literature, which reports better results for sidewall covalent amination rather than tip-defect amination.[21]

Impact strength

Epoxy resins possess high strength and stiffness, although a relatively low toughness, which is a crucial and limiting factor for the design of structural components. Therefore, an improvement in the impact strength of epoxies is a desired goal. To evaluate the toughness of the different composites, room temperature Charpy impact tests were performed on the SWCNT-dba and SWCNT-asg composites, and quantitative results are shown in Figure 5.7.

The impact strength of the pure resin is approximately 2 kJ/m^2, and decreases by almost 25% for the blank sample, since the integration process leads to some damage on the epoxy network, hence premature failure. Non-functionalized SWCNTs lead to an increase in the epoxy toughness at low nanofiller loadings (about 21% at 0.1 wt % SWCNT content), while it decreases at higher filler contents. The composites with 1 wt% SWCNT-asg exhibit similar toughness to the blank sample.

Toughness is very sensitive to the state of dispersion of the nanofillers and their interfacial adhesion with the matrix. At very low loadings, the non-functionalized SWCNTs should be well-dispersed through the matrix, leading to a large epoxy-CNT surface area, thus minimizing the stress concentration nuclei. However, when the filler concentration increases, aggregate formation is favoured. These aggregates serve as stress concentration sites that promote the formation of dimples, nucleating cracks. This

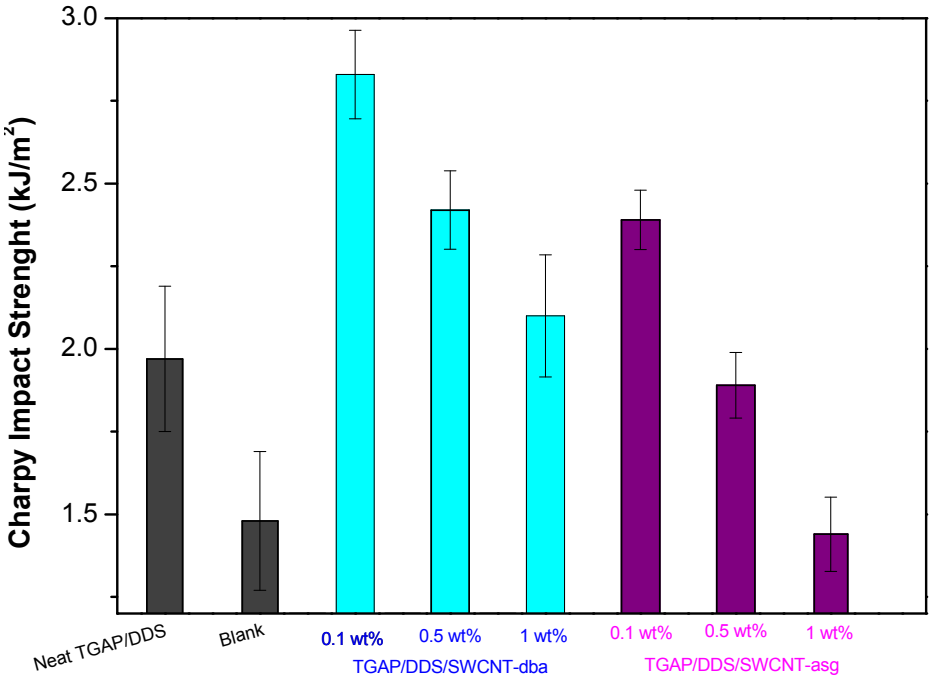

Figure 5.7. Charpy impact strength for the neat epoxy, the SWCNT-dba and SWCNT-asg composites at different nanotube loadings. Error bars represent confidence intervals calculated using Student's "t-test" (statistical significance = 0.1).

aggravates the brittleness under high strain rates, resulting in a small decrease in the impact strength and premature system failure. In contrast, composites incorporating SWCNT-dba show improved toughness compared to the matrix for all the concentrations studied. At 0.1 wt % loading, a 44% improvement in impact strength is observed in comparison to the neat matrix (about a 90% increase as compared to the blank sample). This is consistent with the increase in elongation at break at 0.1 wt% loading. The enhancement is less significant at higher loadings, only about 7% at 1 wt% SWCNT content.

The improved behavior found for composites reinforced with these amino-functionalized SWCNTs is probably related to their improved dispersibility within the matrix as well as the CNT- matrix covalent bonding, hence a higher effective interfacial area, which provides a strong barrier for pinning and bifurcation of the advancing cracks. Moreover, these composites absorb more energy during fracturing, owing to the additional rupture of the strong covalent bonds between the amino groups of the SWCNTs and the epoxide moieties. These results demonstrate that it is possible to

enhance the impact resistance of epoxy composites by means of strong interfacial bonding at the molecular level with crosslinked polymer chains. The simultaneous increase in stiffness, strength and toughness observed for composites obtained through the diazonium route makes them particularly suitable for structural applications, such as aeronautic and aerospace industries.

Electrical conductivity measurements

Direct current (DC) conductivity measurements were conducted on the different composite samples and the obtained results are given in Figure 5.8. As a general statement, all composite samples show higher electrical conductivity than the bare matrix, and those containing functionalized SWCNTs exhibit equal or lower conductivity than samples containing unfunctionalized SWCNTs. This is explained on the basis that covalent modifications to the structure of SWCNTs lead to an impurity state near the Fermi level that can lead to dramatic changes in conductive properties.[37,38]

The functionalization procedure determines the electrical conductivity values of the composites. In the entire range of studied compositions, it is clear how epoxy composites containing SWCNT-oxa as filler present the lowest conductivities observed at the lowest loading. This confirms the poor dispersibility of this filler, which hinders its potential to create conductive pathways within the bulk matrix, and also the fact that this functionalization route induces a high level of damage to SWCNTs. Indeed, the nitric acid treatment is known to be particularly harmful to the conductive properties of epoxy/CNT composites.[18,39]

The sidewall functionalization of SWCNTs does not cause noticeable disruption of conductive properties, except for the diazonium route (at the lowest loading). The diazonium reaction on SWCNT sidewalls has been reported to occur preferentially over

[37] Zhao, J. J.; Park, H. K.; Han, J.; Lu, J. P., Electronic properties of carbon nanotubes with covalent sidewall functionalization. *J. Phys. Chem. B* 2004, *108* (14), 4227-4230.
[38] Park, H.; Zhao, J. J.; Lu, J. P., Effects of sidewall functionalization on conducting properties of single wall carbon nanotubes. *Nano Lett.* 2006, *6* (5), 916-919.
[39] Kim, Y. J.; Shin, T. S.; Choi, H. D.; Kwon, J. H.; Chung, Y. C.; Yoon, H. G., Electrical conductivity of chemically modified multiwalled carbon nanotube/epoxy composites. *Carbon* 2005, *43* (1), 23-30.

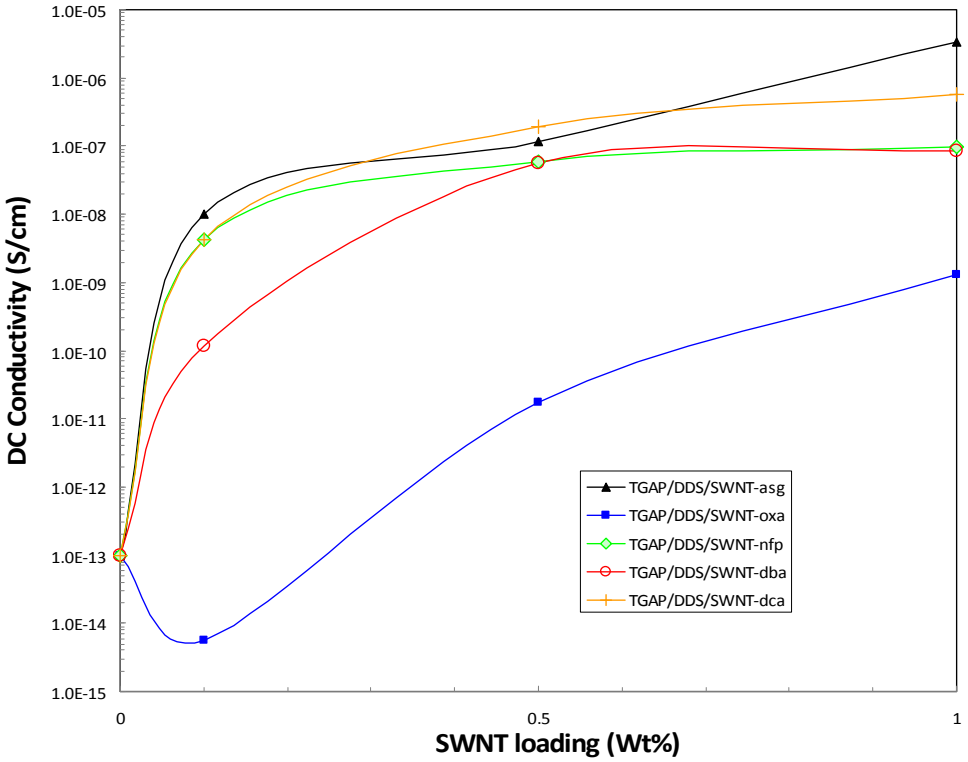

Figure 5.8. DC conductivity values as a function of SWCNT loading

SWCNTs with metallic behavior,[40] which are mainly responsible for the macroscopic conductive properties in bulk SWCNT samples. At high loadings, the effect of enhanced filler-matrix interactions (owing to functionalization) would compensate for the chemical inhibition of metallic tubes, leading to conductivity values close to SWCNT-asg composites. At the highest loading (1 wt %), the epoxy composite containing SWCNT-dca as filler exhibits the closest conductivity value to that of the SWCNT-asg composite at the same loading (a difference of one order of magnitude between both samples). These conductivity values suggests that the 1,3-dipolar cycloaddition is a suitable functionalization means for preserving the conductive properties of epoxy/SWCNT composites at high loadings while enhancing other physical properties.

AFM characterization

Figure 5.9 presents comparative AFM images of the epoxy nanocomposite with 1 wt% SWCNTs-nfp. Figures 5.9a and 5.9b show the topography image and its

[40] Strano, M. S.; Dyke, C. A.; Usrey, M. L.; Barone, P. W.; Allen, M. J.; Shan, H. W.; Kittrell, C.; Hauge, R. H.; Tour, J. M.; Smalley, R. E., Electronic structure control of single-walled carbon nanotube functionalization. *Science* 2003, *301* (5639), 1519-1522.

associated stiffness map, respectively. The stiffness map for the neat epoxy (image not shown) reveals a very homogeneous profile with a stiffness average value close to 3 GPa. The nanocomposite sample stiffness mapping shows different features; there is a green area (showing comparatively higher stiffness than the neat matrix) and small areas in pink with higher stiffness (about 5 GPa) that seem to correspond to small (around 200 nm) aggregates of SWCNTs. AFM stiffness mapping is consistent with the composites

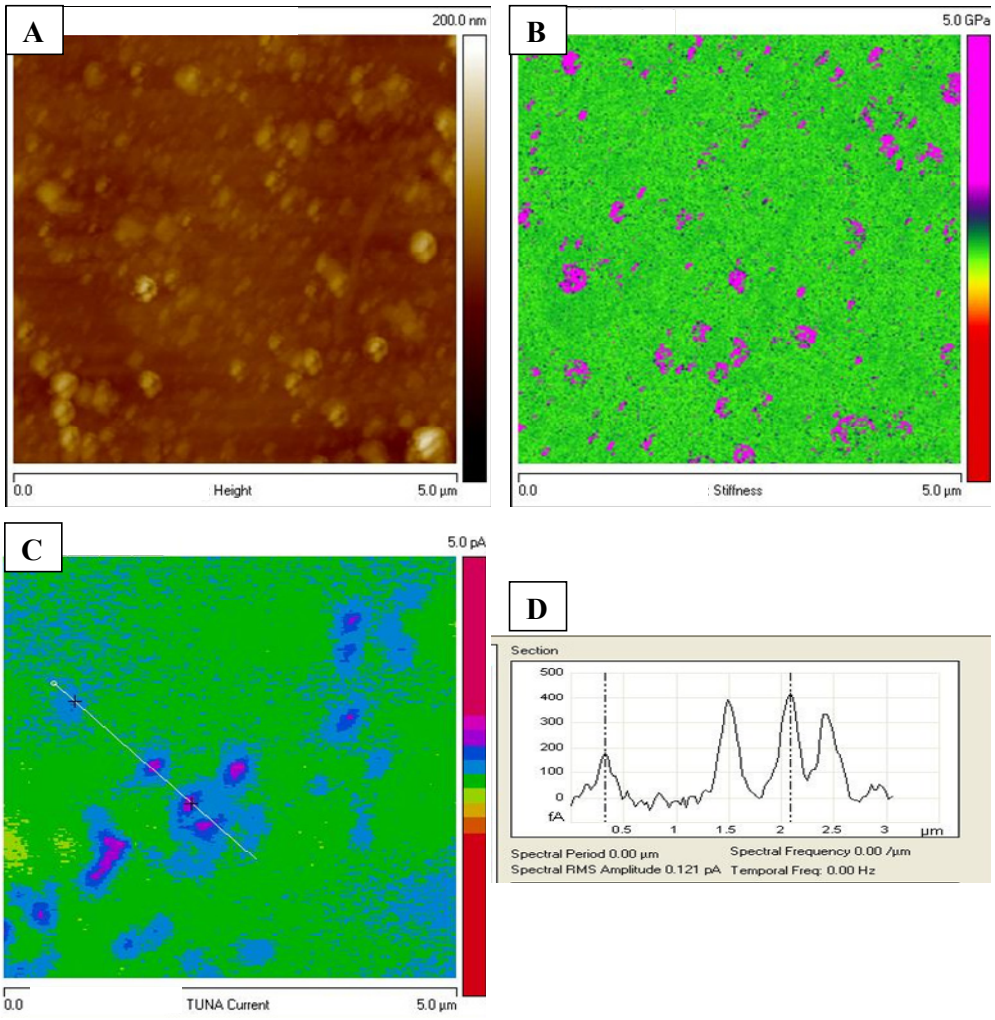

Figure 5.9. AFM images corresponding to SWCNTs- nfp composite at 1 wt % loading a) topography image; b) stiffness map of the same area as Fig. 5.9a; c) electrical current map; d) electrical current profile as indicated in Fig. 5.9c.

storage modulus at 1 wt% loading (Figure 5.4a). Therefore, a proper transfer of properties is suggested owing to the covalent bonding between matrix and the filler, despite a higher level of dispersion could still be achieved. Figures 5.9c and 5.9d show

electrical current mapping and the corresponding profile of another area in the same composite, respectively. In the current map, it is possible to see areas of higher conductivity corresponding to the presence of SWCNTs surrounding by areas of lower conductivity but higher than the rest of the composite, which confirms the observations in Figure 5.9b concerning the formation of aggregates or non-disaggregated SWCNTs bundles. AFM observations match with those made by SEM regarding the different state of dispersion in the SWCNT-nfp nanocomposite.

5.3.2. Epoxy nanocomposites containing SWCNTs functionalized with matrix-based moieties

Chemical functionalization is known to provide the most significant improvements in CNT-reinforced polymer matrices.[4,7] There are several key aspects in the reinforcement of polymer matrices with CNTs, including proper load transfer, good dispersion and (less critically) SWCNT alignment.[41] Covalent bonding between the matrix and filler creates strong interfacial interaction which, as seen in the previous section, enables an efficient stress transfer, providing mechanical reinforcement.

Works related to epoxy/amine-SWCNT composites involving multifunctional epoxy networks, which have scarcely been reported in the literature, are of particular interest for high-performance applications. When the molecular composition of the functionalization moieties is different from that of the parent epoxy matrix, a heterogeneous crosslinking of the polymer at the CNT-epoxy interface takes place. This could locally increase the polymer chains alignment and molecular mobility at the interface favouring the epoxy fatigue resistance and toughening through crack bridging by epoxy fibrils at the interface.[42] This mechanism is different from the classical conception of toughening in fibre-reinforced epoxy composites, where the crack interfaces are bridged by the fibrous filler and not by epoxy chains or fibrils. SWCNTs functionalized with matrix-based moieties were employed to develop a uniform cross-linking of epoxy at the CNT-epoxy interface, so the toughening mechanism is expected

[41] Coleman, J. N.; Khan, U.; Gun'ko, Y. K., Mechanical reinforcement of polymers using carbon nanotubes. *Adv. Mater.* 2006, *18* (6), 689-706.
[42] Zhang, W.; Srivastava, I.; Zhu, Y. F.; Picu, C. R.; Koratkar, N. A., Heterogeneity in epoxy nanocomposites initiates crazing: significant improvements in fatigue resistance and toughening. *Small* 2009, *5* (12), 1403-1407.

to depend exclusively on the filler potential to hinder crack propagation, which, coupled to a robust covalent bonding between filler and matrix, should ensure improved transfer of properties hence improved nanocomposites features. The SWCNTs functionalization with matrix-based moieties was chosen to obtain functionalized SWCNTs capable of exhibiting high miscibility in the epoxy matrix, and to improve the dispersion state and rheological features of the epoxy-SWCNT blends.[43]

In this case, the chemical nature of the attached moiety is identical to that of the parent matrix. The incorporation of these fillers into the epoxy system was carried out without the participation of organic solvents, expecting an increase in the SWCNT/ epoxy miscibility as compared to unfunctionalized SWCNTs (and some other aminated SWCNTs). The miscibility enhancement was much more pronounced in the SW-DDS and SW-AD samples.[43] The tailored functionalization in our nanocomposites was expected to deliver as much interfacial bonding as that of the polymer chains with one another because the epoxy molecular architecture is unmodified at the nanotube-matrix interface. The reinforcement potential of our functionalized SWCNTs was evaluated by measuring their mechanical properties in two different ways: DMA performance, and tensile (stress-strain) tests on cured composite samples at different SWCNT loadings.

DMA characterization

DMA curves were registered for a set of nanocomposite materials with functionalized and unfunctionalized A-SWCNTs and L-SWCNTs that were integrated solvent-free (see experimental section). The storage modulus values at room temperature were compared to those of the neat epoxy matrix and the obtained improvements are given in Figure 5.10a.

The incorporation of unfunctionalized SWCNTs provides an improvement in the epoxy modulus of about 30% for both types of SWCNTs at the highest loading tested (1 wt%). In addition to these results, functionalization of SWCNTs with the DDS molecules or the AD derivative greatly increases the DMA performance of the epoxy

[43] Martinez-Rubi, Y.; González-Domínguez, J. M.; Ansón-Casaos, A.; Kingston, C.; Martínez, M. T.; Simard, B.; Tailored SWCNT functionalization optimized for compatibility with epoxy matrices, *Nanotechnology (submitted).*

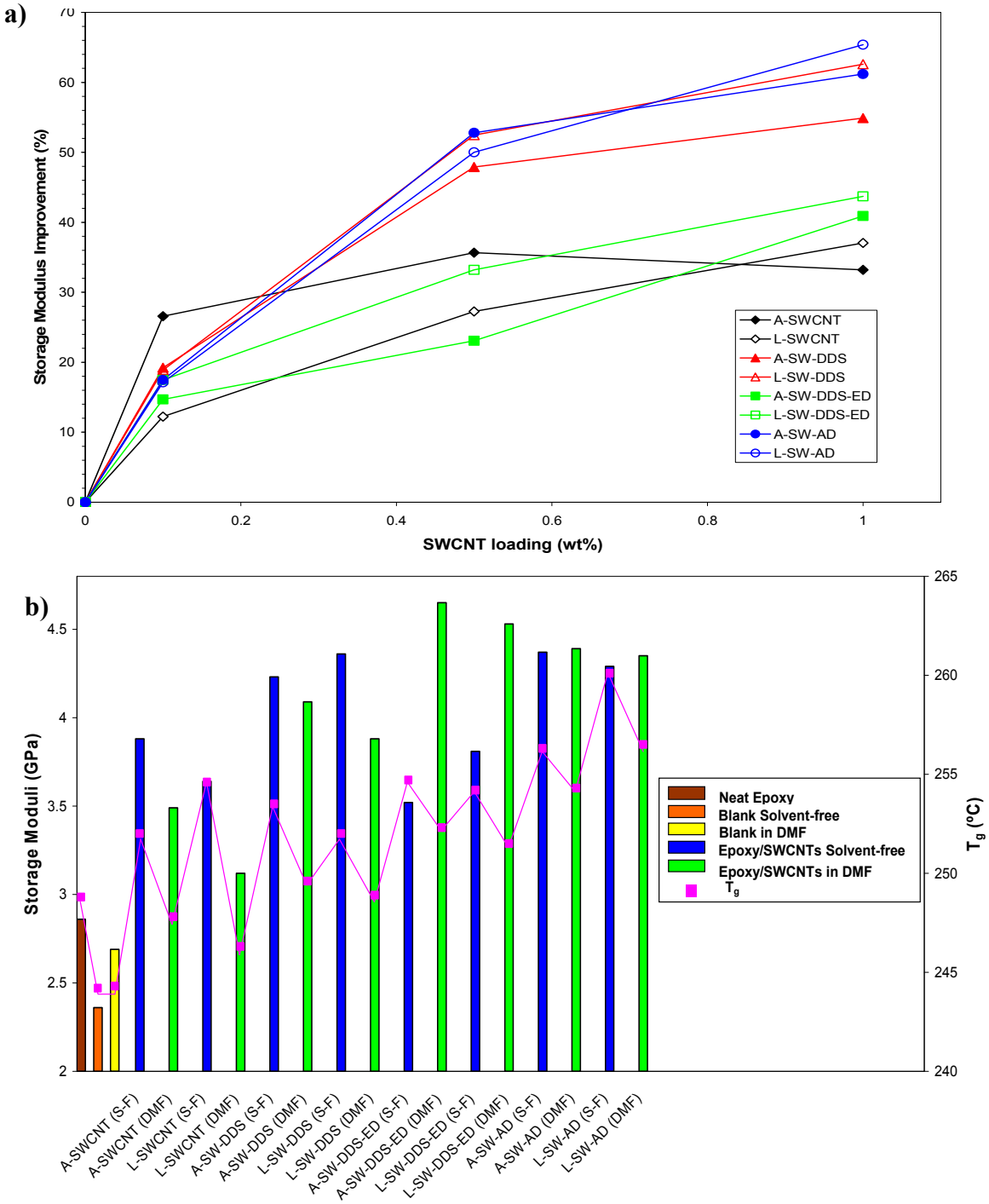

Figure 5.10. (a) Room-temperature storage modulus improvements for the nanocomposite samples integrated *via* solvent-free at different filler loadings, referred to the TGAP/DDS baseline epoxy matrix; (b) Storage modulus and T_g values for the nanocomposite samples at 0.5 wt% with different preparation protocols.

matrix, achieving modulus improvements up to 65% (1 wt% L-SW-AD), which represents a storage modulus value as high as 4.75 GPa and a glass transition

temperature (T_g) increase of *ca.* 15ºC (see Figure 5.11 for absolute Storage modulus and T_g values).

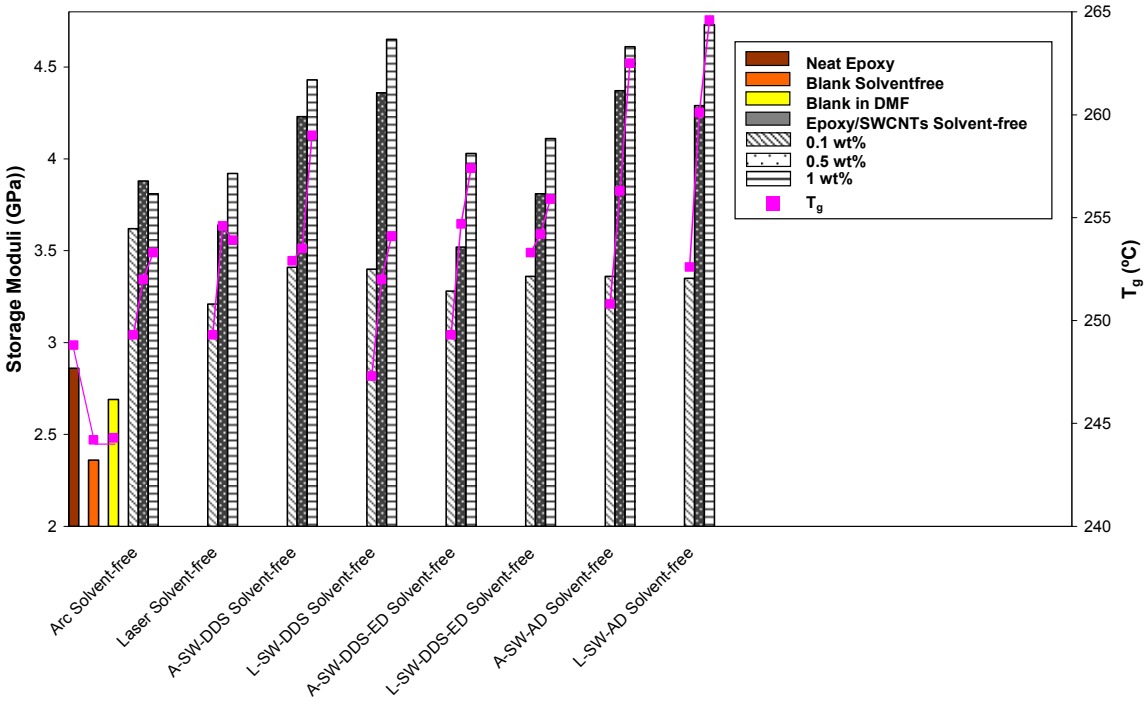

Figure 5.11. Storage modulus and T_g values for all epoxy nanocomposites prepared solvent-free at different SWCNT loadings.

The DDS and AD covalently grafted chemical moieties (Figure 5.1) contain terminal amine groups, and these groups would create a very efficient covalent anchoring to the matrix which, jointly with the good level of dispersion achieved (due to the chemical affinity for the matrix) explains these enhancements. Although both covalent functionalizations increase the storage modulus to similar values, the grafting with the AD derivative shows a higher improvement in T_g, particularly for L-SWCNT. However, the grafted moiety containing epoxide rings (ED derivative) causes poor modulus improvement, with this being only slightly higher than that achieved for unfunctionalized SWCNTs at 1 wt%.

This unexpected behavior of the ED moiety and the unsatisfactory SWCNT dispersibility tests in the epoxy matrix[43] led us to think that the direct interface interaction between SW-DDS-ED and the epoxy matrix was not as good as initially expected. Despite SW-DDS-ED exhibited better miscibility and dispersibility in the

epoxy matrix than unfunctionalized SWCNTs, the DMA performance of the cured composites showed that the solvent-free integration of these SWCNTs was ineffective in order to achieve a satisfactory transfer of properties with these specific functional groups. For this reason, we tried an alternative integration method based on the previous dispersion of functionalized SWCNTs in organic solvent, followed by mixing with the epoxy and then evaporation of the solvent (see experimental section). The organic solvent chosen in this case was N,N'-dimethylformamide (DMF). A set of nanocomposite materials containing each of the functionalized SWCNT fillers, was prepared at 0.5 wt% SWCNT loading.

A comparison between the storage modulus values at room temperature of nanocomposites containing solvent-free or DMF-integrated SWCNTs is given in Figure 5.10b. The blank samples are pure epoxy matrix subjected to the same preparation procedure as that of the nanocomposites, in order to assess the influence of the experimental procedure on the matrix performance. The storage modulus and T_g values for the blank samples are lower than those of the parent matrix, with the solvent-free blank being visibly lower. This could be ascribed to the sonication steps applied in the experimental protocol, which would have caused damage to the matrix, and in the case of the DMF method, to the residual solvent traces after evaporation.

The effect of enhanced dispersion and interfacial interaction in all the nanocomposite materials compensates for the sonication or the solvent treatment drawbacks, as seen in the storage modulus and T_g (Figure 5.10b). It is clear that there is a great difference between both preparation methods, which depend on the functional attached moiety. For non-functionalized SWCNTs or the amine-terminated functional groups, the DMF processing method offers results that are worse (in the case of SW-DDS) or equal (in the case of SW-AD) than their solvent-free counterparts.

Nanocomposites containing epoxide-terminated SWCNTs (SW-DDS-ED) exhibit a drastic increase in storage modulus compared to their analogous nanocomposites *via* solvent-free integration. These surprising results indicate that interfacial interactions between SWCNTs and epoxy can be different depending on the chemical nature of the grafted covalent moiety and the integration method. The solvent processing method can have a detrimental effect on the storage modulus, as was

observed for the case of the neat resin and nanocomposites containing unfunctionalized SWCNTs (Figure 5.10b). However, depending on the type of functionalization, this drawback can be overcome by improvements in dispersion and interfacial interaction. Finally, the T_g values are systematically lower (~4ºC, on average) for DMF-integrated nanocomposites in comparison to their solvent-free counterparts, which could be attributed to the aforementioned solvent treatment drawback.

Static mechanical properties

YM, σ_y, ε_b and tensile toughness (calculated as the area under the curve) obtained from stress-strain tests for epoxy reference samples and nanocomposites at 0.5 wt% are shown in Figure 5.12. Again, the blank samples present worse results than the parent matrix as a consequence of the preparation procedures. On the contrary, the solvent-free incorporation of non-functionalized SWCNTs into the epoxy system produces a fair improvement in YM and σ_y of *ca.* 25% and 36%, respectively, but a detrimental effect in toughness and ε_b. The latter parameter tends to decrease drastically in epoxy resins upon incorporation of CNTs,[6,36,44,45] which provokes a less ductile fracture behavior, hence a detrimental effect on toughness.

The functionalization of SWCNTs with tailored molecules exhibits a significant increase in the tensile parameters of the resulting nanocomposites (as compared to the TGAP/DDS neat matrix) when the filler is integrated solvent-free. On the average, YM values attain improvements of 47% and 54%, while σ_y reaches 55% and 73%, for SW-DDS and SW-AD nanocomposites, respectively. Improvements in tensile strength are higher than the improvements that are attained for YM values, suggesting that our approach is even more effective for enhancing the strength of the polymer rather than its stiffness. These significant enhancements indicate the existence of strong epoxy-SWCNT interfacial adhesion, which is capable of transferring the stress load effectively and preventing the sliding of nanotube bundles during tension. However, as previously mentioned for the DMA results, nanocomposites containing SW-DDS-ED show poor

[44] Allaoui, A.; Bai, S.; Cheng, H. M.; Bai, J. B., Mechanical and electrical properties of a MWNT/epoxy composite. *Compos. Sci. Technol.* 2002, *62* (15), 1993-1998.
[45] Zhu, J.; Kim, J. D.; Peng, H. Q.; Margrave, J. L.; Khabashesku, V. N.; Barrera, E. V., Improving the dispersion and integration of single-walled carbon nanotubes in epoxy composites through functionalization. *Nano Lett.* 2003, *3* (8), 1107-1113.

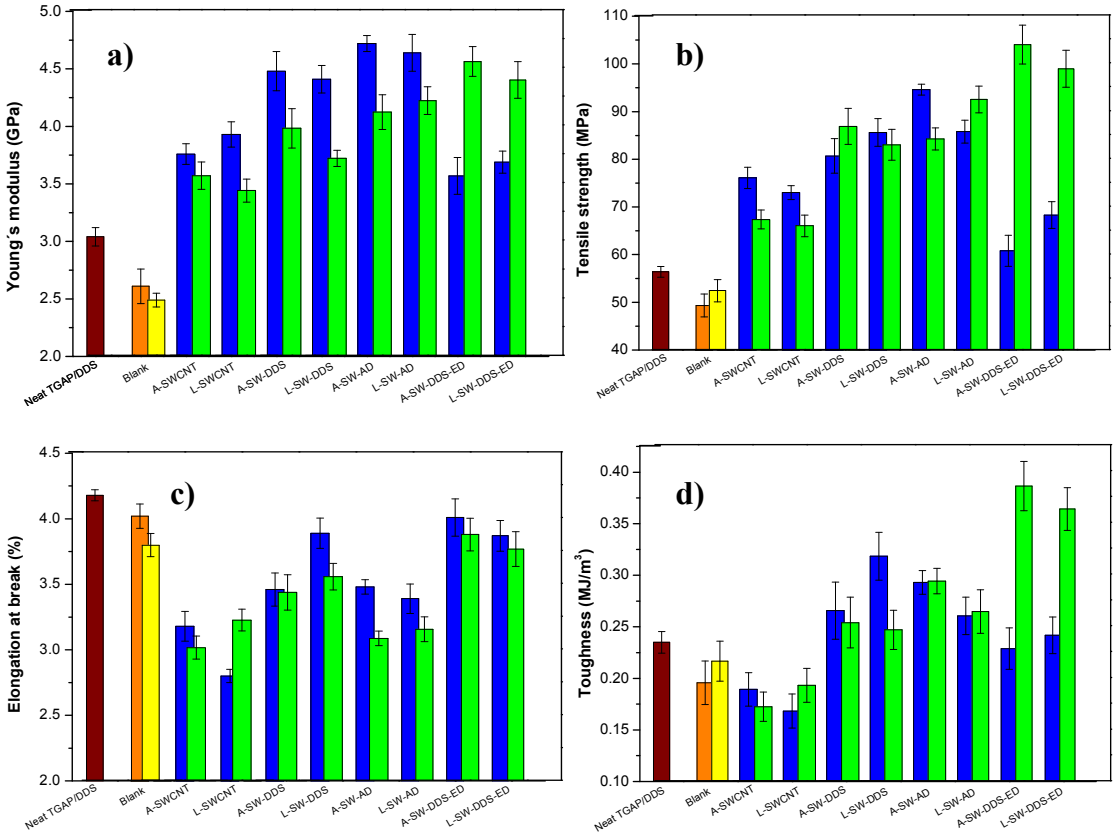

Figure 5.12. Mechanical parameters obtained from tensile tests of nanocomposite samples at 0.5wt% filler loading. a) YM, b) σ_y, c) ε_b, and d) toughness. The same colour code from Figures 5.10 and 5.11, is applied: Brown, neat TGAP/DDS epoxy matrix; Orange, blank solvent-free; Yellow, blank in DMF; Blue, nanocomposites integrated *via* solvent-free; Green, nanocomposites integrated in DMF.

improvement when integrated solvent-free, exhibiting tensile properties that are lower than or comparable to those achieved for unfunctionalized SWCNTs. The general effect of all the functionalized SWCNTs incorporated *via* solvent-free processing, with the exception of SW-DDS-ED, is to prevent the large decrease in ε_b, as compared to unfunctionalized SWCNTs. The maximum improvement in toughness for solvent-free-integrated samples is 39% (L-SW-DDS), which is noticeably large considering the high brittleness of epoxy matrices and the difficulty involved in toughening them without sacrificing other mechanical properties.

The incorporation of SWCNTs *via* solvent processing leads to nanocomposite materials with tensile parameters that are worse than their solvent-free counterparts, with the only exception of SW-DDS-ED. As observed for DMA results, nanocom-

posites containing SW-DDS-ED show drastically enhanced properties when compared to their solvent-free counterparts, achieving the highest σ_y and toughness values with this approach (91% and 65% improvement as compared to the neat matrix, respectively). These improvements are among the best ever reported for SWCNT-filled epoxy resins[7,41] with such low filler content. The interface interaction between SW-DDS-ED and the epoxy matrix is strongly enhanced by the DMF integration protocol, thus exhibiting large improvements in tensile parameters.

The most significant mechanical improvements in nanocomposites of this section (as compared to the neat matrix) can be summarized as follows: approximately 65% improvement in storage modulus is achieved by solvent-free integration of L-SW-AD (1 wt%) or by DMF-based integration of A-SW-DDS-ED (0.5 wt%); additionally, 91% improvement in the ultimate tensile strength and 65% improvement in tensile toughness are also achieved for the latter sample. This is indicative of the possibility of tuning the nanocomposite performance by means of the tailored functional groups and a suitable preparation procedure. In general, the functionalization of SWCNTs with higher molecular weight architectures (AD and ED derivatives) causes higher improvements in mechanical properties than those seen with the bare hardener molecules (SW-DDS). By functionalizing SWCNTs with moieties having the same molecular architecture than the epoxy, we were able to modify the filler/matrix interaction without changing the chemical composition of the interface. This functionalization strategy leads to stiffer and stronger nanocomposite materials.

Thermal and thermo-oxidative stability

Thermal and thermo-oxidative stability was studied by TGA under inert (nitrogen) or oxidant (air) atmospheres. TGA plots for nanocomposite samples containing 0.5 wt% filler loading are displayed in Figure 5.13. These samples experience a single weight loss under inert atmosphere (in the range of 400 - 450ºC), while two consecutive weight losses are found in air atmosphere (in the range of 400 – 450ºC and 550 – 600ºC respectively), which is in agreement with earlier TGA studies on the same matrix.[14,19] The temperature of maximum weight loss (T_{max}), obtained as the inflection point in a TGA curve, was used to compare the thermal stability of

nanocomposites in inert atmosphere for solvent-free (Figure 5.13a) or DMF-processed (Figure 5.13c) nanocomposites.

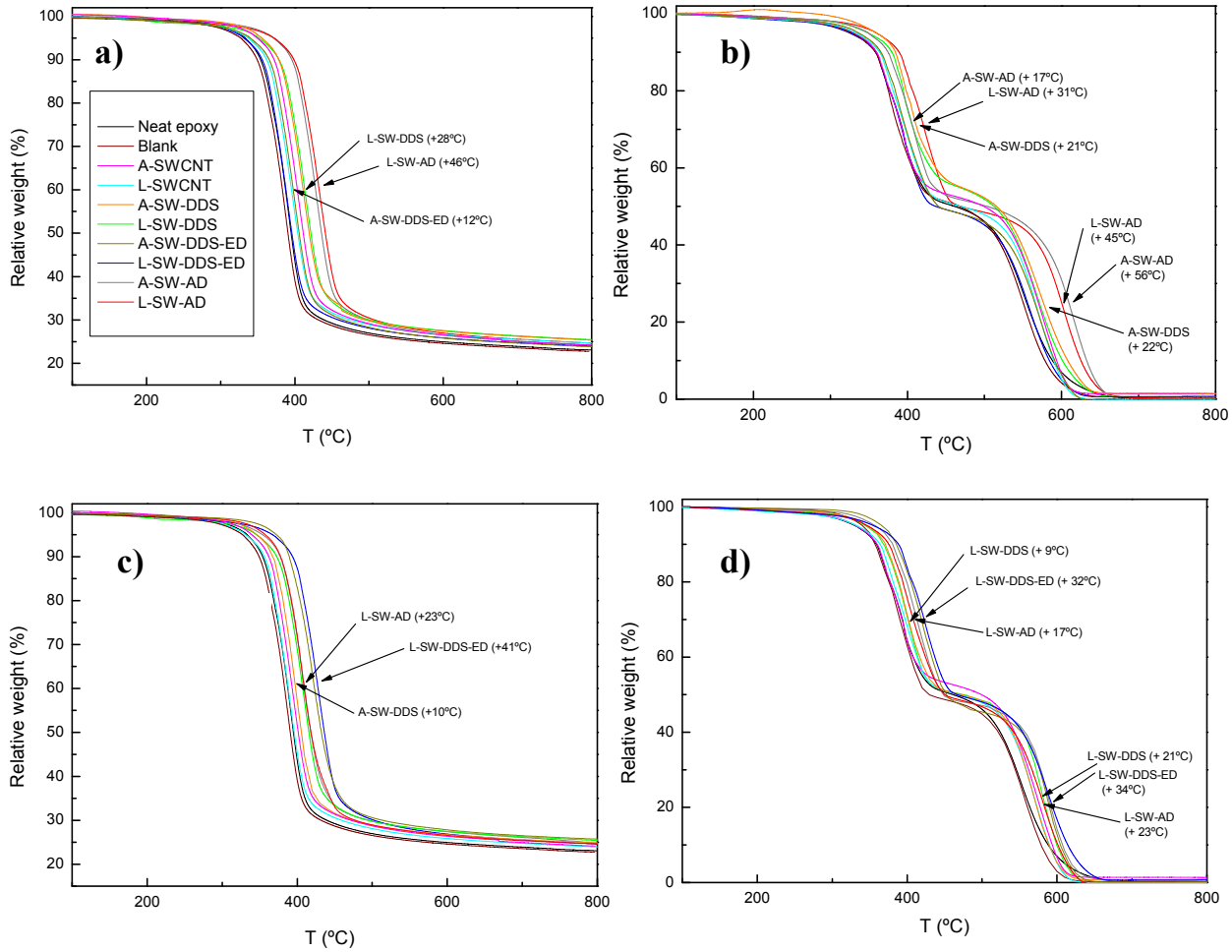

Figure 5.13. TGA plots at 10ºC/min in nitrogen (a, c) and air (b, d) atmospheres for epoxy and nanocomposite samples at 0.5 wt% loading prepared by solvent-free method (a, b) or DMF processing (c, d)

In all cases, the blank samples present slightly lower T_{max} values than the parent matrix, evidencing the inherent drawbacks of the preparation procedures. Nanocomposite samples present exceedingly higher T_{max} values as compared to reference samples or nanocomposites with unfunctionalized SWCNTs in both types of processing. The effectiveness of each filler in raising T_{max} follows the order SW-AD > SW-DDS > SW-DDS-ED (for solvent-free samples) and SW-DDS-ED > SW-AD > SW-DDS (for DMF-processed samples), reaching maximum T_{max} increases of 46ºC (SW-AD, solvent-free) and 41ºC (SW-DDS-ED, in DMF), respectively.

TGA plots indicate that the synergistic combination of chemical functionalization and preparation procedure determine the thermal stability. A strong interfacial bonding is suggested on the basis of TGA results, since it is known that the fraction of polymer matrix intimately surrounding the filler may degrade at a slower rate, causing the T_{max} upshift.[46] These results would agree with an enhanced interaction between matrix and filler, and also with a better filler distribution, since well-dispersed CNTs would provide the higher thermal conductivity that promotes the heat dissipation,[47] and effectively hinder the diffusion of the degradation products from the bulk polymer to the gas phase, thus delaying matrix degradation.

Nanocomposites containing SW-DDS-ED present the best results when processed in organic solvent, while for SW-DDS and SW-AD the solvent-free integration method provides the best results, with the SW-AD filler presenting the best improvements in both air and nitrogen atmospheres.

Thermo-oxidative stability was ascertained from TGA experiments under air atmosphere. The results are shown in Figure 5.13b and 5.13d for solvent-free and DMF-processed samples, respectively. A similar discussion to that of the inert atmosphere TGAs can be made in this case. In the solvent-free nanocomposites, the first degradation step exhibited a maximum loss rate temperature ($T_{max}1$) that was highly upshifted for nanocomposites with SW-DDS and SW-AD, showing a maximum upshift of 31ºC (L-SW-AD). The second weight loss presented a similar trend in its maximum loss rate temperatures ($T_{max}2$), with the most significant increase being that of the A-SW-AD nanocomposite (56ºC upshift). In DMF-processed nanocomposites, the SW-DDS-ED nanocomposites again stand out for their enhanced thermo-oxidative stability, with upshifts in $T_{max}1$ and $T_{max}2$ of 32ºC and 34ºC, respectively. The effect of DMF processing on these parameters for SW-DDS and SW-AD samples is to cause a lower upshift, a further evidence of the possibility to tune physical properties through the combination of functionalization and a suitable integration protocol.

[46] Moniruzzaman, M.; Winey, K. I., Polymer nanocomposites containing carbon nanotubes. *Macromolecules* 2006, *39* (16), 5194-5205.
[47] Huxtable, S. T.; Cahill, D. G.; Shenogin, S.; Xue, L. P.; Ozisik, R.; Barone, P.; Usrey, M.; Strano, M. S.; Siddons, G.; Shim, M.; Keblinski, P., Interfacial heat flow in carbon nanotube suspensions. *Nat. Mater.* 2003, *2* (11), 731-734.

It is worthy of note that the thermal and thermo-oxidative stability enhancements attained in our nanocomposites are, to the best of our knowledge, the highest reported for epoxy/CNT composites so far, especially considering the relatively low loading of filler (0.5 wt%). In other TGA studies in inert atmosphere, Ma et al.,[48] dealing with epoxy/CNT nanocomposites with functionalized CNTs, reported a T_{max} upshift of 3.9ºC using silane-modified multi-walled carbon nanotubes (MWCNTs) at 0.5 wt%; higher thermal improvements were achieved by Shen et al., who found a 26ºC increase for epoxy nanocomposites containing 4,4'-diaminodiphenylmethane-modified MWCNTs (1 wt%)[25] and a 31ºC increase for ethylenediamine-modified MWCNTs at 0.25 wt%, while it was shown to decrease for 1 wt% loading.[49] Spitalsky et al.[21] found a 25ºC upshift in T_{max} for chemically-modified MWCNTs (*via* the diazonium reaction) while epoxy thermal stability was further increased (up to 30ºC upshift) with physically modified MWCNTs (using polyaniline), in both cases at 1 wt% filler loading. The highest thermal stability improvement we could find in the literature for epoxy/functionalized-CNTs was reported by Chen et al.[35] with an upshift of 49.3ºC for an epoxy nanocomposite containing 2 wt% of covalently-modified MWCNTs with terminal amines. This result is in the same order as our highest improvement (46ºC upshift in T_{max} for solvent-free L-SW-AD nanocomposite sample at 0.5 wt%), although they achieved their result with a much higher CNT loading.

In air atmosphere, TGA literature data for epoxy/CNT nanocomposites is somewhat more limited. One of the best results found in the literature is the aforementioned work by Spitalsky et al.[21] who obtained a $T_{max}1$ upshift of 34ºC (for chemically-modified MWCNTs) and 40ºC (for physically-modified MWCNTs), both at 1 wt%. Moreover, Yang et al.[50] reported a $T_{max}1$ and $T_{max}2$ upshift of 5.8ºC and 44.5ºC, respectively, for epoxy nanocomposites containing 0.6 wt% MWCNTs functionalized with triethylenetetramine. In those works, the indicated improvements are attained at higher CNT loadings than our nanocomposites, with our best results (at 0.5 wt%) in air atmosphere for $T_{max}1$ (31ºC upshift in solvent-free L-SW-AD nanocomposite) and

[48] Ma, P. C.; Kim, J. K.; Tang, B. Z., Effects of silane functionalization on the properties of carbon nanotube/epoxy nanocomposites. *Compos. Sci. Technol.* 2007, *67* (14), 2965-2972.
[49] Shen, J. F.; Huang, W. S.; Wu, L. P.; Hu, Y. Z.; Ye, M. X., Thermo-physical properties of epoxy nanocomposites reinforced with amino-functionalized multi-walled carbon nanotubes. *Composites: Part A* 2007, *38*, 1331-1336.
[50] Yang, K.; Gu, M. Y., The Effects of Triethylenetetramine Grafting of Multi-Walled Carbon Nanotubes on Its Dispersion, Filler-Matrix Interfacial Interaction and the Thermal Properties of Epoxy Nanocomposites. *Polym. Eng. Sci.* 2009, *49* (11), 2158-2167.

$T_{max}2$ (56ºC upshift for solvent-free A-SW-AD nanocomposite) being noticeable. The improvements with this strategy are even greater than those achieved in the previous section, where the functionalization of SWCNTs via the 1,3-dipolar cycloaddition reaction provided a filler that raised the epoxy $T_{max}1$ by 22ºC (which represents an increase of 12ºC as compared to epoxy nanocomposites with unfunctionalized SWCNTs).

The reason for such good results in this section could be the outcome of two facts. First, our covalently grafted moieties contain sulfone groups flanked by benzene rings, which are well known to provide excellent thermal resistance in polymers,[51] including the neat TGAP/DDS epoxy matrix. Second, the preservation of the matrix molecular architecture at the interface not only provides strong interfacial bonding between filler and matrix, but it could also boost the intrinsic thermal features of the parent polymer so that the degradation rate is greatly lowered.

Electrical conductivity measurements

In addition to the thermal and mechanical properties, the electrical conductivity of the nanocomposites (Figure 5.14) was also dependent on the functionalization and preparation procedures. Firstly, epoxy blanks (either solvent-free or DMF-processed) exhibited identical conductivity values as the neat matrix (data not shown), hence the changes in conductivity observed for the nanocomposite samples are not a consequence of the experimental protocol impact on the parent matrix. Electrical conductivity measurements for nanocomposites prepared solvent-free at different filler loadings are shown in Figure 5.14a.

Nanocomposites incorporating unfunctionalized SWCNTs display the highest conductivity values, up to $\sim 10^{-3}$ and $\sim 10^{-6}$ S/cm (for L-SWCNT and A-SWCNT, respectively). The lower conductivity found for nanocomposite samples containing functionalized SWCNTs can be explained in terms of the covalent disruption of the SWCNT electronic structure. SWCNTs underwent covalent functionalization through the diazonium reaction, which has been reported to act preferentially on SWCNTs with

[51] Balashova, I. M.; Danner, R. P.; Puri, P. S.; Duda, J. L., Solubility and diffusivity of solvents and nonsolvents in polysulfone and polyetherimide. *Ind. Eng. Chem. Res.* 2001, *40* (14), 3058-3064.

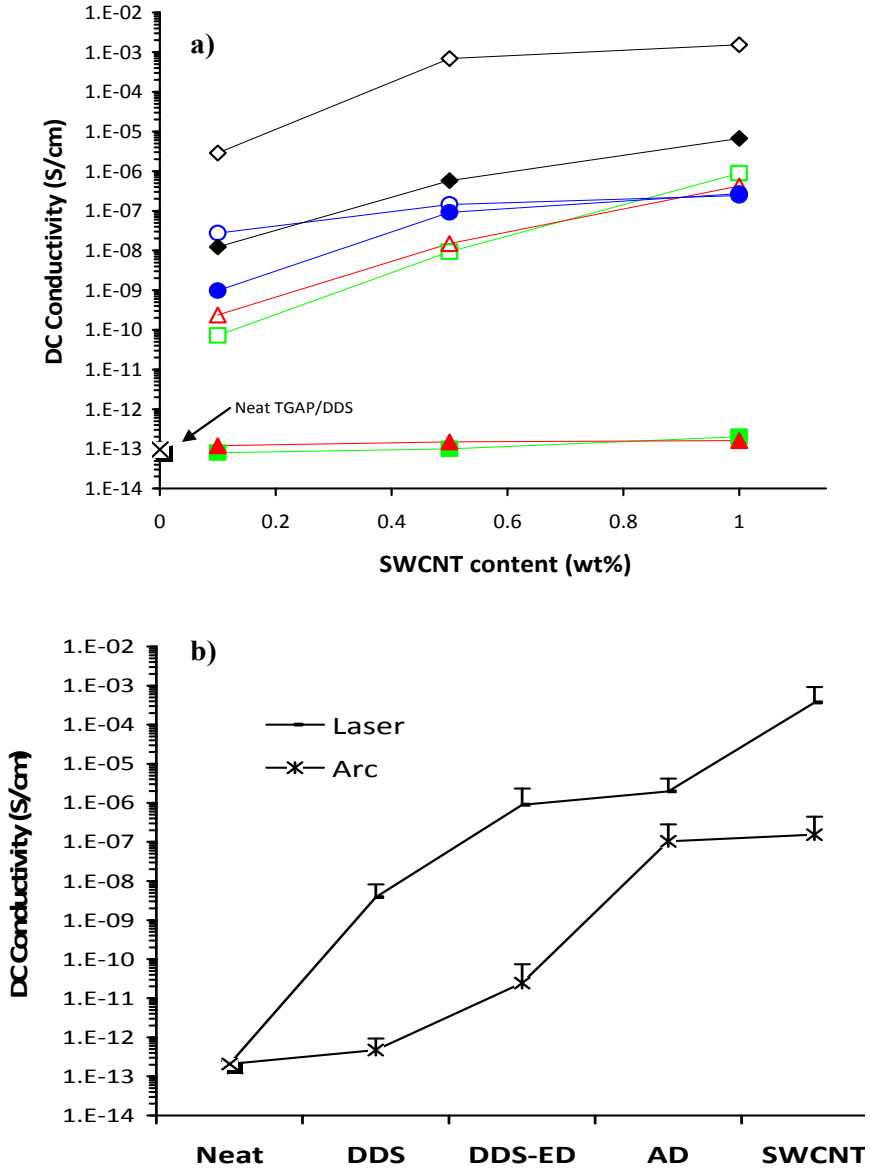

Figure 5.14. DC conductivity plots for (a) solvent-free nanocomposite samples as a function of the SWCNT loading, (b) DMF-processed nanocomposites at 0.5 wt% loading. The same colour coding from Figure 5.10a is applied: diamonds, unfunctionalized SWCNTs; triangles, SW-DDS; squares, SW-DDS-ED; circles, SW-AD; solid symbols, arc SWCNTs; hollow symbols, laser SWCNTs.

metallic behavior.[40] These types of SWCNTs are mainly responsible for the SWCNT conductive properties, and their chemical inhibition would explain the results observed in Figure 5.14. This is a general behavior already observed in the previous section, related to the electrical conductivity of nanocomposites with functionalized and non-functionalized SWCNTs. Arc-grown SWCNTs seem to be the most sensitive to the

diazonium route, since nanocomposites containing functionalized A-SWCNTs possess the lowest conductivity values in this work.

Nanocomposites containing A-SW-DDS and A-SW-DDS-ED show the same conductivity values as the parent matrix in the studied range of loadings. Such nanocomposites would be especially useful in applications where electrical insulating epoxies with highly enhanced mechanical performance would be required. An electrical percolation is observed for the other nanocomposites (generally around the 0.1 wt% loading), which shows an increase in conductivity with increasing filler loading, and reaching maximum conductivity values of ~10^{-3} S/cm at 1wt% (L-SWCNTs). Nevertheless, SWCNTs functionalized with DDS showed a higher degree of functionalization in comparison to AD[43] (see chapter 2), being an explanation for the strong difference in electrical performance between both types of nanocomposites.

The incorporation of SWCNTs *via* DMF processing again provides better features for SW-DDS-ED-based nanocomposites, tested at 0.5 wt% loading (Figure 5.14b). While electrical conductivity values for all nanocomposites at 0.5wt% loading remain nearly unchanged in comparison to their respective solvent-free counterparts, in those samples containing SW-DDS-ED, electrical conductivity is raised by 2 orders of magnitude as compared to their solvent-free analogous nanocomposites. This again shows the importance of the combination between SWCNT functionalization and integration protocol, enabling the physical properties of the nanocomposites to be tuned readily through the choice of accessible experimental variables. The electrical conductivity (especially where percolation thresholds and maximum conductivity values are concerned) in polymer/CNT nanocomposites is highly dependent on dispersion, disentanglement, uniform distribution, CNT aspect ratio and type of polymer.[7,41,52] The results presented in this section suggest that the combined effect of tailored functionalization and the integration method may lead to a strong interfacial interaction and enhanced dispersion. This causes great improvements in mechanical and thermal properties), with additional modification of electrical properties owing to the electronic effects of covalent functionalization.

[52] Bauhofer, W.; Kovacs, J. Z., A review and analysis of electrical percolation in carbon nanotube polymer composites. *Compos. Sci. Technol.* 2009, *69* (10), 1486-1498.

Dispersion assessment by SEM and Raman spectroscopy

In the previous discussions regarding the mechanical, thermal and electrical properties of epoxy/SWCNT nanocomposites, the improvements achieved have been ascribed mostly to filler-matrix interfacial interactions, as well as to good dispersion of the filler. The observation of fracture surfaces on nanocomposites in this section by means of SEM provided additional insights into the state of dispersion and interfacial interaction of SWCNTs within the epoxy matrix. Some representative images are shown in Figure 5.15. The observation of the fracture surface of the nanocomposites allowed the SWCNT bundle morphology to be recognized. However, as this technique is limited to small areas of the composites, the discussions are made after thoroughly exploring different fracture areas. Nanocomposites containing non-functionalized SWCNTs generally present a number of aggregates and entanglements, regardless of the processing method employed in the integration (DMF (Figure 5.15a) or solvent-free (Figure 5.15b)). It is worth noting that laser SWCNT bundles are thicker and heavily entangled, whereas arc SWCNT bundles are thinner and tend to form micron-sized agglomerates rather than network-like entanglements.

When SWCNTs are functionalized with DDS and integrated solvent-free, a drastic change in the fracture edge is noted. The filler is much better dispersed, with almost no presence of agglomerates or entanglements, and the length of the protruded bundles dramatically decreases, particularly for the A-SW-DDS nanocomposite (Figure 5.15c). This would agree with a strengthened interfacial bonding, since SWCNTs that are strongly bound to the matrix avoid the slippage that would lead to their pull-out, appearing as long ropes hanging from the fracture edge.[53] Instead, SWCNTs are broken together with the polymer matrix (enabled by their structural defects), which provides the "dot-like" view in Figure 5.15c. This explanation can equally be applied to solvent-free SW-AD nanocomposites (Figure 5.15d).

Nanocomposite samples containing SW-DDS or SW-AD integrated using DMF exhibit worse features than those seen in their solvent-free counterparts. SWCNTs appear somewhat more pulled-out and slightly more aggregated (Figure 5.15e),although

[53] Mirjalili, V.; Hubert, P., Modelling of the carbon nanotube bridging effect on the toughening of polymers and experimental verification. *Compos. Sci. Technol.* 2010, *70* (10), 1537-1543.

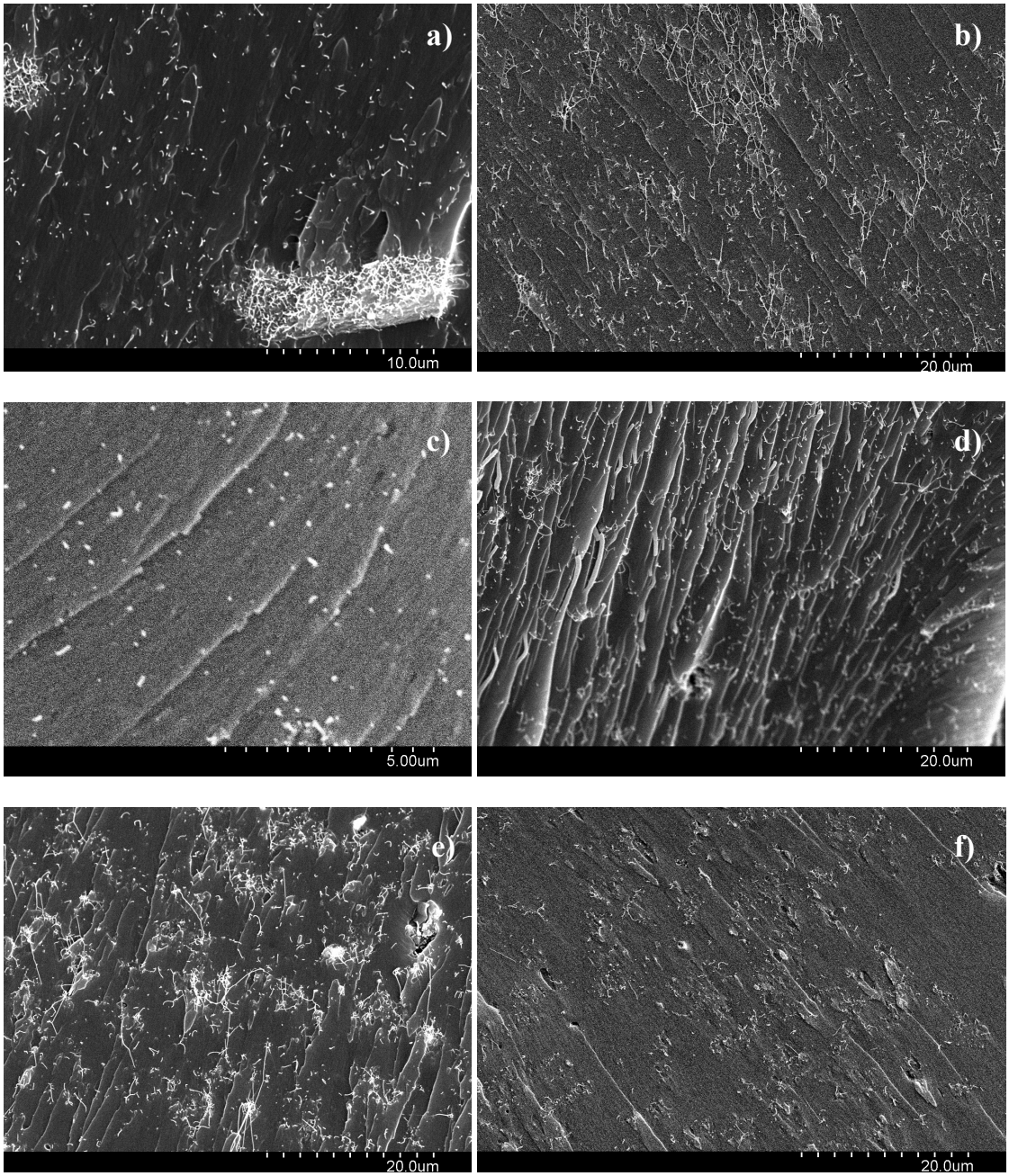

Figure 5.15. Fracture surface SEM images for the DMF-processed (a, e, f) and solvent-free (b, c, d) nanocomposites containing 0.5 wt% loading of (a) A-SWCNTs, (b) L-SWCNTs, (c) A-SW-DDS, (d and e) L-SW-AD, (f) L-SW-DDS-ED

in all cases, the fracture morphology is visibly better than that of non-functionalized SWCNT nanocomposites. This is in consonance with results obtained essentially from mechanical and thermal properties, where SW-DDS- and SW-AD-based nanocomposites present higher improvements when integrated solvent-free. SEM observations support the fact that DDS and AD functional groups achieve stronger

interfacial bonding using the solvent-free method, as observed from the lack of pull-out and aggregation.

Nanocomposites containing SW-DDS-ED present the opposite trend. Samples prepared by DMF processing exhibited much better dispersion and much less aggregation (Figure 5.15f), as compared to the rest of DMF-processed nanocomposites. This is again consistent with the former characterization, being the DMF processing especially favourable in SW-DDS-ED nanocomposites.

Additional insights into the state of dispersion in our nanocomposites were obtained with Raman spectroscopy. Raman intensity maps were used for quantitative evaluation of the 2-dimensional SWCNT dispersion at a 1 μm length scale. As the intensities of the Raman modes are proportional to SWCNT concentration within the sampling volume, the G-band intensity distribution can therefore be used to evaluate the distribution of SWCNTs along the surface of the nanocomposite sample.

The SWCNT distribution was evaluated using a method described by Du et al.[54] in which the Raman intensities for each image are normalized to a mean of 100, and the standard deviation for that average is calculated. Representative Raman images of the G-band intensity distribution of 80 x 120 μm regions are shown in Figure 5.16 for SWCNTs integrated using DMF. The 3-D contour plot of normalized Raman intensity of nanocomposites containing functionalized SWCNTs (Figure 5.16 B-C-D) is clearly flatter than that of L-SWCNT composites (Figure 5.16A), with a standard deviation of 22 for L-SWCNT, whereas L-SW-DDS, L-SW-DDS-ED and L-SW-AD composites have standard deviation values of 17, 9 and 18, respectively. This indicates that the functionalization procedures improve the distribution of SWCNT in the matrix, with L-SW-DDS-ED composites (in DMF) exhibiting the best filler distribution within this series of samples.

[54] Du, F. M.; Scogna, R. C.; Zhou, W.; Brand, S.; Fischer, J. E.; Winey, K. I., Nanotube networks in polymer nanocomposites: Rheology and electrical conductivity. *Macromolecules* 2004, *37*, 9048-9055.

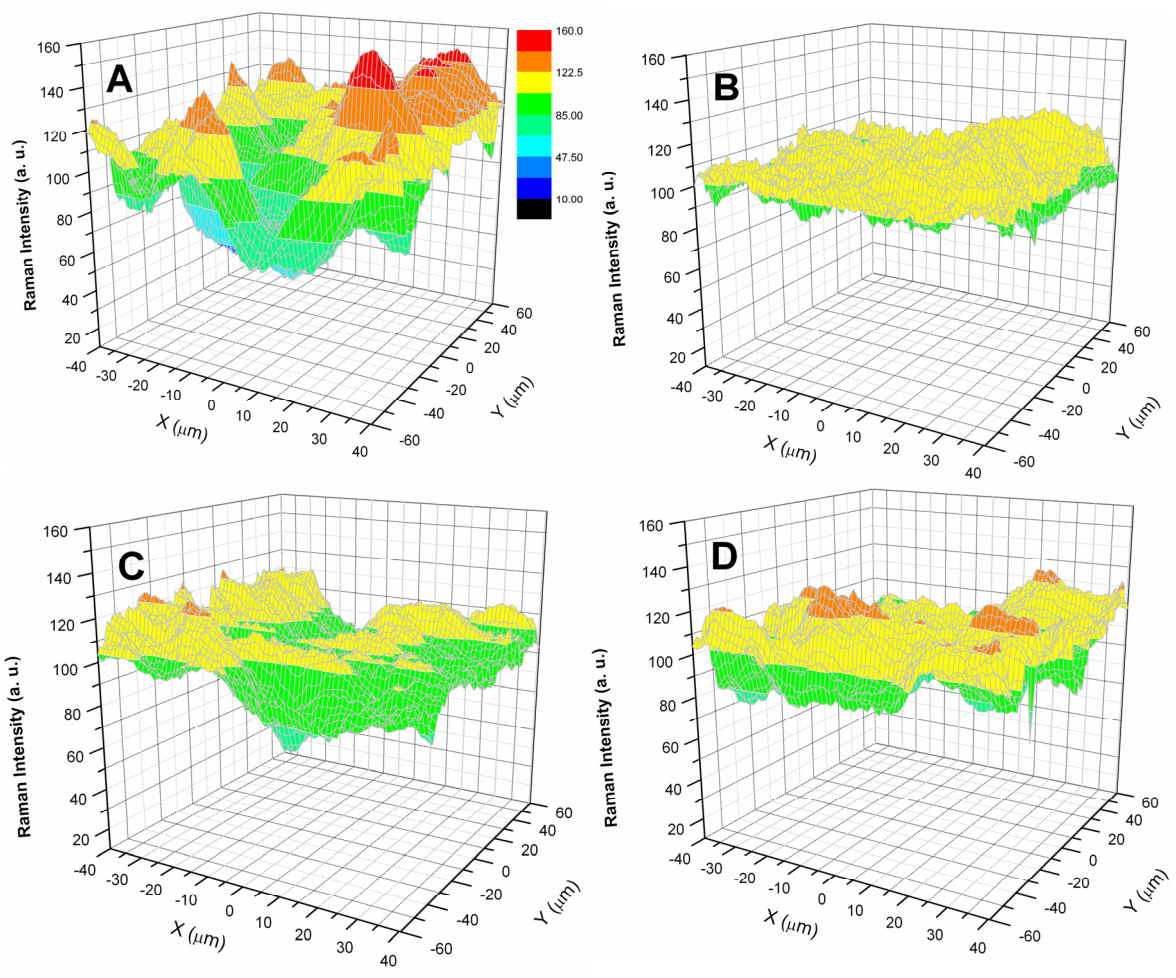

Figure 5.16. Raman imaging of DMF-processed nanocomposites containing 0.5 wt% loading of (A) L-SWCNT, (B) L-SW-DDS (C) L-SW-DDS-ED and (D) L-SW-AD. (λ_{exc} 785 nm).

5.4. Conclusion

The solvent-free incorporation of as-produced arc-discharge or laser SWCNTs into the TGAP/DDS epoxy matrix leads to composite materials with fairly enhanced mechanical and thermal properties together with the highest electrical conductivities from among all the studied samples.

The previous functionalization of these SWCNTs by sidewall covalently grafting amine moieties provides epoxy composites with improved performance as compared to those containing as-grown SWCNTs. In a first approach, the incorporation of arc-discharge SWCNTs functionalized with terminal aliphatic amines (described in section 2.2.2.) into the epoxy matrix has been addressed. With the exception of the SWCNT-

oxa sample, covalently aminated SWCNTs present better direct dispersibility in the epoxy medium. The chemical nature of the grafted moieties promotes the SWCNT reaction with the matrix epoxide groups, leading to covalent anchoring to the matrix, during the crosslinking reactions.

This study shows that particular amino-functionalization routes can be applied to preferentially enhance specific features of the epoxy matrix. Amination *via* the diazonium reaction with 4-aminobenzylamine is especially effective in enhancing the mechanical performance of the epoxy composites with enhanced stiffness (especially at medium-high SWCNT loadings) and one of the highest YM increases ever reported for aminated CNTs in epoxy resin at 1 wt% (45% increase).

The highest T_g and tensile parameters measured in this part of the work correspond to composites prepared with SWCNT-dba as filler and the increments observed in T_g (10ºC) are among the highest reported for similar epoxy/amino-functionalized CNT composites. The excellent mechanical features of this series of composites are supported by impact resistance tests and also by SEM, where the lowest bundle pull-out and degree of agglomeration were observed. As a matter of fact, a noticeable increase in the impact strength is observed with only 0.1 wt % of SWCNT-dba (44% increase), coupled with a more ductile fracture behavior as inferred from ε_b values. These composites would be particularly useful for structural applications in the aerospace or automotive industries.

Nanocomposites incorporating aminated SWCNTs throughout the 1,3-dipolar cycloaddition reaction stand out for their thermal, thermo-oxidative (between 6 and 12 ºC higher $T_{max}1$ than the rest of samples) and electrical properties (only one order of magnitude lower conductivity than the SWCNT-asg composite at 1 wt %, and about six orders of magnitude higher than the neat matrix at this SWCNT loading), while possessing excellent mechanical performance (the highest storage modulus at 1 wt % loading, 45% increase). In this regard, composites with SWCNT-dca as fillers are particularly attractive as coatings or adhesives with mechanical resistance and conductive properties.

The amination of SWCNTs *via* alkaline reduction + diacyl peroxides provides a filler whose epoxy composites display a well-balanced set of physical properties, with some emphasis in the stiffness at the lowest loadings (highest T_g and nearly the highest storage modulus at 0.1 wt %). AFM and SEM observations indicate that the improvement of mechanical performance is determined by the degree of dispersion of the SWCNTs in the matrix and, thus, by the chemical nature of the amine. Table 5.4 summarizes this information.

Table 5.4. Amino-functionalized types of arc-discharge SWCNTs used and their specific improvements in the epoxy matrix

Sample Nomenclature	Functionalization route and outcome		Specific improvements
SWCNT-dba	In situ formation and reaction of an aryl diazonium salt	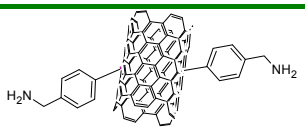	**Best tensile and impact properties** - 45% increase of Young's Modulus (1 wt %) - 44% increase in impact strenght (0.1 wt %) **And, highly enhanced dynamic mechanical properties** - 10ºC increase in T_g (1 wt %) - 40% increase in Storage Modulus (1 wt %)
SWCNT-dca	1,3-dipolar cycloaddition reaction of an azomethine ylide	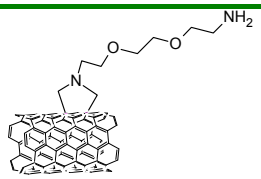	**Best thermo-oxidative and thermomechanical performance** - 45% increase of Storage Modulus (1 wt %) - 22ºC increase in $T_{max}1$ (air) at 1 wt %
SWCNT-nfp	Alkaline reduction and subsequent reaction with a diacyl peroxide	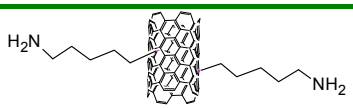	**Good balance of physical properties**, with enhanced stiffness at the lowest loading
SWCNT-oxa	Chemical oxidation followed by carboxylic activation and amidation	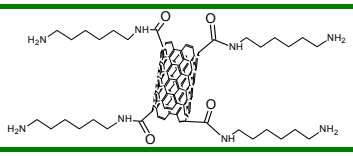	None

In parallel, a new approach is presented for developing high-performance light-weighted epoxy/SWCNT nanocomposites. The functionalization of SWCNTs with tailored molecules coming directly or synthesized from the epoxy matrix native structure *via* the diazonium reaction provides different fillers ending in primary amine or epoxide groups (see section 2.2.2.). The integration of these functionalized SWCNTs into the bulk matrix ensures strong filler-matrix interfacial bonding, plus the added advantage of having an unchanged molecular architecture at the interface, since the

covalently grafted moieties on the SWCNT surface possess a chemical nature that is equal to the parent matrix.

The experimental integration procedure also plays an important role. SWCNTs functionalized with terminal amines exhibit the best results when integrated solvent-free, while epoxide-terminated SWCNTs present the best improvements if integrated by solvent-assisted method. This enables the tuning of the nanocomposites physical properties with the combination of functional group and preparation procedure.

The as-prepared nanocomposites exhibited excellent mechanical properties, with improvements of both maximum storage modulus and tensile toughness by 65%, or an increase in the tensile strength of 91%, in comparison to the neat matrix. Most of the nanocomposites exhibited superior thermal and thermo-oxidative stability, determined by TGA, with upshifts in the maximum loss rate temperature as high as 46ºC (inert atmosphere) or 56ºC (air atmosphere) at only 0.5 wt.%. Moreover, these nanocomposites can behave as conductive or insulating agents depending on the type of SWCNTs, combination of functional group and preparation procedure, with conductivity values ranging from $\sim 10^{-13}$ to $\sim 10^{-3}$ S/cm.

Summarizing, the physical properties of epoxy nanocomposites with covalently functionalized SWCNTs can be readily tuned through specific functionalizations, leading to enhancements that can be ranked among the highest ever achieved in the field of epoxy/CNT nanocomposites.

"You were right. It's not about changing the world. It's about doing our best to leave the world the way it is. It's about respecting the will of others, and believing in your own. […] Isn't that what you fought for?"

Metal Gear Solid 4: Guns of the Patriots
Konami (2008)

CHAPTER 6:

HIGH-PERFORMANCE EPOXY/SWCNT NANOCOMPOSITES, PART II: MATRIX REINFORCEMENT WITH BLOCK COPOLYMER-WRAPPED SWCNTs

6.0. Abstract

Multicomponent nanocomposite materials based on the TGAP/DDS high-performance epoxy system and arc-discharge SWCNTs have been prepared. The non-covalent wrapping of SWCNTs with PEO-based amphiphilic block copolymers leads to a highly disaggregated filler with a boosted miscibility in the epoxy matrix, allowing its dispersion without organic solvents. Although direct dispersion of as-grown or acid-treated SWCNTs results in modest improvements of mechanical properties, the incorporation of wrapped SWCNTs is able to produce a noticeable increase in toughness and impact strength with no detrimental effect on the elastic properties. From mechanical characterization data a synergistic effect between SWCNTs and the block copolymer is revealed. The electrical conductivity of the matrix increases significantly, even at low filler loading, and the percolation threshold can be greatly reduced. This approach provides an efficient way to disperse SWCNTs without solvents into an epoxy matrix, and to generate substantial improvements with small amounts of SWCNTs. Manufacturing and comprehensive characterization of these nanocomposite materials is reported in the present chapter.

6.1. Introduction

Epoxy resins are electrically insulating thermosetting materials widely used in structural applications because of their intrinsic stiffness, chemical and heat resistance derived from a heavily cross-linked structure. The base material is brittle and often provides low wear resistance and low toughness that hinder its use in some structural, adhesive, or coating applications. The possibility of toughening and tuning other physical properties of these materials would widen their spectrum of potential applications. This is typically achieved by the addition of reinforcing and/or conductive fillers. For example, an epoxy resin can become conductive by adding silver particles, creating the potential for a conductive adhesive in electronic applications.

Reinforcement with nanoscale fillers currently represents an active field of research for advanced high-performance applications. Carbon nanotubes, in particular

single-walled (SWCNTs), have outstanding properties[1,2] and are low density, which is of critical interest in applications where the weight reduction is crucial, such as in the aircraft or automotive industries. Poor interfacial adhesion, lack of transfer of their properties, agglomeration and low uniformity of SWCNT distribution are the biggest challenges when dealing with nanotube-reinforced polymer composites.[3] Achieving an optimum nanotubes dispersion and/or individualization in a nanocomposite material is of a great importance, since its final properties (e.g., mechanical or electrical performance) can be dramatically enhanced[4] and also because new features may arise, such as optical transparency,[5] which may provide unique applications to these materials.

The integration of SWCNTs into an epoxy thermosetting material is accomplished through blending with the epoxide precursor and/ or the curing agent, followed by thermally-activated crosslinking reactions in the presence of SWCNTs.[6] Mechanical treatments, such as high shear strains[7] or ultrasounds[8] (generally in organic solvents[1,6]) are the most widely used integration methods. The use of SWCNTs has the added difficulty of achieving bundle exfoliation, which is not easy using these methods. More recently, there has been a growing interest in chemical functionalization of SWCNTs to improve integration and dispersion in epoxy resins.[1,3,6] One of the most interesting works was reported by Zhu et al.[9] in which the combination of acid treatment and fluorination produced functionalized SWCNTs that were successfully dispersed into a

[1] Coleman, J. N.; Khan, U.; Gun'ko, Y. K., Mechanical reinforcement of polymers using carbon nanotubes. *Adv. Mater.* 2006, *18* (6), 689-706.
[2] Thostenson, E. T.; Ren, Z. F.; Chou, T. W., Advances in the science and technology of carbon nanotubes and their composites: a review. *Compos. Sci. Technol.* 2001, *61* (13), 1899-1912.
[3] Moniruzzaman, M.; Winey, K. I., Polymer nanocomposites containing carbon nanotubes. *Macromolecules* 2006, *39* (16), 5194-5205.
[4] Jung, Y. C.; Shimamoto, D.; Muramatsu, H.; Kim, Y. A.; Hayashi, T.; Terrones, M.; Endo, M., Robust, Conducting, and Transparent Polymer Composites using Surface-Modified and Individualized Double-Walled Carbon Nanotubes. *Adv. Mater.* 2008, *20* (23), 4509-4512.
[5] Jung, Y. C.; Muramatsu, H.; Park, K. C.; Shimamoto, D.; Kim, J. H.; Hayashi, T.; Song, S. M.; Kim, Y. A.; Endo, M.; Dresselhaus, M. S., Transparent and Conductive Polyethylene Oxide Film by the Introduction of Individualized Single-Walled Carbon Nanotubes. *Macromol. Rapid Commun.* 2009, *30* (24), 2084-2088.
[6] Coleman, J. N.; Khan, U.; Blau, W. J.; Gun'ko, Y. K., Small but strong: A review of the mechanical properties of carbon nanotube-polymer composites. *Carbon* 2006, *44* (9), 1624-1652.
[7] Gojny, F. H.; Schulte, K., Functionalisation effect on the thermo-mechanical behavior of multi-wall carbon nanotube/epoxy composites. *Compos. Sci. Technol.* 2004, *64* (15), 2303-2308.
[8] Guo, P.; Chen, X. H.; Gao, X. C.; Song, H. H.; Shen, H. Y., Fabrication and mechanical properties of well-dispersed multiwalled carbon nanotubes/epoxy composites. *Compos. Sci. Technol.* 2007, *67* (15-16), 3331-3337.
[9] Zhu, J.; Kim, J. D.; Peng, H. Q.; Margrave, J. L.; Khabashesku, V. N.; Barrera, E. V., Improving the dispersion and integration of single-walled carbon nanotubes in epoxy composites through functionalization. *Nano Lett.* 2003, *3* (8), 1107-1113.

diglycidyl ether of bisphenol A (DGEBA)-based epoxy system by sonication in organic solvent. The filler exhibited more homogeneous distribution in the epoxy matrix as compared to unfunctionalized SWCNTs. There have been other attempts to disperse carbon nanotubes into epoxy resins based on non-covalent wrapping. Commercial surfactants[10-14] or natural polymers (i.e., Gum Arabic,[15] proteins[16]) have been utilized with the aim of dispersing pristine or functionalized nanotubes in organic solvents prior to their integration. In general, functionalization (covalent or not) is pursued to increase the dispersibility of nanotubes in organic solvents in which sonication is carried out followed by evaporation and curing of the resulting epoxy blend. This enhanced solubility in organic media often provides temporarily stable nanotube dispersions, and the solvent evaporation process leads to inhomogeneous distributions when not done quickly enough.[3,17] Furthermore, the final properties of the nanocomposites can be compromised by the solvent traces remaining after evaporation.[18]

A non-covalent approach with BCs has not been widely used in SWCNT-reinforced epoxy resins, and has been limited to the use of Disperbyk-2150 dispersant,[19-21] or, more recently, to the grafting of synthetic acrylic-based diblock

[10] Zhang, W.; Srivastava, I.; Zhu, Y. F.; Picu, C. R.; Koratkar, N. A., Heterogeneity in Epoxy Nanocomposites Initiates Crazing: Significant Improvements in Fatigue Resistance and Toughening. *Small* 2009, *5* (12), 1403-1407.
[11] Cui, S.; Canet, R.; Derre, A.; Couzi, M.; Delhaes, P., Characterization of multiwall carbon nanotubes and influence of surfactant in the nanocomposite processing. *Carbon* 2003, *41* (4), 797-809.
[12] Geng, Y.; Liu, M. Y.; Li, J.; Shi, X. M.; Kim, J. K., Effects of surfactant treatment on mechanical and electrical properties of CNT/epoxy nanocomposites. *Composites: Part A* 2008, *39* (12), 1876-1883.
[13] Gong, X. Y.; Liu, J.; Baskaran, S.; Voise, R. D.; Young, J. S., Surfactant-assisted processing of carbon nanotube/polymer composites. *Chem. Mater.* 2000, *12* (4), 1049-1052.
[14] Pecastaings, G.; Delhaes, P.; Derre, A.; Saadaoui, H.; Carmona, F.; Cui, S., Role of interfacial effects in carbon nanotube/epoxy nanocomposite behavior. *J. Nanosci. Nanotechnol.* 2004, *4* (7), 838-843.
[15] Wang, S. R.; Liang, Z. Y.; Gonnet, P.; Liao, Y. H.; Wang, B.; Zhang, C., Effect of nanotube functionalization on the coefficient of thermal expansion of nanocomposites. *Adv. Funct. Mater.* 2007, *17* (1), 87-92.
[16] Graff, R. A.; Swanson, J. P.; Barone, P. W.; Baik, S.; Heller, D. A.; Strano, M. S., Achieving individual-nanotube dispersion at high loading in single-walled carbon nanotube composites. *Adv. Mater.* 2005, *17* (8), 980-984.
[17] Grady, B. P., Recent Developments Concerning the Dispersion of Carbon Nanotubes in Polymers. *Macromol. Rapid Commun.* 2010, *31* (3), 247-257.
[18] Lau, K. T.; Lu, M.; Lam, C. K.; Cheung, H. Y.; Sheng, F. L.; Li, H. L., Thermal and mechanical properties of single-walled carbon nanotube bundle-reinforced epoxy nanocomposites: the role of solvent for nanotube dispersion. *Compos. Sci. Technol.* 2005, *65* (5), 719-725.
[19] Li, Q. Q.; Zaiser, M.; Koutsos, V., Carbon nanotube/epoxy resin composites using a block copolymer as a dispersing agent. *Phys. Stat. Sol. A* 2004, *201* (13), R89-R91.
[20] Cho, J.; Daniel, I. M., Reinforcement of carbon/epoxy composites with multi-wall carbon nanotubes and dispersion enhancing block copolymers. *Scripta Mater.* 2008, *58* (7), 533-536.
[21] Cho, J.; Daniel, I. M.; Dikin, D. A., Effects of block copolymer dispersant and nanotube length on reinforcement of carbon/epoxy composites. *Composites: Part A* 2008, *39* (12), 1844-1850.

copolymers.[22] Amphiphilic BCs have been shown to cause a toughening effect by self-assembled nanostructure formation in epoxy resins.[23,24] A judicious choice of the respective blocks allows favoring their miscibility into the epoxy resin, causing the formation of different vesicular and micellar structures that are responsible for the toughening effect. On the other hand, this tuneable lyophilicity difference between polymer blocks can be employed in liquid media to obtain highly dispersed SWCNTs. Processing these dispersed SWCNTs leads to powders with a high content of individual tubes.[25] Combining both effects provides a toughness improvement along with the advantages inherent to the integration of debundled SWCNTs. Filler-matrix adhesion is also expected to improve, since the epoxyphobic block would possess more affinity for the SWCNTs and thus interconnect them to the matrix throughout the epoxy-miscible block (Figure 6.1).

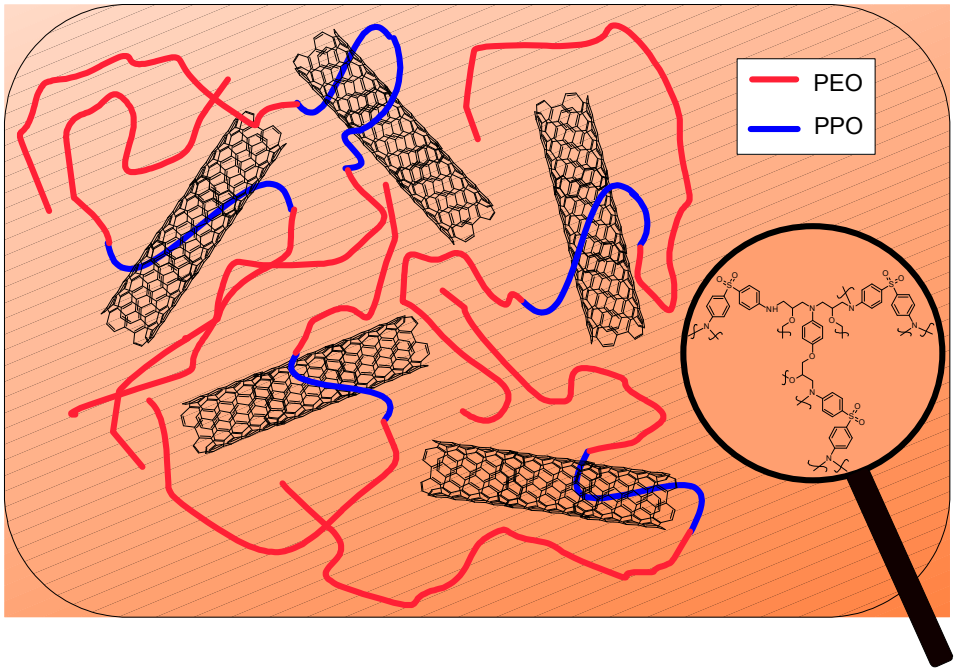

Figure 6.1. Conceptual visualization of the dispersion method based on Pluronic wrapping, (elements not to scale).

[22] Gilbert, A. C. C.; El Bounia, N. E.; Pere, E.; Billon, L.; Derail, C., Dispersion improvement of carbon nanotubes in epoxy resin using amphiphilic block copolymers. In *Advances in Structural Analysis of Advanced Materials*, Karama, M.,Ed. Trans Tech Publications Ltd:Stafa-Zurich, 2010;Vol. 112,pp 29-36.
[23] Ruzette, A. V.; Leibler, L., Block copolymers in tomorrow's plastics. *Nat. Mater.* 2005, *4* (1), 19-31.
[24] Ruiz-Perez, L.; Royston, G. J.; Fairclough, J. P. A.; Ryan, A. J., Toughening by nanostructure. *Polymer* 2008, *49* (21), 4475-4488.
[25] Gonzalez-Dominguez, J. M.; Castell, P.; Anson, A.; Maser, W. K.; Benito, A. M.; Martinez, M. T., Block Copolymer Assisted Dispersion of Single Walled Carbon Nanotubes and Integration into a Trifunctional Epoxy. *J. Nanosci. Nanotechnol.* 2009, *9* (10), 6104-6112.

In the present work, we have employed the aforementioned approach in order to achieve effective reinforcement in an aerospace-grade high performance epoxy system. We have used the ability of BCs to disperse and disentangle SWCNTs thus producing reasonably debundled arc-discharge SWCNTs wrapped in Pluronic F68 BC[25] and other amphiphilic PEO-based BCs. Their effect on curing kinetics was demonstrated by means of differential scanning calorimetry studies of the epoxy blends (see Chapter 4). The solubility of the BC-wrapped SWCNTs powders into the epoxy resin was so high that the dispersion could be carried out solvent-free by stirring and mild sonication. A complete and comprehensive study of these epoxy nanocomposite materials properties is provided in the present chapter to assess the BC-wrapped SWCNTs potential as epoxy matrix filler.

6.2. Experimental section

6.2.1. Nanocomposites preparation

Neat (TGAP/DDS) epoxy was prepared by directly blending TGAP and DDS in a stoichiometric functionality ratio (100/67) at 60ºC for 15min. Different nanocomposites containing 0.1, 0.25, 0.5, 1, and 2 wt % of Pluronic-wrapped or acid-treated SWCNTs were prepared by a solvent-free method including hot stirring (at 60ºC) and tip sonication (see section 4.2.2). The Epoxy + BC blank samples were prepared by the same solvent-free procedure, mixing the neat resin with the same amounts of BC present in each nanocomposite sample, according to the final BC content in the wrapped SWCNTs. For dynamic mechanical analysis (DMA) and electrical characterization the curing was performed as follows: the epoxy blend after the mixing protocol was cast into a steel dish mold sealed by teflon plates (3 mm thick), followed by curing at 200ºC for 30min in a Perkin Elmer hydraulic press coupled to a Greaseby Specac controlled heater, under 3 tones of pressure. The sample was removed from the mold, transferred to a Carbolite LHT4/30 oven and postcured at 200ºC for 4h. The curing cycle applied to nanocomposites based on diblock copolymer-wrapped SWCNTs was slightly different: 160ºC for 45 min + 200ºC for 30 min curing in the hot press, followed by postcuring in Carbolite ovent at 200ºC/4h.

6.2.2. Characterization techniques

► TEM images were taken in the same equipment specified in section 3.2.3. Cured samples were sliced using a microtome and deposited on a copper grid for their further use. **(UNIZAR)**

► Thermally programmed desorption coupled to mass spectrometry (TPD-MS) experiments were carried out in a home-made oven with a Eurotherm 2408 temperature controller, coupled to a Balzers Instruments GSD 300-O mass spectrometer. Two different atmospheres were used: inert (argon) and oxidative (synthetic air made by O_2 in argon), respectively, under a 50 ml/min flow, starting from room temperature and using a 10ºC/min heating ramp. The oven was calibrated with a calcium oxalate standard together with the TGA device, in order to assure the reproducibility of the heating ramp. **(ICB)**

► Fourier transform infrared (FTIR) spectroscopy was used to study partially degraded residues obtained by heating approximately 40mg of sample in standard 100 μL aluminium crucibles using the Mettler DSC-823e device under a 100 mL/min flow of N_2 or air at a 20ºC/min heating rate. When the desired temperature was reached during the heating cycle, corresponding to a specific weight loss, the sample crucible was removed and quickly cooled on an ice surface. The partially degraded residues generated were cryogenically ground using a SPEX Model 6770 Freezer/Mill and subsequently prepared as dispersions in KBr for the infrared measurements. Spectra were acquired using a Perkin-Elmer System 2000 FTIR spectrometer incorporating a MIR-DTGS detector, and spectra were recorded over the spectral range 400-4000 cm^{-1} at a resolution of 4 cm^{-1}. **(ICTP)**

► Tensile testing was performed on different devices depending on the nanocomposite sample.

For Pluronic-based nanocomposites: Tensile measurements were carried out on an MTS 858 Table Top Servohydraulic test frame equipped with hydraulic grips. Each dog-bone coupon was placed in the grips and tested in displacement control at a loading rate of 0.050 inches/min (1.27 mm/min) to failure. A 3D digital image correlation

system (Correlated Solutions Inc, Columbia, SC) comprised of two AVT Marlin cameras was used to acquire full field strain measurements in the gauge region of each coupon. The AVT Marlin cameras had a spatial resolution of 1000 pixels x 1000 pixels and provided images with a magnification of approximately 30.1 pixels/mm. For the purpose of determining elastic modulus and elongation at failure, the virtual extensometer function in Vic 3D (Correlated Solutions Inc.) was used, which allowed for displacement changes to be accurately measured in the gauge region and converted to engineering strain. Dog-bone coupons were manufactured through liquid molding to dimensions required by ASTM D638.[26] In order to obtain statistically representative data, six specimens were manufactured for each sample, and those which broke beyond the gauge region were automatically discarded in further calculations. **(IAR)**

For diblock copolymer-based nanocomposites: Tensile mechanical properties of the composites were measured in the same conditions stated in section 5.2.2. **(ICTP)** At least five specimens for each type of composite were tested to ensure repeatability and those which broke beyond the gauge region were automatically discarded in further calculations.

Both test sample surfaces were polished prior to the measurements. Low magnification optical microscopy was applied to the broken surface after each tensile test to verify that coupons were broken due to normal failure rather than by the existance of a superficial flaw.

► Charpy impact strength measurements were carried out in the same conditions stated in section 5.2.2. The presented data correspond to the average value of 6 - 8 specimens. **(ICTP)**

►TGA and DSC characterizations were applied according to the experimental details provided in sections 2.2.3. and 4.2.3. respectively. On the other hand, SEM, DMA, AFM and electrical conductivity measurements were performed in the same conditions as described in section 5.2.2.

[26] ASTM D638. Standard Test Method for Tensile Properties of Plastics. ASTM International, West Conshohocken, PA, USA, 2008.

6.3. Results and discussion

6.3.1. Pluronic-based Epoxy/SWCNT nanocomposites. Mechanical and electrical properties

The state of dispersion was firstly controlled by optical microscopy. These observations have been performed in a blend containing TGAP and filler (prior to the hardener incorporation and curing). The obtained images (see section 4.4.1) show how the solvent-free mixing protocol provides a highly homogeneous epoxy blend with no visible agglomerates in the case of Pluronic-wrapped SWCNTs. In contrast, acid-treated SWCNTs present a very rough and aggregated view, visibly different from that of the Pluronic-wrapped filler. In Figure 1, typical SEM and TEM images are shown for composite samples containing 0.5 wt % SWCNTs (acid-treated and Pluronic-wrapped). In the SEM images, performed on the fractured edge of a cured test sample, the difference between the two kinds of SWCNTs is evident. The incorporation of acid-treated SWCNTs into the epoxy matrix results in a visible inhomogeneity, with appreciable amounts of large domains of aggregated SWCNTs (Figure 6.2a). The adhesion to the matrix seems to be poor because SWCNTs in the agglomerates appear to be "pulled out" intact rather than broken.

When Pluronic-wrapped SWCNTs are used as the reinforcement, a drastic change in the fracture edge morphology is denoted. Homogeneity in the SWCNT distribution increases considerably, no agglomerates can be observed, and the thickness of SWCNT bundles is greatly reduced (Figure 6.2b). The fracture edge overview in this case consists of SWCNTs randomly oriented and broken, that appear as bright dots, indicating a very good adhesion to the matrix, as well as the possible presence of defects in the SWCNT structure that enables the SWCNT/matrix joint breakage. Spherical morphologies formed by the BC are easily seen at higher filler loadings (2 wt % SWCNT-Pluronic), as will be shown in Figure 6.9.[27] A closer look at both samples was made by TEM, using test samples cut with a microtome. For the nanocomposite containing acid-treated SWCNTs, large areas with no filler were observed, containing

[27] Gonzalez-Dominguez, J. M.; Anson-Casaos, A.; Castell, P.; Diez-Pascual, A. M.; Naffakh, M.; Ellis, G.; Gomez, M. A.; Martinez, M. T., Integration of block copolymer-wrapped single-wall carbon nanotubes into a trifunctional epoxy resin. Influence on thermal performance. *Polym. Degrad. Stab.* 2010, *95* (10), 2065-2075.

some nanometric-sized aggregates of SWCNTs (Figure 6.2c). On the other hand, the nanocomposite containing Pluronic-wrapped SWCNTs showed a different pattern wherein different nanostructures formed by the BC could be seen (Figure 6.2d), with no evidence of aggregates. In this latter sample, SWCNTs were fully embedded in the epoxy matrix and therefore barely visible, indicating important improvements in the disentanglement and distribution of the filler inside the matrix. Optical microscopy is consistent with observations made by SEM and TEM.

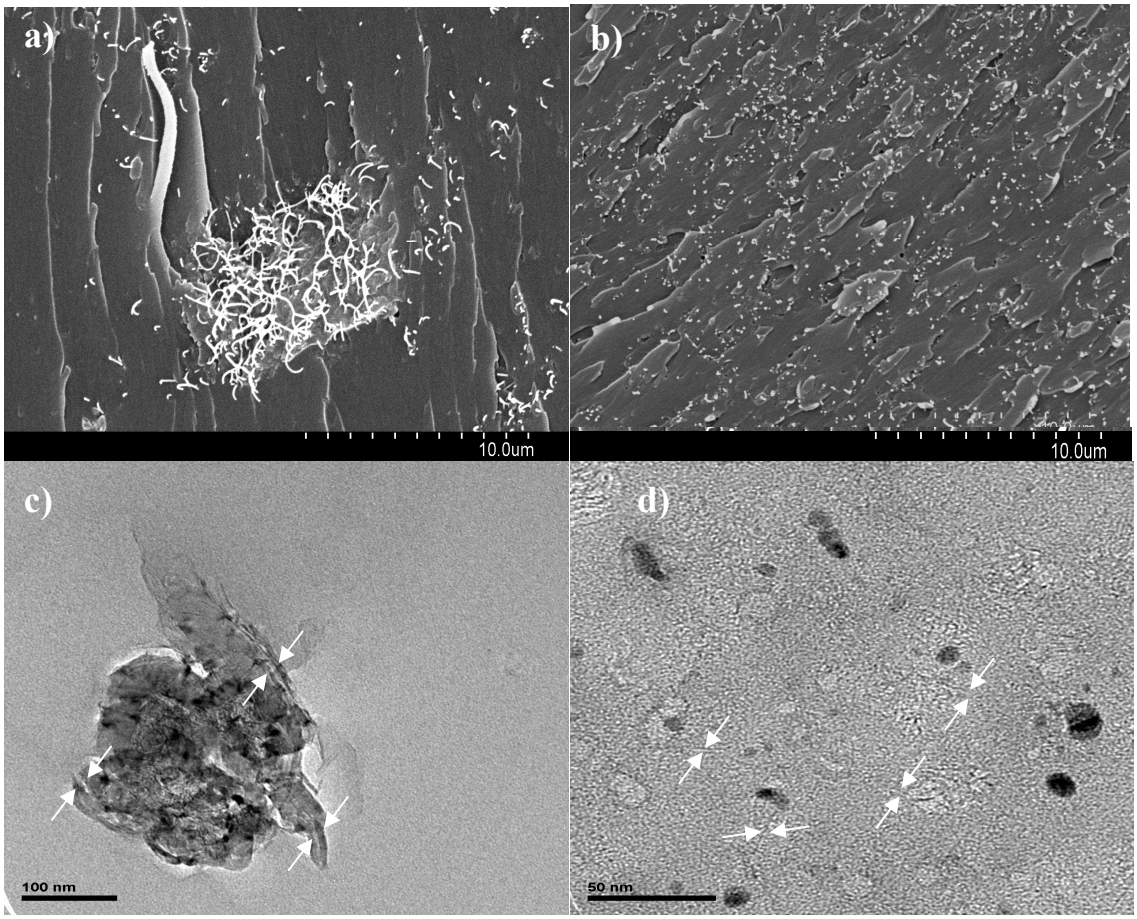

Figure 6.2. SEM (top) and TEM (bottom) images for the nanocomposite sample containing 0.5 wt% of filler: a) and c) correspond to acid-treated SWCNTs nanocomposites, while b) and d) belong to the Pluronic-wrapped containing sample. Arrows indicate the presence of SWCNTs.

Dynamic mechanical characterization

DMA over a wide temperature range is very sensitive to the physical and chemical structure of epoxy resins and their composites. A study of the storage modulus and tan δ curves is very useful in ascertaining the relaxation behavior of a sample under

load and temperature. A clear understanding of the storage modulus-temperature curve obtained during DMA provides valuable insights into the stiffness of a material as well as the molecular relaxations taking place, both as a function of temperature.

In Figure 6.3a the room temperature storage modulus data are shown for different nanocomposite and blank samples. Epoxy nanocomposites based on acid-treated SWCNTs experience a moderate increase in the storage modulus. The reinforcing role of SWCNTs in the dynamic mechanical performance of epoxy resin is controlled by the SWCNT concentration. Composites with 1 wt% of acid-treated SWCNTs increased the storage modulus of the epoxy resin at room temperature by 28%. The 0 wt% baseline blank represents the epoxy matrix subjected to the same mixing protocol as the rest of nanocomposite samples.

The utilized procedure causes slight damage to the neat matrix. The incorporation of small amounts of Pluronic F68 BC leads to a decrease in the storage moduli of 33.5%, which is apparently independent of Pluronic concentration in the studied range. This is consistent with observations reported by other authors working with different epoxy matrices modified with PEO-based BCs.[28,29] This fact may be attributed to a strong plasticizing effect caused by the BC. The presence of a BC within the epoxy matrix leads to spherical nanostructure formation by self-assembly which may encapsulate epoxy material, leading to a nano-segregated feature consisting of BC and epoxy as will be shown in AFM images. The rubbery layer between the inner and outer part of the spherical nanostructures is probably weakly bonded to the epoxy, causing this plastic behavior.

The addition of Pluronic-wrapped SWCNTs produces a large increase in the storage modulus of all samples compared with their respective Epoxy + Pluronic blanks. This leads to modulus values close to the neat epoxy (Fig. 6.3a), with no dependence on filler concentration in the studied range. As an example, the modulus increase with respect to its own blank sample for the lowest loading of Pluronic-wrapped SWCNTs (0.1 wt% filler) is 0.99 GPa (an increase of 47%). This represents a large increase with a

[28] Dean, J. M.; Grubbs, R. B.; Saad, W.; Cook, R. F.; Bates, F. S., Mechanical properties of block copolymer vesicle and micelle modified epoxies. *J. Polym. Sci. B-Polym. Phys.* 2003, *41* (20), 2444-2456.
[29] Dean, J. M.; Lipic, P. M.; Grubbs, R. B.; Cook, R. F.; Bates, F. S., Micellar structure and mechanical properties of block copolymer-modified epoxies. *J. Polym. Sci. B-Polym. Phys.* 2001, *39* (23), 2996-3010.

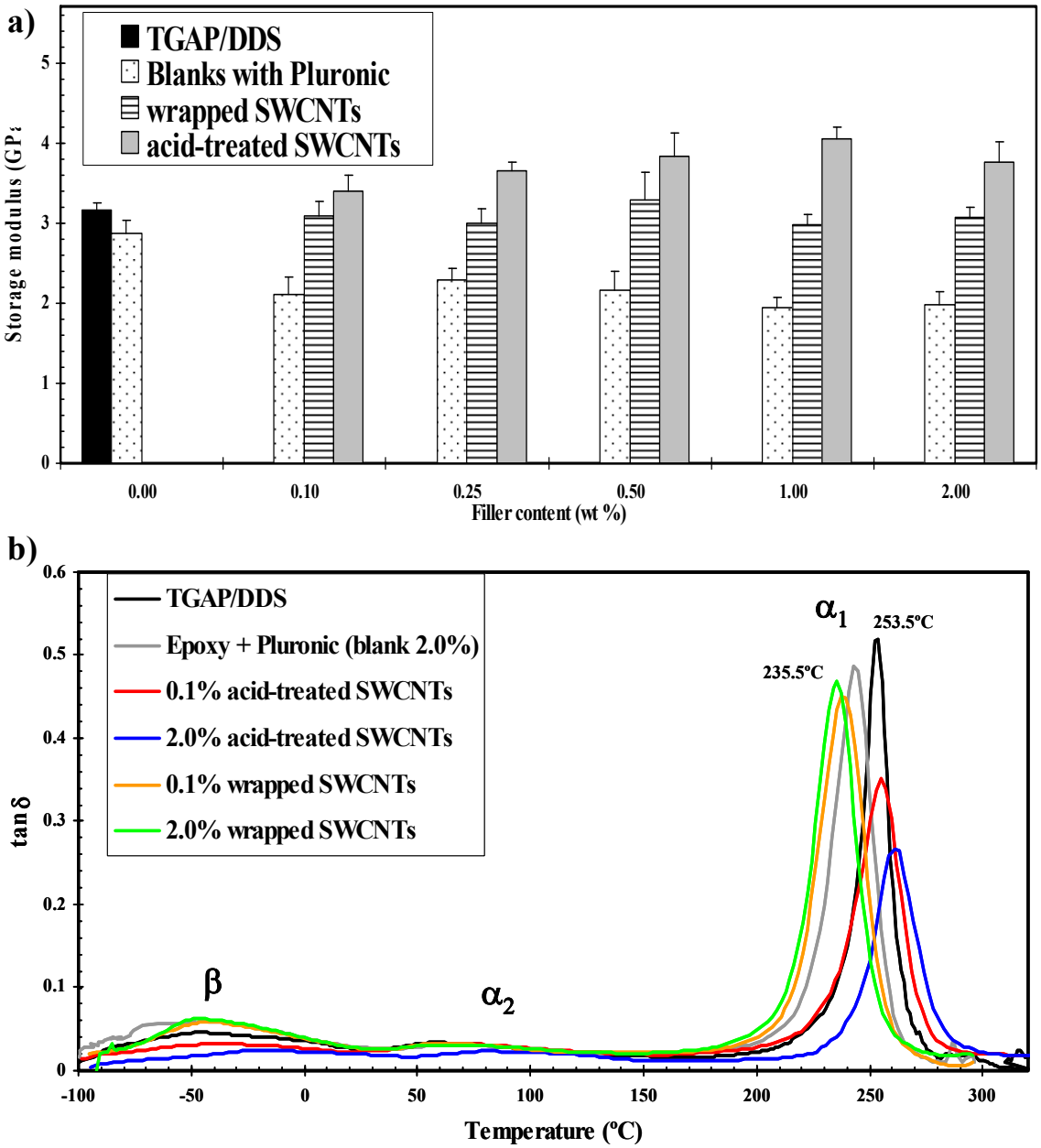

Figure 6.3. Dynamic mechanical analysis of epoxy nanocomposites obtained at the frequency of 1Hz and 25ºC; a) value of storage modulus obtained at room temperature *versus* filler concentration, and b) Evolution of tan δ for some different compositions of epoxy resin *vs.* temperature at 1Hz.

very small amount of the filler (30 wt% BC and 70 wt% SWCNTs in the filler, thus 0.07 wt% of SWCNTs in the composite, see section 3.3.2.1). The reinforcement role of SWCNTs seems to be enhanced when wrapped in Pluronic and this fact compensates for the plasticizing effect of the BC, leaving the storage modulus values unchanged with respect to the neat matrix.

The damping factor (tan δ) tests allow studying glass or secondary transitions. As can be seen in Figure 6.3b, the resin system displays three transition peaks in the curve. The transition at the lowest temperatures is the secondary relaxation associated with the β-transition while the other relaxations are associated with different α-transition temperatures of the cured network. The α_1-transition (glass transition) can be related to Brownian motion of the main chains at the transition from the glassy to the rubbery state and the relaxation of associated dipoles, at a specific temperature (T_g). The β-transition occurs at significantly lower temperatures and it is well known to be related to crankshaft rotation of hydroxyl ether segments (-CH_2-CH(OH)-CH_2-O-) of the crosslinked network in the glassy state.[30]

The appearance of these two α transitions related to the epoxy network, while not common, has been reported previously for high-performance structural epoxy resins possessing high functionality monomers.[31] For the sake of clarity, only the extreme compositions (0.1 and 2 wt%) are shown in Figure 6.3b. The addition of acid-treated SWCNTs leads to a progressive increase in both β and α_1 transition temperatures of the neat epoxy (initially about -50ºC and 253.5ºC, respectively). The height of the α_1 transition peak also progressively decreases with the addition of acid-treated SWCNTs, in good agreement with an increase in the rigidity of the system. However, the α_2 transition temperature appears unchanged. Upon addition of Pluronic a reduction in T_g (α_1) was found, about 18ºC for samples containing Pluronic-wrapped SWCNTs and 10.5ºC for the Epoxy + Pluronic blank references. Furthermore, the presence of Pluronic strongly influences the α_2 transition of the neat epoxy resin. The value of the α_2 transition temperature decreased drastically with the addition of Pluronic. These facts confirm the strong plasticizing effect of Pluronic.

Similar observations were reported by other authors working with Pluronic and other epoxy resins.[32] The broadening of the α_1 peak might be related to restrained chain mobility that usually occurs in compatible blends, slowing down the mobility of the

[30] Yi, F. P.; Zheng, S. X.; Liu, T. X., Nanostructures and Surface Hydrophobicity of Self-Assembled Thermosets Involving Epoxy Resin and Poly(2,2,2-trifluoroethyl acrylate)-block-Poly(ethylene oxide) Amphiphilic Diblock Copolymer. *J. Phys. Chem. B* 2009, *113* (7), 1857-1868.
[31] Varley, R. J.; Hodgkin, J. H.; Simon, G. P., Toughening of a trifunctional epoxy system - Part VI. Structure property relationships of the thermoplastic toughened system. *Polymer* 2001, *42* (8), 3847-3858.
[32] Larrañaga, M.; Serrano, E.; Martin, M. D.; Tercjak, A.; Kortaberria, G.; de la Caba, K.; Riccardi, C. C.; Mondragon, I., Mechanical properties-morphology relationships in nano-/microstructured epoxy matrices modified with PEO-PPO-PEO block copolymers. *Polym. Int.* 2007, *56*, 1392-1403.

matrix chains, hence creating a wider temperature transition.[33] It can be assumed that matrix chains located close to the nanofiller possess different mobility than those fully embedded in an epoxy environment, leading to a broadening of the relaxation peaks. Opposed to the epoxy + acid-treated SWCNT samples, the nanocomposites with Pluronic-wrapped SWCNTs do not show significant changes in α_1 width, with respect to their corresponding blanks, suggesting that SWCNTs are not able to fully develop their ability to restrict motion when wrapped in the BC.

On the whole, the results provided by this technique show that the incorporation of SWCNTs wrapped in this BC into the epoxy does not damage the elastic properties of the matrix. The storage moduli of the samples containing Pluronic-wrapped SWCNTs experience a very pronounced increase as compared to the epoxy + Pluronic blank references, regardless of the filler content, while giving modulus values comparable to that of the neat epoxy. Pluronic-containing samples (nanocomposites with wrapped SWCNTs and related blanks) exhibit significantly lower T_g values even with small additions of the filler.

Static mechanical properties

One of the epoxy-SWCNT samples was selected to carry out a series of tensile experiments. As a compromise between nanotube loading and dynamical mechanical properties, the nanocomposite with 0.5 wt % filler was chosen. Four different samples were prepared: the TGAP/DDS neat epoxy, the 0.5 wt % nanocomposite containing Pluronic-wrapped SWCNTs, the blank sample (epoxy + 0.15 wt % of Pluronic) and the nanocomposite sample containing 0.5 wt % of acid-treated SWCNTs. In a typical tensile experiment, the stress-strain curve obtained is shown in Fig. 6.4. The ultimate strain or elongation (ε_b) and ultimate tensile stress (σ_y) are extracted from the curve just before the failure. Young'smodulus (YM) is obtained from the slope of the linear fit in the initial section of the curve (up to 5000 με, i.e. 0.05% strain). Finally, the toughness was estimated by calculating the area under the curve using equation 1:

[33] Lin, M. S.; Lee, S. T., Mechanical behaviors of fully and semi-interpenetrating polymer networks based on epoxy and acrylics. *Polymer* 1997, *38* (1), 53-58.

$$G = \sum_{\varepsilon=0}^{\varepsilon_{max}} \sigma \Delta \varepsilon \qquad [1]$$

Mechanical parameters drawn from tensile curves for the different samples are depicted in Figure 6.5. In this figure, error bars represent confidence intervals calculated through the Student's "t-test" (statistical significance >90%).

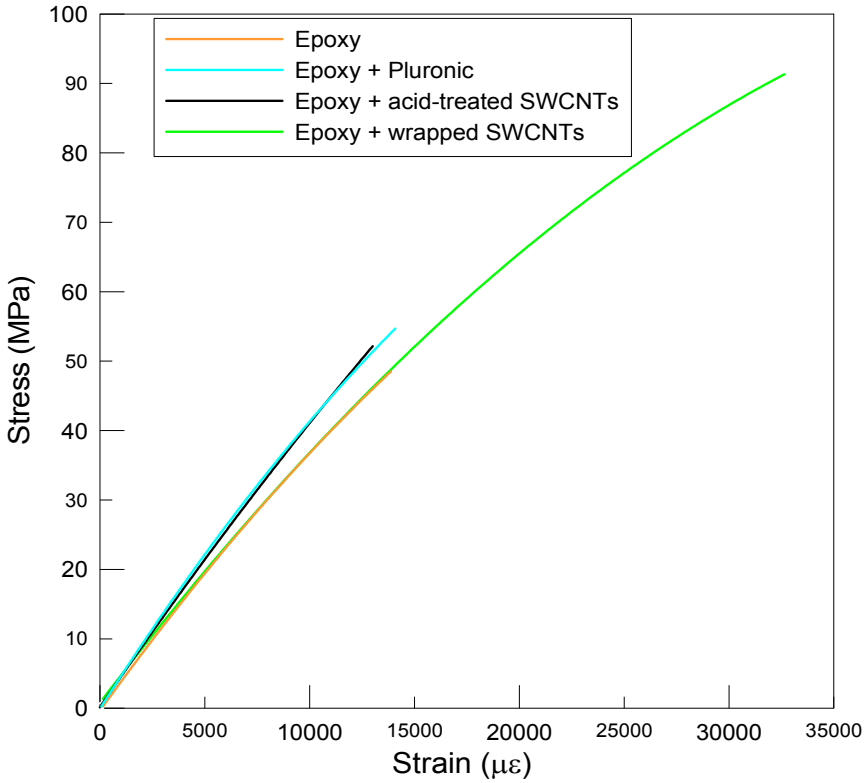

Figure 6.4. Representative stress-strain curves for the epoxy + 0.5 wt% wrapped-SWCNTs nanocomposite sample and different control samples.

The neat epoxy matrix possesses a high YM value (4.3 GPa) but low toughness (0.34 MJ/m^3), as expected with an inherently brittle material. It is clear that the incorporation of acid-treated SWCNTs (0.5 wt %) slightly increased the matrix YM and increased toughness by 4.7% and 35% respectively. It was also found that ε_b decreases by 6.5% and σ_y increases by 37%. The presence of the BC in the same amount as in the Epoxy + wrapped SWCNTs sample (0.15 wt % BC) was found to have a more pronounced effect on toughness, resulting in an increase of 71% with respect to the neat resin. This latter is consistent with the fact that BCs are well-known to toughen epoxy matrices.[23,24] In our case, Pluronic F68 itself is causing a visible toughness improvement

despite the low amounts in which it is present. YM for Epoxy + BC sample, however, remains unchanged with respect to the neat matrix, whereas ε_b and σ_y values increase by 2.5% and 31%, respectively.

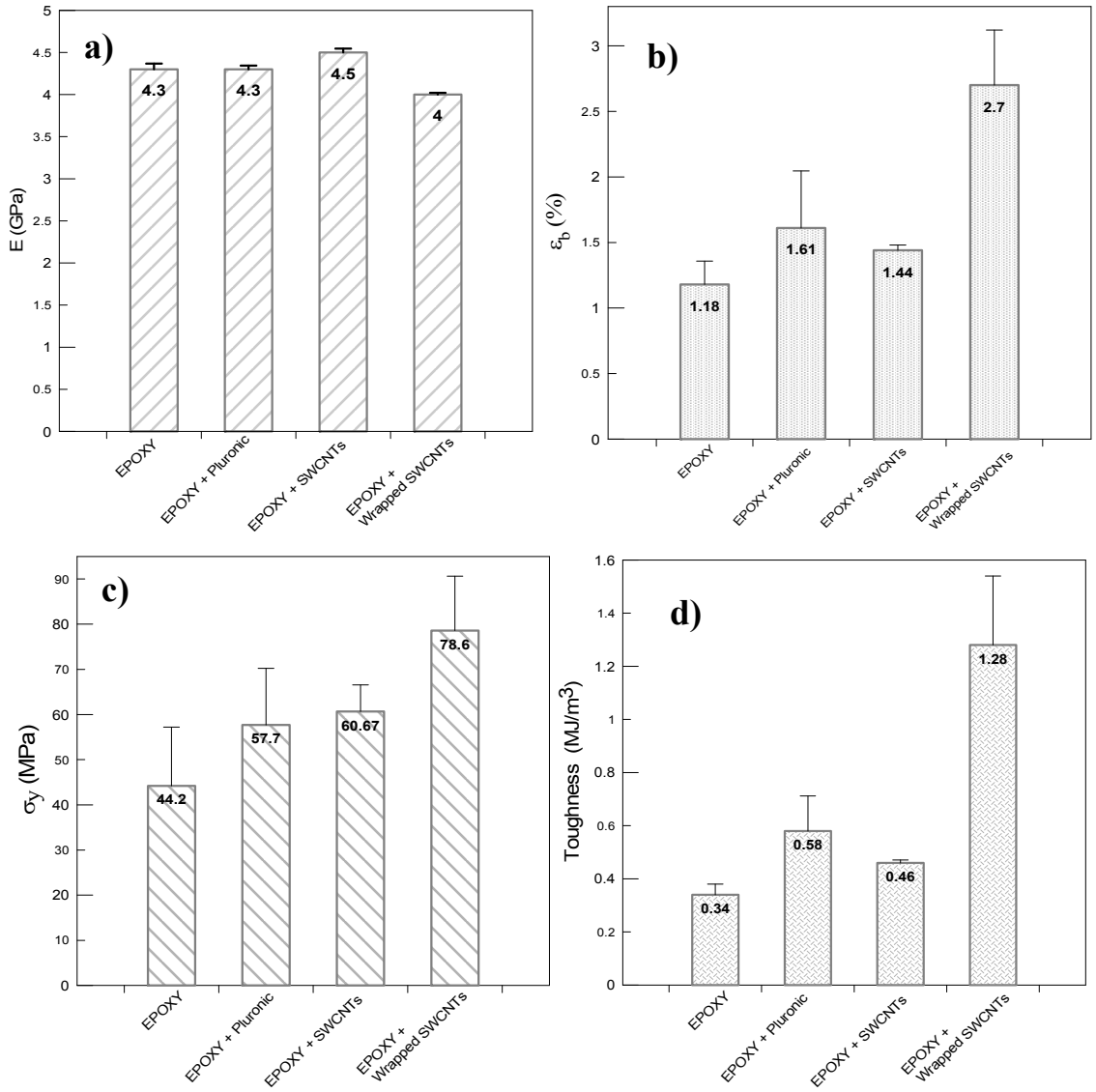

Figure 6.5. Mechanical parameter extracted from stress-strain curves in Pluronic-based nanocomposites: a) Young's modulus, b) Maximum strain, c) Ultimate tensile strength, and d) Toughness.

Finally, for the Epoxy + wrapped SWCNTs sample there was huge increase in toughness with respect to the neat matrix (276%), which evidences the synergistic toughening effect between acid-treated SWCNTs and Pluronic F68. While acid-treated SWCNTs or BC do not separately cause such toughening, the combination of both (in the form of Pluronic-wrapped SWCNTs) produces a remarkable toughness enhance-

ment. This synergistic behavior was also detected for ε_b and σ_y, which exhibit an improvement of 72% and 78%, respectively, with regard to the neat matrix, indicating a more ductile fracture behavior. The YM seems to be slightly worsened in this last case, decreasing 7.5% with respect to the neat matrix (Table 6.1).

Table 6.1. Tensile percentage improvements for the different Pluronic-based nanocomposite samples at 0.5 wt% filler (or the associated Pluronic amount) with respect to the baseline TGAP+DDS matrix

	Epoxy + Pluronic	**Epoxy + SWCNTs**	**Epoxy + wrapped SWCNTs**
YM	0%	+4.7%	-7.5%
σ_y	+31%	+37%	+78%
ε_b	+2.5%	-6.5%	+72%
Toughness	+71%	+35%	+276%

Although YM enhancements in epoxy/CNT nanocomposites have extensively been reported over the past years, available toughness data in these systems are limited.[34] In general, extensive storage and YM enhancements have been reported in the literature but no increase or significant decrease in toughness.[6] Some few studies have shown moderate tensile toughness improvements,[7,35] but to the best of our knowledge no tensile toughness improvement comparable with the 276% found here have been demonstrated, particularly with such small amounts of filler. In addition to this, the classical methods to toughen epoxy matrices usually sacrifice other mechanical properties.[36] The mechanical data reported here shows how to selectively enhance toughness and maximum strain of an epoxy resin with virtually no change in other mechanical properties.

The Pluronic-wrapping of SWCNTs provides an epoxy-miscible filler with high capability for toughening the matrix whereas, composites with a moderate increase in storage moduli and tensile properties can be achieved by solvent-free dispersion of acid-treated SWCNTs.

[34] Spitalsky, Z.; Tasis, D.; Papagelis, K.; Galiotis, C., Carbon nanotube-polymer composites: Chemistry, processing, mechanical and electrical properties. *Progr. Polym. Sci.* 2010, *35* (3), 357-401.
[35] Gojny, F. H.; Wichmann, M. H. G.; Fiedler, B.; Schulte, K., Influence of different carbon nanotubes on the mechanical properties of epoxy matrix composites - A comparative study. *Compos. Sci. Technol.* 2005, *65* (15-16), 2300-2313.
[36] Johnston, N. J. Toughened Composites, ASTM special technical publication, Philadelphia PA, 1895, p. 937.

The BC binds to the SWCNTs during the wrapping process, thanks to the van der Waals forces, polar interactions between oxygen groups in both BC and SWCNTs, and by a noticeable steric stabilization. It could be assumed that the interface between BC-wrapped SWCNTs and the matrix is ruled by the interactions between the BC and the epoxy. The chemical similarity and miscibility, but non-reactivity of PEO with the target matrix allows interfacial bonding throughout polar interactions (dipole forces) and the possible existence of hydrogen bonds (i.e., between PEO ethers and epoxy's unreacted OHs). The PPO block would remain more strongly bound to the SWCNTs than PEO within the epoxy environment, being responsible of the interfacial connection of the filler with the matrix.

Recent studies about the adsorption and self-assembly of Pluronic block copolymers on SWCNTs[37] propose the formation of new hybrid SWCNT-polymer elongated-micelle-like structures where a SWCNT is located at the core of a cylindrical aggregate. According to these studies, it seems feasible that the presence of SWCNTs would hinder the typical spherical micellation within the epoxy matrix, favoring the formation of micrometer- long cylindrical aggregates with increased surface area which would be more efficient in toughening the epoxy matrix. This could be an explanation for the huge toughness increase reported herein.

Impact strength

To further characterize the toughness of the composites, room temperature Charpy notched impact strength measurements were carried out, and the results are shown in Figure 6.6. The impact strength of the pure resin is around 1.4 kJ/m^2 and increases by about 66% for the blank sample, with Pluronic, because of the toughening effect of the BC which increases the flexibility of the epoxy. Acid-treated SWCNTs lead to a moderate increase in the impact strength (~41% at 0.5 wt % SWCNT content); whilst for composites incorporating the same amount of Pluronic-wrapped nanofillers, the increase was exceptionally higher (193%), close to that observed in toughness obtained from tensile data.

[37] Shvartzman-Cohen, R.; Monje, I.; Florent, M.; Frydman, V.; Goldfarb, D.; Yerushalmi-Rozen, R., Self-assembly of amphiphilic block copolymers in dispersions of Multiwalled Carbon Nanotubes as reported by spin probe Electron Paramagnetic Resonance Spectroscopy. *Macromolecules* 2010, *43* (2), 606-614.

This unprecedented toughness enhancement is ascribed to a strong increase in the energy dissipated, because of the synergistic effect between SWCNTs and the BC. This percentage improvement in Charpy impact strength is, to the best of our knowle-dge, considerably higher than the best found in the literature, which were achieved by covalent integration of aminated multi-walled carbon nanotubes into DGEBA-based epoxy systems.[38-41] Any molecular process which promotes energy dissipation enhances the impact resistance of polymers.[42] Composites with Pluronic-wrapped SWCNTs present considerably larger area under tan δ peak (Fig. 6.3b), hence are able to dissipate more energy than those reinforced with acid-treated fillers.

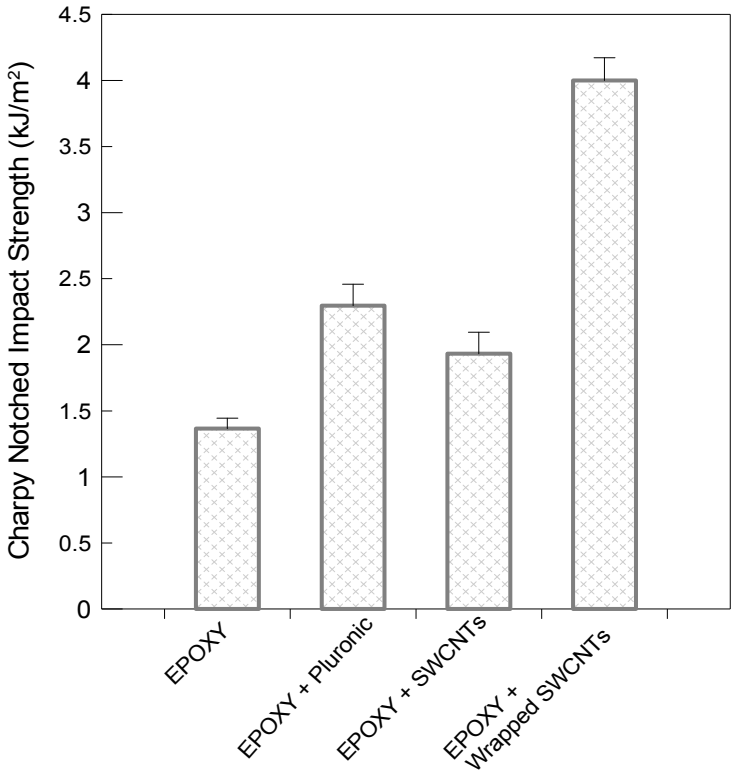

Figure 6.6. Room temperature notched impact toughness of the neat epoxy matrix, the composite containing 0.5 wt% Pluronic-wrapped SWCNTs and reference composites.

[38] Wang, J. G.; Fang, Z. P.; Gu, A. J.; Xu, L. H.; Liu, F., Effect of amino-functionalization of multi-walled carbon nanotubes on the dispersion with epoxy resin matrix. *J. Appl. Polym. Sci.* 2006, *100* (1), 97-104.
[39] Yang, K.; Gu, M. Y.; Guo, Y. P.; Pan, X. F.; Mu, G. H., Effects of carbon nanotube functionalization on the mechanical and thermal properties of epoxy composites. *Carbon* 2009, *47* (7), 1723-1737.
[40] Li, S. Q.; Wang, F.; Wang, Y.; Wang, J. W.; Ma, J.; Xiao, J., Effect of acid and TETA modification on mechanical properties of MWCNTs/epoxy composites. *J. Mater. Sci.* 2008, *43* (8), 2653-2658.
[41] Byun, J.; Kim, D. S., Curing behavior and physical properties of epoxy nanocomposites comprising amine-functionalized carbon nanofillers. *Polym. Compos.* 2010, *31* (8), 1449-1456.
[42] Jafari, S. H.; Gupta, A. K., Impact strength and dynamic mechanical properties correlation in elastomer-modified polypropylene. *J. Appl. Polym. Sci.* 2000, *78* (5), 962-971.

The results provided by the different mechanical tests indicate that the addition of Pluronic-wrapped SWCNTs reduces the detriment in energy dissipation caused by the incorporation of the stiff nanotubes, thereby leading to a huge improvement in the toughness of the composites.

Electrical conductivity measurements

Figure 6.7 shows electrical conductivity measurements for all the samples in the presence or absence of Pluronic BC. According to the final Pluronic content in the Pluronic-wrapped SWCNTs (see experimental section) the SWCNT wt % was recalculated for the series of samples containing Pluronic. Conductivity values are higher when using Pluronic-wrapped SWCNTs as reinforcement, particularly at low loading. Samples without Pluronic do not show a substantial increase in conductivity with increasing content of SWCNT until 0.5 wt% (~$1 \cdot 10^{-7}$ S/cm). However, Pluronic-containing nanocomposites reach the highest conductivity values at lower SWCNT wt% (1-2 wt % wrapped SWCNTs, equivalent to 0.7-1.4 wt % of bare acid-treated SWCNTs). The latter samples achieve conductivity values increased by about 7 orders of magnitude (as compared to the neat matrix) with a low effective amount of SWCNTs (<1 wt %).

Considering the percolation threshold defined by the universal percolation law[43] (where conductivity is proportional to the $(p - p_c)^t$ factor, for $p > p_c$, being p the filler fraction and p_c the threshold value) the application of percolation theory to both series of samples provides significantly different results. Conductivity values in both cases follow a similar trend, which can be fitted to the aforementioned scaling law (Figure 6.7, solid lines) but with very different threshold values. For Pluronic-wrapped SWCNT nanocomposites, an approximate percolation threshold of 0.03 wt % can be derived from curve fitting (with t = 2.35), whereas a value of 0.31 wt % is obtained for acid-treated SWCNT nanocomposites (t = 1.1). The series of samples with Pluronic-wrapped SWCNTs reached the electrical percolation threshold at the lowest filler loading, 0.1 wt % of Pluronic-wrapped SWCNTs, exhibiting a very sharp conductivity increase to $0.14 \cdot 10^{-8}$ S/cm. This conductivity represents an increase of 4.1 orders of magnitude with

[43] Stauffer, D.; Aharony, A. in Introduction to percolation theory. Taylor & Francis, London 1994.

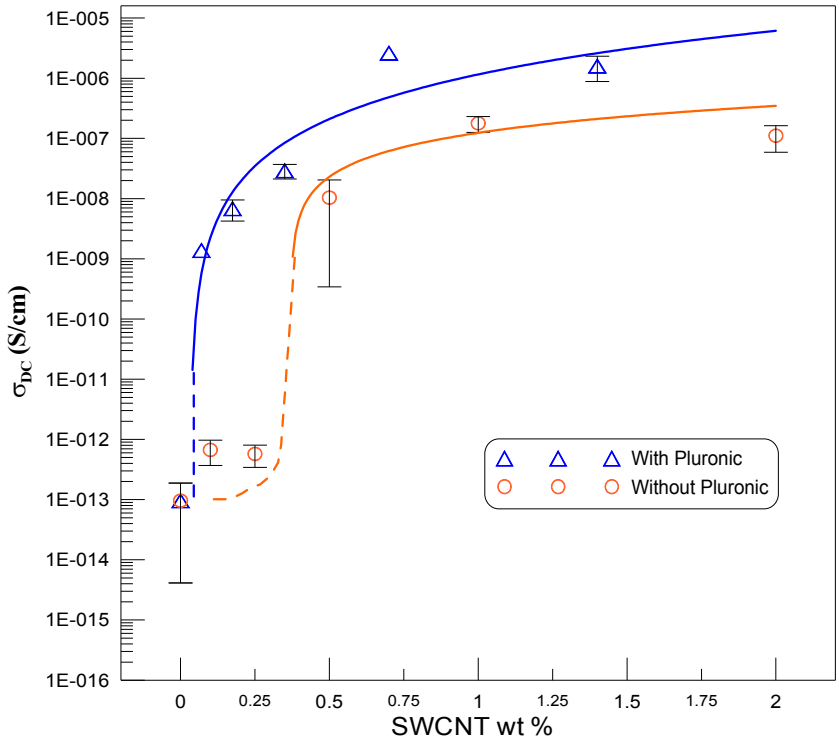

Figure 6.7. Electrical conductivity *vs*. SWCNTs actual content for samples containing acid treated and Pluronic-wrapped SWCNTs. Solid lines correspond to the percolation theory fitting. Dashed lines provide additional visual aid.

respect to the neat matrix, achieved with a very low effective content of SWCNTs (0.07 wt %) and a corresponding associated amount of BC (0.03 wt %).

This is comparable to the remarkable data reported by Liu et al.[44] who achieved an increase of 4.3 orders of magnitude in electrical conductivity by incorporating clay-dispersed SWCNTs (0.05 wt % SWCNTs and 0.2 wt % clay) into an epoxy matrix. In our system, it is necessary to go beyond 0.25 wt % of bare acid-treated SWCNTs in the binary composites to achieve the percolation threshold. The nitric acid purification applied promotes SWCNT compaction (manifested by a drastic reduction in the specific surface area[45]), becoming an obstacle to solvent-free dispersion into the epoxy matrix. This would explain the high percolation threshold and lower overall conductivity values.

[44] Liu, L.; Grunlan, J. C., Clay assisted dispersion of carbon nanotubes in conductive epoxy nanocomposites. *Adv. Funct. Mater.* 2007, *17* (14), 2343-2348.
[45] Martinez, M. T.; Callejas, M. A.; Benito, A. M.; Cochet, M.; Seeger, T.; Anson, A.; Schreiber, J.; Gordon, C.; Marhic, C.; Chauvet, O.; Fierro, J. L. G.; Maser, W. K., Sensitivity of single wall carbon nanotubes to oxidative processing: structural modification, intercalation and functionalisation. *Carbon* 2003, *41* (12), 2247-2256.

This latter data are also in agreement with the fact that chemically treated (in this case, oxidized) nanotubes show higher percolation thresholds, because of the functionalization process[46] that induces disruption of the conjugated electronic structure as well as length cutting (lower aspect ratio) of the nanotubes. In fact, this kind of oxidative treatment has been reported as one of the most harmful for electrical conductivities in epoxy nanocomposites.[47,48] It has been previously stated[49] that in a given epoxy system, there is a critical SWCNT aspect ratio value above which nanotubes disentanglement and the uniform distribution of individual nanotubes in the matrix are crucial, allowing the percolation threshold to vary several orders of magnitude. Below this limit, percolation threshold tends to increase rapidly with decreasing aspect ratio. Therefore, Pluronic wrapping on acid-treated SWCNTs counteracts this effect. Electrical conductivity measurements show how the Pluronic-wrapping dispersion method induces a more pronounced enhancement of properties (compared to acid-treated SWCNTs), particularly at the lowest loadings. This can be ascribed to the highly homogeneous distribution of disentangled SWCNTs across the matrix. Additionally there is a reduction of the needed amount of SWCNTs to reach the percolation threshold because of the presence of the BC.

AFM characterization

In Figure 6.8, topography and stiffness images are shown for two epoxy samples: epoxy + 0.6 wt% Pluronic and epoxy + 2wt% Pluronic-wrapped SWCNTs. Topography views (Figure 6.8a, c, e, g) depict the morphological features observed. The neat epoxy matrix (not shown) has a very smooth and regular surface. Incorporation of 0.6 wt % Pluronic leads to the formation of surface holes and a "peak-valley" topographic profile resulting from the BC micellar or vesicular nanostructures. The app-

[46] Gojny, F. H.; Wichmann, M. H. G.; Fiedler, B.; Kinloch, I. A.; Bauhofer, W.; Windle, A. H.; Schulte, K., Evaluation and identification of electrical and thermal conduction mechanisms in carbon nanotube/epoxy composites. *Polymer* 2006, *47* (6), 2036-2045.
[47] Kim, Y. J.; Shin, T. S.; Choi, H. D.; Kwon, J. H.; Chung, Y. C.; Yoon, H. G., Electrical conductivity of chemically modified multiwalled carbon nanotube/epoxy composites. *Carbon* 2005, *43* (1), 23-30.
[48] Spitalsky, Z.; Krontiras, C. A.; Georga, S. N.; Galiotis, C., Effect of oxidation treatment of multiwalled carbon nanotubes on the mechanical and electrical properties of their epoxy composites. *Composites: Part A* 2009, *40* (6-7), 778-783.
[49] Li, J.; Ma, P. C.; Chow, W. S.; To, C. K.; Tang, B. Z.; Kim, J. K., Correlations between percolation threshold, dispersion state, and aspect ratio of carbon nanotubes. *Adv. Funct. Mater.* 2007, *17* (16), 3207-3215.

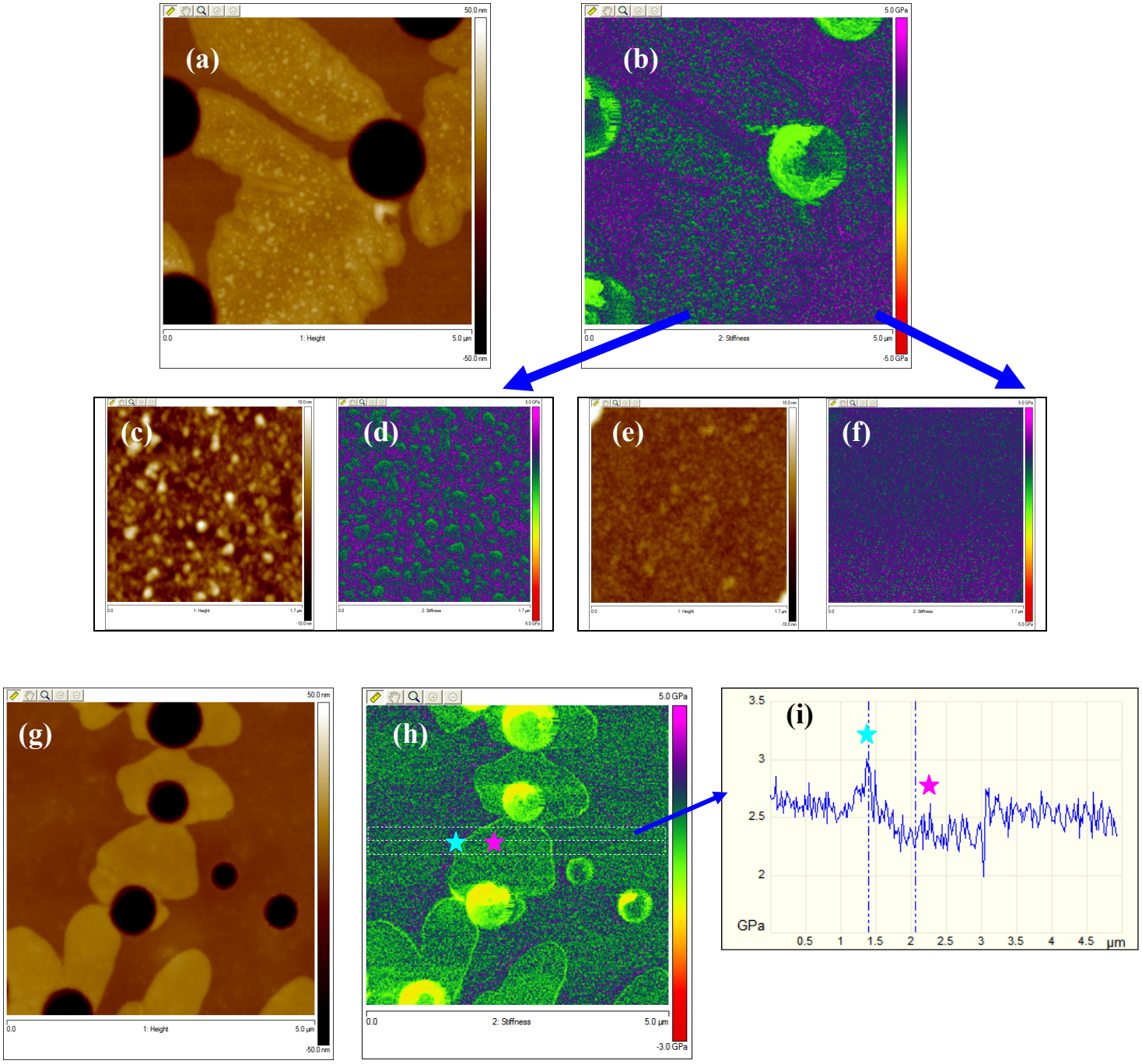

Figure 6.8. Topography images (a, c, e and g) and stiffness maps (b, d, f and h) for two samples: (a, b) Epoxy + Pluronic (0.6 wt%) sample; (c, d) high resolution scan of the patch area in Figure 6a,b; (e, f) high resolution scan of the area between patches in Figure 6a,b; (g, h) Epoxy + 2wt% Pluronic-wrapped SWCNTs sample; (i) cross-section profile along the line in Figure 6h.

earance of elevated patch areas next to deep valleys is observed as a consequence of this nanostructure formation (Figure 6.8a). The incorporation of Pluronic-wrapped SWCNTs shows similar overall topographic features as the epoxy + Pluronic sample, with the

formation of deep surface holes surrounded by patch areas, although with both features in smaller areas, and with less pronounced nanostructures (Figure 6.8g). The AFM stiffness mapping indicates that the neat epoxy possesses a very homogeneous profile (not shown), with high stiffness (~3 GPa).

The patches formed upon Pluronic addition (0.6 wt %) exhibit, on the average, a lower stiffness (~2.6 GPa, Figure 6.8d), while the areas between patches (Figure 6.8e, f) correspond to a stiffness closer to the neat matrix (~2.8 GPa, Figure 6.8f). The patch region seems to be a Pluronic-rich phase and experiences nanoscale separation into two components with different stiffness. A line profiling analysis of the patch region (not shown, but analogous to Figure 6.8i) reveals that the softer component has a stiffness of about 2.2 GPa, whereas the stiffer component is similar to the neat matrix (again ~2.8 GPa). Addition of SWCNTs (2 wt % Pluronic-wrapped) affects both the patch area and the area between the patches: the patch area becomes smaller, softer (overall similar to the soft component in the patches on the epoxy + Pluronic sample, ~2.3 GPa) and more homogeneous, as shown in Figures 6.8g and 6.8h.

At difference of the patch area, two more-or-less homogeneous phases coexist in the area between the patches (Figure 6.8h). One of these phases has comparable stiffness and surface structure to that of the neat epoxy; the other one has a stiffness value close to that of the patch area on the epoxy + Pluronic sample. However, the latter phase is not identical to the patches in Figure 6.8b, as can be concluded from the difference in the nanostructure. The three phases identified on this sample are discernible both in the imaged cross-section (Figure 6.8i) and in the stiffness map (Figure 6.8h). It seems that, on the sample with 2 wt % Pluronic wrapped-SWCNTs, the stiffest region forms some sort of band around the two softer regions.

AFM stiffness correlates with that obtained through the DMA technique. The neat epoxy matrix exhibits a stiffness value corresponding to its storage modulus (Figure 6.3a). The epoxy + Pluronic sample has a storage modulus of about 2 GPa, in good agreement with the AFM stiffness value, in particular with that of the nanostructured features contained within the patches. These nanostructures would dominate the macroscopic mechanical behavior of this sample. However, for Pluronic-

wrapped samples containing SWCNTs, the storage modulus (3 GPa) corresponds to the stiffness of the phase surrounding the patches, and is comparable to the neat matrix. In this case, this phase dominates the macroscopic mechanical behavior. Thus, the influence of Pluronic and Pluronic-wrapped SWCNTs on the dynamical mechanical properties was reasserted with the AFM measurements.

6.3.2. Pluronic-based Epoxy/SWCNT nanocomposites. Thermal properties

For the study of thermal features of epoxy nanocomposites with Pluronic-wrapped SWCNTs, a test sample containing 2 wt% filler was selected together with the corresponding reference samples. These samples have been prepared as stated in section 6.2.1 and can be summarized as follows (information in parenthesis indicate the nomenclature used hereafter): [27]

- Neat epoxy matrix (*Epoxy*)
- Nanocomposite sample containing 2 wt% of nitric acid-treated SWCNTs (*SWCNT/Epoxy*)
- Nanocomposite sample containing 2 wt% of Pluronic-wrapped SWCNTs (*Plu/SWCNT/Epoxy*)
- Epoxy matrix filled with the same amount of Pluronic contained in the former sample (*Plu/Epoxy*)

Table 6.2. Sample specifications for the thermal study of Pluronic-based epoxy/SWCNT nanocomposites

Sample Name	Type of SWCNTs	Filler ratio (wt%)	Amount of Pluronic (mg/gTGAP)
Epoxy	---	0	0
Plu/Epoxy	---	0	10
SWCNT/Epoxy	Acid treated	2	0
Plu/SWCNT/Epoxy	Pluronic wrapped	2	10

Representative SEM micrographs of the *Plu/SWCNT/Epoxy* and *Plu/Epoxy* samples are shown in Figure 6.9. The homogeneous distribution of the wrapped SWCNTs (indicated with arrows) can be clearly appreciated, and is considerably improved when compared to the dispersion of acid-treated SWCNTs, as previously reported (see figure 6.2). Spherical self-assembled morphologies of ≤ 1μm diameter can

be observed as a consequence of the BC presence. The epoxyphilic block volume ratio within Pluronic F68 would favour this microstructure, even at a low loading, which is consistent with the literature.[28,29] In this context, J. M. Dean and co-workers[29] found vesicular morphologies in an epoxy system filled with a PEO-based BC at low BC load-

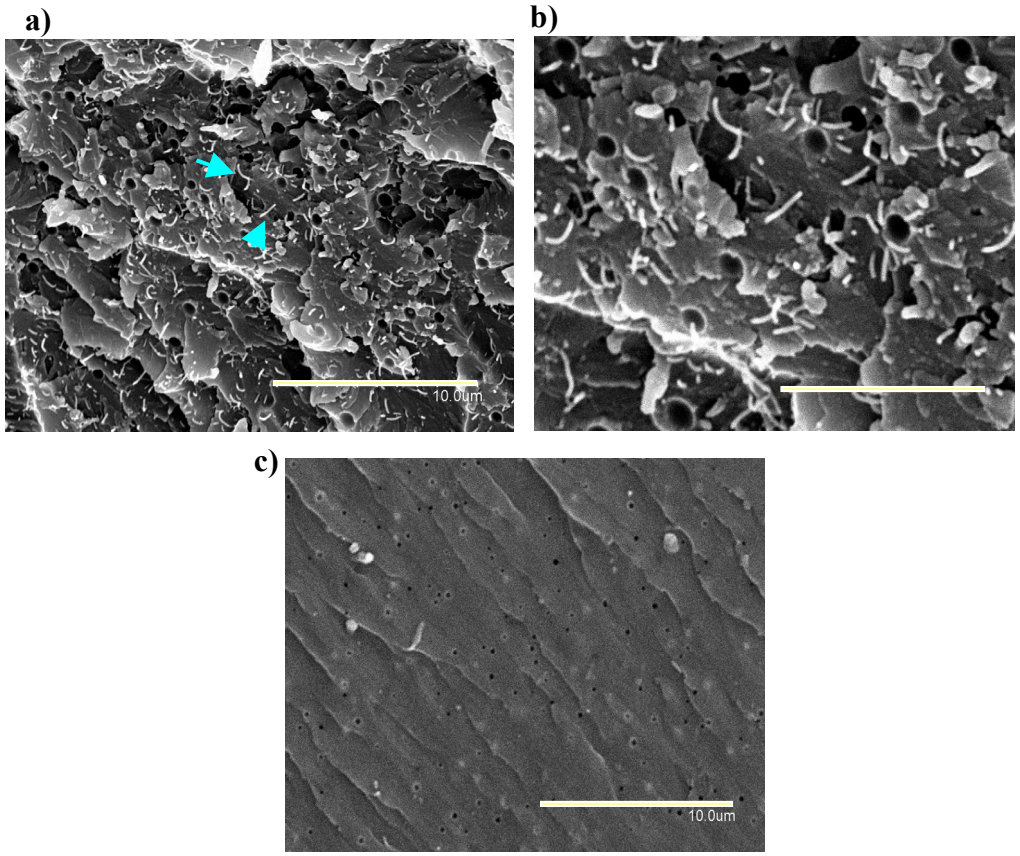

Figure 6.9. (a) SEM image of a *Plu/SWCNT/Epoxy* sample fracture surface. Scale bar = 10μm. Arrows point the filler ; (b) magnification of the central area in figure 1a. Scale bar = 4μm; (c) *Plu/Epoxy* sample fracture surface. Scale bar = 10μm

ing (2.5 wt%). These vesicles had a typical size of 0.6 μm which is nearly that observed in our nanocomposite sample, also with a very low BC content (0.6 wt% for Pluronic containing samples). These vesicles have a clear toughening effect, as was reported for many epoxy systems.[24,50] The presence of the BC and SWCNTs also affect the T_g values of the neat epoxy matrix as determined by DSC. The *Epoxy* sample has a T_g = 218.0 ºC. while *Plu/Epoxy*, *SWCNT/Epoxy*, and *Plu/SWCNT/Epoxy* samples exhibit a T_g value of 212.7, 220.9 and 200.7 ºC respectively. The presence of Pluronic, which acts as plastificant, decreased the T_g of the neat epoxy resin (as observed by other authors[32])

[50] Thompson, Z. J.; Hillmyer, M. A.; Liu, J.; Sue, H. J.; Dettloff, M.; Bates, F. S., Block Copolymer Toughened Epoxy: Role of Cross-Link Density. *Macromolecules* 2009, *42* (7), 2333-2335.

while the SWCNTs slightly increased the T_g probably due to restrictions in the mobility of the polymeric chains.[34] When wrapped SWCNTs are present (*Plu/SWCNT/Epoxy* sample) the T_g decreased even more than in the *Plu/Epoxy* sample and the microstructure (Figure 6.9a and 6.9b) exhibits differences in vesicles sizes, when compared to the *Plu/Epoxy* sample (Fig. 6.9c).

Figure 6.10 shows TGA plots at a heating rate of 10ºC/min. As expected, the nanocomposite samples behave differently in the presence of oxidative (air) or inert (N_2) atmospheres. Figure 6.10 also shows differential thermograms (dTG) for both environments. There is a weight loss at around 385ºC under inert atmosphere, which is also visible under air, where the maximum weight loss shifts by ~10ºC to lower temperatures. The similarity between the peaks suggests that the same thermal process is occurring in both cases. However, the higher complexity in air, manifested by several associated shoulders, provides evidence to suggest that this thermal process is partly overlapped with an oxidative reaction. The mass loss observed by TGA supports this premise since in air the second process starts when the weight loss is lower than that corresponding to the end of the thermal process in inert atmosphere. The second weight loss, only observed under air, can be associated with an oxidative step leading to the almost complete consumption of the epoxy matrix. These observations are in agreement with previously reported work for other epoxy systems.[51,52]

Table 6.3 shows some data drawn from the aforementioned thermograms (10ºC/min). The T_5 parameter represents the temperature at which the material has experienced 5% weight loss and is a useful value for the estimation of the thermal stability. Under air atmosphere, T_5 is increased by adding SWCNTs, Pluronic or Pluronic-wrapped SWCNTs to the resin. Under N_2 atmosphere, the Pluronic BC causes a reduction in the thermal stability of the epoxy, with a decrease in T_5 of 8.8ºC in the *Plu*/*Epoxy* sample. This is also observed in the presence of Pluronic-wrapped SWCNTs (*Plu/SWCNT/Epoxy* sample) with respect to the non-wrapped SWCNTs (*SWCNT/Epoxy* sample). These decreases correlate with the decrease observed previously in the T_g values determined by DSC.

[51] Lin, S. T.; Huang, S. K., Thermal degradation study of siloxane-DGEBA epoxy copolymers. *Eur. Polym. J.* 1997, *33* (3), 365-373.
[52] Liu, Y. F.; Du, Z. J.; Zhang, C.; Li, H. Q., Thermal degradation of bisphenol-A type novolac epoxy resin cured with 4,4 '-diaminodiphenyl sulfone. *Int. J. Polym. Anal. Charact.* 2006, *11* (4), 299-315.

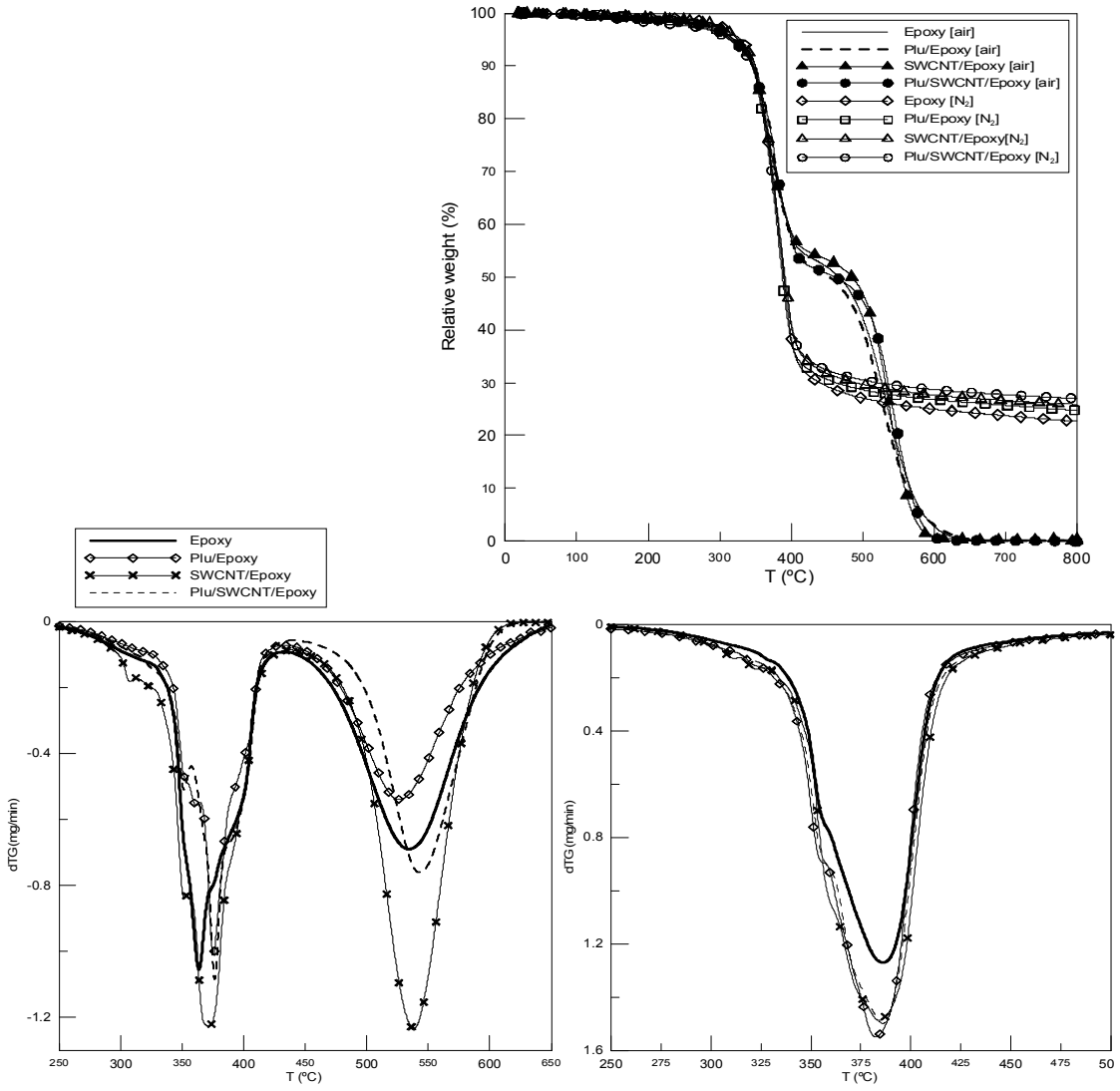

Figure 6.10. TG (above) and dTG plots (below) of the studied samples at 10ºC/min. dTG plots are represented under air (below left) and N_2 (below right) atmospheres.

The temperature of the maximum rate of weight loss (T_{max}) is another parameter associated to thermal stability. The observed T_{max} is the highest for the *Plu/SWCNT/Epoxy* sample in air (both peaks), surpassing effects due to Pluronic or SWCNTs. This is specially relevant considering that, owing to the presence of BC in the filler composition (30 wt%), 2 wt% of Pluronic-wrapped SWCNTs contains a lower effective amount of nanotubes than 2 wt% of acid-treated SWCNTs.

Table 6.3. Temperature and residue data from different TGA experiments at 10ºC/min. T_5 = Temperature in which a 5% of degradation has occurred; T_{max} = Temperature of maximum loss rate; R_{700} = residue at 700ºC.

Sample	Air atmosphere				N_2 atmosphere			
	T_5 (ºC)	T_{max} 1 (ºC)	T_{max} 2 (ºC)	R_{700} (wt%)	T_5 (ºC)	T_{max} (ºC)	R_{700} (wt%)	OI (%)
Epoxy	314.3	363.7	533.9	0.1	328.8	386.3	23.7	26.7
Plu/Epoxy	319.8	375.7	526.1	0.1	320.0	382.5	25.7	27.3
SWCNT/Epoxy	320.5	371.0	536.4	0.3	325.6	384.1	26.6	27.8
Plu/SWCNT/Epoxy	317.0	376.5	543.3	0.1	313.8	386.1	27.7	28.3

According to the literature, the most plausible reason for the thermal stabilization seems to be the improved SWCNT dispersion resulting from the polymer wrapping. Well-dispersed nanotubes may hinder the degradation process thus delaying the degradation reaction, since the fraction of the polymer matrix intimately surrounding nanotubes may degrade at a slower rate provoking a shift of T_{max} to higher values.[3] A better filler distribution would promote the heat dissipation within the nanocomposite and thus delay its degradation.[53]

The parameter R_{700} corresponds to the residue remaining at 700ºC. The R_{700} values under air are very low and the differences between samples are insignificant. The R_{700} parameter in N_2 increases when SWCNTs or Pluronic are incorporated into the epoxy. The *Plu/SWCNT/Epoxy* sample has the highest value among the samples studied.

The N_2 (char) residues are useful parameters for the study of flame retardant ability of the composite material since they can be easily correlated with the Oxygen Index (OI) through the empirical equation derived by D. W. van Krevelen[54] (see section 5.3.1). The limiting OI is defined as the minimum amount of oxygen needed in a nitrogen-oxygen (air) mixture to maintain combustion after ignition. A material may be considered flammable when OI is ≤ 26%, and TGA in inert atmosphere provides the necessary data to calculate OI. In table 6.3, OI data for the different prepared samples are exhibited. The neat resin sample is non-flammable but remains at the borderline

[53] Huxtable, S. T.; Cahill, D. G.; Shenogin, S.; Xue, L. P.; Ozisik, R.; Barone, P.; Usrey, M.; Strano, M. S.; Siddons, G.; Shim, M.; Keblinski, P., Interfacial heat flow in carbon nanotube suspensions. *Nat. Mater.* 2003, *2* (11), 731-734.
[54] van Krevelen, D. W., Some basic aspects of flame resistance of polymeric materials. *Polymer* 1975, *16* (8), 615-620.

between flammability and non-flammability. Both additives, Pluronic and SWCNTs, improve this parameter. The sample containing Pluronic-wrapped SWCNTs (*Plu/SWCNT/Epoxy*) manifests the maximum OI value. The integration of SWCNTs by prior dispersion in Pluronic allows an improvement in the epoxy resin thermo-oxidative resistance with a substantial lower filler concentration. For example, in our case the addition of such small amounts of SWCNTs to an epoxy resin has improved the OI parameter in a ratio that other authors have reported with amounts of ≥ 10 wt% of siloxane oligomer[51] or a combination of carbon-fibre and organic phosphate hardener (2.6wt% P).[55] In the aerospace industry, in which this epoxy system could be employed, the reported results provide important insights into the stability in different environments, such as enhanced fire resistance and the reduction of thermal ageing.

Degradation kinetics study

The advanced isoconversional method (AIM) kinetic calculations (see section 4.3) were carried out with TGA data from both inert and oxidative atmospheres and the obtained data are plotted in Figure 6.11. The average AE value in inert atmosphere (approximately 230 kJ/mol) is perfectly consistent with AE data reported for thermal cleavages of other epoxy systems.[56] In the early stages of the thermal process (up to 30% conversion, approximately) a dependence of AE with α for all samples is observed. The AE of the *Plu/Epoxy* sample shows the lowest value (40 kJ/mol below the others) at α between 10-40%, which is in agreement with the T_5 and T_{max} decrease from the *Epoxy* to the *Plu*/*Epoxy* sample in TGA (see table 6.3). The incorporation of Pluronic-wrapped SWCNTs into the TGAP+DDS epoxy resin (*Plu/SWCNT/Epoxy* sample) produces an increase of AE, indicating higher thermal resistance in the range of 50-90% α. For all the samples, the latest stage of the thermal process shows a significant increase in the AE during the formation of the thermal residue. The most thermally resistant residue is that of the *Plu/SWCNT/Epoxy* nanocomposite, which exhibits the highest AE values in the α range of 90-100%.

[55] Braun, U.; Balabanovich, A. I.; Schartel, B.; Knoll, U.; Artner, J.; Ciesielski, M.; Doring, M.; Perez, R.; Sandler, J. K. W.; Altstadt, V.; Hoffmann, T.; Pospiech, D., Influence of the oxidation state of phosphorus on the decomposition and fire behavior of flame-retarded epoxy resin composites. *Polymer* 2006, *47* (26), 8495-8508.

[56] Montserrat, S.; Malek, J.; Colomer, P., Thermal degradation kinetics of epoxy-anhydride resins: II. Influence of a reactive diluent. *Thermochim. Acta* 1999, *336* (1-2), 65-71.

Figure 6.11b shows AIM plots for thermal cleavage under air atmosphere. The first TGA weight loss (solid lines) exhibits a strong AE dependence with α, consistent with a complex multi-step process. Average AE values are noticeably lower than those of the thermal process under inert atmosphere, and consistent with AE data reported for

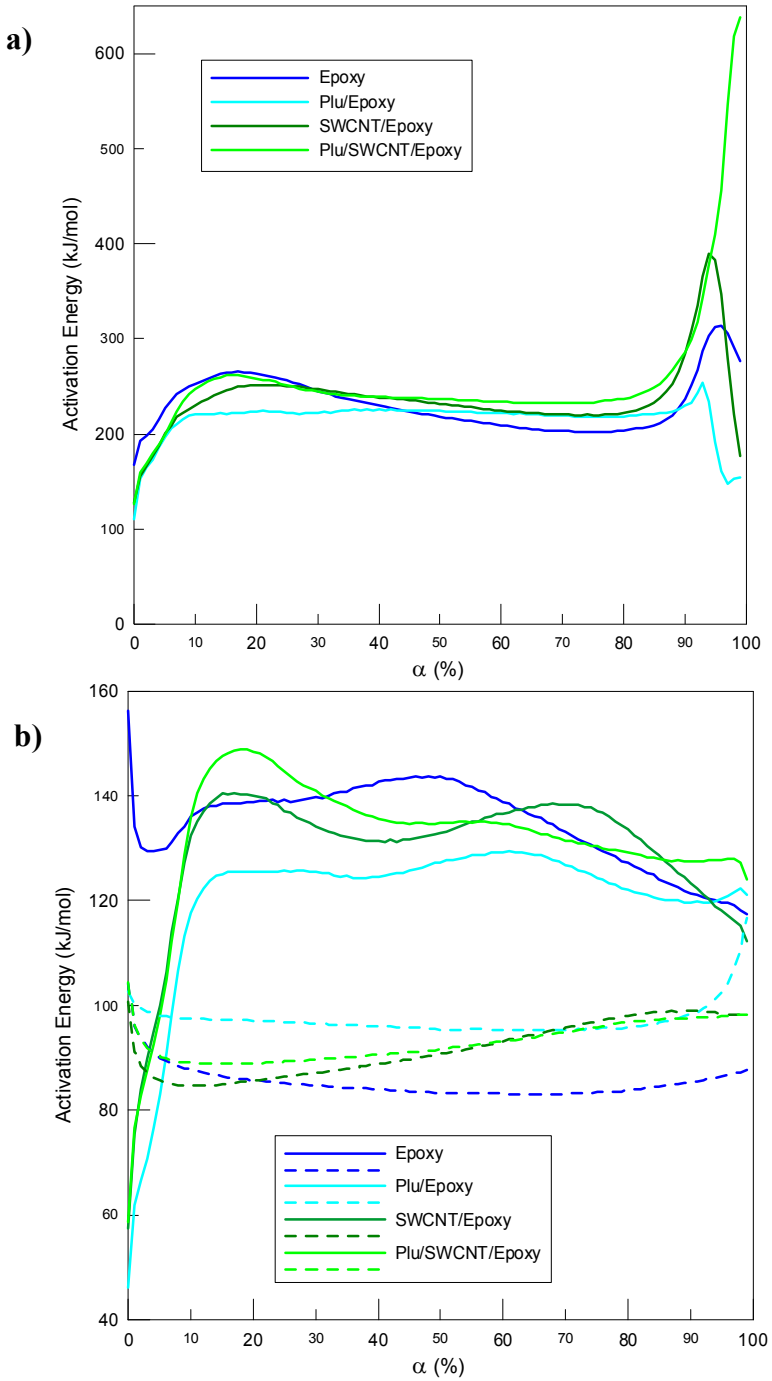

Figure 6.11. AIM plots for all samples applied to the TGA data in N_2 (a) and air (b) data. AIM plots in air are applied in the first (solid lines) and the second (dashed lines) TGA weight losses.

other epoxy systems in similar conditions.[57] Up to 10% α the plots show a pronounced linear AE dependence on α for *Plu*/*Epoxy*, *SWCNT/Epoxy* and *Plu/SWCNT/Epoxy* samples and AE values are lower than those of the *Epoxy* sample. The AE for the *Plu/SWCNT/Epoxy* sample is the highest (≈10 kJ/mol higher) in the range of 10-30% α, which points to an enhanced thermo-oxidative stability at low α in accordance to the increase in T_5 and $T_{max}1$ (Table 6.3). For the second TGA weight loss, Figure 6.11b (broken lines) average AE values are lower than those of the first TGA weight loss. For samples without SWCNTs, steady AE versus α profiles are observed that stand for a single-step process. Samples containing SWCNTs show a slight linear dependence on AE with α indicating differences in the cleavage mechanism. The *Plu/Epoxy* sample shows the highest AE in the second oxidative steps, whereas it shows the lowest AE in the first step.

The information from all the plots in Figure 6.11 can be summarized as follows. The thermal cleavage of TGAP+DDS epoxy system under inert atmosphere and in presence of Pluronic, SWCNTs or both together is mechanistically similar, with higher AE values for the *Plu/SWCNT/Epoxy* sample at the highest α values. Under air atmosphere, the first weight loss indicates a complex multi-step process, the mechanism of which is slightly different when adding Pluronic and/or SWCNTs. The *Plu/SWCNT/Epoxy* sample exhibits the highest AE in the range of 10-30% α. In the second oxidative step, both additives increase the AE values for α higher than 20 %.

TPD-MS was applied to all samples to identify the evolved products during the degradation process. In this case, the inert environment selected was argon and the oxidative medium synthetic air (O_2+Ar, in the same ratio as natural air). The choice of argon instead of N_2 was made in order to prevent interferences in the mass detection of the CO molecule (both with peaks at m/z = 28). A continuous qualitative monitoring of specific m/z values was carried out in all the experiments.

Figure 6.12 shows the evolved species under Ar atmosphere for the *Plu/SWCNT/Epoxy* sample. The first evolved species are CO, CO_2 and OH (m/z = 28,

[57] Budrugeac, P.; Segal, E., Application of isoconversional and multivariate non-linear regression methods for evaluation of the degradation mechanism and kinetic parameters of an epoxy resin. *Polym. Degrad. Stab.* 2008, *93* (6), 1073-1080.

44 and 17 respectively) indicating that the loss of oxygen is responsible of the first degradation step. The maximum signal temperatures (T_{ms}) observed for the three oxygenated species are between 330 and 400ºC. The second degradation step is related to the evolution of nitrogenated species NH_2, NO and N_2O (m/z = 16, 30 and 44, respectively). Finally the species evolved at the highest temperatures are the S species H_2S, SO and SO_2 (m/z = 34, 48 and 64, respectively). These data indicate that the degradation mechanism progresses through a continuous loss of oxygen, which gives rise to the loss of carbon, then nitrogen and finally sulphur species.

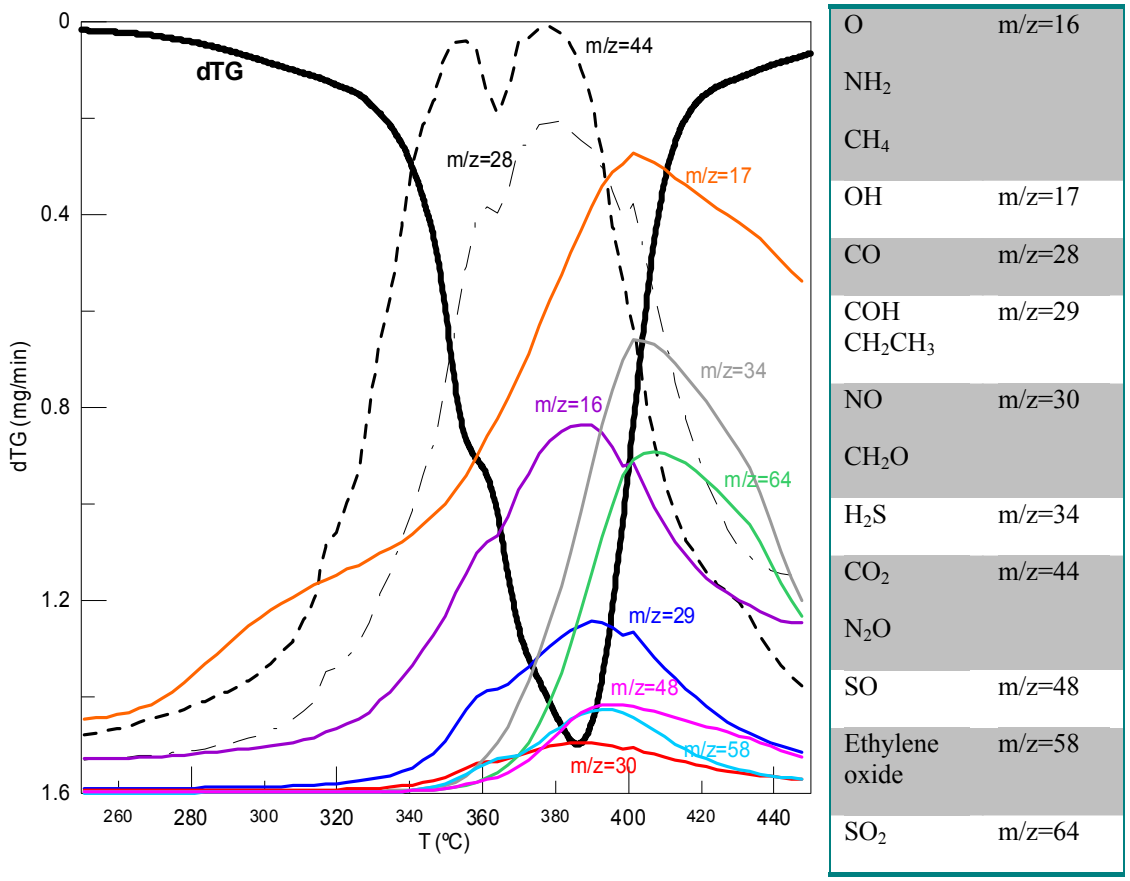

Figure 6.12. TPD-MS plots for *Plu/SWCNT/Epoxy* sample heated at 10ºC/min under argon atmosphere compared with its corresponding TGA peak.

The maximum signal temperature (T_{ms}) of CO (m/z = 28) and CO_2 (m/z = 44) evolved during the dynamic heating decreases in the samples containing Pluronic (Fig. 6.13), thus indicating the lower thermal stability of these samples. This is in agreement with the TGA data under inert environment. There are no significant differences regarding the aromatic moieties detected by MS, the phenyl (m/z = 78) and aniline

species (m/z = 91) evolve at similar temperatures in all the samples, suggesting that there are no noticeable effects of either Pluronic or SWCNTs in their formation.

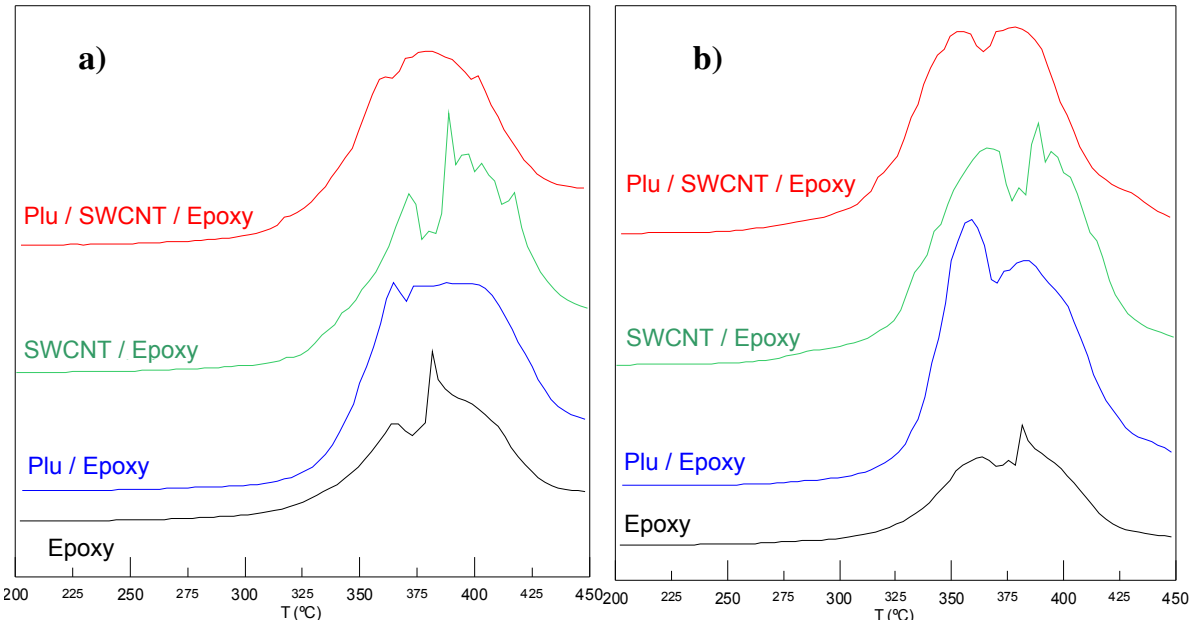

Figure 6.13. TPD-MS plots under Ar atmosphere: a) CO and b) CO_2 qualitative monitoring.

The cleavage mechanism under air shows a more complex pattern as discussed earlier. The different monitored species in both degradation processes are shown in Figures 6.14a, b and c. The second dTG peak is mainly governed by the formation of CO and CO_2 species (Figure 6.14a); the rest of the monitored evolved species display considerably lower concentration. Under air, the first observed species are CH_3, CH_2CH_3, and CH_2O (m/z = 15, 29 and 30, respectively) generated from the degradation of the aliphatic chains that possess a lower thermal stability. These species were detected from 320ºC and above. In the $T_{max}1$ range, oxygenated, nitrogenated and sulphur containing species are evolved. All these species were detected in the interval between 340-400ºC. The degradation of the nanocomposites is initiated firstly in the aliphatic parts passing later to the rest of the structure (oxygen peak at m/z = 17; nitrogen peak at m/z = 30; sulphur peaks at m/z = 34, 48, 64), being these species evolved at similar temperatures.

In the second TGA peak the CO and CO_2 formation is predominant, as mentioned earlier. Nevertheless other minor species are observable at approximately 550ºC such as COH, NO, NO_2, SO and SO_2 (m/z = 29, 30, 46, 48 and 64 respectively). The oxidation of the residue produced in the first peak is responsible for the formation of these species. It should be mentioned that NO and NO_2 were perfectly observed at these temperatures under air atmosphere due to the presence of oxygen in the reactive environment. These molecules possessed the highest T_{ms} of all the measured species.

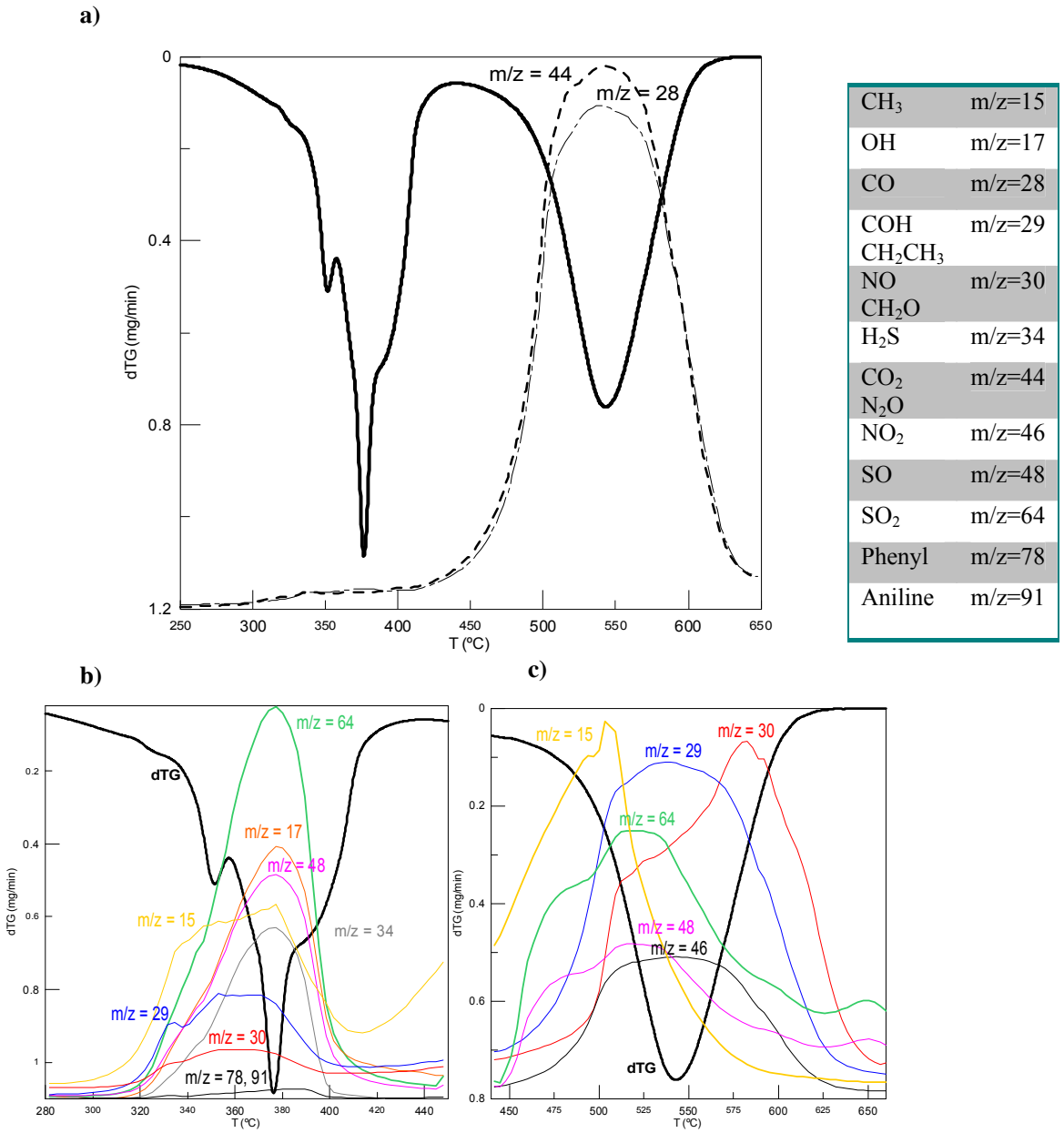

Figure 6.14. TPD-MS plots for *Plu/SWCNT/Epoxy* sample heated at 10ºC/min under synthetic air atmosphere and compared with its corresponding TGA peaks in air: a) CO and CO_2 qualitative monitoring; b) and c) show other species also qualitatively monitored, covering different ranges of temperature.

The presence of Pluronic decreases the T_{ms} of both CO and CO_2 released, while SWCNTs increase these temperatures, indicating a thermo-oxidative stability enhancement of the samples owing to the SWCNTs (Fig. 6.15a and b). It is worth mentioning that this effect is even more noticeable when wrapped SWCNTs are incorporated, indicating a better transfer of properties owing to improved distribution in the matrix. This supports the TGA data, regarding the increase of $T_{max}2$ peak value for *Plu/SWCNT/Epoxy* sample. The same positive effect is observed when SO and SO_2 are monitored (Fig. 6.15c and d). Both SWCNTs and wrapped SWCNTs increase the T_{ms} at which they are released, indicating higher thermal stability of the samples containing nanotubes.

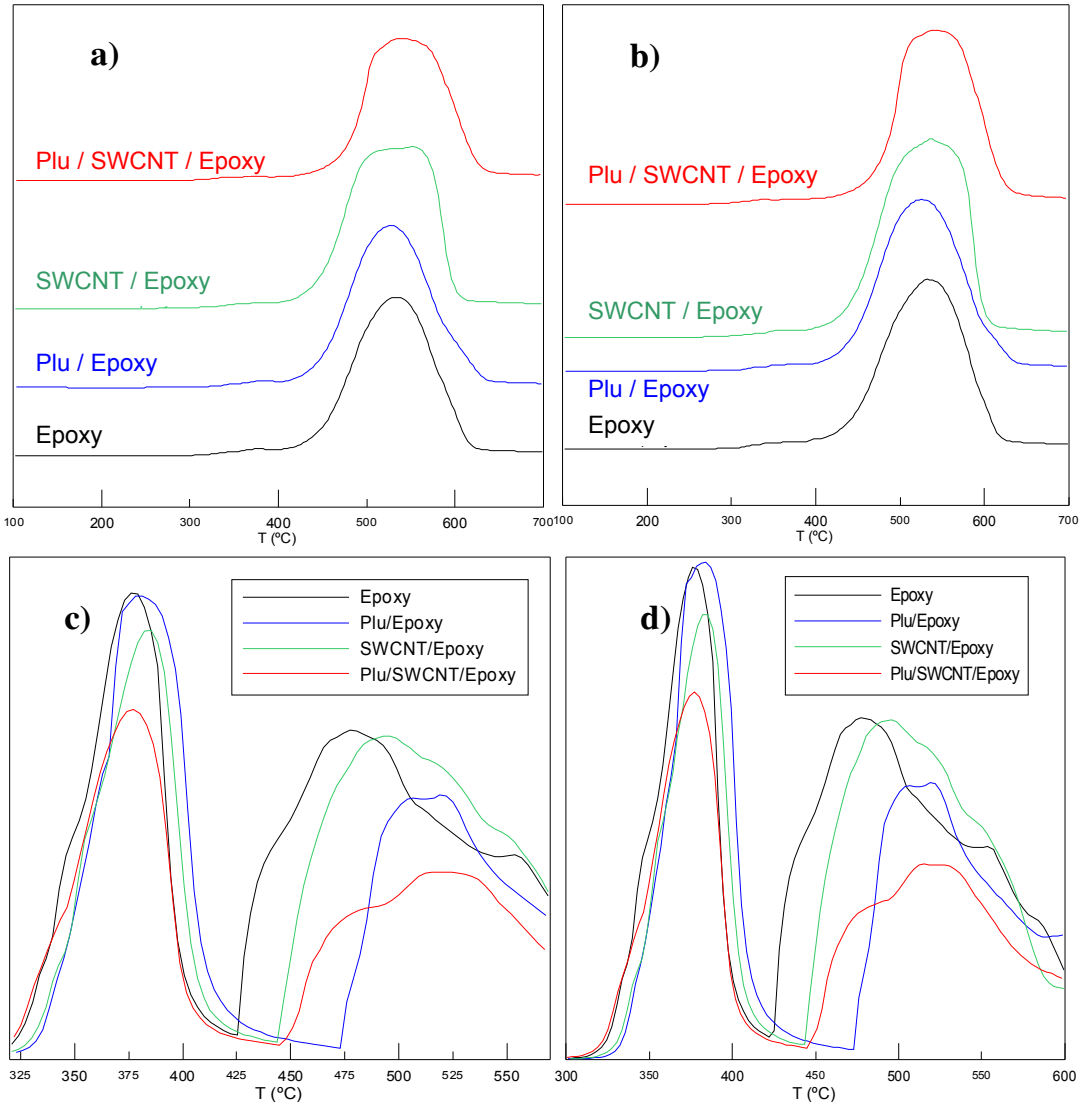

Figure 6.15. TPD-MS plots under synthetic air: a) CO, b) CO_2, c) SO and d) SO_2 qualitative monitoring

Although the degradation mechanism is very complex (particularly when air is present) the monitoring of the released species during the different TPDs showed that samples containing SWCNTs have an improved thermo-oxidative stability with respect to the neat resin and samples containing wrapped SWCNTs showed the most enhanced thermo-oxidative performance of all the samples studied. This is a clear indication of the positive effect of SWCNT wrapping on the thermal behavior of these nanocomposites in air environment.

In addition to identify the evolved gases and to give us some insight into the degradation mechanism, the cleavage reactions were monitored by infrared spectroscopy, studying the solid residues generated during controlled heating experiments. As an example, Figures 6.16a and b show the infrared spectra of *SWCNT/Plu*/*Epoxy* and *Plu/Epoxy* samples, after heat treatment in N_2 at three temperatures around T_{max}. A more expanded representation of the features in the IR spectra is presented in Figure 6.17. A number of common features can be observed that are associated to characteristic vibrational bands[58] in the composite. Evidence of a progressive loss of oxygen was observed by the decrease in intensity of bands correspo-

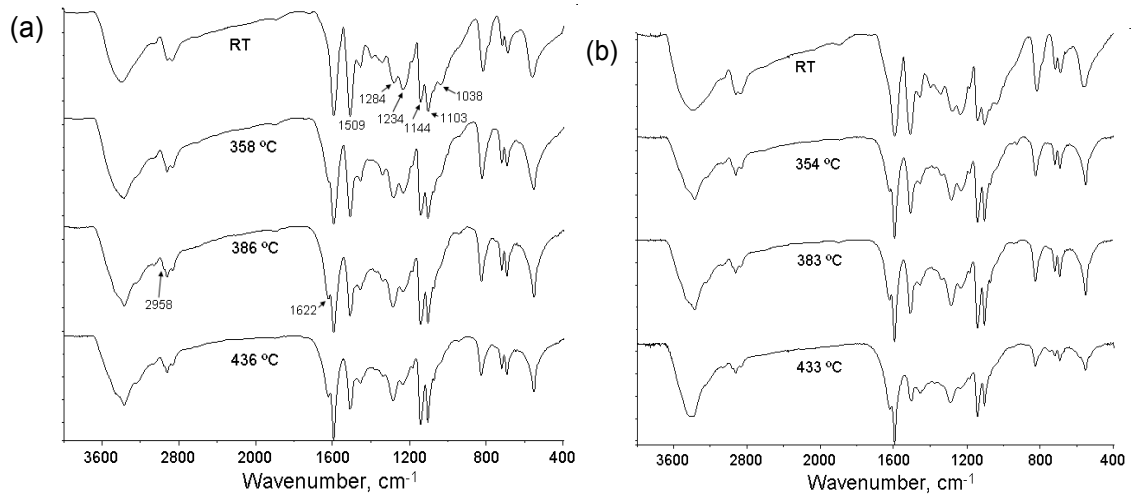

Figure 6.16. FTIR spectra (transmittance units) for different residues during thermal treatments: a) *Plu/SWCNT/Epoxy* sample solid residues extracted at the indicated temperatures during a thermal treatment under N_2 at 10ºC/min; b) *Plu*/*Epoxy* sample solid residues extracted at the indicated temperatures during a thermal treatment under N_2 at 10ºC/min.(Scale change at 2000 cm^{-1}).

[58] Colthup NB, Daly LH, Wiberley SE in Introduction to Infrared and Raman Spectroscopy, 3rd Edn., Academic Press, London 1990.

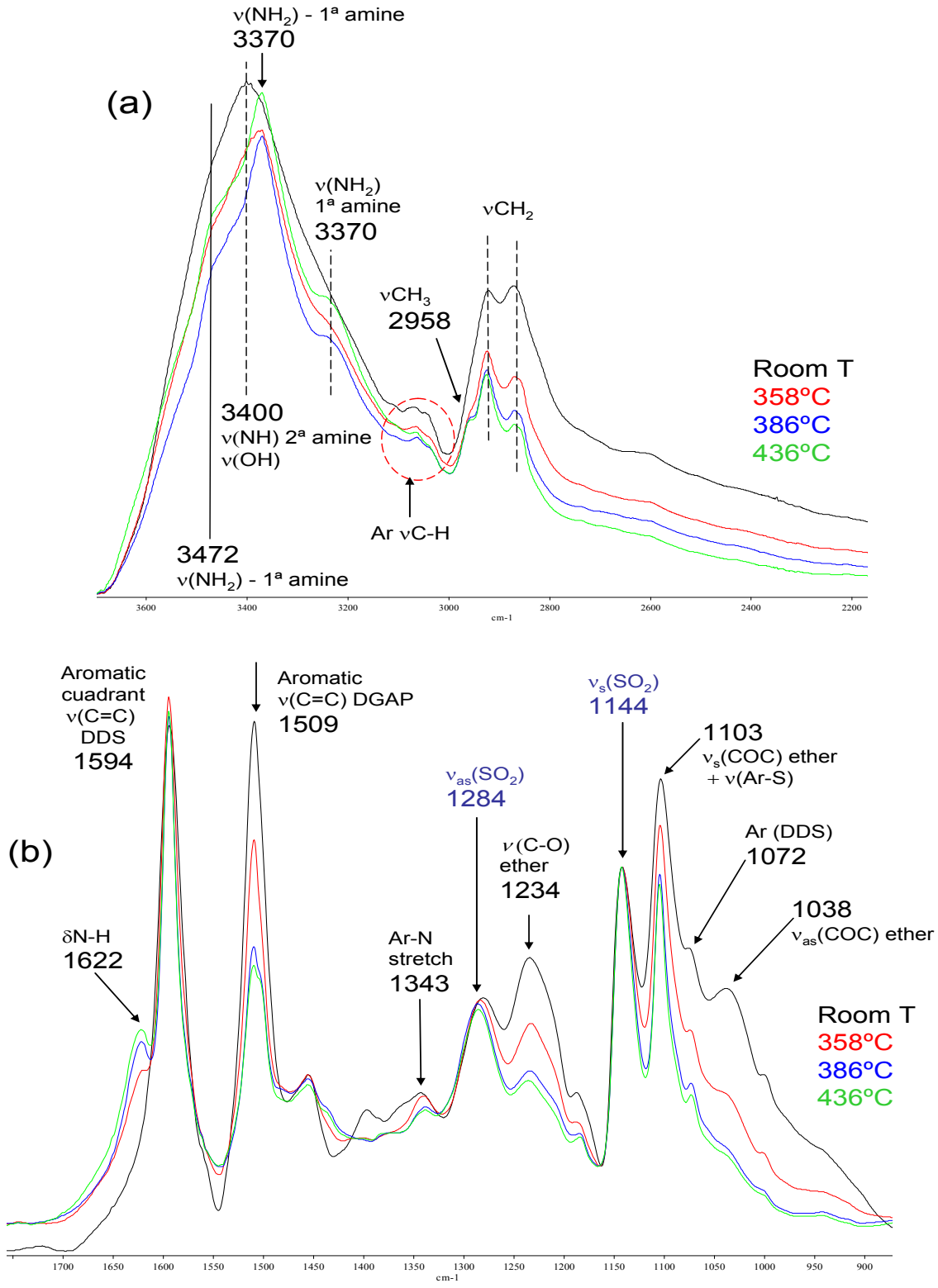

Figure 6.17. Infrared spectra (in Absorbance units) for *Plu/Epoxy/SWCNT* sample corresponding to Figure 6.15a, with details of band assignments expanded for the ranges (a) 3700 – 2200 cm^{-1}, and (b) 1800 – 900 cm^{-1}.

nding to ether moieties at around 1234 and 1038 cm^{-1}. Some aromatization of the sample was also observed by the sharpening of the 1594 cm^{-1} band, characteristic of polycondensed aromatic systems. In contrast, the aromatic ring mode at 1509 cm^{-1}, associated with TGAP[59] also decreased as the degradation progressed, suggesting that within the epoxy network the chain segments formed by DDS units appear to be more stable than those formed by TGAP units. We also observed that the strong band at around 1103 cm^{-1} experienced a progressive decrease, manifested by the reduction in its relative intensity compared to the bands at 1144 and 1284 cm^{-1} band, assigned to the symmetric and asymmetric SO_2 stretching modes, respectively.[59] Whilst the overall intensity of the 1103 cm^{-1} band certainly includes a significant contribution from the aryl–S stretching vibration, it also overlaps with the symmetric C–O–C stretching mode of the ether group whose contribution decreases as the degradation progresses, along with that of the previously mentioned asymmetric C–O–C stretching mode at 1038 cm^{-1}.

The sustained relative intensity of the SO_2 stretching modes compared to those of the aromatic ring vibrations suggests minimal Aryl–S cleavage and the retention of most of the sulfone groups, which is in agreement with other authors that have reported a slow degradation rate for DDS aromatic ring moieties.[60] Indeed, it is well known that sulfone moieties in aromatic polymers have excellent thermal stability. Some evidence for the formation of methyl groups was also detected by the appearance of a characteristic C-H stretching mode at around 2958 cm^{-1}. Likewise, the formation of amine groups is suggested by the progressive growth of the 1622 cm^{-1} band, corresponding to a N-H bending mode, and the sharpening of the heavily overlapped N-H stretching modes (~3400 cm^{-1}) typically observed for primary amines. The generation of amine moieties would be consistent with cleavage at the oxygen atoms originating from the initial epoxide and ether functional groups in the TGAP monomer.

Summarizing, Pluronic-wrapped SWCNTs have a positive effect on the thermal and thermo-oxidative performance of the epoxy, beyond the effect of acid-treated SWCNTs. The kinetic study based on Vyazovkin's AIM revealed the highest AE values

[59] Carrasco, F.; Pages, P.; Lacorte, T.; Briceno, K., Fourier transform IR and differential scanning calorimetry study of curing of trifunctional amino-epoxy resin. *J. Appl. Polym. Sci.* 2005, *98* (4), 1524-1535.
[60] Musto, P.; Ragosta, G.; Russo, P.; Mascia, L., Thermal-oxidative degradation of epoxy and epoxy-bismaleimide networks: Kinetics and mechanism. *Macromol. Chem. Phys.* 2001, *202* (18), 3445-3458.

for *Plu/SWCNT/Epoxy* sample in N_2 during the latter stages of the thermal cleavage. Likewise, in air atmosphere AE increases at low to medium conversions. TPD-MS profiles showed a delay in the evolution of the main molecular species, such as carbon or sulphur oxides for *Plu/SWCNT/Epoxy* sample, consistent with its higher thermo-oxidative stability. IR spectroscopy helped in elucidating the degradation mechanism in both oxidative and inert atmospheres.

6.3.3. Diblock copolymer-based Epoxy/SWCNT nanocomposites

The incorporation of diblock copolymer-wrapped SWCNTs into the epoxy system allowed the preparation of nanocomposite materials with improved properties. A series of nanocomposite samples were prepared, containing as-grown SWCNTs wrapped in PEO-*b*-PPO or PEO-*b*-PE, and [ox]-SWCNTs wrapped in PEO-*b*-PE. For comparative purposes, different reference samples were manufactured and character-rized.

Mechanical properties

Results from DMA characterization are shown in Figure 6.18 and 6.19. As in previous trials, it is visible that the preparation procedure (the sonication and heating) induces some damage to the parent matrix. In general, diblock copolymers induce a plastic behavior to the epoxy since storage moduli and T_g values experience a significant decrease as compared to the neat matrix (and apparently independent on the BC amount in the studied range). However, wrapped SWCNTs are able to compensate for this effect, leaving the moduli and T_g values comparable to that of the neat matrix, or even surpassing the matrix values at medium-low loadings (in the case of PEO-*b*-PE). Despite nanocomposites with bare SWCNTs exhibit higher storage moduli in some cases (especially at higher loadings), those achieved for wrapped SWCNTs are fairly high for a non-covalent approach, particularly considering the incorporation of a BC with a strong plasticizing effect.

The mechanical characterization was fulfilled with tensile (stress-strain) measurements, which are shown in table 6.4, for all nanocomposite and reference samples with 0.5 wt% SWCNTs and/or the corresponding associate amount of BC. The

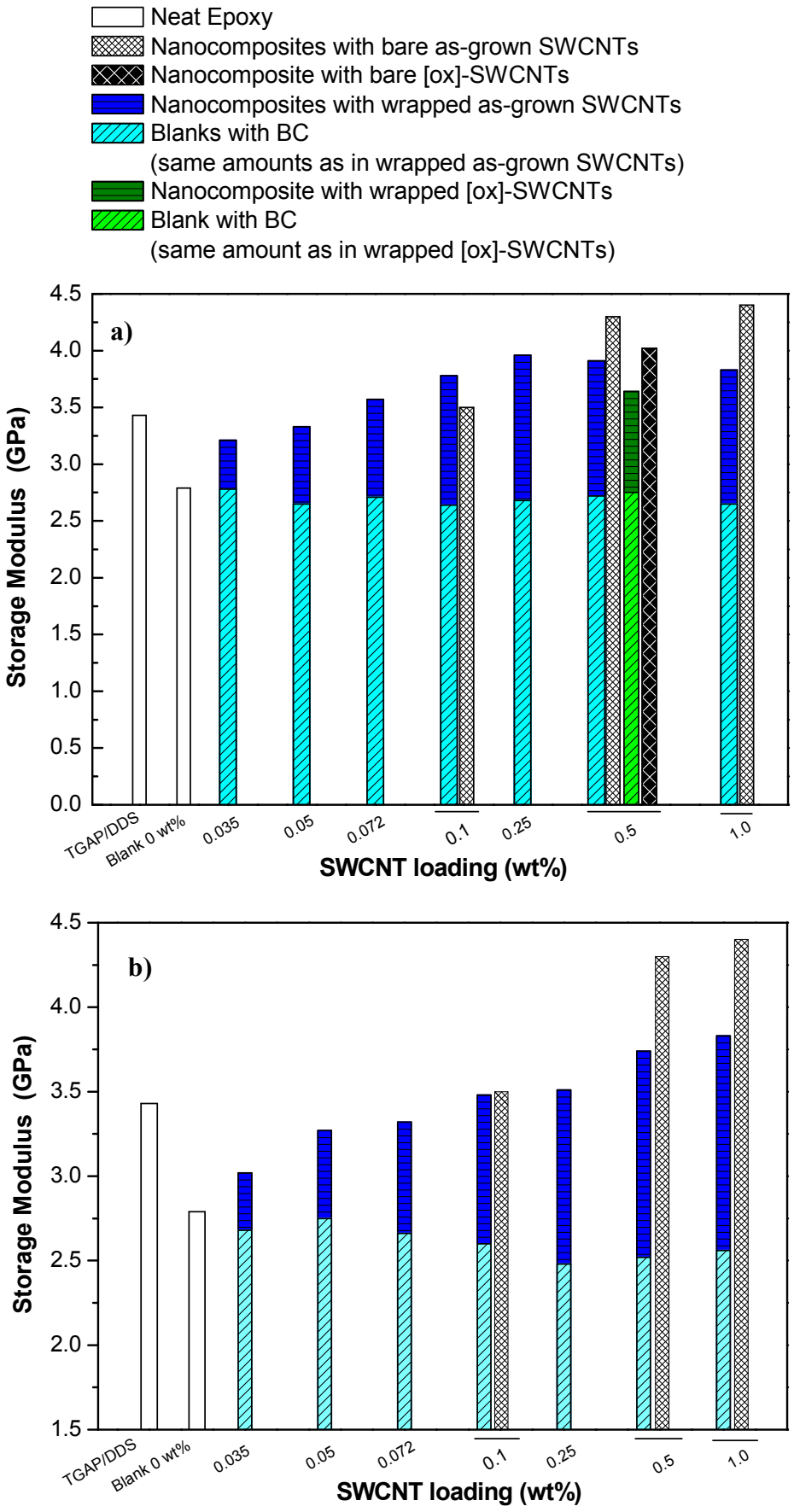

Figure 6.18. Storage modulus data (room temperature, 1Hz) for the different nanocomposite and reference samples based on a) PEO-*b*-PE, and b) PEO-*b*-PPO.

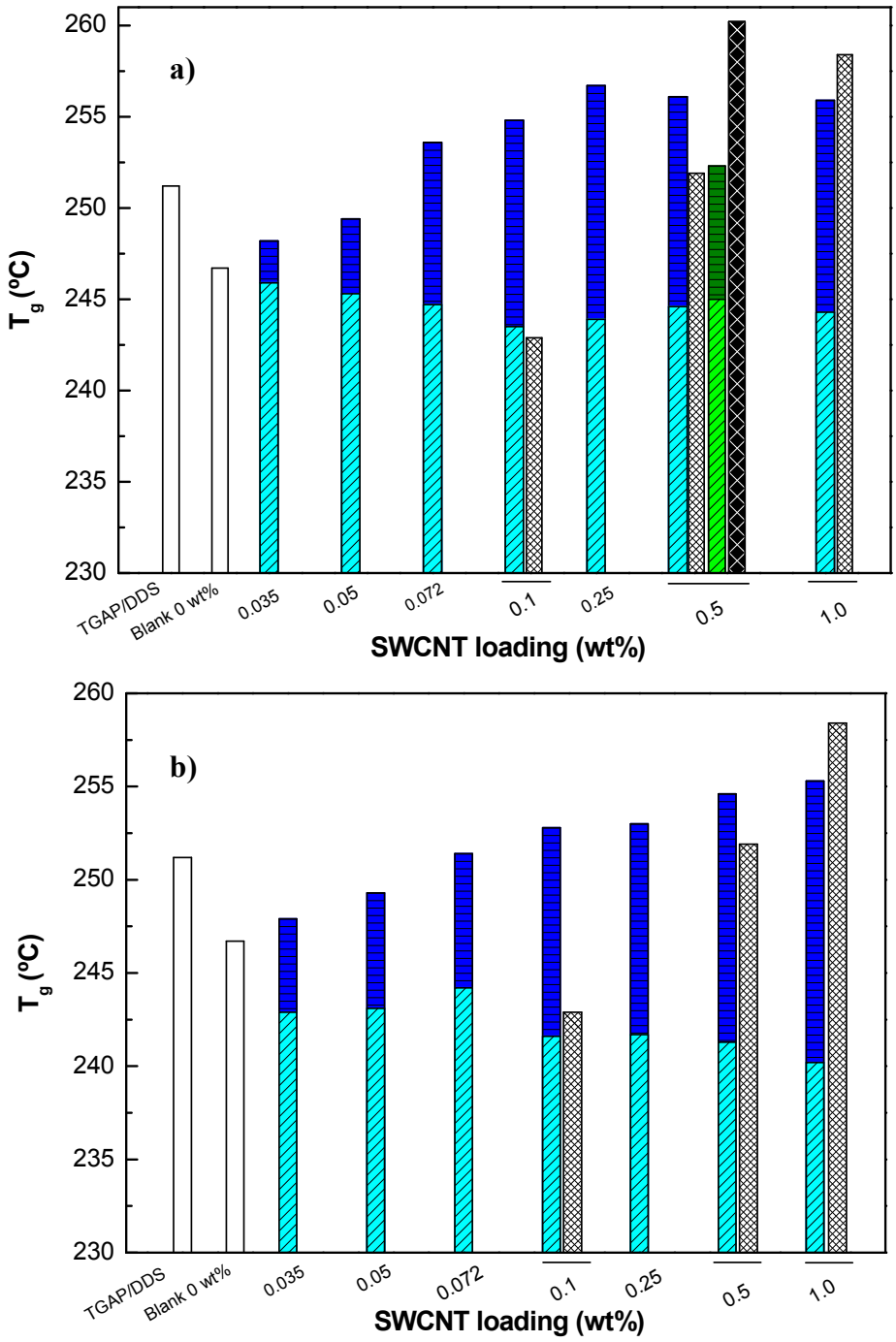

Figure 6.19. Glass transition temperature data (DMA at 1Hz) for the different nanocomposite and reference samples based on a) PEO-*b*-PE, and b) PEO-*b*-PPO. NOTE: The same legend as in Figure 3.17 is applied.

YM of the different studied samples show that the elastic properties of the neat epoxy matrix shift to a more plastic behavior upon BC incorporation, which is in agreement with the DMA results. Moreover, wrapped SWCNTs again compensate for the effect of BCs ending up in improved modulus in comparison to the neat epoxy.

The improvements attained in YM values, for wrapped and non-wrapped SWCNTs are very similar, about 35% improvement as compared to the neat matrix. Ultimate tensile strength (σ_y) values follow an analogous trend. Neat epoxy and blank samples containing BCs display similar σ_y values, while the incorporation of SWCNTs (mostly wrapped in the BCs) increases significantly this parameter. The highest increase is achieved for the nanocomposite sample containing as-grown SWCNTs wrapped in PEO-*b*-PE (50% increase in σ_y in comparison to the neat matrix).

Table 6.4. Tensile parameters drawn from stress-strain curves for the epoxy nanocomposites and reference samples studied in this section, all at 0.5 wt.-% SWCNT loading.

Sample	YM (GPa)	σ_y (MPa)	ε_b (%)	Toughness (MJ/m^3)
Neat Epoxy	3.0 ± 0.8	58 ± 1	4.0 ± 0.2	0.23 ± 0.01
Blank (0 wt%)	2.7 ± 0.3	52 ± 4	3.6 ± 0.4	0.21 ± 0.03
Blank + PEO-*b*-PPO	2.7 ± 0.1	51 ± 3	3.2 ± 0.1	0.20 ± 0.02
Blank + PEO-*b*-PE *	2.9 ± 0.1	53 ± 3	3.6 ± 0.1	0.23 ± 0.02
Blank + PEO-*b*-PE **	2.9 ± 0.1	54 ± 3	3.9 ± 0.1	0.20 ± 0.01
Nanocomposite with bare as-grown SWCNTs	4.1 ± 0.4	70 ± 5	3.1 ± 0.4	0.26 ± 0.01
Nanocomposite with bare [ox]-SWCNTs	4.3 ± 0.2	84 ± 4	2.8 ± 0.2	0.20 ± 0.01
Nanocomposite with as-grown SWCNTs wrapped in PEO-*b*-PPO	3.9 ± 0.2	80 ± 5	3.2 ± 0.1	0.26 ± 0.3
Nanocomposite with as-grown SWCNTs wrapped in PEO-*b*-PE	4.2 ± 0.1	87 ± 4	3.6 ± 0.1	0.31 ± 0.3
Nanocomposite with [ox]-SWCNTs wrapped in PEO-*b*-PE	3.8 ± 0.3	78 ± 4	4.8 ± 0.2	0.43 ± 0.3

***** Epoxy blank containing the same BC amount as those nanocomposites with wrapped as-grown SWCNTs

****** Epoxy blank containing the same BC amount as those nanocomposites with wrapped [ox]-SWCNTs

Another important mechanical parameter is the elongation at break (ε_b), which tends to decrease in epoxy/CNT nanocomposites as a consequence of an increase of the rigidity, induced by the presence of CNTs,[61-64] that could be detrimental for the

[61] Allaoui, A.; Bai, S.; Cheng, H. M.; Bai, J. B., Mechanical and electrical properties of a MWNT/epoxy composite. *Compos. Sci. Technol.* 2002, *62* (15), 1993-1998.

material's toughness. As a matter of fact, the incorporation of bare SWCNTs into the epoxy (either as-grown or oxidized) significantly lowers the ε_b value as compared to the parent epoxy, while BCs by themselves scarcely affect it (in the amounts studied here). More interestingly, the incorporation of wrapped SWCNTs causes the recovering of the ε_b value (especially in PEO-*b*-PE, the one having the highest lyophilicity difference between blocks in both BCs) hence exhibiting a more ductile fracture. This effect is enhanced in wrapped [ox]-SWCNTs, which seems to indicate a synergy between the SWCNTs oxidized surface and the BC, also reflected in the toughness values. This parameter noticeably increases in [ox]-SWCNTs wrapped in PEO-*b*-PE, achieving an 87% improvement of the matrix toughness (or 105% improvement as compared to the unfilled blank sample). This is a significant achievement in the field of epoxy nanocomposites, which typically suffer from a high brittleness. The wrapping of oxidized SWCNTs in BCs, in addition to cause the sample purification and debundling, it is also useful for toughening epoxy matrices.

In summary, mechanical properties show that this approach (particularly when preceded by the SWCNT surface oxidation) is useful to obtain highly purified and disentangled SWCNTs which additionally provide ductile epoxy nanocomposites with enhanced toughness, good balance between stiffness and toughness, but without sacrificing the elastic moduli.

Electrical conductivity measurements

The effect of the BC wrapping on electrical properties of the epoxy nanocomposites was determined by direct current conductivity measurements (Figure 6.20). This shows that the effect of wrapping in PEO-based diblock copolymers is to increase the maximum conductivity values of the matrix, up to a maximum of 9-10 orders of magnitude, in as-grown SWCNTs (at 1 wt%). The BC having lower lyophilicity difference between blocks (PEO-*b*-PPO) achieves higher conductivity values than the

[62] Zhu, J.; Peng, H. Q.; Rodriguez-Macias, F.; Margrave, J. L.; Khabashesku, V. N.; Imam, A. M.; Lozano, K.; Barrera, E. V., Reinforcing epoxy polymer composites through covalent integration of functionalized nanotubes. *Adv. Funct. Mater.* 2004, *14* (7), 643-648.
[63] Rafiee, M. A.; Lu, W.; Thomas, A. V.; Zandiatashbar, A.; Rafiee, J.; Tour, J. M.; Koratkar, N. A., Graphene Nanoribbon Composites. *ACS Nano* 2010, *4* (12), 7415-7420.
[64] Gonzalez-Dominguez, J. M.; Diez-Pascual, A. M.; Anson-Casaos, A.; Gomez-Fatou, M. A.; Martinez, M. T., Epoxy composites with covalently anchored amino-functionalized SWNTs: towards the tailoring of physical properties through targeted functionalization. *J. Mater. Chem.* 2011, *21* (20), 14948-14958.

other one (globally ~1 order of magnitude). The electrical conductivity in CNT/epoxy nanocomposites not only depends on the dispersion state of the sample but also in the intertube connection ability for creating conductive pathways within the bulk matrix.

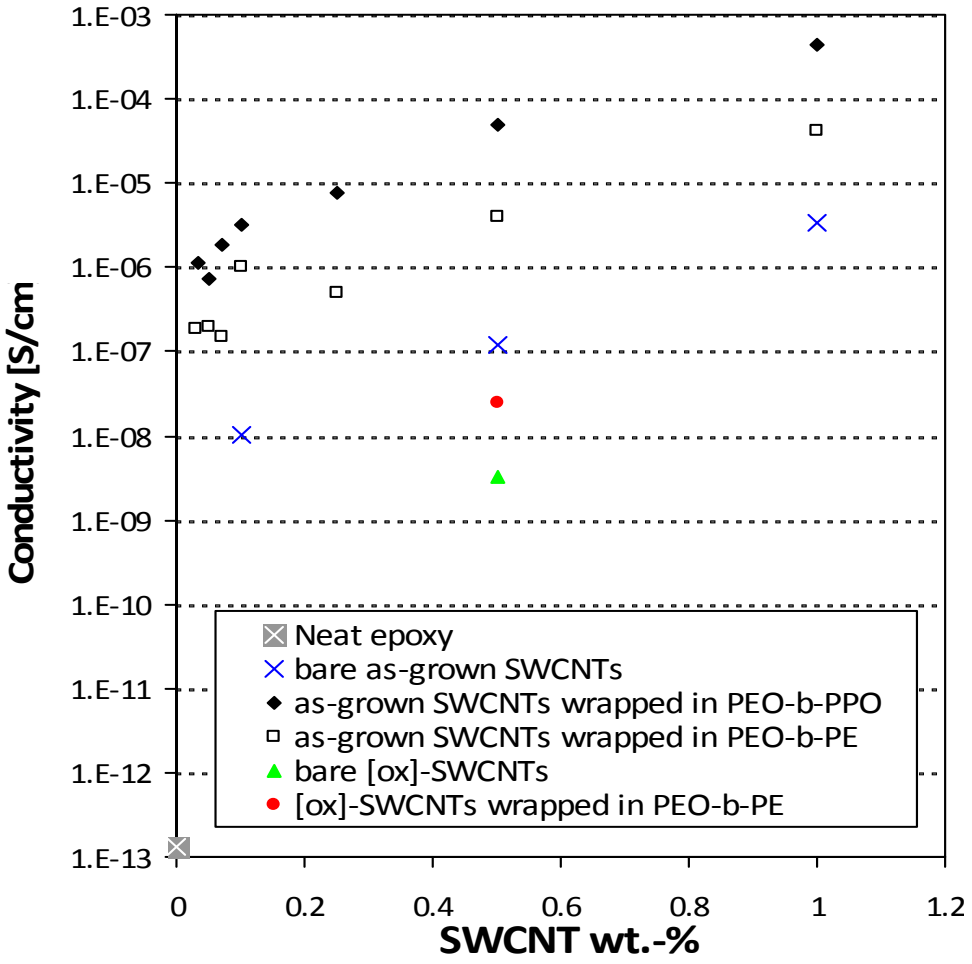

Figure 6.20. DC conductivity values for epoxy nanocomposites wrapped in PEO-based diblock copolymers and their corresponding reference samples.

On the other hand, the electrical percolation threshold of epoxy/SWCNT nanocomposites is very low when SWCNTs are wrapped in the BCs. According to Figure 6.20, for wrapped as-grown SWCNTs, it seems to be lower than 0.03 wt% (without visible differences between both BCs).

In the nanocomposite containing [ox]-SWCNTs, the conductivity value is two orders of magnitude lower than its as-grown counterpart. This difference is maintained for the nanocomposite containing wrapped [ox]-SWCNTs (in comparison to as-grown

wrapped SWCNTs nanocomposite), which points to an effect of the surface oxidation of SWCNTs. The insertion of oxygen groups by covalent bonding to the SWCNT surface disrupts the delocalized electronic structure of the pristine tubes, worsening their intrinsic electrical properties. Nevertheless, the BC wrapping counteracts this effect, since it causes an increase of ~1 order of magnitude, as compared with the unwrapped [ox]-SWCNT nanocomposites.

SEM observation

Finally, the dispersion state and morphology of nanocomposites was examined through a microscopic technique. SEM images of the fracture edge of different nanocomposites are shown in Figure 6.21.

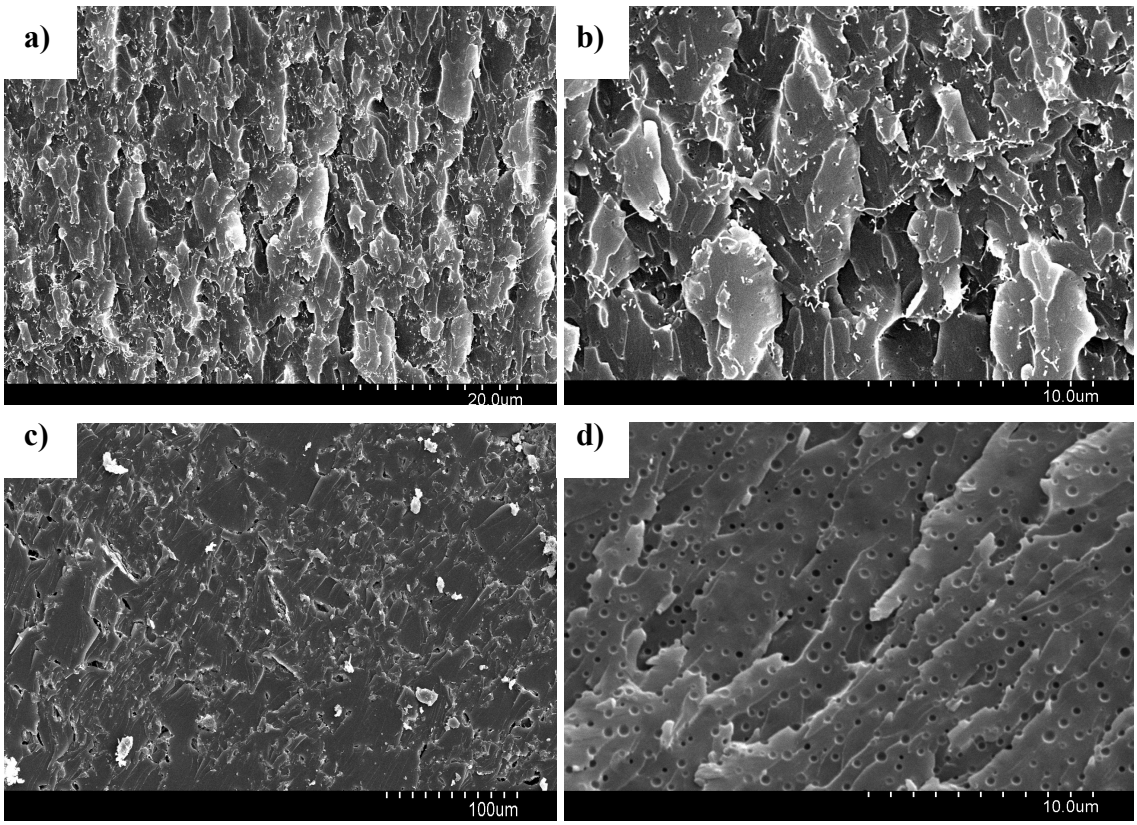

Figure 6.21. Representative SEM images of different nanocomposites: a) and b) Epoxy nanocomposite with 0.5 wt% as-grown SWCNTs wrapped in PEO-*b*-PE; c) Epoxy nanocomposite with 0.5 wt% [ox]-SWCNT wrapped in PEO-*b*-PE; d) Blank epoxy with PEO-*b*-PE in the same amount as in the nanocomposite sample of Figure 6.20c.

As previously stated by SEM, the solvent-free incorporation of as-grown arc discharge SWCNTs into the TGAP/DDS epoxy system ends up in inhomogeneous

distribution of the filler across the fracture edge, with numerous aggregates and pulled-out SWCNT bundles (see sections 5.3.1. and 5.3.2.).[64,65] A higher homogeneity is seen in nanocomposites containing diblock copolymer-wrapped SWCNTs. Similar images can be visualized in nanocomposites reinforced with as-grown SWCNTs wrapped in both BCs. As an example, the PEO-*b*-PE case is displayed in SEM images of Figure 6.21a and 6.21b. The homogeneity of the filler distribution is greatly improved. For nanocomposite with wrapped [ox]-SWCNTs (Figure 6.21c) the filler distribution over the fracture edge is even more homogeneous, and SWCNT are almost indiscernible, owing to the great debundling experienced by the filler upon wrapping in the BC. The reference epoxy nanocomposites filled with BC (Figure 6.21d) shows the typical toughening vesicular structures of the self-assembled BC,[23,24] also present in the nanocomposite samples with wrapped SWCNTs.

6.4. Conclusion

In the present chapter, different epoxy nanocomposites, containing BC-wrapped SWCNTs have been prepared and characterized. The non-covalent strategy based on the SWCNTs wrapping in PEO-based BCs led in all cases to the successful integration of the filler into the matrix, exhibiting high miscibility, which enabled the integration process to undergo efficiently in absence of organic solvents.

For Pluronic F68-based epoxy nanocomposites the wrapped SWCNTs caused remarkable improvements in the epoxy toughness (276% increase in tensile toughness and 193% increase in impact strength, at only 0.5 wt% filler loading, which means ~0.35 wt% SWCNTs) leaving the elastic properties unharmed. These nanocomposites also exhibited significant improvements in electrical conductivity as compared to the neat epoxy matrix (maximum conductivity values achieved were around 7 orders of magnitude higher) and to the epoxy/non-wrapped SWCNTs reference composites. The nanocomposites thermal and thermo-oxidative properties improved noticeably when containing Pluronic-wrapped SWCNTs (higher T_{max} values, lower flammability and a slowing down of the degradation mechanism). A synergistic effect between SWCNTs

[65] González-Domínguez, J. M.; Martínez-Rubí, Y.; Díez-Pascual, A. M.; Ansón-Casaos, A.; Gómez-Fatou, M. A.; Simard, B.; Martínez, M. T., Reactive fillers based on SWCNTs functionalized with matrix-based moieties for the preparation of epoxy composites with superior and tuneable properties, *Nanotechnology (submitted).*

and the BC is therefore suggested given that these improvements are greater than the sum of individual effects.

In the case of nanocomposites containing PEO-based diblock copolymers (PEO-*b*-PPO and PEO-*b*-PE), the effect of SWCNT surface oxidation prior to the BC wrapping causes differences in the properties of the obtained nanocomposite materials. Epoxy nanocomposites with as-grown wrapped SWCNTs presented improved elastic properties (higher storage moduli, higher tensile strength, and lower elongation at break values), without detriment on the toughness or even with a slight improvement (~35% increase in tensile toughness of nanocomposites containing 0.5 wt% as-grown SWCNTs wrapped in PEO-*b*-PE, in comparison to the neat epoxy matrix). However, [ox]-SWCNTs wrapped in PEO-*b*-PE presented a higher ductile behavior, reflected in a much higher elongation at break and also a tensile toughness improvement (87% increase at 0.5 wt% SWCNTs, as compared to the epoxy matrix) but without increasing, nor decreasing, the elastic modulus values. Higher conductivity values and lower percolation thresholds are achieved for nanocomposites with as-grown wrapped SWCNTs, reaching the maximum conductivity values achieved in the present thesis work with arc SWCNTs (close to 10^{-3} S/cm).

The non-covalent approach with PEO-based BCs offers the versatility of providing highly unbundled and purified SWCNTs and, simultaneously, the way of obtaining a suitable filler for successful reinforcement of epoxy matrices. The solvent-free integration of this filler into the epoxy ends up in nanocomposite materials with improved mechanical, thermal and electrical properties. These improvements will depend on the use of untreated or previously oxidized SWCNTs wrapped fillers. Oxidized SWCNTs wrapped in BCs provide higher ductility and toughness to the epoxy matrix, with no negative effect on the elastic or conductive properties. On the other hand, nanocomposites with wrapped as-grown SWCNTs stand out for their electrical conductivity, with unchanged or slightly improved mechanical properties.

"Life,… dreams,…hope,…
Where do they come from?
And where do they go?"

Final Fantasy VI
Squaresoft (1994)

CHAPTER 7:

GENERAL CONCLUSIONS

Different strategies have been developed to modify SWCNTs seeking their rational integration in specific polymer matrices, with emphasis in a high-performance epoxy thermoset for aerospace and automotive applications. The main conclusions drawn from the work presented here can be summarized in the following points:

1) SWCNTs can be efficiently purified by several methods, each one having its own advantages and limitations. The oxidative acid treatments (mainly with nitric acid) allow removing important part of the metallic particles and induce a certain degree of debundling, but some structural damaging is produced. This treatment also serves to generate surface oxygen groups with potential for further derivatization *via* nucleophilic attack. However, it also causes the compaction of the sample and therefore hinders SWCNTs dispersion into the polymer matrix. On the other hand, the SWCNT purification using BCs is able to eliminate graphitic impurities and metal particles from raw samples, particularly when the BC dispersion is combined with centrifugation. The air oxidation of SWCNTs prior to centrifugation in a BC solution increases the sample purity and the obtained wrapped SWCNTs are particularly suitable to be integrated as fillers in epoxy nanocomposites.

2) The covalent functionalization of SWCNTs with different terminal amine groups has been carried out for their subsequent integration as reactive fillers into epoxy resins. In a first approach, SWCNTs covalently functionalized with terminal aliphatic amines have been obtained through four different widespread chemical routes (namely: carboxylation + amidation; alkaline reduction + diacyl peroxide; 1,3-dipolar cycloaddition of azomethyne ylides; *in situ* generation and reaction of aryl diazonium salts). Each functionalization pathway provides aminated SWCNTs with different functionalization degree and different chemical nature of the attached moiety. In a second approach, SWCNTs have been covalently functionalized with pre-synthesized molecules derived from the epoxy matrix structure *via* the *in situ* diazonium reaction. By this means, SWCNTs ending in aromatic amines or epoxide rings are obtained.

3) Non-covalent interactions in liquid media between SWCNTs and different polymers can be conveniently undertaken in order to obtain polymer-wrapped

SWCNTs for different purposes. A rational choice of polymeric dispersants has been carried out attending to the target matrix and the relative chemical affinities between filler and matrix. The wrapping of SWCNTs in PEO-based BCs, besides causing significant purity improvements, induces the filler debundling and boosts its miscibility with epoxy. SWCNTs wrapped in thermo-plastic polymers, namely polyetherimide (PEI) or polysulfones (PSF or PEES), also end up with certain degree of debundling, and are interesting fillers to reinforce PEEK matrices, as it has been demonstrated in the framework of the project.

4) The effect of several functionalized SWCNTs in the epoxy curing reaction (all integrated solvent-free) has been studied by isoconversional kinetics, from DSC measurements, the main conclusions being:
   - **a.** The incorporation of SWCNTs wrapped in Pluronic F68 block copolymer causes the activation energy reduction in the extreme stages of the curing reaction, possibly due to a positive effect of Pluronic on the species mobility without negatively affecting the epoxy cross-linking process.
   - **b.** The incorporation of SWCNTs functionalized with aliphatic terminal amines leads to nanocomposites that exhibit different features depending on the chosen functionalization pathway. Non-functionalized SWCNTs or those aminated *via* nitric acid treatment raise the curing enthalpy (with slight change in glass transition temperature) and cause a sudden increase in the activation energy during the initial curing stages. The nanocomposites prepared with the rest of aminated SWCNTs exhibit a decrease in enthalpy and a big increase in glass transition temperature, coupled to a sharp decrease in activation energy during the initial curing stages. This is consistent with a covalent anchoring of the sidewall-functionalized SWCNTs to the epoxy matrix. This study reveals that the chemical nature of the attached moiety plays a crucial role, since it is intimately related with the filler's dispersibility and affinity to the epoxy matrix.

5) Neither of the SWCNT functionalization procedures employed provides an optimum reinforcement to the epoxy matrix. The improvements attained in the epoxy physical properties are dependent on the kind of functionalization applied to SWCNTs.

   a. The enhancement of dynamic mechanical and tensile properties of the epoxy matrix is more effectively accomplished through covalent functionalization with terminal amines than by non-covalent BC wrapping. All nanocomposites containing aminated SWCNTs prepared solvent-free in the present thesis (with the exception of those with SWCNT-oxa) exhibit improved mechanical properties, but only specific functionalizations have shown remarkable results. SWCNTs with benzylamine moieties provides higher Young's modulus than the neat matrix (45% increase at 1 wt% loading), and improved impact strength (44% increase at 0.1 wt% loading). On the other hand, the functionalization with matrix-based moieties has presented the best static and dynamic mechanical results in the whole thesis work: ~54% increase in Young's modulus and ~73% increase in tensile strength (SW-AD, 0.5 wt%), and ~65% increase in storage modulus (SW-AD 1 wt%).

   b. The use of epoxide-terminated SWCNTs through functionalization with matrix-based moieties allows similar, or even higher, improvements in mechanical properties, than those previously stated for amine-terminated moieties, if they are integrated using organic solvent. In this way, the highest tensile strength improvement in the present thesis work has been achieved (91% increase, at 0.5 wt% SW-DDS-ED), and also the highest tensile toughness improvement using a covalent functionalization approach (65% increase with 0.5 wt% SW-DDS-ED).

   c. The epoxy toughness can be greatly improved by means of the non-covalent approach with PEO-based BCs. Using SWCNTs wrapped in PEO-*b*-PE, noticeable toughness enhancements are attained (87% increase at 0.5 wt% wrapped [ox]-SWCNTs). The incorporation of nitric acid-treated SWCNTs wrapped in Pluronic F68 BC provides the highest toughness enhancements of the present thesis work: 276%

improvement in tensile toughness and 193% improvement in impact strength (at an effective SWCNT loading of ~0.35 wt%). These improvements in toughness are the highest reported so far for epoxy/CNT nanocomposites.

d. Thermal and thermo-oxidative stability of the neat epoxy can be efficiently improved with the covalent and non-covalent strategies studied here. The best results in this property have been achieved for nanocomposites containing covalent functionalization with matrix-based moieties. The maximum degradation rate temperature (inert atmosphere) exhibits an upshift of 41ºC (with 0.5 wt% SW-DDS-ED, integrated in organic solvent) and in air atmosphere exhibits a maximum upshift of 56ºC (with 0.5 wt% SW-AD, integrated solvent-free). The maximum improvements in thermomechanical properties, as studied through the glass transition temperature, are also attained by using the covalent approach with matrix-based moieties (15ºC increase in this parameter for SW-AD at 0.5 wt% loading).

e. The electrical conductivity of the epoxy is typically increased with the addition of SWCNTs. However, the covalent functionalization has shown to decrease the electrical conductivity as compared to nanocomposites containing as-grown SWCNTs. Only the non-covalent approach with BCs has proven to increase the electrical conductivity values, regarding nanocomposites prepared with unfunctionalized arc SWCNTs. The best results achieved have been obtained with as-grown arc SWCNTs wrapped in PEO-*b*-PPO (1 wt% SWCNT loading), whose epoxy nanocomposites exhibit a maximum conductivity of ~10^{-3} S/cm (the same order as the maximum achieved with laser as-grown SWCNTs at the same loading). The wrapping of acid-treated SWCNTs in Pluronic causes significant reduction of the percolation threshold (about tenfold).

6) The aforementioned improvements (particularly those regarding mechanical properties) are among the best reported in the literature so far for analogous epoxy/CNT nanocomposites (always comparing each result with its respective epoxy matrix) to the very best of the author's knowledge.

"Starting a new journey may not be so hard. Or maybe it's already begun. There are many worlds, but they share the same sky; one sky, one destiny"

Kingdom Hearts II
Square Enix (2006)

CONCLUSIONES

A lo largo de la presente tesis se han desarrollado distintas estrategias de funcionalización de SWCNTs con el objetivo de mejorar la integración de los mismos en matrices poliméricas específicas; una matriz termoestable de epoxi y una matriz termoplástica de PEEK, utilizadas para aplicaciones aeroespaciales y en automoción. Las principales conclusiones extraídas del trabajo que aquí se presenta se pueden resumir en los siguientes puntos:

1) Los SWCNTs se pueden purificar eficientemente mediante distintos métodos, cada uno de ellos con sus propias ventajas y limitaciones. Los tratamientos oxidativos con ácidos (principalmente con ácido nítrico) permiten la eliminación de una parte importante de las partículas metálicas y además inducen cierto grado de desagrupamiento de los SWCNTs, pero inducen daño estructural. Estos tratamientos también sirven para generar grupos oxigenados superficiales con potencial para posteriores derivatizaciones *via* ataque nucleofílico. Sin embargo, estos tratamientos conllevan la compactación de la muestra y por lo tanto impiden su adecuada dispersión en matrices poliméricas. Por otro lado, la purificación de SWCNTs usando copolímeros de bloque es capaz de eliminar las impurezas grafíticas y las partículas metálicas en muestras brutas, especialmente cuando se combinan con ciclos de centrifugación. La oxidación de los SWCNTs con aire, previa a su dispersión en copolímeros de bloque, aumenta su pureza y los SWCNTs así obtenidos son especialmente adecuados para su integración en matriz epoxi.

2) La funcionalización covalente de SWCNTs con diversos grupos amino terminales se ha llevado a cabo para su integración como reforzantes reactivos en matriz epoxi. En una primera aproximación, los SWCNTs covalentemente funcionalizados con grupos amino terminales alifáticos fueron obtenidos a través de cuatro rutas químicas establecidas (carboxilación + amidación; reducción alcalina + peróxido de diacilo; cicloadición 1,3-dipolar de iluros de azometina; generación *in situ* y reacción de sales de aril diazonio). Cada una de las rutas de funcionalización

proporciona SWCNTs aminados con distintos grados de funcionalización y distinta naturaleza química del grupo funcional incorporado. En una segunda aproximación, los SWCNTs se funcionalizaron con moléculas pre-sintetizadas derivadas de la estructura de la matriz epoxi *via* reacción de diazonio. De este modo, se obtienen SWCNTs con grupos amino terminales aromáticos ó anillos oxirano terminales.

3) Se pueden llevar a cabo interacciones no covalentes en medio líquido entre SWCNTs y distintos polímeros y que pueden satisfacer distintos propósitos. En la presente tesis se ha llevado a cabo una elección racional de los dispersantes poliméricos atendiendo a la matriz objetivo y a las afinidades químicas entre reforzante y matriz. El recubrimiento de los SWCNTs con copolímeros de bloque basados en PEO, además de causar importantes mejoras en la pureza de los mismos, proporciona cierto grado de desagrupamiento del reforzante y potencia su miscibilidad en epoxi. Los SWCNTs recubiertos de polímeros termoplásticos, tal como poliéterimida (PEI) ó polisulfonas (PSF ó PEES), también proporcionan un cierto grado de desagrupamiento, y constituyen interesantes agentes reforzantes para PEEK, tal y como se ha demostrado en el transcurso del proyecto de investigación en el cual se enmarca la presente tesis.

4) El efecto de los distintos SWCNTs modificados en las reacciones de curado (entrecruzamiento) de la epoxi tras su integración sin disolventes ha sido estudiado a través de calorimetría diferencial de barrido, siendo las principales conclusiones las siguientes:
    a. La incorporación de SWCNTs recubiertos con el copolímero de bloque Pluronic F68 produce una reducción de la energía de activación en las etapas extremas del proceso de curado, posiblemente debido a un efecto positivo del Pluronic en la movilidad de las especies sin afectar negativamente el proceso de entre-cruzamiento de la matriz.
    b. La incorporación en epoxi de SWCNTs funcionalizados con aminas terminales alifáticas proporciona un material con diferentes características dependiendo de la ruta de funcionalización elegida.

Los SWCNTs sin funcionalizar, o aquellos SWCNTs aminados mediante oxidación previa con ácido nítrico, aumentan la entalpía de curado (con un ligero cambio en la temperatura de transición vítrea) y causan un súbito incremento de la energía de activación en las etapas iniciales del curado. El resto de SWCNTs aminados muestran un decrecimiento de la entalpía de curado y un gran incremento en la temperatura de transición vítrea, unido a un descenso pronunciado de la energía de activación en las etapas iniciales del curado, que es consistente con un anclaje covalente de dichos SWCNTs aminados a la matriz epoxi. Este estudio muestra que la naturaleza química del grupo funcional juega un papel crucial, ya que está íntimamente relacionada con la dispersabilidad del reforzante y su afinidad por la matriz epoxi.

5) No existe un procedimiento de funcionalización único de SWCNTs que proporcione un refuerzo óptimo en matriz epoxi. Las mejoras conseguidas en las propiedades físicas de la matriz dependen del tipo de funcionalización aplicado a los SWCNTs.
   a. La mejora de las propiedades dinamo-mecánicas y de tracción en la matriz epoxi que se consigue mediante funcionalización covalente con aminas terminales es mayor que la obtenida con copolímeros de bloque. Todos los nanomateriales compuestos reforzados con SWCNTs aminados (y preparados sin disolventes orgánicos), con la excepción de aquellos funcionalizados con oxidación + amidación, exhiben propiedades mecánicas mejoradas, pero sólo algunas funcionalizaciones concretas han mostrado resultados notables. Los SWCNTs funcionalizados con bencilamina proporcionan un aumento del módulo de Young de la matriz epoxi del 45% (con una carga del 1% en peso), y una resistencia al impacto del 44% (0.1% en peso). Por otro lado, la funcionalización de SWCNTs con moléculas derivadas de la matriz epoxy, conteniendo grupos amino terminales, ha proporcionado los mejores resultados en propiedades mecánicas de la presente tesis: ~54% de aumento en el módulo de Young, ~73% de aumento en la fuerza máxima de tracción (σ_y) (SW-AD al 0.5% en

peso), y ~65% de aumento en el módulo de almacenamiento (SW-AD al 1% en peso).

b. El uso de SWCNTs funcionalizados con anillos oxirano terminales (a través de funcionalización con moléculas derivadas de la matriz epoxi) proporciona aumentos similares o incluso mayores de las propiedades mecánicas que aquellos previamente mencionados, siempre y cuando la integración se lleve a cabo usando disolvente orgánico. De este modo se alcanzaron los mayores aumentos en σ_y presentados en esta tesis (91% de aumento al 0.5% en peso de SW-DDS-ED), y también el mayor aumento de tenacidad alcanzado con una funcionalización covalente (65% de aumento al 0.5% en peso de SW-DDS-ED).

c. La tenacidad de la matriz epoxi puede aumentarse sustancialmente a través de la estrategia no covalente con copolímeros de bloque basados en PEO. Mediante la incorporación de SWCNTs recubiertos del copolímero PEO-*b*-PE se consiguió un notable aumento de la tenacidad (87% de aumento al 0.5% en peso de [ox]-SWCNTs). Sin embargo, la incorporación de SWCNTs oxidados con ácido nítrico y recubiertos con Pluronic F68 proporcionó el mayor aumento de tenacidad en la presente tesis: 276% de aumento + un 193% de aumento en la resistencia al impacto (con un contenido efectivo de SWCNTs de ~0.35% en peso), siendo el mayor aumento publicado en materiales epoxi/CNT en la literatura científica.

d. La estabilidad térmica y termo-oxidativa de la matriz epoxi se pueden aumentar eficientemente con las estrategias covalentes y no covalentes estudiadas en la presente tesis. Los mejores resultados conseguidos en esta propiedad se alcanzaron en aquellos nanomate-riales compuestos reforzados con SWCNTs funcionalizados con moléculas derivadas de la matriz epoxi. La temperatura de máxima degradación medida por TGA (en atmósfera inerte) experimenta un incremento de 41ºC (con 0.5% en peso de SW-DDS-ED, integrado con disolvente) y en atmósfera de aire el incremento es de 56ºC (con 0.5% en peso de SW-AD, integrado sin disolvente). Las mejoras más notables en propiedades termomecánicas, estudiadas a partir de la

temperatura de transición vítrea, se obtienen mediante el uso de la ruta de funcionalización mencionada en este subapartado (15ºC de aumento en la temperatura de transición vítrea para el nanomaterial compuesto con 0.5% en peso de SW-AD).

e. La conductividad eléctrica de la matriz epoxi aumenta tras la adición de SWCNTs. Sin embargo, la integración de SWCNTs funcionalizados covalentemente proporciona menores aumentos de conductividad eléctrica que cuando se integran SWCNTs no funcionalizados. Solamente la estrategia no covalente con copolímeros de bloque ha mostrado ser capaz de superar los valores de conductividad eléctrica en los nanomateriales compuestos preparados con SWCNTs de arco sin funcionalizar. Los mejores resultados obtenidos en la presente tesis se han conseguido con SWCNTs de arco eléctrico recubiertos de PEO-*b*-PE (1% en peso de SWCNTs), cuyos nanomateriales compuestos con epoxi exhibieron una conductividad máxima de $\sim 10^{-3}$ S/cm (valor del mismo orden de magnitud que el conseguido con SWCNTs de láser sin funcionalizar a igual carga). Adicionalmente, los SWCNTs oxidados con ácido nítrico y recubiertos de Pluronic F68 causan una notable reducción del umbral de percolación eléctrica (alrededor de diez veces).

6) Las mejoras anteriormente citadas (en particular aquellas relativas a las propiedades mecánicas) están entre las mejores de la literatura científica accesible hasta la fecha en nanomateriales compuestos epoxi/CNT análogos (siempre en comparación con sus respectivas matrices epoxi).

"The answer lies in the heart of battle"

Street Fighter IV
Capcom (2009)

ANNEX I:

HIGH-PERFORMANCE PEEK/SWCNT NANOCOMPOSITES. APPLICATION OF THE INTEGRATION STRATEGIES STUDIED

I.0. Abstract

The manufacturing and characterization of nanocomposite materials with thermoplastic matrices and SWCNTs can be undertaken through the different approaches studied along the present thesis. The target matrix for such nanocomposites has been Poly(ether ether ketone) (PEEK). By a simple melt blending approach, new interesting PEEK/SWCNT nanocomposites can be developed. Moreover, the wrapping of arc discharge or laser grown SWCNTs with different thermoplastic polymers (PEI, PSF and PEES) has been utilized as a means to improve the filler integration into the PEEK matrix and thus the resulting nanocomposite properties. PEEK/glass fibre (GF) laminates have also been successfully improved using this non-covalent functionalization. A covalent anchoring of SWCNTs to the polymer matrix was carried out *via* chemical modification of the target matrix. Reducing PEEK carbonyl groups to hydroxyl led to a polymer derivative able to anchor to oxidized arc discharge SWCNTs by esterification reaction. The results contained in the present chapter demonstrates the effectiveness of the designed strategies, as well as the possibility to extend these concepts to any other CNT-reinforced polymer matrix.

I.1. Introduction

Over the last decade, the outstanding mechanical, electrical and thermal properties of CNTs have motivated their use as reinforcing materials for a wide variety of polymer matrices.[1,2] The successful utilization of CNTs in composite applications depends on their homogenous dispersion throughout the matrix. A strong CNT–polymer interfacial adhesion is also required to fabricate materials with enhanced properties. One of the typical initial steps in the development of a Polymer/CNT nanocomposite is to remove the impurities accompanying CNTs. There have been many reports on the purification with strong acids, such as nitric or sulfuric.[3] Carboxylic groups are formed with the acid treatment, which increase the reactivity of the CNTs and their ability to

[1] Thostenson, E. T.; Ren, Z. F.; Chou, T. W., Advances in the science and technology of carbon nanotubes and their composites: a review. *Compos. Sci. Technol.* 2001, *61* (13), 1899-1912.
[2] Moniruzzaman, M.; Winey, K. I., Polymer nanocomposites containing carbon nanotubes. *Macromolecules* 2006, *39* (16), 5194-5205.
[3] Hu, H.; Zhao, B.; Itkis, M. E.; Haddon, R. C., Nitric acid purification of single-walled carbon nanotubes. *J. Phys. Chem. B* 2003, *107* (50), 13838-13842.

interact with other molecules. This functionalization approach has been further extended to covalently graft polymer matrices onto their surfaces.[4,5] The direct attachment of the polymeric structures to defect sites (side-walls or open ends) of the CNTs results in nanocomposites with both enhanced filler dispersion and miscibility with the two phases; as a result, the properties of these materials are able to surpass those containing pristine CNTs. An efficient way to ensure compatibility between the composite phases is to incorporate a polymer derivative with functional groups that present affinity with both the fillers and the matrix. Hill et al.[6] used a derivatized polyimide with hydroxylic pendant groups to functionalize CNTs for further integration in a polyimide matrix. Since minor hydroxyl moieties are present in many polymers or can be introduced without significantly changing their structure, this strategy may find increasing application in the functionalization of CNTs, which can be directly employed for the fabrication of composites.

Poly(ether ether ketone) (PEEK) is a semicrystalline high-performance thermoplastic with excellent mechanical properties,[7] thermal[8,9] and chemical stability,[10] which combined with its easy processability make it suitable for a wide range of applications, such as automobile, aeronautic, medical and electronic industries.[11,12] The insolubility of this polymer in most organic solvents represents the main obstacle for its functionalization, hence the ability to interact with other substances. The aromatic rings

[4] Blake, R.; Coleman, J. N.; Byrne, M. T.; McCarthy, J. E.; Perova, T. S.; Blau, W. J.; Fonseca, A.; Nagy, J. B.; Gun'ko, Y. K., Reinforcement of poly(vinyl chloride) and polystyrene using chlorinated polypropylene grafted carbon nanotubes. *J. Mater. Chem.* 2006, *16* (43), 4206-4213.
[5] Yang, B. X.; Pramoda, K. P.; Xu, G. Q.; Goh, S. H., Mechanical reinforcement of polyethylene using polyethylene-grafted multiwalled carbon nanotubes. *Adv. Funct. Mater.* 2007, *17* (13), 2062-2069.
[6] Hill, D.; Lin, Y.; Qu, L. W.; Kitaygorodskiy, A.; Connell, J. W.; Allard, L. F.; Sun, Y. P., Functionalization of carbon nanotubes with derivatized polyimide. *Macromolecules* 2005, *38* (18), 7670-7675.
[7] Cebe, P.; Chung, S. Y.; Hong, S. D., Effect of thermal history on mechanical-properties of polyetheretherketone below the glass-transition temperature. *J. Appl. Polym. Sci.* 1987, *33* (2), 487-503.
[8] Kruger, K. N.; Zachmann, H. G., Investigation of the melting behavior of poly(aryl ether ketones) by simultaneous measurements of saxs and waxs employing synchrotron-radiation. *Macromolecules* 1993, *26* (19), 5202-5208.
[9] Diez-Pascual, A. M.; Naffakh, M.; Gomez, M. A.; Marco, C.; Ellis, G.; Martinez, M. T.; Anson, A.; Gonzalez-Dominguez, J. M.; Martinez-Rubi, Y.; Simard, B., Development and characterization of PEEK/carbon nanotube composites. *Carbon* 2009, *47* (13), 3079-3090.
[10] Searle, O. B.; Pfeiffer, R. H., Victrex poly(ethersulfone) (pes) and victrex poly(etheretherketone) (PEEK). *Polym. Eng. Sci.* 1985, *25* (8), 474-476.
[11] Le Guen, A.; Klapper, M.; Mullen, K., Synthesis and properties of flexible poly(ether ketone) backbones, grafted with stiff, monodisperse side chains. *Macromolecules* 1998, *31* (19), 6559-6565.
[12] Harrison, W. L.; Hickner, M. A.; Kim, Y. S.; McGrath, J. E., Poly(arylene ether sulfone) copolymers and related systems from disulfonated monomer building blocks: Synthesis, characterization, and performance - A topical review. *Fuel Cells* 2005, *5* (2), 201-212.

in the PEEK structure (see Figure 3.2a) are crucial for its chemical modification, since they provide electrons for electrophilic substitution reactions. Furthermore, the ketone group in the benzophenone segment is also a versatile reactant for selective modifications of this polymer, as reported by Conceição et al.[13,14] and Henneuse et al.,[15,16] who prepared different derivatives through carbonyl reduction, and Colquhoun and co-workers,[17] who developed a derivatization procedure based on the dithioketalization of the ketone groups under strong acid conditions.

The integration of carbon nanofillers into these modified polymers would lead to nanocomposites with superior physical properties, expected to be used in technological applications. To our knowledge, there are very few studies to date related to the incorporation of CNTs into PEEK derivatives. A recent study reported by Babaa et al.[18] deals with the functionalization of MWCNTs with sulfonated PEEK; using a similar approach, Feng and co-workers[19] described the synthesis and characterization of MWCNT/poly-(phthalazinone ether sulfone ketone) composites. Baek et al.[20-22] focused on the in situ electrophilic grafting of linear and hyperbranched poly(ether ketones)s

[13] Conceiçao, T. F.; Bertolino, J. R.; Barra, G. M. O.; Mireski, S. L.; Joussef, A. C.; Pires, A. T. N., Preparation and characterization of poly(ether ether ketone) derivatives. *J. Braz. Chem. Soc.* 2008, *19* (1), 111-116.

[14] Conceiçao, T. F.; Bertolino, J. R.; Barra, G. M. O.; Pires, A. T. N., Poly (ether ether ketone) derivatives: Synthetic route and characterization of nitrated and sulfonated polymers. *Mater. Sci. Eng. C* 2009, *29* (2), 575-582.

[15] Noiset, O.; Henneuse, C.; Schneider, Y. J.; MarchandBrynaert, J., Surface reduction of poly(aryl ether ether ketone) film: UV spectrophotometric, H-3 radiochemical, and X-ray photoelectron spectroscopic assays of the hydroxyl functions. *Macromolecules* 1997, *30* (3), 540-548.

[16] Henneuse-Boxus, C.; Boxus, T.; Duliere, E.; Pringalle, C.; Tesolin, L.; Adriaensen, Y.; Marchand-Brynaert, J., Surface amination of PEEK film by selective wet-chemistry. *Polymer* 1998, *39* (22), 5359-5369.

[17] Colquhoun, H. M.; Hodge, P.; Paoloni, F. P. V.; McGrail, P. T.; Cross, P., Reversible, Nondegradative Conversion of crystalline aromatic poly(ether ketone)s into organo-soluble poly(ether dithioketal)s. *Macromolecules* 2009, *42* (6), 1955-1963.

[18] Babaa, M. R.; Bantignies, J. L.; Alvarez, L.; Parent, P.; Le Normand, F.; Gulas, M.; Mane, J. M.; Poncharal, P.; Doyle, B. P., NEXAFS study of multi-walled carbon nanotubes functionalization with sulfonated poly(ether ether ketone) chains. *J. Nanosci. Nanotechnol.* 2007, *7* (10), 3463-3467.

[19] Feng, X. B.; Liao, G. X.; He, W.; Sun, Q. M.; Jian, X. G.; Du, J. H., Preparation and Characterization of Functionalized Carbon Nanotubes/Poly(phthalazinone ether sulfone ketone)s Composites. *Polym. Compos.* 2009, *30* (4), 365-373.

[20] Jeon, I. Y.; Tan, L. S.; Baek, J. B., Nanocomposites derived from in situ grafting of linear and hyperbranched poly(ether-ketone)s containing flexible oxyethylene spacers onto the surface of multiwalled carbon nanotubes. *J. Polym. Sci. A-Polym. Chem.* 2008, *46* (11), 3471-3481.

[21] Choi, J. Y.; Han, S. W.; Huh, W. S.; Tan, L. S.; Baek, J. B., In situ grafting of carboxylic acid-terminated hyperbranched poly (ether-ketone) to the surface of carbon nanotubes. *Polymer* 2007, *48* (14), 4034-4040.

[22] Oh, S. J.; Lee, H. J.; Keum, D. K.; Lee, S. W.; Wang, D. H.; Park, S. Y.; Tan, L. S.; Baek, J. B., Multiwalled carbon nanotubes and nanofibers grafted with polyetherketones in mild and viscous polymeric acid. *Polymer* 2006, *47* (4), 1132-1140.

(PEKs) onto MWCNTs by Friedel–Crafts acylation in polyphosphoric acid. These methods are difficult to scale up, since specific monomers must be employed to obtain high-molecular weight polymers.

The present annex reports the improvements that arise from the application of the different covalent or non-covalent SWCNT integration strategies studied along the present thesis work, in a high-performance PEEK matrix. On the one hand, the incorporation of SWCNTs wrapped in thermoplastic polymers (specifically chosen to improve the compatibility with the PEEK matrix) provides a non-covalent means for the effective reinforcement of the matrix. On the other hand, the covalent attachment of the HPEEK derivative onto the surface of purified arc-grown SWCNTs, which incorporate carboxylic groups on their sidewalls, is carried out. The manufacturing of PEEK/SWCNT nanocomposites, through a melt blending approach, and their characterization allows comparing the effectiveness of the different strategies applied.

I.2. Experimental section

I.2.1. Materials and reagents

Low viscosity grade poly(ether ether ketone), PEEK 150P, was supplied by Victrex plc, UK (Mw ~40000 g/mol, T_g = 147ºC, T_{melt} = 345ºC). The polymer, provided as a coarse powder, was ground with a ball mill in order to diminish the particle size, vacuum dried at 120ºC for 4h and stored in a dry environment. Chemicals and solvents were all purchased from Sigma Aldrich (in the desired purity degree) and used without further purification. SWCNTs, either arc-discharge or laser grown were those described in chapters 2 and 3. Arc-discharge SWCNTs treated with nitric acid and subsequently wrapped in thermoplastic polymers (PEI, PSF or PEES) were prepared as described in section 3.2.2.1. These nitric acid-treated SWCNTs will be called CNT-COOH hereafter. The HPEEK sample was directly obtained from the group of M. A. Gómez-Fatou (ICTP-CSIC), which was synthesised by PEEK reduction with $NaBH_4$.[23] The HPEEK sample used in this work had a ~37% hydroxylation degree (in wt%), which was shown to be the highest reduction extent that avoided a dramatic worsening of the parent PEEK

[23] Diez-Pascual, A. M.; Martinez, G.; Gomez, M. A., Synthesis and Characterization of Poly(ether ether ketone) Derivatives Obtained by Carbonyl Reduction. *Macromolecules* 2009, *42* (18), 6885-6892.

properties.[23] For the covalent grafting of oxidized SWCNTs to HPEEK, the arc-discharge SWCNTs treated with nitric acid in severe conditions (acid treatment which precedes the PEES and PSF wrapping) was used, as described in section 3.2.2.1.

I.2.2. Experimental procedures

Grafting reaction between oxidized SWCNTs and HPEEK

The covalent grafting between HPEEK and oxidized arc-discharge SWCNTs (which contain a large amount of carboxylic groups in their surface) was conducted *via* esterification reaction. The esterification was performed in a collaborative research work through two different routes. The first route was conducted by Díez-Pascual and co-workers. It consisted of a one-pot esterification reaction using a carboxylic activation with Dicyclohexyl carbodiimide (DCC) and Dimethylamino pyridine (DMAP) in mild conditions.[24] The resulting composite is called HPEEK-CNT-1 hereafter. In a second approach, developed in our laboratory, the esterification reaction was made in two steps. Firstly, acid-treated SWCNTs (257 mg) were submerged in anhydrous DMF (35 mL) and sonicated in an ultrasound bath for 15 min. Subsequently, they were reacted with excess $SOCl_2$ (40 mL) at 120ºC for 18 h under reflux and constant stirring. The residual $SOCl_2$ was removed by reduced pressure distillation to yield the acyl-chloride-functionalized SWCNTs. Secondly, HPEEK (2.7 g) was suspended in DMF (65 mL) and bath sonicated for 30 min. Subsequently pyridine (2 mL) was added and the system was maintained under stirring at ~60ºC until further use. The acylated nanotubes were then added to the polymer suspension and the reaction was allowed to proceed for 20 h at 60ºC under Ar flow and mechanical stirring. The reaction mixture was diluted in anhydrous methanol (300 mL) for 1 h under vigorous stirring. The resulting compound (HPEEK–CNT-2, hereafter) was filtered through a PTFE membrane (0.1 mm pore size) and washed with methanol until the falling filtrate was observed to be colourless. Then it was rinsed with aqueous ethanol (96% v/v) and dried under vacuum at 120ºC for 10 days. Figure I.1. depicts the grafting process.

[24] Diez-Pascual, A. M.; Martinez, G.; Gonzalez-Dominguez, J. M.; Anson, A.; Martinez, M. T.; Gomez, M. A., Grafting of a hydroxylated poly(ether ether ketone) to the surface of single-walled carbon nanotubes. *J. Mater. Chem.* 2010, *20* (38), 8285-8296.

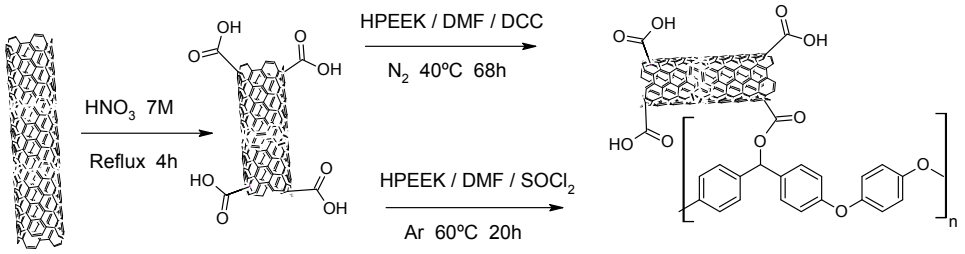

Figure I.1. Covalent grafting scheme between oxidized arc-discharge SWCNTs and HPEEK

PEEK/SWCNT Nanocomposites preparation

The processing route to manufacturing PEEK/SWCNT nanocomposites was undertaken at the ICTP. It consisted in a joint dispersion of SWCNTs and PEEK by bath-sonicating the powder mixture (obtained by ball milling) in ethanol. Then, after solvent evaporation, the resulting mixture was processed by conventional melt blending inside an extruder device.[9,25] This was applied for all PEEK/SWCNTs nanocomposites except for the HPEEK grafted derivative obtained from the esterification reaction, which was directly molded for its characterization with no melt processing. This grafted derivative was eventually incorporated into pure PEEK by the aforementioned predispersion-melting approach.

I.2.3. Characterization techniques

► X-Ray photoelectron spectroscopy (XPS) measurements were recorded on a Kratos AXIS ultra DLD equipment, using an Al/Kα X-ray source (10 mA, 12 kV). Prior to the experiments, the samples were oven-dried at 100ºC for 15 h in order to remove moisture. Subsequently, they were placed in the same sample holder and registered consecutively. For all the samples, high resolution spectra of C1s and O1s core levels were recorded. The applied lens mode was a Hybrid Slot, corresponding to an analysis area of 700 - 300 microns. The reported values are referenced to the C1s C–C binding energy at 284.9 eV. For backgrounds, Shirley functions were used. Peak deconvolutions

[25] Diez-Pascual, A. M.; Naffakh, M.; Gonzalez-Dominguez, J. M.; Anson, A.; Martinez-Rubi, Y.; Martinez, M. T.; Simard, B.; Gomez, M. A., High performance PEEK/carbon nanotube composites compatibilized with polysulfones-I. Structure and thermal properties. *Carbon* 2010, *48* (12), 3485-3499.

were carried out using Gaussian functions with no asymmetry corrections, in order to estimate the relative surface abundance of the different types of atoms.

I.3. Results and discussion

I.3.1. Effects of incorporation of thermoplastic-wrapped SWCNTs into a PEEK matrix. Comparison with nanocomposites containing bare SWCNTs.

The reinforcement obtained by the integration of thermoplastic-wrapped SWCNTs could be briefly stated as follows.

- An efficient dispersion of all SWCNTs (arc-discharge or laser grown, bare or acid-treated) in the matrix was achieved by the combination of polymer ball milling and mechanical pre-treatments in ethanol, as revealed by SEM micrographs of fractured films.[9] TGA thermograms show a substantial increase in the matrix degradation temperatures by the incorporation of SWCNTs (20ºC upshift in T_{max} for 1 wt% arc SWCNTs). Higher thermal stability is found for samples with improved CNT dispersion.

- DSC experiments indicate a decrease in the crystallization temperature with increasing SWCNT content, whereas the melting temperature remains almost constant. This behaviour can be explained by a confinement effect of the polymer chains within the CNT network, which delays the crystallization process and leads to lower values of crystallization temperatures for the composites. No significant differences are found within the level of crystallinity of these composites calculated from DSC measurements. At room temperature, samples containing 0.1 wt% SWCNTs exhibit larger crystallite size than the raw matrix. At higher concentrations, the CNT network restricts the polymer chain diffusion and hinders the formation of large-size crystals. Furthermore, over the whole concentration range, composites including purified SWCNTs present bigger crystals.[9]

- DMA studies reveal a non-linear growth in the storage modulus of the matrix by the addition of increasing SWCNT contents. This phenomenon can be

attributed to weaker nanotube–matrix interfacial interactions taking place when a larger concentration regime is reached (27% increase in E' at 1 wt% arc SWCNTs loading). SWCNTs restrict molecular mobility and consequently increase slightly the glass transition temperatures. The largest shift is found among composites with more homogeneous and fine distribution of the CNTs, that also exhibit enhanced rigidity.[9]

- When incorporating PEI-wrapped SWCNTs into the PEEK matrix, the presence of such compatibilizer significantly reduced the size of the filler phase and improved their dispersion within the matrix and maintains the level of thermal stability attained in the binary nanocomposites.[26] DMA measurements indicate that the compatibilization leads to a significant enhancement in the storage modulus of the nanocomposites, beyond the effect of bare SWCNTs (30% higher E' for 1 wt% arc SWCNTs than that achieved for bare SWCNTs), due to an improved interfacial adhesion and stress transfer ability between the reinforcement and the matrix.

  The wrapping of PEI around the SWCNTs leads to a diminution in the number of contacts between the tubes, and consequently a reduction in the conductivity. Despite this decrease, their conductivity is far superior to that of the PEEK matrix, and sufficient to effectively dissipate heat and prevent the build up of static charge. Considering all the analyses performed, it can be concluded that PEI is able to compatibilize SWCNTs and PEEK, particularly at higher nanotube loading, where the enhancement in stiffness is more significant.[26]

- In the case of polysulfones, the incorporation of PEES- or PSF-wrapped SWCNTs into the PEEK matrix showed (by SEM) that the wrapped SWCNTs were homogenously dispersed in the thermoplastic matrix using the aforementioned processing process. TGA thermograms demonstrated a remarkable increase in the degradation temperatures of the composites by the incorporation of the polysulfones (35ºC upshift in T_{max} and 38ºC upshift in

[26] Diez-Pascual, A. M.; Naffakh, M.; Gomez, M. A.; Marco, C.; Ellis, G.; Gonzalez-Dominguez, J. M.; Anson, A.; Martinez, M. T.; Martinez-Rubi, Y.; Simard, B.; Ashrafi, B., The influence of a compatibilizer on the thermal and dynamic mechanical properties of PEEK/carbon nanotube composites. *Nanotechnology* 2009, *20* (31).

$T_{max}2$ for 1 wt% PEES-wrapped arc SWCNTs), attributed to the compatibilizing effect and the high thermal stability of these amorphous polymers.[25] The addition of 0.1 wt.% wrapped SWCNTs increased the crystallization temperature and level of crystallinity of PEEK, whereas it decreased slightly at higher concentrations, due to the inactive nucleating effect of the nanofillers, the restrictions on chain diffusion imposed by the CNT network and the presence of an amorphous compatibilizer miscible with the matrix.[25] As regards to mechanical properties, a noticeable increase in E' (39% improvement for 1 wt% PEES-wrapped SWCNTs), in Young's moduli, and other mechanical parameters were observed.[27] Similar trends in the thermal and electrical conductivity as the PEI case were measured.

I.3.2. Covalent strategy. Characterization of the SWCNT-HPEEK grafting reaction

Due to the insolubility of the polymer, the esterification approaches employed for the synthesis of the HPEEK-grafted SWCNTs are surface reactions that lead to mixtures composed by non-reacted HPEEK segments interacting physically with the acid-oxidized SWCNTs and HPEEK chains covalently attached to the surface of the SWCNTs. Taking into account their heterogeneous composition, the analysis of different fractions of these samples provides a broad distribution of properties. Thus, it is important to notice that the results obtained from the different characterization techniques should be considered as representative average values. The hydroxylation degree of the polymer derivative (~37%) and the extent of the grafting reactions (~12% and 9% for HPEEK–CNT-1 and HPEEK–CNT-2, respectively) were calculated from the TGA curves under inert atmosphere considering that the first stage of weight loss after 300ºC of PEEK derivatives is related to the elimination of hydroxyl groups from the polymer backbone.[23]

XPS was used to characterize the functional groups present on the surface of the different samples. The O1s spectra are displayed in Figure I.2, and the position as well

[27] Diez-Pascual, A. M.; Naffakh, M.; Gonzalez-Dominguez, J. M.; Anson, A.; Martinez-Rubi, Y.; Martinez, M. T.; Simard, B.; Gomez, M. A., High performance PEEK/carbon nanotube composites compatibilized with polysulfones-II. Mechanical and electrical properties. *Carbon* 2010, *48* (12), 3500-3511.

as assignation of the different peaks are included in Table I.1. In the spectrum of the acid-treated SWCNTs (Figure I.2a), two clear contributions can be observed, typical of highly oxidized nanotubes. The first peak centred at 532.1 eV corresponds to C=O bonds,[28-30] and the second at 533.7 eV is ascribed to single bonds C–O.[28-30] Both contributions can also be visualized in the spectra of the HPEEK (531.7 and 533.3 eV respectively, Figure I.2b) and the HPEEK-grafted SWCNTs (531.7 and 533.5 eV, Fig. 7.2c and d, respectively). Moreover, all the HPEEK samples present a low intensity broad band at 539.9 eV that can be assigned to π interactions, and another feature centred at 532.8 eV attributed to hydroxyl groups[30] arising from the reduction of the carbonyl groups of PEEK. The similarity between the O1s spectra of both HPEEK–CNT samples confirms the presence of the same type of oxygen bonds. Moreover, a new contribution at 534.5 eV can be visualized in their spectra, typical of the ester bond,[30,31] supporting the success of the grafting reactions. In addition, their O–C peak (533.5 eV) appears in an intermediate position between that of the CNT–COOH (533.7 eV) and the HPEEK (533.3 eV), which also indicates the esterification of the HPEEK functional groups.

Regarding the peak areas, noticeable changes from the polymer derivative to the different HPEEK–CNT samples can be observed. The C=O band increases its area from 1.5% (for the HPEEK) to an average of 9% (for both HPEEK–CNT samples), which is an intermediate value between that of the CNT–COOH (59.3%) and the hydroxylated polymer. In contrast, the C–O band experiences a strong reduction, from 69.7% in the HPEEK to ~31% and 40% for the HPEEK–CNT-1 and HPEEK–CNT-2, respectively. This decrease is coupled to the appearance of the ester band and is consistent with the esterification process, since the formation of an ester group creates O=C–O–C bonds at the expense of O–H moieties. Furthermore, the area of the ester band is larger for the HPEEK–CNT-1, hinting that it presents a higher esterification degree than HPEEK–CNT-2. However, area data can not be employed to quantify the esterification degree,

[28] Yang, K.; Gu, M. Y.; Guo, Y. P.; Pan, X. F.; Mu, G. H., Effects of carbon nanotube functionalization on the mechanical and thermal properties of epoxy composites. *Carbon* 2009, *47* (7), 1723-1737.
[29] Zhang, G. X.; Sun, S. H.; Yang, D. Q.; Dodelet, J. P.; Sacher, E., The surface analytical characterization of carbon fibers functionalized by H_2SO_4/HNO_3 treatment. *Carbon* 2008, *46* (2), 196-205.
[30] Lopez, G. P.; Castner, D. G.; Ratner, B. D., XPS O1s Binding-energies for polymers containing hydroxyl, ether, ketone and ester groups. *Surf. Interface Anal.* 1991, *17* (5), 267-272.
[31] A. Dilks, in *Electron Spectroscopy: Theory, Techniques and Applications*, ed. A. D. Baker and C. R. Brundle, Academic Press, London, 1981, p. 277.

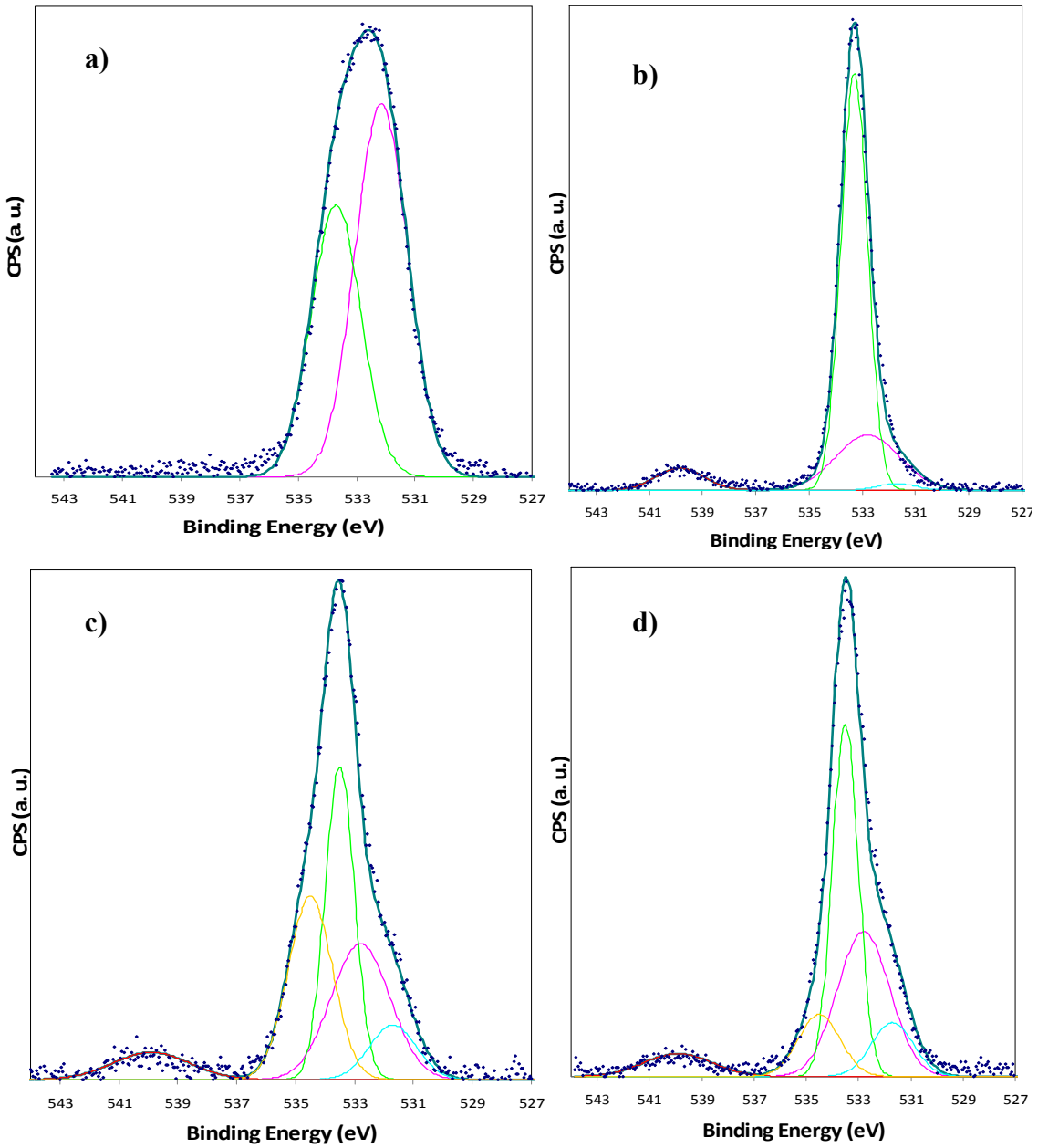

Figure I.2. O1s core level XPS spectra and signal deconvolutions for the studied samples: a) CNT-COOH, b) HPEEK, c) HPEEK–CNT-1, and d) HPEEK–CNT-2.

since XPS is a surface technique and does not consider the bulk of the sample. On the other hand, the area corresponding to the π contribution remains almost unchanged for all the HPEEK-related samples. In summary, the O1s spectra demonstrate the existence of the ester bond and give some insights into the type of oxygen bonds in the different samples.

The covalent attachment of the HPEEK to the SWCNTs was also monitored by FTIR spectroscopy and solid-state NMR at the ICTP.[24]

Table I.1. XPS results: O1s peak positions (E), referenced to the C1s C-C binding energy at 284.9 eV, peak areas (A) and assignations.

CNT- COOH		HPEEK		HPEEK-CNT-1		HPEEK-CNT-2		Assignation
E(eV)	A(%)	E(eV)	A(%)	E(eV)	A(%)	E(eV)	A(%)	
		539.9	6.6	539.9	6.9	539.9	6.7	π
				534.5	27.1	534.5	11.2	O=C-O
533.7	40.7	533.3	69.7	533.5	30.7	533.5	39.7	O-C
		532.8	22.1	532.8	26.7	532.8	32.7	O-H
532.1	59.3	531.7	1.5	531.7	8.6	531.7	9.7	O=C

I.3.3. Covalent strategy. Improvements achieved in the PEEK matrix

A thorough study of these HPEEK-CNT grafted polymers, conducted at the ICTP[24] revealed that these samples present higher thermal stability than the HPEEK, suggesting that the covalent attachment to the SWCNTs hinders the scission of the polymer chains. Moreover, DSC thermograms revealed a decrease in the crystallization and melting temperature as well as in the degree of crystallinity of the HPEEK with the esterification reaction. The crystallite size of the polymer determined from X-Ray diffractograms also diminished after the grafting process. DMA measurements demonstrated an exceptional enhancement in the storage modulus and glass transition temperature of the HPEEK-grafted SWCNTs in relation to those of the polymer derivative and neat PEEK. Slightly improved thermal and mechanical properties were found for the sample synthesized by carbodiimide-based esterification compared to that obtained *via* acylation, in agreement with its higher extent of covalent bonding. The tests performed confirm that the use of a hydroxylated derivative is an effective strategy to covalently graft polymer matrices onto the surface of carbon nanotubes, which may find increasing applications for the fabrication of nanocomposites with relatively high CNT content.

An extension of this study[32] showed that the incorporation of the grafted samples into pure PEEK promotes the filler dispersion within the matrix. DSC thermograms indicate a decrease in the crystallization and melting temperature of PEEK by the

[32] Diez-Pascual, A. M.; Martinez, G.; Martinez, M. T.; Gomez, M. A., Novel nanocomposites reinforced with hydroxylated poly(ether ether ketone)-grafted carbon nanotubes. *J. Mater. Chem.* 2010, *20* (38), 8247-8256.

addition of HPEEK-grafted SWCNTs, attributed to the restrictions on mobility imposed by the strong interactions between the functional groups of the nanotubes and the polymer chains. TGA studies show an exceptional thermal stability enhancement by the addition of these fillers. DMA experiments demonstrate a strong increase in both the storage modulus and glass transition temperature of the matrix by the polymer grafting. Furthermore, the Young's modulus, tensile strength and toughness greatly improve in comparison with composites reinforced with non-grafted fillers, since the additional covalent interactions and hydrogen bonds enhance the reinforcement effect.

The electrical conductivity increases drastically at very low CNT contents, indicating typical percolation behavior. The tests performed at the ICTP confirm that the addition of a polymer derivative covalently attached to the SWCNTs is more effective in enhancing the overall performance of these nanocomposites in comparison to the direct reinforcement or the incorporation of nanotubes wrapped in compatibilizers. This approach is promising for use in the preparation of multifunctional high-performance composites with relatively high CNT loading, to be employed in lightweight structural applications.

I.4. Conclusion

In the present chapter, the different functionalization strategies studied (non-covalent, in chapter 3; covalent, in annex I) have been successfully applied for the integration of SWCNTS into a high-performance thermoplastic PEEK matrix. The comparison between covalent and non-covalent strategies (namely, thermoplastic polymer wrapping or esterification grafting on hydroxylated PEEK) has been taken from the works performed in collaboration with Prof. M. A. Gomez-Fatou's research group.

Among the different compatibilizers tested, the best mechanical properties were attained with the incorporation of poly(1-4-phenylene ether ether sulfone) (PEES), amorphous thermoplastic polymer miscible and structurally similar to PEEK, that presents chemical affinity to both the matrix and the fillers. The mechanical properties of PEEK/CNT + PEES nanocomposites are compared to those of PEEK/HPEEK–CNT

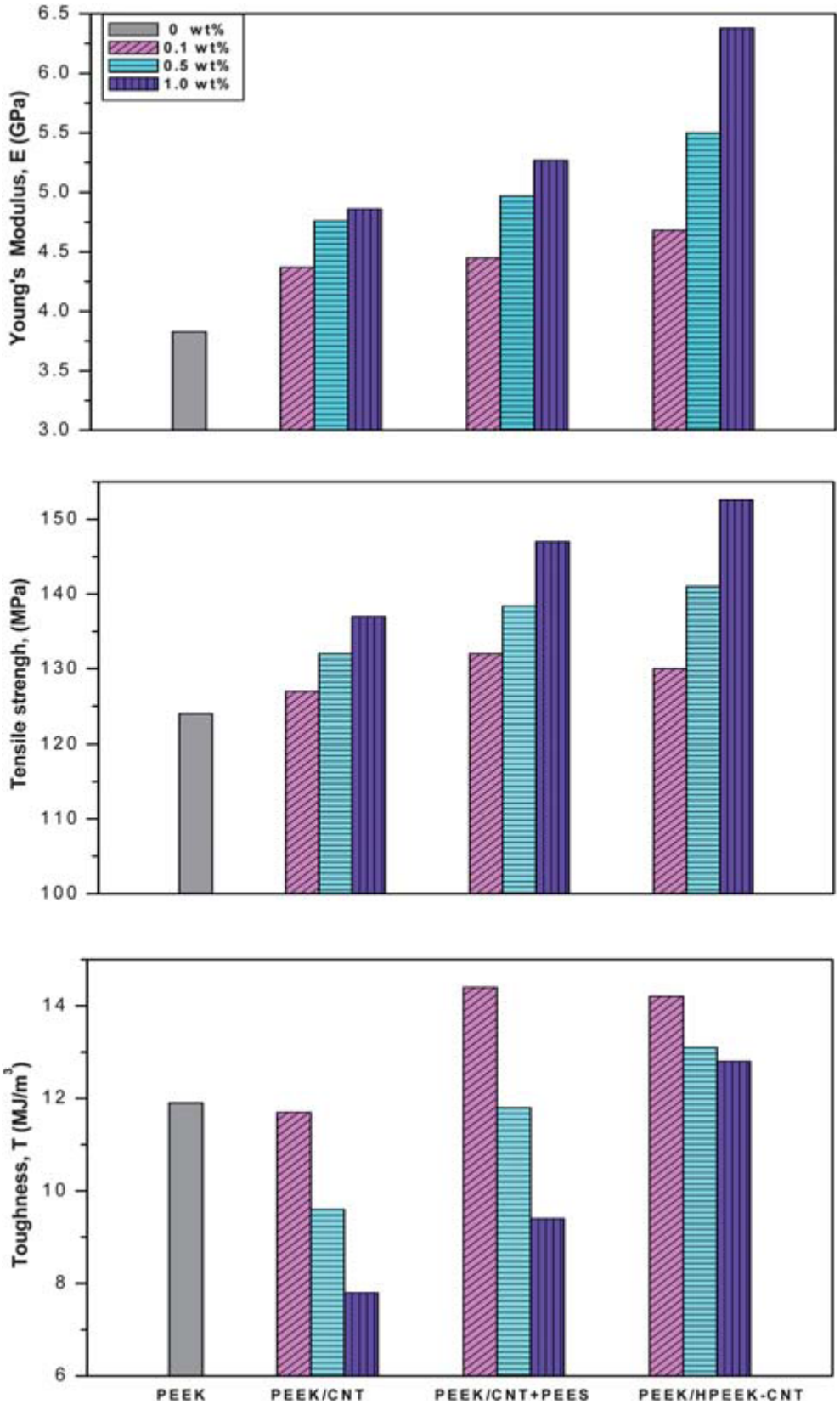

Figure I.3. Comparison between the mechanical properties of different PEEK nanocomposites.[32] Data of PEEK/CNT are taken from ref. 9; samples involving PEES are taken from references 25 and 27.

and PEEK/CNT in Figure I.3. Regarding to the Young's modulus, greater improvements are attained with the addition of polymer-grafted fillers in relation to those wrapped in PEES, particularly at 1.0 wt% CNT loading, where YM increases by 58% and 36%, respectively, in comparison to neat PEEK. This investigation confirms that the addition of a hydroxylated derivative covalently attached to the surface of SWCNTs is the most efficient way to improve the overall performance of the polymer; this opens up new perspectives for the development of nanocomposites with relatively high CNT loading, suitable for structural applications, particularly for the aeronautic industry. However, due to processing issues, the PEES wrapping strategy has become a suitable way to develop new and enhanced PEEK/GF laminates for the same application purposes.[33,34]

[33] Diez-Pascual, A. M.; Ashrafi, B.; Naffakh, M.; Gonzalez-Dominguez, J. M.; Johnston, A.; Simard, B.; Martinez, M. T.; Gomez-Fatou, M. A., Influence of carbon nanotubes on the thermal, electrical and mechanical properties of poly(ether ether ketone)/glass fiber laminates. *Carbon* 2011, *49* (8), 2817-2833.
[34] Ashrafi, B.; Díez-Pascual, A. M.; Johnson, L.; Genest, M.; Hind, S.; Martinez-Rubi, Y.; González-Domínguez, J. M.; Martínez, M. T.; Gómez, M. A.; Johnston, A., Influence of interfacial characteristics on properties of PEEK/Glass fibre laminates modified with single-walled carbon nanotubes, *Composites A (submitted)*.

"Let's see what you're made of"

Mortal Kombat 9
Konami (2011)

ANNEX II:

LIST OF SCIENTIFIC CONTRIBUTIONS DERIVED FROM THE PRESENT THESIS WORK

Research Papers:

SWCNTs purification

- Anson-Casaos, A.; Gonzalez-Dominguez, J. M.; Martinez, M. T., *Separation of single-walled carbon nanotubes from graphite by centrifugation in a surfactant or in polymer solutions.* ***Carbon*** **2010, *48* (10), 2917-2924.**
- Anson-Casaos, A.; Gonzalez, M.; Gonzalez-Dominguez, J. M.; Martinez, M. T., *Influence of Air Oxidation on the Surfactant-Assisted Purification of Single-Walled Carbon Nanotubes.* ***Langmuir*** **2011, *27* (11), 7192-7198.**

SWCNTs covalent functionalization and processing

- Anson-Casaos, A.; Gonzalez-Dominguez, J. M.; Terrado, E.; Martinez, M. T., *Surfactant-free assembling of functionalized single-walled carbon nanotube buckypapers.* ***Carbon*** **2010, *48* (5), 1480-1488.**
- Gonzalez-Dominguez, J. M.; Gonzalez, M.; Anson-Casaos, A.; Diez-Pascual, A. M.; Gomez, M. A.; Martinez, M. T., *Effect of various aminated single-walled carbon nanotubes on the epoxy cross-linking reactions.* ***J. Phys. Chem. C*** **2011, *115* (15), 7238-7248.**
- Martinez-Rubi, Y.; González-Domínguez, J. M.; Ansón-Casaos, A.; Kingston, C.; Martínez, M. T.; Simard, B.; *Tailored SWCNT functionalization optimized for compatibility with epoxy matrices,* ***Nanotechnology*** **(submitted).**

Epoxy/SWCNTs nanocomposites

- Gonzalez-Dominguez, J. M.; Castell, P.; Anson, A.; Maser, W. K.; Benito, A. M.; Martinez, M. T., *Block copolymer assisted dispersion of single walled carbon nanotubes and integration into a trifunctional epoxy.* ***J. Nanosci. Nanotechnol.*** **2009, *9* (10), 6104-6112.**
- Gonzalez-Dominguez, J. M.; Anson-Casaos, A.; Castell, P.; Diez-Pascual, A. M.; Naffakh, M.; Ellis, G.; Gomez, M. A.; Martinez, M. T., *Integration of block copolymer-wrapped single-wall carbon nanotubes into a trifunctional epoxy resin. Influence on thermal performance.* ***Polym. Degrad. Stab.*** **2010, *95* (10), 2065-2075.**
- Gonzalez-Dominguez, J. M.; Anson-Casaos, A.; Diez-Pascual, A. M.; Ashrafi, B.; Naffakh, M.; Backman, D.; Stadler, H.; Johnston, A.; Gomez, M.; Martinez, M. T., *Solvent-free preparation of high-toughness epoxy-SWNT composite materials.* ***ACS Appl. Mater. Interfaces*** **2011, *3* (5), 1441-1450.**
- Gonzalez-Dominguez, J. M.; Diez-Pascual, A. M.; Anson-Casaos, A.; Gomez-Fatou, M. A.; Martinez, M. T., *Epoxy composites with covalently anchored amino-functionalized SWNTs: towards the tailoring of physical properties through targeted functionalization.* ***J. Mater. Chem.*** **2011, *21* (20), 14948-14958.**
- González-Domínguez, J. M.; Martínez-Rubí, Y.; Díez-Pascual, A. M.; Ansón-Casaos, A.; Gómez-Fatou, M. A.; Simard, B.; Martínez, M. T., *Reactive fillers based on SWCNTs functionalized with matrix-based moieties for the production of epoxy nanocomposites with superior and tuneable properties*, ***Nanotechnology*** **(submitted).**

- González-Domínguez, J. M.; Tesa-Serrate, M. A.; Ansón-Casaos, A.; Díez-Pascual, A. M.; Gómez-Fatou, M. A.; Martínez, M. T., *Wrapping of SWCNTs with amphiphilic PEO-based diblock copolymers: an approach to purification, debundling and integration into epoxy matrix,* ***J. Phys. Chem. C*** **(submitted).**

PEEK/SWCNTs nanocomposites

- Diez-Pascual, A. M.; Naffakh, M.; Gomez, M. A.; Marco, C.; Ellis, G.; Gonzalez-Dominguez, J. M.; Anson, A.; Martinez, M. T.; Martinez-Rubi, Y.; Simard, B.; Ashrafi, B., *The influence of a compatibilizer on the thermal and dynamic mechanical properties of PEEK/carbon nanotube composites.* ***Nanotechnology*** **2009,** ***20*** **(31).**
- Diez-Pascual, A. M.; Naffakh, M.; Gomez, M. A.; Marco, C.; Ellis, G.; Martinez, M. T.; Anson, A.; Gonzalez-Dominguez, J. M.; Martinez-Rubi, Y.; Simard, B., *Development and characterization of PEEK/carbon nanotube composites.* ***Carbon*** **2009,** ***47*** **(13), 3079-3090.**
- Diez-Pascual, A. M.; Naffakh, M.; Gonzalez-Dominguez, J. M.; Anson, A.; Martinez-Rubi, Y.; Martinez, M. T.; Simard, B.; Gomez, M. A., *High performance PEEK/carbon nanotube composites compatibilized with polysulfones-I. Structure and thermal properties.* ***Carbon*** **2010,** ***48*** **(12), 3485-3499.**
- Diez-Pascual, A. M.; Naffakh, M.; Gonzalez-Dominguez, J. M.; Anson, A.; Martinez-Rubi, Y.; Martinez, M. T.; Simard, B.; Gomez, M. A., *High performance PEEK/carbon nanotube composites compatibilized with polysulfones-II. Mechanical and electrical properties.* ***Carbon*** **2010,** ***48*** **(12), 3500-3511.**
- Diez-Pascual, A. M.; Martinez, G.; Gonzalez-Dominguez, J. M.; Anson, A.; Martinez, M. T.; Gomez, M. A., *Grafting of a hydroxylated poly(ether ether ketone) to the surface of single-walled carbon nanotubes.* ***J. Mater. Chem.*** **2010,** ***20*** **(38), 8285-8296.**
- Diez-Pascual, A. M.; Ashrafi, B.; Naffakh, M.; Gonzalez-Dominguez, J. M.; Johnston, A.; Simard, B.; Martinez, M. T.; Gomez-Fatou, M. A., *Influence of carbon nanotubes on the thermal, electrical and mechanical properties of poly(ether ether ketone)/glass fiber laminates.* ***Carbon*** **2011,** ***49*** **(8), 2817-2833.**
- Ashrafi, B.; Díez-Pascual, A. M.; Johnson, L.; Genest, M.; Hind, S.; Martinez-Rubi, Y.; González-Domínguez, J. M.; Martínez, M. T.; Gómez, M. A.: Johnston, A., *Influence of interfacial characteristics on properties of PEEK/Glass fibre laminates modified with single-walled carbon nanotubes*, ***Composites A*** **(submitted).**

Book Chapters:

- Díez-Pascual, A. M.; González-Domínguez, J. M.; Martínez-Rubi, Y.; Naffakh, M.; Ansón, A.; Martínez, M. T.; Simard, B.; Gómez, M. A.; *Synthesis and Properties of PEEK/Carbon nanotube nanocomposites*. Chapter 11th of the book entitled *Polymer/Carbon nanotube nanocomposites*, Editorial Scrivener Publishing (Salem, USA), Wiley, pp 281-313, **ISBN: 9780470625927.**

Patents:

- **"**MATERIAL NANOCOMPUESTO REFORZADO CON UN DERIVADO POLIMÉRICO INJERTADO EN UN NANOMATERIAL DE CARBONO" (*Nanocomposite material reinforced with a polymer derivative grafted to a carbon nanomaterial)* Spanish patent application number **P201030947**.
- International extension of the aforementioned Spanish patent. Application number **PCT/ES2011/070443**.